Reports of the Department of Geodetic Science
Report No. 231

PROCEEDINGS OF THE GEODESY/SOLID EARTH AND OCEAN PHYSICS (GEOP) RESEARCH CONFERENCES

1972-1974

Edited by
Ivan I. Mueller

Prepared for
Defense Mapping Agency
Washington, D.C. 20036
National Aeronautics and Space Administration
Washington, D.C. 20036
National Oceanic and Atmospheric Administration
Rockville, Maryland 20852
U.S. Geological Survey
Washington, D.C. 20242

Contract No. NASW-2435
OSURF Project No. 3511-A1

The Ohio State University
Research Foundation
Columbus, Ohio 43212

September, 1975

Table of Contents

Introduction

The idea of the Geodesy/Solid Earth and Ocean Physics (GEOP) research conferences was born on October 6, 1971 in the bar of the Sonesta Beach Hotel in Key Biscayne, Florida, while Jerome Rosenberg of NASA Headquarters and the future director of the conferences were trying to recover from the hardship imposed upon them by the conference on "Sea Surface Topography from Space". The following thoughts were recorded:

- It may be the way to accelerate the development of interdisciplinary forbearance and skills so necessary for applying the newer technologies to a prompt and beneficial attack on critical problems.

- Emphasis would be on the application of space-based technologies; however, such a restriction should not be imposed.

- A small steering committee (similar to a board of directors) should be appointed/selected to plan and run the seminars.

- The seminars would meet at regular intervals (every 2 - 4 months).

- The seminar should be sponsored by a respected scientific organization such as the American Geophysical Union. Voluntary cosponsors and contributions should be solicited from the government and non-government communities.

- One of the secondary objectives of the seminar should be to involve and interest better graduate students in the critical problems of geodesy/earth and ocean physics. On that basis, the academic environment would be the most suitable one for the meetings.

- Each seminar should have at least one invited review or tutorial paper. This will help maintain the thrust for interdisciplinary exchange. The invited papers should be by accepted experts and should be based on guidelines established by the steering committee.

- At least one-third of the meeting time should be for informal discussion. In addition, panel discussions wherein the panel members and the audience exchange views should be emphasized. To further encourage inquiry, each paper should be followed by an equal time for questions from the floor.

Based on these preliminary thoughts the Charter of the GEOP Conferences was formulated and the sponsorships of the American Geophysical Union, National Aeronautics and Space Administration, National Oceanic and Atmospheric Administration and the U.S. Geological Survey were sought. The AGU Council at its December 5, 1971 meeting, authorized the sponsorship, and the other organizations followed suit shortly afterwards. The Charter is reproduced below:

Purpose:

The conferences are established to stimulate interdisciplinary research in the fields of geodesy, solid-earth and ocean physics within universities, research foundations, industrial and governmental organizations. This is to be achieved by an informal type of meeting consisting of scheduled speakers and discussion groups where sufficient time is available to stimulate discussion among the members of each conference. This type of meeting is a valuable means of disseminating information and ideas to an extent that could not be achieved through the usual channels of publication and presentation at scientific meetings. In addition, scientists in these related fields become acquainted and valuable associations are formed that often result in collaboration and cooperative efforts.

Meetings are held at regular intervals (every 2 - 4 months) during a two day period. The morning of the first day is reserved for a tutorial lecture presented by an eminent scientist. The topic of the lecture is determined by the subject of the conference in question and generally is a review of known information. It is hoped that each conference will extend the frontiers of science by fostering a free and informal exchange of ideas among persons actively interested in the subject under discussion.

The primary purpose of the program is to bring experts up-to-date on the latest developments, to analyze the significance of these developments, to provoke suggestions concerning the underlying theories and profitable methods of approach for scientific research and to accelerate the development of interdisciplinary forebearance and skills necessary for applying the newer technologies to an efficient attack on critical problems. Emphasis is on the application of space and astronomic techniques, however, other techniques are not necessarily excluded.

The secondary purpose of the program is to interest and involve talented graduate students in the critical problems of geodesy/solid-earth and ocean physics.

In order to protect individual rights and promote discussion, it is an established requirement of each conference that no new information presented is to be used without specific authorization of the individual making the contri-

bution, whether in formal presentation or in discussion. Scientific publications, with the exception of the tutorial-review paper, are not prepared as emanating from the conferences.

Administration:

The conferences are sponsored by the American Geophysical Union, NASA, NOAA, USGS and the Department of Geodetic Science, The Ohio State University. The program is under the direction of the Steering Committee, members of which are appointed by the various Sections of the American Geophysical Union. The Steering Committee elects the Chairman of the Conferences and appoints a subcommittee from its membership for each conference. An Executive Director is appointed by the Department of Geodetic Science, The Ohio State University.

Registration:

Attendance at the conferences is by application, which must be submitted on the standard application form obtainable from the American Geophysical Union. This procedure is important because certain specific information is required in order that a fair and equitable decision on the application may be made. Attendance at each conference is limited to approximately fifty conferees.

AGU submits the applications of those requesting permission to attend a conference to the committee for the conference. This committee reviews the applications and selects the members in an effort to distribute the attendance as widely as possible among the various organizations represented by the applications. A registration card is then mailed to those selected. Advance registration by mail for each conference is required and is completed on receipt of the card. There is no registration fee, however, each registrant is expected to cover his own travel, lodging and other expenses.

Most conferences will be scheduled in the Center for Tomorrow on the campus of The Ohio State University in Columbus. The center is equipped with lodging and conference facilities, all in the same building. The conferees are expected to live at this location because one of the objectives of the conference is to provide a place where scientists can get together informally for discussion of scientific research.

The Steering Committee appointed by the AGU Council (see title page) met on February 22, 1972 on the New York University campus, and the GEOP conference series was on its way, with the first conference to be held in October 1972. After the 1972/73 academic year the Defense Mapping Agency joined the list of sponsors and a second year was authorized. A total of eight conferences were held during

these two years. It is hoped that the following pages reflect not just the work accomplished but also portray at least a part of the atmosphere of excitement, discovery and friendship which was present throughout. It is also hoped that these pioneering efforts of organizing conferences covering limited interdisciplinary subject areas (topical conferences) will be followed by others organized by the scientific community. The GEOP experience clearly shows that future conference series should retain the following GEOP features:

1. limited interdisciplinary subject area
2. not longer than two days
3. not more than 60 attendees
4. organization delegated to four panel chairmen
5. located at an intermontane university strong in the area of geophysics.

Recommended modifications are:

1. broaden scope to "Geophysical Interaction" conferences
2. change responsibility and location every two or three years.

First Geodesy/Solid-Earth and Ocean Physics (GEOP) Research Conference

Solid Earth and Ocean Tides

Keynote Speaker: Walter H. Munk, University of California

CENTER FOR TOMORROW
OHIO STATE UNIVERSITY
COLUMBUS, OHIO
OCTOBER 26–27, 1972

Sponsored by: **American Geophysical Union**
National Aeronautics and Space Administration
National Oceanic and Atmospheric Administration
Ohio State University, Department of Geodetic Science
U.S. Geological Survey

The theme for the first GEOP Research Conference will be set by an introductory review relating to earth and ocean tides. The conference will be divided into the following sub-topics, each introduced by an invited moderator and discussed by a panel:

1. **Perturbations: Ocean Tides-Earth Tides**; *Chairman:* John Kuo, Lamont-Doherty Geological Observatory.
2. **Tidal Instrumentation, Data Acquisition and Analysis**; *Chairman:* Chris Harrison, University of Colorado.
3. **Global Oceanic Tidal Measurements and Prediction**; *Chairman:* Myrl C. Henderschott, University of California.
4. **Coastal Tidal Measurements and Prediction**; *Chairman:* Carl Wunsch, Massachusetts Institute of Technology.

Individuals interested in attending the conference are requested to send their applications on the standard application form available from the American Geophysical Union, 1707 L Street, N.W., Washington, D.C. 20036. Information on the membership in the GEOP Research Conferences may be found on page 305 of the April 1972 issue of E⊕S.

Further details on the program, accommodations, and registration will be sent to those applicants selected by the committee to attend the conference.

American Geophysical Union ★ 1707 L Street, N.W. ★ Washington, D.C. 20036

D1

N76-20567

Ocean Tides

M.C. Hendershott

Progress in the understanding of ocean tides since the field was reviewed two years ago by *Hendershott and Munk* [1970] has confirmed their characterization of the field as rapidly developing. The First Geodesy/Solid-Earth and Ocean Physics (GEOP) Research Conference on Solid-Earth and Ocean Tides provided an opportunity to gather subsequent results and to view them in the context of long-term trends in the development of the field. This review, therefore, largely picks up where that of *Hendershott and Munk* [1970] left off; the two reviews together are intended to provide a modern view of our state of understanding of ocean tides. Vital progress in instrumentation, in data analysis, and in the closely related field of solid-earth tides is outlined in the accompanying summary of conference discussions beginning on page 96 of this issue.

Tidal Dissipation, Continental Shelf and Marginal Sea Tides, Baroclinic Tides

The total rate of tidal dissipation in the atmosphere–ocean–solid-earth system has been fixed at about 3×10^{19} erg/sec by ascribing the astronomically or paleontologically observed increase in the length of day to a retarding torque arising from the frictionally induced phase lag between actual tides and tide-generating forces [*Munk and MacDonald*, 1960]. Thus the problem is not the determination of the rate of tidal dissipation but rather the determination of the mechanism by which the known dissipation occurs.

Most of the dissipation is thought to occur in the ocean, and the greater part of that evidently occurs in shallow marginal seas and over certain continental shelves. Atmospheric dissipation is probably quite small, and the effect of atmospheric tides on ocean–solid-earth tides is known to be small. (The reverse, however, is not true; ocean surface tide displacements alone are as effective as heating and cooling in driving atmospheric tides [*Hollingsworth*, 1971].) The grave mode of solid-earth free oscillation has the same second-order spherical harmonic form as does the greatest part of the solid-earth tide itself, and studies of solid-earth 'ringing' after strong earthquakes suggest that the Q of this mode is of the order of 10^2 ($Q = 2\pi E/TE_t$, where E is the total stored energy that escapes at a rate E_t and T is the period of the motion). Thus solid-earth dissipation is also likely to be small. We are left, then, with the oceans as evidently the major dissipators, although a definitive discussion of the partition of dissipation has not yet been given.

By estimating the energy flux from the deep sea onto shoal regions or by estimating directly the rate of working by bottom stresses as tidal currents flow over shoal regions, *Jeffreys* [1921], *Heiskanen* [1921], and, most recently, *Miller* [1966] have been able to ascribe most of the total dissipation to shoal regions. But the accuracy of these estimates is very poor, especially because of the kind of tidal current data available; Miller finds that the shoal area dissipation may fall between 0.7×10^{19} erg/sec and 2.5×10^{19} erg/sec. The difference between his upper limit and the astronomically determined 3×10^{19} erg/sec is probably not significant. The importance of a few regions in this estimate is striking. According to Miller, the five most important regions, together with their approximate dissipations (in 10^{17} erg/sec), are the Bering Sea (24), the Sea of Okhtosk (21), the Timor Sea (15), the Patagonian shelf (13), and the Hudson Straits (12). They sum to 0.85×10^{19} erg/sec, nearly one-third of the total.

A number of recent studies have resulted in improvements in our understanding of tides in marginal seas and over continental shelves. *Hendershott and Speranza* [1971] have suggested a way to compute the rate of tidal energy flow along certain long and relatively narrow marginal seas having primarily cross basin variation of bottom relief. They capitalize on the fact that many such basins are sufficiently narrow and deep that only Kelvin waves propagate semidiurnal tidal energy; in principle, therefore, only two tide stations at which harmonic constants are known permit deduction of the direction and magnitude of the semidiurnal tidal energy flux along the basin. *Hendershott and Speranza* [1971] interpreted the net inflow of energy thus calculated for the Adriatic Sea and the Gulf of California as shallow water dissipation at the shoaling closed end of the basin. Garrett (private communication) has pointed out that the local rate of working by tide-generating forces may also have to be considered if shallow water dissipation itself is to be deduced. Systematic application of this technique should make possible a useful revision of some of *Miller*'s [1966] estimates of marginal sea dissipation.

Munk et al. [1970] attempt to represent California coastal tides as a superposition of the possible motions, free and forced, of a plane, rotating ocean that has a straight coast with a continental shelf. In the absence of rotation, a family of Stokes edge waves are refractively trapped over the shelf. Rotation splits the formerly identical phase speeds of oppositely traveling modes and also makes possible a new set of

This article was taken from the keynote address presented at the first GEOP Research Conference on Tides, which was held at The Ohio State University, Columbus, October 26–27, 1972.

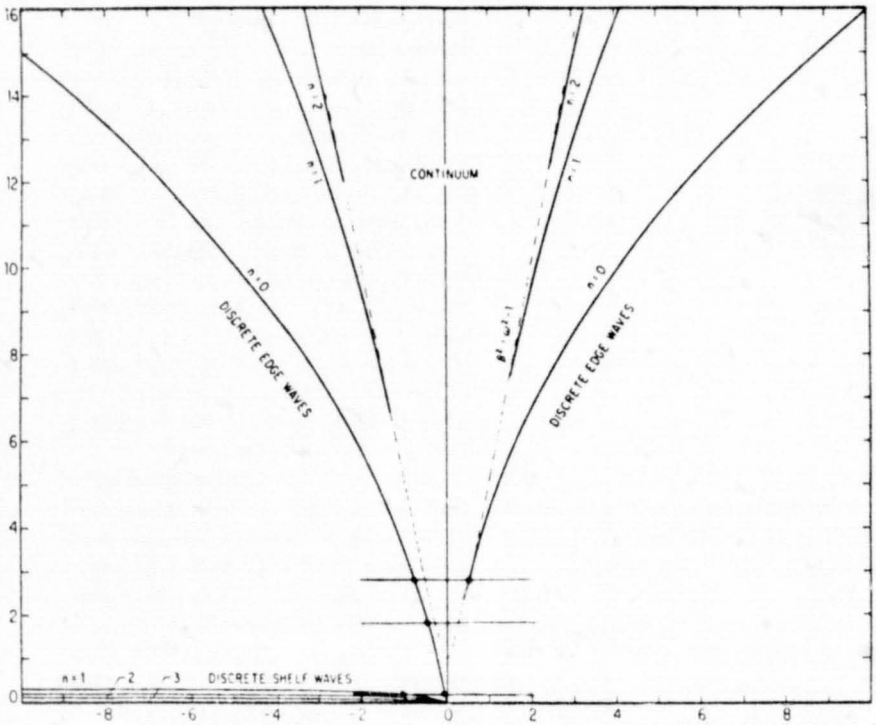

Fig. 1. Typical dispersion relation (frequency in units of the local inertial frequency plotted against longshore wave number in units of reciprocal shelf width) for a continental shelf, after Munk, Snodgrass and Wimbush (1970). The discrete edge waves are the rotationally modified Stokes modes of §2; the n = 0 edge wave having negative longshore wave number becomes the Kelvin mode for dimensionless frequencies of order one or smaller. The three short horizontal lines of constant frequency near the origin cross the dispersion curves of the various modes which may be excited in tides at low latitudes (uppermost line), mid latitudes, i.e., California (central line), and high latitudes (lowest line).

quasigeostrophic low-frequency shelf modes trapped over the shelf. (However, the lowest order Stokes mode, which travels with the coast to the right in the northern hemisphere, approaches the usual Kelvin wave at frequencies of the order of the local inertial frequency.) A continuum of leaky Poincare waves (essentially rotationally modified gravity waves reflected at the shore-shelf) also exists (Figure 1). Besides these free modes, *Munk et al.* [1970] additionally require a forced shelf solution that allows for both local working by tide-generating forces as well as for the yielding of the solid earth to those forces.

For the California coastal $M2$ tide, a combination of the Kelvin-Stokes mode, a single wave of the Poincare continuum, and the forced solution in the amplitude ratio 54:16:4 cm gives a good representation of the coastwise and seaward variation of the tide. This mix of modes predicts a semidiurnal amphidrome off the California coast, roughly half way to Hawaii, a prediction that has subsequently been confirmed by direct deep sea observation [*Irish et al.*, 1971]. The success of this dissipationless model is a strong, although indirect, confirmation of *Miller*'s [1966] low estimate of California coastal tidal dissipation. *Miles* [1972] has shown how coastline curvature modifies the dominant Kelvin mode.

The variety of shelf modes (Figure 1) allows for coastal tides of quite different character from those of California. At very low latitudes, the lowest order Stokes mode whose direction of travel is opposite to that of the Kelvin-Stokes mode may be excited in semidiurnal tides. At high latitudes, one or more quasigeostrophic shelf modes may be excited in diurnal tides. Because these quasigeostrophic modes tend to have much more kinetic than potential energy, one would expect to observe in this latter case strong diurnal tidal currents without correspondingly large diurnal fluctuations of sea level. *Cartwright* [1969] has observed diurnal tides of this kind in the region west of Scotland.

A number of observational studies of continental shelf and marginal sea tides have recently been initiated, including studies of continental shelf tides around the British Isles [*Cartwright*, 1968] and Australia [*Irish*, 1971]. Filloux (unpublished data) has recently completed a series of observations in the Gulf of California. All of this important observational work is too recent to have strongly influenced theoretical studies and a great deal more is as yet unpublished.

The dynamics of tides in shoal regions are thus being sorted out, but the vital question of whether all or merely some of the oceans' tidal dissipation occurs there is not yet resolved. By far the most interesting alternative to the total dissipative dominance of shoal regions is the possibility that an appreciable amount of dissipation occurs via baroclinic or internal tides. The small-scale turbulence and consequent mixing that would result from 'breaking' tidal internal waves make this prospect one of great interest to oceanographers. However, the physics of internal wave generation and decay are only beginning to be understood. Observations of internal tides, both over continental shelves and in the deep sea, are commonplace, although perhaps not so much so as observations of inertial currents [*Webster*, 1968]. *Defant* [1950] has summarized the evidence available before the advent of long-term deep sea moorings. Subsequent reports or discussions of relevant observations have been given by *Lafond* [1962], *Cox* [1962], *Lee and Cox* [1966], *Wunsch and Dahlen* [1970], *Halpern* [1971], *Fofonoff and Webster* [1971], *Gould* [1971], and many others. No modern review of the internal tide problem exists, and I will not attempt to present one here.

Internal tidal waves owe the possibility of their existence to the stable density stratification of the oceans. They manifest themselves largely as marked but irregular departures of

the vertical profile of horizontal tidal currents from the uniformity implicit in the usual form of the long-wave, shallow water equations; their effects on sea-surface displacement would be barely detectable [*Radok et al.*, 1967]. Internal tidal currents are nearly always phase incoherent with either the tide-generating forces or local barotropic, i.e., surface, tides (see, for example, *Munk et al.* [1970]). This situation has been widely interpreted as being the result of the very low phase speeds of free internal waves and the consequent likelihood of their strong nonlinear interaction with ocean currents having appreciable variation over weeks or months. *Regal and Wunsch* [1972] note the sole exception to this: at a location (Woods Hole Site D) seaward of the continental slope in the western North Atlantic they find semidiurnal tidal currents phase locked to the surface tide.

Internal tides are generated and dissipated by unknown mechanisms. The possible importance of scattering of barotropic tidal energy into baroclinic tides via interaction with bottom roughness has been stressed by *Rattray et al.* [1969] and by *Baines* [1971] for the continental shelves and large-scale bottom slopes and by *Cox and Sandstrom* [1962] for small-scale mid-ocean bottom roughness. The relative importance of the different topographic regions is unknown. Observations by *Reid* [1956] and by *Summers and Emery* [1963] suggest that the seaward edge of the California continental shelf is an important local source of semidiurnal internal tides. The unusual observation by *Regal and Wunsch* [1972] of internal tides having phase coherence with the surface tide, strongly suggests generation over the nearby continental slope, especially when the vertical structure of the observations is considered. *Cox* [1968] has estimated the energy density in internal tides at a location 350 km off the southern California coast to be 4.5×10^5 erg/cm^2, about 30% of the energy present in the semidiurnal barotropic tide there; but until recently there have been no observations allowing even a guess at the rate of energy input or energy loss for internal tides.

Wunsch and Hendry [1972] have placed a closely spaced array of current meters on the continental slope of the western North Atlantic, not far from Woods Hole Site D. Their wave number spectra suggest that the tide there is almost all baroclinic and, at the nearshore part of the array, propagates towards the shore from that region where the slope of the characteristics of the internal wave equation [*Sandstrom*, 1969] is locally equal to the bottom slope. The slope of the bottom *at* the nearshore part of the array is not far from that of a characteristic, and the enhancement, expected under such circumstances [*Wunsch*, 1967], of tidal currents towards the bottom is observed. From the observed wavelength (about 12 km) of the internal tides, *Wunsch and Hendry* [1972] are able to estimate the vertical mode number (2) and can thus compute the energy flux shoreward away from the presumed region of generation (where bottom and characteristic slopes coincide). They obtain 2.2×10^9 erg/cm sec, a result that, when extrapolated at face value to the length (3×10^9 cm) of oceanic coastline and multiplied by 2 to allow for both seaward and shoreward radiation, gives more than 10^{19} erg/sec for the rate at which tidal energy is scattered into internal tides at the world's continental shelves.

Tidal Admittance, Tidal Q, and Tidal Resonance

Estimates of the amount of energy stored in the tide and of the distribution over the oceans of that energy have been more difficult to construct than traditional estimates of dissipation, which require primarily near coastal observations or astronomical observations. The closely related problem of estimating the resonant frequencies and Q factors of oceanic normal modes from the observed response of the ocean to forcing at various tidal frequencies has only recently received attention.

In determining the resonant frequencies of the solid earth, seismologists have the advantage of very broad-band forcing functions, i.e., earthquakes. But earthquakes are (perhaps fortunately) not sufficiently rich in energy at near tidal periods to make analogous studies of ocean normal modes feasible. However, tide-generating forces are not entirely monochromatic, and it has become feasible to study the frequency response of the oceans by looking at the variation of ocean admittance across diurnal and semidiurnal tidal bands.

Because of the nonlinearity of the orbital equations of motion, the fundamental astronomical frequencies

$\omega_1 = 2\pi/$(period, 27.3 days, of lunar declination)

$\omega_2 = 2\pi/$(period, 365.24 days, of solar declination)

$\omega_3 = 2\pi/$(period, 8.85 years, of lunar perigee)

$\omega_4 = 2\pi/$(period, 18.61 years, of lunar node)

$\omega_5 = 2\pi/$(period, 20,940 years, of perihelion)

$\omega_0 = 2\pi/$(one solar day)

$\omega_c = 2\pi/$(one lunar day)

appear as sum and difference frequencies

$$\sigma = S\left(\frac{\omega_0}{\omega_c}\right) + \sum_{k=1}^{5} M_k \omega_k$$

$$S = 0, 1, 2$$

in the harmonic representation

$$\sum_j C_j \cos(\sigma_j t + S\Phi + \theta_j)$$

of the long period ($S = 0$), the diurnal ($S = 1$), or the semidiurnal ($S = 2$) tide-generating potential (at time t, longitude ϕ; the potential at Greenwich when $t = 0$ has the value $C_j \cos(\theta_j)$). The tide-generating forces thus contain energy in frequency bands of width ~ 0.3 cpd centered about 0, 1, and 2 cpd. This analysis is from *Doodsen* [1921]; a succinct review has been given by *Platzman* [1971].

Munk and Cartwright [1966] were the first to examine the variation of mid-ocean (Hawaii) tidal

admittance across these bands. They found little systematic variation across the bands, but they did note that the magnitude and frequency variation of admittance for tides having second-order spherical harmonic spatial variation of the force-producing potential were different than those for tides whose potential has third-order spherical harmonic spatial variation. (The latter admittances, however, were determined only within very wide error bars.) This means that the coupling between a second-order potential Φ_2 and Pacific normal modes may be quite different from that between a third-order potential Φ_3 and those same normal modes.

More recent studies of the frequency dependence of the admittance have been conducted by *Garrett and Munk* [1971] and by *Wunsch* [1972]. *Garrett and Munk* [1971] discuss their work in terms of the 'age of the tide.' Solar and lunar tides reinforce when sun, moon, and earth are colinear (spring tides) but oppose when these three bodies form a right triangle (neap tides). In the Fourier analysis of tide-generating forces, spring and neap tides appear as the 'beat' between lunar semidiurnal ($M2$) and solar semidiurnal ($S2$) tides, but spring tides are generally observed to occur a day or two (the 'age') *after* full or new moon (when the tide-generating forces are greatest). This means that the phase of the ocean's response to $M2$-forcing is different from that of the response to $S2$-forcing; an age of one hour corresponds to a difference in phase lag of 1.016°.

If one supposes that a single ocean normal mode is being excited by tide-generating forces and that its response is that of a simple harmonic oscillator

$$Ae^{i\theta} = \frac{\text{constant}}{\omega - \omega_R - i\omega_R/2Q}$$

then observations of $Ae^{i\theta}$ at several frequencies ω allow one to draw conclusions about the resonant frequency ω_R and the Q of the mode. *Garrett and Munk* [1971] note that $Q > (\omega_R/2)\, d\theta/d\omega$, and they estimate $d\theta/d\omega$ from the global distribution of the maximum age to find roughly $Q > 25$ for the world's oceans. Excitation of many modes appears unlikely to modify their result.

Wunsch [1972] has examined Bermuda tide gauge data, reanalyzing a particularly favorable portion of the record to resolve as many lines as possible. He found the semidiurnal admittance growing by 400% (towards lower frequencies) across the semidiurnal band with a concomitant phase shift of over 120°. Similar behavior occurs in the Azores. This strongly suggests that the North Atlantic is in fact resonant at a period not too much longer than 12 hours; *Wunsch* [1972] combines diurnal, semidiurnal, and (one) terdiurnal admittances to estimate the shape of the admittance curve. That estimated curve shows peaks at 36.6, 14.8, and 9.3 hours; the evident resonance at 14.8 hours has, from its half power width $\Delta\omega$ a Q given by $\omega_R/\Delta\omega$ as $Q > 5$.

In view of the difference in Φ_2-ocean and Φ_3-ocean coupling found by *Munk and Cartwright* [1966], we may wonder about the effect of the difference in coupling between the ocean and the diurnal, semidiurnal, and terdiurnal tide-generating potentials (whose spatial dependence is quite different) on the shape of this admittance curve. But the suggestion of a resonance just below the semidiurnal band is compelling, especially in view of *Platzman*'s [1972*b*] recent theoretical estimate of North Atlantic resonant periods of 21.2, 14.0, and 11.5 hours.

Both the *Garrett and Munk* [1971] and the *Wunsch* [1972] estimates of Q are lower bounds and they are not in direct conflict; but it is puzzling that the North Atlantic, which in *Miller*'s [1966] estimate is relatively dissipationless, should have such a low Q relative to the global ocean.

Simultaneously, *Hendershott* [1972] estimated the energy stored in the global $M2$ tide as 7×10^{24} ergs by a direct numerical integration of Laplace's tidal equations. His Q for $M2$ was thus 34. Similar estimates from other numerical tidal models would be useful.

Historical estimates [*Hendershott and Munk*, 1970] of the Q of ocean tides as of the order of two or three thus require upward revision. It is certain that studies of the admittance curve in various parts of the world will now be vigorously pursued. *Garrett* [1972] has applied the method to the tides of the Bay of Fundy with results that are of engineering as well as of scientific importance.

Earth Tides and Ocean Tides

Students of solid-earth tides have long been aware of the importance of ocean effects in the interpretation of their observations, but the reverse is not true. Of the various large-scale tidal models summarized in Table 1, only those of *Gohin* [1961], *Munk et al.* [1970], *Cartwright* [1971], and *Hendershott* [1972] acknowledge the solid earth to be other than rigid. In these models, the yielding of the solid earth to the direct action of the astronomical tide-generating forces is introduced in Love number approximation, but the yield of the solid earth to the weight of the overlying ocean tidal column is neglected.

Hendershott [1972] points out that the full tide-generating potential Γ is of the form

$$\Gamma = (1 + k_2)U_2 + \sum_n (1 + k_n')\,(3g/2n + 1)\,(\rho_w/\rho_e)\zeta_{0n}$$

while the geocentric solid-earth tide δ is

$$\delta = h_2 U_2/g + \sum_n h_n' \cdot [3/(2n + 1)]\,(\rho_w/\rho_e)\zeta_{0n}$$

in which U_2 is the (dominantly second-order spherical harmonic) astronomical tide-generating potential, ρ_w and ρ_e are the mean densities of ocean and solid earth, h_n, k_n, h_n', k_n' are the Love numbers defined by *Munk and MacDonald* [1960], g is the acceleration of gravity, and ζ_{0n} is the nth spherical harmonic component of the observed (relative to the deforming ocean floor) ocean tide ζ_0. The models of *Gohin* [1961], *Munk et al.* [1970], and *Cartwright* [1971] noted above disregard the terms Σ_n in these expressions for Γ and δ. Using these expressions, *Hendershott* [1972] rewrites Laplace's tidal equations as a set of integro-differential equations in which all

driving terms appear in the single combination

$$(1 + k_2 - h_2)U_2/g$$
$$-\sum_n (1 + k_n' - h_n') [3/(2n + 1)]$$
$$\cdot (\rho_w/\rho_e)\zeta_{0n}$$

The size of the second term in this expression relative to the first is one measure of the importance of ocean self-attraction and of solid-earth yielding to the weight of the oceanic tidal column relative to that of forces derived directly from the astronomical potential U_2 after solid-earth yielding to those forces has been considered. Using *Hendershott*'s [1972] estimate of ζ_0 for the global $M2$ ocean tide, *Farrell* [1972*a*] has evaluated the second term by convolution of ζ_0 with Green functions derived for realistic solid-earth models [*Farrell*, 1972*b*]. The result (Figure 2) is startling; the two terms are of equal orders of magnitude. Although the detailed shape of this field is influenced by the estimate of ζ_0, which is not free of errors, it is nevertheless clear that the heretofore neglected ocean-loading and ocean-self-attraction effects must be retained in models of ocean tides aspiring to more than qualitative accuracy. *Hendershott* [1972] has discussed the way in which ocean tide models must consequently be modified but notes that there are technical difficulties in the way of solving the resulting equations.

Farrell [1972*c*] has also used the same ζ_0 to estimate the effect of ocean loading on gravity tides in the continental United States. The ocean-loading correction thus derived reduces the discrepancy between the theoretical gravity tide and the observed gravity tide by well over 50%. It is thus clear that precision earth tide measurements carry with them much information about the tides of the ocean. In principle, this information could be extracted in an optimal manner by solving an inverse problem for ocean tides using earth tides as observables, but this is a development for the future.

Global Numerical Models of Ocean Tides

One of the striking things about the ensemble of numerical global tidal models discussed in the literature is the evident nearness of the semidiurnal tide to resonance at many places. Thus *Pekeris and Accad* [1969], in refining their pioneering dissipationless global model of the $M2$ tide by changing the coastlines slightly or by refining the finite difference mesh from 2° to 1°, sometimes found amplitude changes as great as three meters. Similar effects are noticeable in other models (see discussion below).

This proximity to semidiurnal resonance should not be surprising in view of the rich spectrum of free oscillations possible in even a regular

TABLE 1. Summary of Large-Scale Tidal Models

Investigator	Type of Model	Boundary Condition	Dissipation	Earth Tide
Zahel [1970]	$M2$ tide for globe	Impermeable coast	Bottom stress in shallow water	None
Pekeris and Accad [1969]	$M2$ tide for globe	Impermeable coast	Linearized artificial bottom stress in shallow water	None
Hendershott [1972]	$M2$ tide for globe	Coastal elevation specified	At coast only	See §5
Bogdanov and Magarik [1967]	$M2$, $S2$ tides for globe	Coastal elevation specified	At coast only	None
Tiron et al. [1967]	$M2$, $S2$, $K1$, $O1$ tides for globe	Coastal elevation specified where data exist, otherwise impermeable coast	At coast only	None
Gohin [1961]	$M2$ tide for Atlantic, Indian oceans	Coastal impedance specified	At coast only	Yielding to astronomical force only
Platzman [1972*a*,*b*]	Normal modes of major basins, esp. Atlantic	Adiabatic boundaries	Zero	—
Munk et al. [1970]	Normal mode representation of California coastal tides	Impermeable coast	Zero, although energy flux parallel to coast may reflect dissipation up coast	Yielding to astronomical force only
Cartwright [1971]	β-plane representation for S. Atlantic tides	Island values specified	Zero, although energy flux may reflect distant dissipation	Yielding to astronomical force only

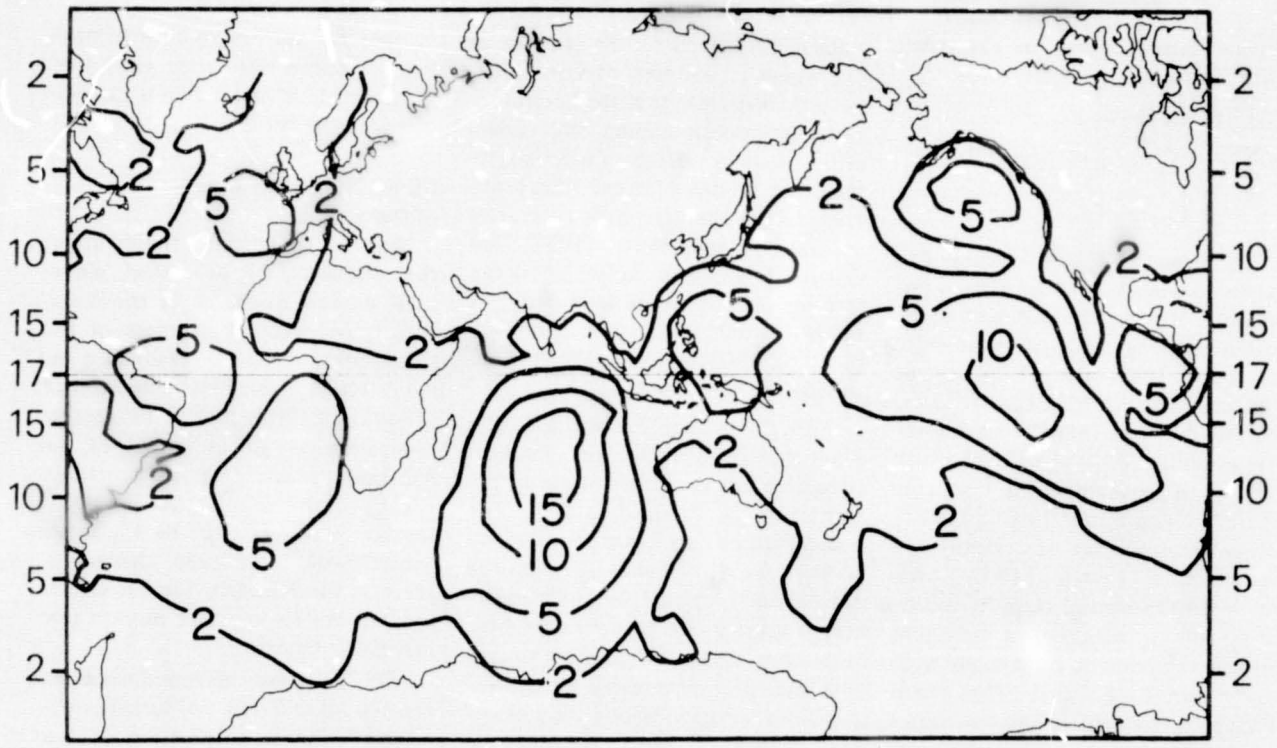

Fig. 2. Cornage lines (cm) of the self potential of ocean tides plus the potential due to the earth's deformation with the height of the tidal column (after Farrell *[1972c]). Numbers on margins are amplitude of astronomical potential plus potential due to yield of solid earth to astronomical force. All potentials divided by* g.

flat-bottom ocean of global extent (i.e., *Longuet-Higgins and Pond* [1970]). In this case we may expect (*a*) inertia-gravity waves modified by rotation and sphericity with free periods of the order of one day or shorter, (*b*) planetary or Rossby waves with free periods of the order of 3 or 4 days or *longer*, (*c*) standing Kelvin waves with periods of the order of one day or less [*Hendershott and Munk*, 1970]. Variable bottom relief introduces additional free oscillations.

The various global numerical models differ from one another primarily in their inclusion of dissipation, their treatment of coastal boundary conditions, and their inclusion of the effects of solid-earth tides. Some modelers attempt to include bottom-drag dissipation directly and require the coasts to be impermeable, while others allow power to flow out of their computational boundaries, thus parameterizing the dissipation as a near coastal process. The pros and cons of such procedures have been discussed by *Hendershott and Munk* [1970]. The numerical models together with several other large-scale models of various sorts are summarized in Table 1. I want to compare here the results of the various models over the globe. In what follows, I refer to semidiurnal models only, although diurnal calculations have also been made in some cases.

The various models are in rather good qualitative agreement in the North Atlantic (Figure 3). The central Atlantic amphidrome appears east of Nova Scotia and south and slightly east of the tip of Greenland but with some variation in its position. *Platzman*'s [1972*b*] 14-hour normal mode displays a similar amphidrome. There is an amphidrome between Iceland and the Faroe Islands, in accordance with the empirical maps of *Dietrich* [1944] and *Villain* [1952].

In the South Atlantic the empirical tidal maps show a uniform northward progression of crests on the basis of coastal data plus island observations at Ascension Island, Trinidad, St. Helena, Tristan, and South Georgia. The numerical maps of everyone except Hendershott show an amphidrome in this region. *Pekeris and Accad* [1969] were the first to take this feature seriously and to suggest that it was realistic. *Cartwright* [1971] repeated tidal measurements at St. Helena and analyzed new data for Tristan in a study intended to confirm or deny the existence of this amphidrome. He attempted various reconstructions of the elevation field in this region, both by linear interpolation and by fitting the island observations to free solution of the β-plane version of Laplace's tidal equations with no coastal boundary conditions. His linear interpolation gives a result very similar to that of *Pekeris and Accad* [1969]; his dynamical interpolations move the amphidrome closer to the coast of South America.

We may scarcely expect any of these models to be entirely faithful to reality in this region because none really takes the coastal boundary conditions into proper account. *Cartwright*'s [1971] dynamical interpolation is for an unbounded ocean, and although the numerical models aim at proper treatment of the coasts, all are demonstrably very inadequate along the Patagonian shelf, and hence all probably do not dissipate the proper amount of energy there. Nevertheless, the totality of all calculations together with *Cartwright*'s [1971] work suggests that the South Atlantic semidiurnal amphidrome is real. If so, it will be the first such

Fig. 3. Atlantic results of global numerical solutions of Laplace's tidal equations for the M2 tide by (left to right, top to bottom) Bogdanov and Magarik [1967], Hendershott [1972], Zahel [1970], Pekeris and Accad [1969],—frictionless, 2° mesh, Dietrich [1944],—an empirical map rather than a numerical solution, redrawn by Villain [1962], Pekeris and Accad [1969],—dissipative, 1° mesh.

feature discovered by the numerical tidalists.

Islands in the Indian Ocean are sufficiently frequent and evenly distributed that a rather good empirical map may be constructed (Figure 4). The salient feature of such a map is a very large region in the south central Indian Ocean within which the sea surface moves nearly synchronously. Every numerical map produces such an 'antiamphidrome.' The computations of *Pekeris and Accad* [1969] and *Hendershott* [1972] suggest that this region is nearly resonant at semidiurnal periods. Hendershott (unpublished) finds that by varying the mean depth by several hundred meters, computed *M2* amplitudes may be changed by a multiplicative factor of 2 or 3. A very realistic prediction of Indian Ocean island semidiurnal tides may be made by proper empirical choice of the mean depth.

In the Pacific, the various numerical and normal mode models show the greatest divergence from one another and from Pacific island observations (Figure 5). This is perhaps not surprising in view of the size of this basin and the consequent diminution of the direct influence of coastal boundary conditions on mid-basin tides.

The empirical cotidal maps show a

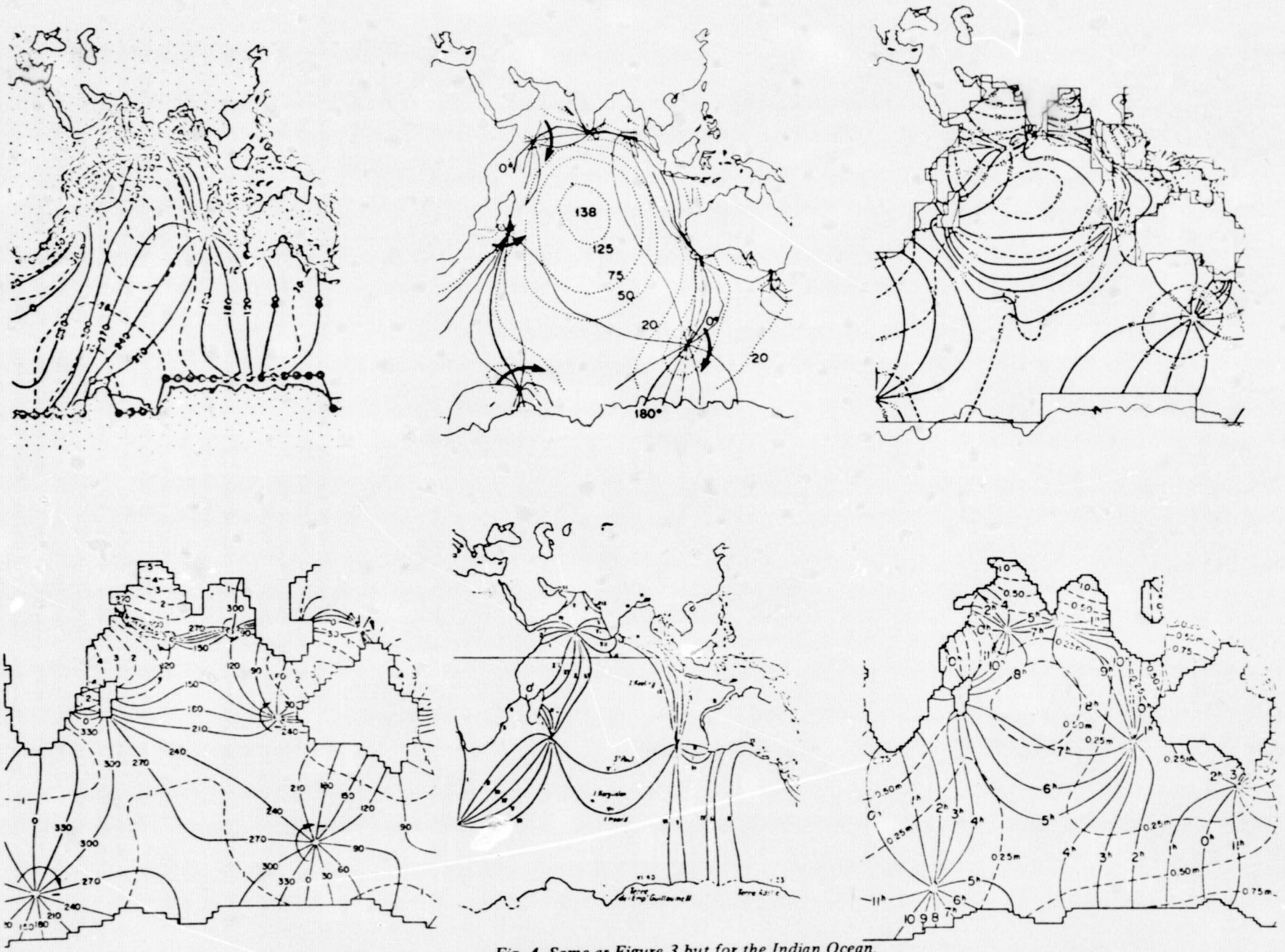

Fig. 4. Same as Figure 3 but for the Indian Ocean.

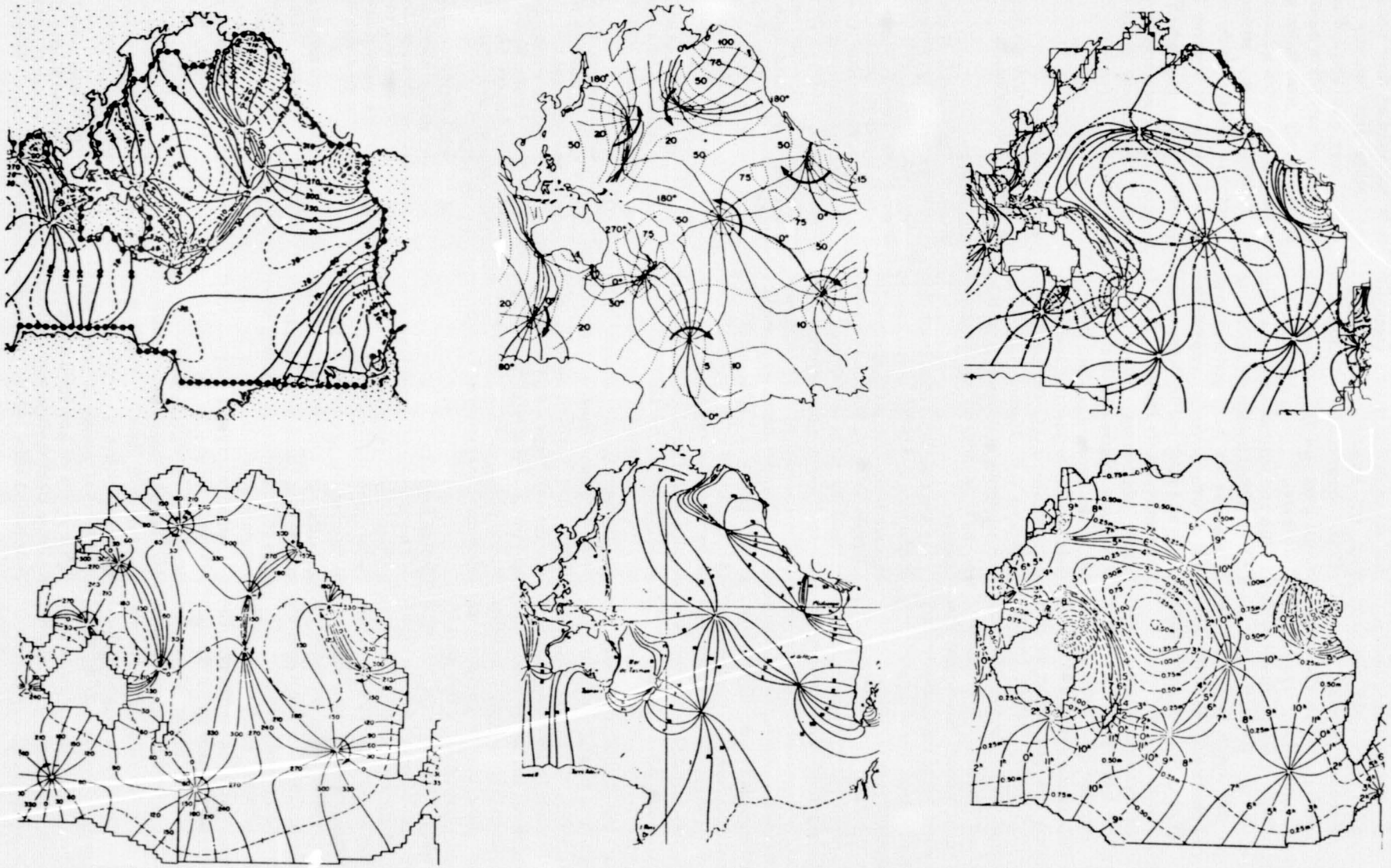

Fig. 5. Same as Figure 3 but for the Pacific Ocean.

number of amphidromes in the Pacific, including one in the northeast Pacific off the northwestern coast of North America, one in the central Pacific just south of the equator, and various others. Cotidal lines bunch together in the Bonin-Mariana Islands; in this region amplitudes are small, and phases shift abruptly along a line running roughly north-south between Japan and New Guinea.

The various numerical maps either resolve this last region into two or three amphidromes [*Hendershott*, 1972; *Pekeris and Accad*, 1969] with realistically low amplitudes, or they fail entirely to be realistic [*Pekeris and Accad*, 1969; *Zahel*, 1970; *Bogdanov and Magarik*, 1967]. Hendershott (unpublished) has found that small variations in imposed boundary values may make the computed tides in this region very realistic.

To the east, at roughly 150°E, 10°N, island observations suggest a broad amplitude maximum in the center of a large region that rises and falls nearly in synchrony, an anti-amphidrome as in the Indian Ocean. The computations of *Bogdanov and Magarik* [1967], *Zahel* [1970], and *Pekeris and Accad* [1969] show such a region, although computed amplitudes vary widely.

Near the California coast, the computations diverge radically. The computations of *Pekeris and Accad* [1969] result in the wrong sense of propagation of semidiurnal tides along the California coast. The other models show the proper sense of crest propagation but differ markedly in where they locate the northeast Pacific amphidrome. All are significantly different from the coastal model of *Munk et al.* [1970], which has been checked by subsequent observation and which is probably the best description of tides between the California coast and Hawaii.

The southeast Pacific is, tidally speaking, unknown territory. The only station between South America and Polynesia is Easter Island, and the Antarctic coast in this quadrant of the globe has no station. The empirical cotidal charts suggest a clockwise amphidrome at 120°W, 40°S, and every numerical chart except that of *Bogdanov and Magarik* [1967] produces an amphidrome of that sense in this region (even the map of *Bogdanov and Magarik* [1967] shows a near confluence of cotidal lines and an amplitude minimum there).

With and without explicit dissipation the global models are disturbingly sensitive to small perturbations: the South Atlantic amphidrome comes and goes, Indian Ocean amplitudes fluctuate by factors of 2 or 3, Pacific amphidromes move about, now nearly coalescing and now rotating in the wrong direction. In toto, these models suggest that such small-scale features as (1) the continental shelf-deep sea transition and (2) island scattering or diffraction must be got right in advance of the global solution.

(1) The California coastal solution of *Munk et al.* [1970] would require an extremely fine mesh spacing for tolerable reproduction of the velocity field by finite difference methods. It is much more natural to use this local normal mode description to generate proper deep sea boundary conditions for a global model. (2) The smoothing of bottom relief required for even the finest finite difference model completely obliterates such features as the Hawaiian island arc, yet semidiurnal tides on the southwestern side of these islands lag over 40° behind those on the northeastern side (Larsen, private communication). Neglect of the effect of this arc is probably a major reason for the poor quality of the numerical solutions in the northeast Pacific.

Closing Remarks

The foregoing omits much of interest. Certain implications [*Munk*, 1968] of tidal dissipation for the history of the earth may become accessible to further study as tidal models and geological reconstructions of ancient oceans mature. Satellite studies of tides, both by orbit perturbations (giving lower order spherical harmonics of terrestrial tides) and by direct satellite altimetry (giving quasi point measurements) will become increasingly important. Earth tide studies will provide areal means of ocean tides that are free of any local distortion resulting from shallow water effects. Long-period tides, whose low amplitude has masked their nonequilibrium nature until recently [*Wunsch*, 1967], may now become accessible to study via earth tide measurement as the already remarkable precision of these measurements increases.

Perhaps the most striking thing about the present study of ocean tides is the fresh impetus for their better understanding which is now coming from other branches of geophysics. The subject is still developing rapidly.

Acknowledgment

The research on tides was supported by the Office of Naval Research.

Bibliography

Baines, P., The reflexion of internal/inertial waves from bumpy surfaces, *J. Fluid Mech., 49*, 113–131, 1971.

Bogdanov, K.T., and V. Magarik, Numerical solutions to the problem of distribution of semidiumal tides M2 and S2 in the world ocean (transl.), *Dokl. Akad. Nauk SSSR, 172*, 1315–1317, 1967.

Cartwright, D.E., A unified analysis of tides and surges round north and east Britain, *Phil. Trans. Roy. Soc. London, Ser. A, 263*, 1–55, 1968.

Cartwright, D.E., Extraordinary tidal currents near St. Kilda, *Nature, 223*, 928–932, 1969.

Cartwright, D.E., Tides and waves in the vicinity of St. Helena, *Phil. Trans. Roy. Soc. London, Ser. A, 270*, 603–649, 1971.

Cox, C.S., Internal waves, *The Sea*, chap. 22, part 2, vol. 1, edited by Hill, Interscience, New York, 1962.

Cox, C.S., Energy in semidiurnal internal waves, Proc. Symp. Math-Hydro Investig. Phys. Process. Sea, *Mitt. Inst. Meereskunde der Univ. Hamburg*, 69–77, 1968.

Cox, C.S., and H. Sandstrom, Coupling of internal and surface waves in water of variable depth, *J. Oceanogr. Soc. Japan*, 30th Anniv. Vol., 499–513, 1962.

Defant, A., On the origin of internal tide waves in the open sea, *J. Mar. Res., 9*(2), 111–119, 1950.

Dietrich, G., Die Schwingungssysteme der halb-und eintägigen Tiden in den Ozeanen, *Veröffentl. Inst. Meereskunde Univ. Berlin, A 41*, 7–68, 1944.

Doodsen, A.T., The harmonic development of the tide generating potential, *Proc. Roy. Soc. London, Ser. A, 100*, 305–329, 1921.

Farrell, W.E., Global calculations of tidal loading, *Nature, 238*, 43, 1972*a*.

Farrell, W.E., Deformation of the earth by surface loads, *Rev. Geophys., 10*(3), 761–797, 1972*b*.

Farrell, W.E., Earth tides, ocean tides, and tidal loading, Royal Society Discussion Meeting, London, May 11, 1972*c*.

Fofonoff, N.P., and F. Webster, Current

measurements in the western Atlantic, *Phil. Trans. Roy. Soc. London, Ser. A, 270*, 423–436, 1971.

Garrett, C.J.R., Tidal resonance in the Bay of Fundy and Gulf of Maine, *Nature, 238*, 441–443, 1972.

Garrett, C.J.R., and W.H. Munk, The age of the tide and the *Q* of the oceans, *Deep Sea Res., 18*, 493–503, 1971.

Gohin, F., Etude des marees oceaniques a l'aide de modeles mathematiques, *Proc. Symp. Math-Hydrodyn. Meth. Phys. Ocean*, Hamburg, 179–198, 1961.

Gould, W.J., Spectral characteristics of some deep current records from the eastern North Atlantic, *Phil. Trans. Roy. Soc. London, Ser. A, 270*, 437–450, 1971.

Halpern, D., Semidiurnal internal tides in Massachusetts Bay, *J. Geophys. Res., 76*(27), 6573–6584, 1971.

Heiskanen, W., Über den Einfluss der Gezeiten auf die Säkuläre Acceleration des Mondes, *Ann. Acad. Sci. Fenn., Ser. A, 18*, 1–84, 1921.

Hendershott, M.C., The effects of solid earth deformation on global ocean tides, *Geophys. J. Roy. Astron. Soc., 29*, 389–403, 1972.

Hendershott, M.C., and W.H. Munk, Tides, *Ann. Rev. Fluid Mech., 2*, 205–224, 1970.

Hendershott, M.C., and A. Speranza, Co-oscillating tides in long, narrow bays, The Taylor problem revisited, *Deep Sea Res., 18*, 959–980, 1971.

Hollingsworth, A., The effect of ocean and earth tides on the semi-diurnal air tide, *J. Atmos. Sci., 28*, 1021–1044, 1971.

Irish, J., Australian-Antarctic tides, Ph.D. thesis, Univ. of Calif., San Diego, 1971.

Irish, J., W. Munk, and F. Snodgrass, M2 amphidrome in the northeast Pacific, *Geophys. Fluid Dyn., 2*, 355–360, 1971.

Jeffreys, H., Tidal friction in shallow seas, *Phil. Trans. Roy. Soc. London, Ser. A, 221*, 237–264, 1921.

Lafond, E.C., Internal waves, *The Sea*, chap. 22, part 1, vol. 1, edited by Hill, Interscience, New York, 1962.

Lee, W.H.K., and C.S. Cox, Time variation of ocean temperatures and its relation to internal waves and oceanic heat flow measurements, *J. Geophys. Res., 71(8)*, 2101–2111, 1966.

Longuet-Higgins, M.S., and G.S. Pond, The free oscillations of fluid on a hemisphere bounded by meridians of longitude, *Phil. Trans. Roy. Soc. London, Ser. A, 266*, 193–233, 1970.

Miles, J.W., Kelvin waves on oceanic boundaries, *J. Fluid Mech., 55*, 113–127, 1972.

Miller, G., The flux of tidal energy out of the deep oceans, *J. Geophys. Res., 71*(4), 2485–2489, 1966.

Munk, W.H., Once again–Tidal friction *Quart. J. Roy. Astron. Soc., 9*, 352–375, 1968.

Munk, W.H., and D. Cartwright, Tidal spectroscopy and prediction, *Phil. Trans. Roy. Soc. London, Ser. A, 259*, 533–581, 1966.

Munk, W.H., and G. MacDonald, *The Rotation of the Earth*, Cambridge University Press, Cambridge, Mass., 1960.

Munk, W.H., F. Snodgrass, and M. Wimbush, Tides off-shore: Transition from California coastal to deep-sea waters, *Geophys. Fluid Dyn., 1*, 161–235, 1970.

Pekeris, C.L., and Y. Accad, Solution of Laplace's equation for the M2 tide in the world oceans, *Phil. Trans. Roy. Soc. London, Ser. A, 265*, 413–436, 1969.

Platzman, G.W., Ocean tides and related waves, Lect. Appl. Math., *14*, American Mathematical Society, Providence, R.I., 1971.

Platzman, G.W., Two-dimensional free oscillations in natural basins, *J. Phys. Ocean., 2*, 117–138, 1972*a*.

Platzman, G.W., North Atlantic Ocean: Preliminary description of normal modes, *Science, 178*, 156–157, 1972*b*.

Radok, R., W. Munk, and J. Isaacs, A note on mid-ocean internal tides, *Deep Sea Res., 14*, 121–124, 1967.

Rattray, M., J. Dworski, and P. Kovala, Generation of long internal waves at the continental slope, *Deep Sea Res., 16*, supplement, 179–195, 1969.

Regal, R., and C. Wunsch, in preparation, 1972.

Reid, J.L., Observations of internal tides in October, 1950, *Eos Trans. Amer. Geophys. Union, 37*, 278–286, 1956.

Sandstrom, H., Effect of topography on propagation of waves in stratified fluids, *Deep Sea Res., 16*, 405–410, 1969.

Summers, H., and K. Emery, Internal waves of tidal period off southern California, *J. Geophys. Res., 68*(3), 827–839, 1963.

Tiron, K.D., Y. Sergeev, and A. Michurin, Tidal charts for the Pacific, Atlantic and Indian Oceans (transl.), *Vestn. Leningrad. Univ., 24*, 123–135, 1967.

Villain, C., Cartes des lignes cotidals dans les oceans, *Ann. Hydrog. (Paris), 3*, 269–388, 1952.

Webster, F. Observations of inertial period motions in the deep sea, *Rev. Geophys., 6*(4), 473–490, 1968.

Wunsch, C., The long-period tides, *Rev. Geophys., 5*(4), 447–475, 1967.

Wunsch, C., Bermuda sea level in relation to tides, weather, and baroclinic fluctuations, *Rev. Geophys., 10*(1), 1–49, 1972.

Wunsch, C., and J. Dahlen, Preliminary results of internal wave measurements in the main thermocline at Bermuda, *J. Geophys. Res., 75*(30), 5899–5908, 1970.

Wunsch, C., and R. Hendry, Array measurements of the bottom boundary layer and the internal wave field on the continental slope, *Geophys. Fluid Dyn.*, in press, 1972.

Zahel, W., Die reproduktion Gezeitenbedingter Bewegungsvorgänge in Weltozean mittels des hydrodynamisch–numerischen Verfahrens, *Mitt. Inst. Meereskunde der Univ. Hamburg, 17*, 1970.

Myrl C. Hendershott is with the Institute of Geophysics and Planetary Physics, University of California, LaJolla, California 92037. He received his B.S. in Physics from the University of Wyoming in 1958 and his M.S. and Ph.D. in Physics from Harvard University in 1963 and 1965, respectively. In 1965 he joined the faculty at the University of California, San Diego, as Assistant Professor of Oceanography.

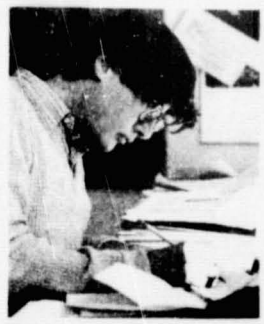

OMIT

AGU

Solid-Earth and Ocean Tides

REPORT ON THE FIRST GEOP RESEARCH CONFERENCE

The Geodesy/Solid-Earth and Ocean Physics (GEOP) Research Conferences were established to stimulate interdisciplinary research in the fields of geodesy, solid-earth and ocean physics within universities, research foundations, industrial and governmental organizations. This aim is to be achieved by an informal type of meeting consisting of invited speakers and a discussion panel supplemented by a small number of contributing speakers, when sufficient time is available, to stimulate discussion among the members. This type of meeting is thought to be a valuable means of disseminating information and ideas to an extent that could not be achieved through the usual channels of publication and presentation at scientific meetings.

Meetings are held at regular intervals (every three months) during a two-day period, generally at The Ohio State University. The morning of the first day is generally reserved for a tutorial lecture presented by an eminent scientist.

The primary purpose of the program is to bring an interdisciplinary group of experts up to date on the latest developments in a specific area, to analyze the significance of these developments, to provoke suggestions concerning the underlying theories and profitable methods of approach for scientific research, and to accelerate the development of new skills necessary for applying the newer technologies to an efficient attack on critical problems. The secondary purpose of the program is to interest and involve talented graduate students in the critical problems of geodesy/solid-earth and ocean physics. Further details on the purpose and administration of the conferences may be found in the April 1972 issue of EOS.

This report concerns the First GEOP Research Conference, which was attended by about 100 persons–60% invited and 40% observers. (The Second Conference on 'Earth Rotation and Polar Motion' will be held on February 8–9, 1973. See announcement on page 103 in this issue.)

The conference was opened by Hyman Orlin (NOS/NOAA) on behalf of the Steering Committee of the GEOP Research Conferences. President Harold L. Enarson welcomed the participants on behalf of The Ohio State University, followed by Myrl C. Hendershott (UCSD), who delivered the keynote address. He mentioned that the progress in the understanding of ocean tides since the field was reviewed two years ago (M.C. Hendershott and W.H. Munk, *Annual Review Fluid Mechanics, 2,* 205–224, 1970) has confirmed that the subject is rapidly developing. His review largely picked up where the other review left off; the two together are intended to provide a modern view of our state of understanding of tides. The keynote address in its entirety is printed on page 76 of this issue.

First Session

Panel on Perturbations: Earth Tides–Ocean Tides

Chairman: John T. Kuo (Columbia)

Members: G.H. Cabaniss (AFCRL), W.E. Farrell (CIRES), R.C. Jachens (Lamont-Doherty), A. Lambert (Dept. of Energy, Mines and Resources, Canada), G.W. Lennon (Institute of Coastal Oceanography and Tides, England), P. Melchior (Observatoire Royal de Belgique), and L.B. Slichter (UCLA).

In his introductory remarks Kuo pointed out that during the last decades great strides have been made in one of the classic areas of geodynamics, i.e., tides, both solid-earth and ocean. Many investigators now realize that neither the problem of solid-earth tides nor that of ocean tides can be solved independently. The conventional concept of applying ocean tidal corrections on solid-earth tidal measurements no longer holds its proper place, since ocean tides in the open oceans are either inferred or theoretically calculated and involve a considerable degree of uncertainty. Ocean tides in the open oceans calculated directly from Laplace's original tidal equations are no longer adequate without considering the elastic yielding of the earth due to the tidal and loading deformation. The interdependency of the problems of the solid-earth and ocean tides thus cast a new frontier in geodynamics. He continued a general review of the static and dynamic theory of solid-earth tides and the present status of experimental results obtained from worldwide gravity, tilt, and strain measurements.

In 1951 Takeuchi, showed that the equations for the deformation of the earth due to surface loads can be derived in a manner similar to that used in the theory of earth tides. Further theoretical work by Slichter, Caputo, and others has been directed toward the problem of determination of the deformation of the earth under the surface load of an arbitrary superficial mass distribution. Using the formulation for free oscillations of the earth given by Pekeris, Jarosch, and Alterman, Takeuchi and Longman calculated the loading deformation coefficients, h_n', k_n', l_n', which correspond to the tidal deformation coefficients of the earth, h_n, k_n, and l_n for the Gutenberg-Bullen earth model. Longman has provided by far the most complete numerical results for the problem of the surface deformation and the perturbation in the superficial gravity field of the Gutenberg-Bullen earth model subject to an idealized unit surface mass load. In the range of less than 30°, however, Longman was forced to resort to extrapolation for realistic values of his parameters in the continuous surface density distribution. Farrell has now extended the work of Longman. In discussing 'Tidal Loading on a Spherical Earth,' Farrell noted that he succeeded in overcoming the problems of convergence for the earth's loading deformation close to a concentrated unit load (including the angular distance of less than 30°). He used the Green-function for a disc-shaped load, taking the limit to allow the vanishing of disc radius. The unit mass distributed uniformly across the disc was expanded in a Legendre series, which in turn was transformed through Krummer and Euler's transformation to speed up the 'convergence.' His formulation alleviates a great deal of difficulty in calculating global ocean-tidal corrections. The value calculated for n was as large as 10,000, compared with that of 40 calculated by Longman and that of 200 calculated by Pertsev of the USSR for determining the global M_2 ocean-tidal corrections.

Lennon, in his discussion on the 'Regional Perturbations of Earth Tides,' pointed out that present experimental results show anomalous perturbations amounting to ±40% in north-south tilt, ±15% in east-west tilt, and ±8% in gravity. A study of the currently used instrumentation fails to provide an explanation and suggests that ±4% should be achieved with little effort and ±1% achieved with care. The systematic differential performance of

This report was prepared by J.C. Harrison, Myrl C. Hendershott, John T. Kuo, Ivan I. Mueller, and Bernard D. Zetler. Material contained herein should not be cited.

north-south and east-west tiltmeters is interesting. This, together with the magnitude of the above anomalies, suggests that local geology, combined with installation difficulties (particularly the use of mines and other underground vaults that represent discontinuities in the earth's crust), must have a greater influence than has previously been realized. Lennon recommended controlled experiments for the examination of the coherency of the solid-tidal signal on a variety of scales and the interaction of theoretical models and experimental exercises in the study of the effects of close-range marine tides in an attempt to understand near-range structure.

One of the major contributions in surface tilt measurements should be accredited to the achievements of 'Borehole Measurements' reported by Cabaniss. Since the birth of the Askania-Graf borehole tiltmeter, I. Simon has developed the Arthur D. Little borehole tiltmeter, a new instrument to investigate crustal tilt from the surface. Cabaniss reported that 85 days of tidal data, taken in 1972 and digitized to a precision of about 5%, were obtained from a biaxial borehole tiltmeter cluster of three in Bedford, Massachusetts. The instruments were installed in water-filled, uncased holes, 20 meters deep (the Askania borehole tiltmeter must be installed in a cased hole if the water table is higher than the depth of the hole). The data, with gaps ranging from 1% to 10%, were analyzed for the M_2 tidal constituent by the least squares method. Depending upon the interval chosen, the observed amplitudes varied by as much as 10% among instruments because of uncertainties in calibration; the observed phases varied by a maximum of 3°. With Green's functions (derived by R.K. McConnell, Jr.) for a multilayered half-space earth model and Tiron's tidal charts computed to a distance of about 1000 km, plus the assumption that the coastal tidal amplitude distribution is equal to one-half the mean tidal range for given coastal stations, the computed load for the east-west component contributed about 60% of the total amplitude. The sum of the computed body tide and load tide agrees with the observed to better than 10%, and the phase difference is reduced from 12° to about 5°

Lambert mentioned that, as Lennon had already pointed out, the interpretation of tidal tilt observations due to ocean loading is still a very difficult problem. However, if we take the perturbation of ocean tides alone on the earth tide, we can take advantage of the tilt Green's function for an average continental and an average oceanic structure overlying a Gutenberg-Bullen nucleus as developed by Farrell to calculate the load tilt. The beauty is that we may adopt any arbitrary crust and upper-mantle structure in the top 200 km by recomputing the near field tilt Green's function. Regional Green's functions can then be convolved with the cotidal charts for ocean tides by using Bower's (unpublished) polygon technique. Regional Green's functions can be obtained, for instance, by

1. Farrell's approach, when one can recompute the higher order Love numbers by numerical integration of the equations of motion for a layered, spherical earth.

2. Kuo's Thompson-Haskell matrix approach, when one can compute a point load response of a layered, either nongravitating or gravitating, half-space.

3. Finite elements technique as done by Jachens, Beaumont, and Lambert, when one can compute a point-load response of regional nongravitating structures; if necessary, these structures can be laterally inhomogeneous.

Despite the observational uncertainties that concerned Lennon, Lambert felt that useful results may emerge from tilt observations in areas where the ocean-tide loading is large. In Nova Scotia tilt measurements of the M_2 tidal constituent were taken at Rawdon near the Bay of Fundy. Beaumont and Lambert found that the observed tilts appear to agree with the loading of a laterally homogeneous elastic model consistent with the previous seismic refraction results for the area.

It is now realized that the greatest uncertainty in tidal loading corrections, even where local loads are large and well known, arises from the incomplete knowledge of the ocean tides both on the continental shelf and in the open ocean.

Jachens noted that the problem of the influence of geological structure on the earth tide remains a challenge. As far as it is known from theoretical and experimental results, the influence of regional geological differences on earth tides is very small. Experimentally, such a small influence is probably masked by experimental uncertainties, local site effects and residual ocean-tidal effects after applying ocean tidal correction with the poor ocean-tidal information. By carefully examining the results of the spatial variations of the O_1 earth-tidal constituent along the Lamont-Doherty's trans-U.S. tidal gravity profile, he found that after correcting for a small ocean tidal perturbation on the constituent, the O_1 tidal gravity residuals displayed no strong systematic anomalies in excess of the experimental uncertainties of about 1.5% in amplitude and of 1° in phase from the eastern coast, through the interior plains, Rocky Mountains, Sierra Nevada, to the west coast. However, there is a slight systematic phase residual of about 0.5° lead found at stations in the Rocky Mountains and the Basin and Range Province and a slight positive gravimetric factor residual found near the extreme western end of the profile. These features are again possibly a result of inaccurate ocean-tidal corrections.

Slichter reported that, under very severe physical conditions, the UCLA group made gravity-tide observations at the south pole and provided a precise value for the gravimetric factor for the fortnightly tide, 1.149 ±0.004. Correction for equilibrium ocean tides would increase this number by 0.6%. Slichter also reported that these observations show that the time lag in the measured tide is small, possibly between 0.00 and 0.34 hours; if so, he estimated that the associated Q value of the earth at that tidal period would be greater than 20, compared with the Q value obtained from the 54-minute free oscillation of the earth about 200–300.

One of the important contributions made by Melchior was to relate the diurnal earth tides to the precession-nutation of the earth in the astronomical frame of reference. Melchior showed astonishing results of the agreement of the diurnal tilts throughout the world with the Molodensky's Model I, which takes into account the dynamic effect of the liquid core of the earth on earth tides, resulting in a diurnal-free nutation of the earth with a period close to a day. Because the K_1 constituent has a frequency close to the frequency of the diurnal-free nutation with a period of about 3 minutes longer than the diurnal-free period of Molodensky's Earth Model I, the K_1 constituent is greatly affected by this resonance. His results are given below.

The first session also included the following contributed papers: 'Tidal Frequency Strain Coherent with Gravity, Air Pressure and Air Temperature,' J.E. Fix (Teledyne Geotech); 'Spectrum and Phase of the Tidal Gravity Measurements at the South Pole,' B.V. Jackson (UCLA); and 'A Reconnaissance of Tidal Gravity in Southeastern United States,' E.S. Robinson (Virginia Polytechnic).

In summarizing the session Kuo concluded that one of the important implications from the foregoing 'give and take' experience seemed to be that unless the problem of ocean tides is solved, further progress on the study of solid-earth tides is rather limited. In solving ocean tides in the open oceans, both theoretical and experimental studies must go hand in hand. The celebrated achievement of numerical integration of Laplace's tidal equations must be ushered into the stage of modifying them to include better friction (Pekeris and Accad use a linear law, while Zahel uses a square law), dissipation (both in deep oceans and shallow waters), and the tidal and loading deformation of the solid earth. Eventually the theory of solid-earth and ocean tides must be treated under a unified system to take into account the damping as well as the lateral inhomogeneity of the earth as a whole.

Observed Tilt	P_1	O_1	K_1
E–W	0.717 ± 0.018	0.674 ± 0.005	0.749 ± 0.005
Molodensky's Earth Model I	0.699	0.688	0.734

Second Session

Panel on Instrumentation, Data Acquisition and Analysis: Marine Tides

Chairman: J.C. Harrison (CIRES)

Members: C. Elachi (JPL), J.H. Filloux (Scripps), A.A. Loomis (JPL), A.A. Nowroozi (Lamont-Doherty), F.E. Snodgrass (UCSD), R.L. Snyder (Nova Univ.), M. Wimbush (Nova Univ.), and B.D. Zetler (UCSD).

In his general review, Snodgrass briefly described the deep sea instrument vehicle and stated that the technology for such devices is adequate for the measurement of diurnal and semidiurnal tides. Advances in solid-state electronics permit the use of elaborate electronic recording systems. Other equipment such as magnetic tape recorders and acoustical recall systems are commercially available. Water velocity sensors continue to present the most serious problems. Pressure and temperature sensors appear to be adequate since the instrumental noise spectra lie well below the sea level noise and the sea-floor temperature spectra, respectively.

Filloux described his design of a sensitive optical lever that he incorporated with a Bourden tube pressure sensor into a free-fall deep-sea tide gauge that has a low temperature dependence. The creep in the six-day record he obtained off the California coast was removed, based on the physics of Andrade's law for a time-dependent plastic strain. He displayed results obtained with his gauges in intensive studies off the Bahamas and later in the Gulf of California. He proposed that a digital readout be included in future versions of the gauge and estimated that the cost could be $7000 or less if produced in large quantities. When asked why he estimated a shallow water gauge to be much cheaper when, in fact, the large temperature changes and waves require more sophistication, he replied that the cost was higher because of the much greater pressure and the need for recovery mechanisms, but he welcomed the suggestion that temperature correction as well as wave filtering are difficult problems usually overlooked.

Nowroozi described results from a gravimeter, a pressure sensor, and a current meter obtained over a period of 6½ years in deep water off the California coast. The equipment was part of a much larger sensor package connected by cable to the shore. The currents were separated into north and east components for separate analysis, and current ellipses were computed from the processed data. The gravimeter records were corrected for the 'slab' of water due to the ocean tide. Spectra were shown for the gravity and pressure records. Tidal constants of the M_2 constituent were compared with eight different cotidal charts for the vicinity of the station and the chart of Tiron and others is in close agreement with the observations, although proof of existence of their alleged amphidromic point requires more pelagic measurements.

Zetler presented a historical review of ocean-tide data analysis, starting with the conventional Coast and Geodetic Survey and Doodson methods designed for use with desk computers. The advent of large electronic computers led Horn to prepare a combined least squares solution for all required constituents; the inversion of the normal equation matrix would have been impossible previously. The least squares solution does not require equal spacing of data, inference of breaks in records, or particular lengths of record (the latter were selected classically to minimize sidebands from nearby frequencies). The Munk-Cartwright response method was described. It uses, as input, time series for the gravitational and radiational potentials as well as complex combinations of these to describe nonlinear tides. It also minimizes the residuals in the least squares sense, using a constraint that the response for any input series is smooth across narrow frequency bands, such as diurnal and semidiurnal tides. It is a complete break with previous analysis procedures that specify a finite set of tidal frequencies. Other procedures mentioned were: (1) Slichter's use of a cross-spectrum analysis of observed data with a time series derived from the gravitational potential to get amplitude from energy calculations and phase lags from the phase of maximum coherence; (2) Filloux's use of a Taylor expansion of the tidal admittances to calculate the harmonic constants; (3) Franco's use of fast Fourier transform coefficients in a narrow tidal band to calculate normal equations leading to harmonic constants for a required set of tidal frequencies; and (4) Myazaki's decimated sampling rate and subsequent analysis for the aliased frequencies of the principal tidal constituents.

Elachi discussed coherent radar techniques and accuracy possibilities in measuring sea level from satellites. He showed that by small changes in frequency the resultant changes in the increment over an integral number of cycles could be used to produce accuracies up to 10 cm, with relative errors even less, for describing sea-surface slopes from a single orbit. He discussed the possible errors due to the ionosphere (reduced by the changes in frequency) and due to the lack of a good model for the atmosphere. A radiometer would be used to permit corrections for water vapor.

Comments were made on the Canadian shallow water gauge, super resolution of tidal lines (separating two frequencies in less than a synodic period), the need for nonharmonic solutions in extreme shallow water areas (such as the St. Lawrence River), the need for numerical models to allow for meteorological factors, the effect of barometric changes on a bottom-sitting pressure gauge, the number and areas of pelagic observations to date, the GEOS-C altimeter, the possibility of satellite observations replacing pelagic measurements (the feeling being that each should complement the other), and an appeal for support of a satellite oceanographic program designed to include tide observations.

The session also included the following contributed papers:

'High [illegible]sion Analysis of Tides,' A.K. Paul (Ei[illegible]OAA). The author described his method (Anharmonic frequency analysis, *Mathematics of Computation, 26*, 437–447, April 1972) for locating unidentified frequencies in time series of data. The accuracy depends on the noise level and was quite good for San Francisco tides.

'A Long-Term Deep Sea Tide Gauge,' J.B. Matthews (Univ. Alaska). The author described the characteristics of his new underwater tide gauge, really an underwater multisensor. He called for an exchange of information on tide gauge development.

'Tidal Studies by Means of the GEOS-C Satellite,' J.W. Siry (GSFC/NASA). The author described the pulse altimeter planned for the GEOS-C satellite, scheduled for 1974, and a proposed tidal experiment that could be conducted in the western North Atlantic. The height uncertainty in orbit is 2 to 3 meters under favorable circumstances. Satellite observations by lasers are now estimated to be accurate to one-half meter, and this measurement will be reduced in the coming years to about 10 cm or better. It was suggested from the floor that consideration should also be given to the areas of antiamphidromes proposed at the 1971 meeting of Working Group No. 27 on 'Tides of the Open Sea.'

Third Session

Panel on Instrumentation, Data Acquisition and Analysis: Earth Tides

Chairman: J.C. Harrison (CIRES)

Members: J. Berger (UCSD), W.E. Farrell (CIRES), R.A. Haubrich (UCSD), J.T. Kuo (Columbia), and L.B. Slichter (UCLA).

Harrison opened the session by commenting that the timing of the conference was very appropriate because important advances were taking place in the field of earth tides, both in theory and instrumentation. On the theoretical side, it is now possible to calculate the effects of ocean loads within our knowledge of these loads; on the instrumental side important advances are taking place in gravimetry with the development of the cryogenic gravity meter, in strain measurement with the advent of laser strain meters, and in tilt instrumentation. It now appears that much of the variability in the parameters of the gravity tide can be explained by ocean loads. In tilt and strain, however, this did not appear to be the case, and it is important to understand the source of this variability.

Modern tidal gravimetry began about 1956 with the development by Clarkson and LaCoste of servoed instruments that have the advantages of avoiding spring hysteresis and using the calibrated measuring screw to measure gravity. The development of capacitative beam-position sensors

using phase locked amplifiers with electrostatic feedback was an important advance and allowed conversion of old prospective instruments into excellent tidal meters. Tidal instruments that measure beam deflection require constant calibration because their sensitivity depends on leveling and because they suffer from phase lags due to spring hysteresis. All spring-type instruments drift, but the cryogenic gravity meter promises to eliminate this problem.

The servoed level bubble tiltmeter developed by the Hughes Research Laboratories was described. This instrument promises exceptional long-term stability and stability of calibration. Tests and calibration have been performed on a tilt table capable of 1 nanoradian resolution. Two instruments of this type are operating alongside each other in the Poorman Mine near Boulder, and the agreement between them is very encouraging.

Berger, in discussing strain instrumentation, said that three types of instruments had been used to measure strain: (1) invar wires, the earliest length standard used for this purpose, were now being employed by King in England and others; (2) Quartz tube instruments developed by Benioff have been improved by Major and used quite extensively in the U.S.; and (3) Laser instruments have the advantage of being extremely stable, having negligible nonlinearities, large dynamic range, wide band frequency range and absolute calibration. Length changes are measured in wavelengths of light from stabilized lasers and the distance between the end piers can be measured by standard survey techniques within an accuracy of about 1 in 10^5, meaning that calibration is known to this accuracy. Two types of installation are in operation: surface mounted instruments in California that employ 800-meter Michelson interferometers and a 30-meter instrument in the Poorman Mine in Colorado.

The strain tides observed in California differ significantly from the oceanless, elastic earth mode. Ocean-load corrections have been made by using the well-known ocean tides off California and Green's functions computed by Farrell for several earth models. The corrections are of the right order of magnitude to account for the discrepancy, but their phases in some cases are incorrect. Thus, it seems that some additional input must be sought to explain the differences between computed and observed tides.

Haubrich said that analysis of earth tides is generally similar to that of ocean tides as already reviewed by Zetler. The response $L(f)$ of a linear system is output $Y(f)$ at frequency f divided by input $X(f)$. The difficulties result from having to determine $L(f)$ from a finite noisy time record. The digital Fourier transform may be used; it is essentially a least squares fit to the frequencies j/N, $j = 0, 1, \ldots N/2$. Unfortunately, the tidal frequencies do not correspond to the frequencies j/N and we must either make side band corrections or apply the same transform to the input function—to do either of these rigorously requires knowing $L(f)$. The response method of Munk and Cartwright eliminates the above problems.

Horn's method of least squares fit to frequencies avoids these complexities but requires choice of a frequency set.

The response method is a least squares fit in the time domain. It should be successful with earth tides because the earth's response should be even smoother than that of the ocean. The fits are made to time series representing the contributions to the theoretical tide from the individual spherical harmonic terms (in earth-fixed coordinates) and to these terms lagged in time. Additional series representing the radiational function, ambient temperature, and pressure variation, together with corresponding lagged series, may also be included.

There was some discussion of gravity meter calibration. J.A. Hammond (AFCRL) suggested that an improved version of the Faller-Hammond free-fall absolute gravity apparatus be used for tidal meter calibration. L.E. Johnson (CIRES) reported on the calibration of a LaCoste prospection meter converted to a feedback tidal instrument. Calibration was accomplished by tilting and by moving between floors of a building on which gravity had been measured with a calibrated geodetic instrument. The two results agreed to 0.4%. There was discussion of proposed calibration of the cryogenic meter by moving lead masses beneath it.

J.H. Suh (Colorado School of Mines), reported briefly on the quartz strain meters of the Colorado School of Mines. The school is now operating 15 strain meters in the Denver area. The tidal strain study for these strain meters is in progress.

Contributed papers in this session included the following:

'The Superconducting Gravimeter,' Richard Warburton (UCSD). Data obtained by using a superconducting gravimeter for the period of June 6 to August 29, 1972, were presented. The data clearly demonstrate the high signal to noise ratios and the long-term stability of such an instrument. Signal to noise ratios of 75 to 80 db for the diurnal and semidiurnal tides, 40 db for the terdiurnal tides, and 30 db for the fortnightly and monthly tides were obtained. A strong correlation between gravity and daily barometric pressure was observed in which 0.1-inch decrease in pressure resulted in a 2.3 μ-gal increase in gravity. This is mainly the result of variations in the direct gravitational attraction between the atmosphere and gravimeter and is not an instrumental effect.

'Observation of Earth Tides Using a 30-m Laser Strainmeter,' J. Levine (NBS). The author reported that they installed a 30-meter laser strainmeter in the Poorman Mine near Boulder, Colorado. The instrument has excellent stability and shows a drift of less than 5×10^{-9} $\Delta L/L$ day. They used the instrument in an investigation of the strain tides and found that the measured strain is significantly smaller than what would be predicted from a theory which neglects ocean loading. They have determined the transfer function of the earth by using least squares techniques and found that the magnitude of the transfer function is 0.78 and that the phase error is a 5° lead for the semidiurnal components and a 2.5° lead for the diurnal components. The residuals of the least squares technique have a peak-to-peak amplitude of the order of 10^{-9} $\Delta L/L$, which is on the order of 5% of the tidal amplitude.

'Methods for Prediction and Evaluation of Tidal Tilt Data from Borehole and Observatory Sites Near Active Faults,' M.D. Wood (USGS). The author reported that tilt has been measured to 10^{-8} radian for up to three years at three locations in the San Francisco Bay region in California. These measurements are part of strain measurement and microearthquake program that has the objective of studying the mechanics of the earthquake generation process. The tilt measurements within this network, conducted for approximately 1000 hours around the occurrence times of the largest earthquakes of 1970–1972, have shown residual tidal-free difference anomaly between two stations accumulating to about 8×10^{-7} radian for events $4.3 < M < 5.0$ of distances $25 < d < 150$ km. Finite element modeling of the response of a tilt station near the fault suggests the possibility of using the ocean as a forcing function for monitoring the dynamic time variations of the (μ) of the fault for secular fault behavior.

Fourth Session

Panel on Deep Sea and Coastal Tides

Chairmen: M.C. Hendershott (UCSD) and C.I. Wunsch (MIT)

Members: W.E. Farrell (CIRES), C. Garrett (Dalhousie Univ.), N. Grijalva (CIC, Mexico), H. Mofjeld (AOML/NOAA), R. Montgomery (Johns Hopkins), G.W. Platzman (Univ. Chicago), W. Sturges (Florida State Univ.), and B. Zetler (UCSD).

The tenor of the discussion was strongly influenced by the earlier presentation of latest results in solid-earth tides, where further development simultaneously offers ocean tide studies the prospect of remarkably refined observations of ocean effects while demanding from ocean tide studies a degree of precision that is now beyond the reach of the most detailed global models. Indeed, most models of ocean tides fail entirely to take into account solid-earth tides. A formalism for remedying this defect was discussed by Hendershott; Laplace's tidal equations are extended to an integro-differential form using Farrell's gravity and vertical displacement surface load Green's functions for a radially stratified earth. Preliminary results were presented. Although no complete solutions including all of the effects of solid-earth yielding are yet available, the importance of these effects for ocean tide models that aspire to better than qualitative accuracy was evident. Kuo briefly reported a some-

what similar correction for solid-earth yielding of a solution by Pekeris with encouraging results.

From the point of view of ocean tides, the logical conclusion of the present efforts by solid-earth tidalists to study ocean tide effects is solution of an inverse problem for ocean tides using observations of gravity, solid-earth tilt and strain tides as the data. This solution would provide the ocean tidalists with weighted areal means of ocean tide elevations (relative to the deformed earth). Inasmuch as such averages would be entirely free of the shallow water distortion that makes coastal and even many island tide gauge observations differ significantly from the tide of the adjoining deep sea, they would be ideal tests of ocean tide models.

Oceanographers have long known of specific examples of the strong distortion of coastal tides relative to those of the deep sea by an intervening shelf, but no reliable predictive parameterization of the effect exists. Mofjeld reported the preliminary results of field work (three tide gauges in a traverse to deep water across the continental shelf of the southeastern United States) aimed at shedding light on this problem. Measurements in a similar spirit are also being conducted around the British Isles and off Antarctica; carefully located earth tide measurements along the coast might ultimately provide useful supplemental material in such studies. J. Larsen (NOAA, Honolulu) noted the presence of significant distortion of Hawaiian tides by the narrow but steep island arc. Island phases probably differ from those of the deep sea by several tens of degrees, but the persistence of the island distortion into the northeastern Pacific is unknown. Here again is a case in which the interpretation of a transect of tide gauge observations normal to the axis of the island arc could be very usefully supplemented by even a single set of earth tide measurements on one of the islands. Such 'local' collaboration between earth and ocean tidalists seems likely to be fruitful in the near future.

The mechanism of tidal dissipation in the oceans is at once one of the principal goals and one of the principal difficulties of ocean tidal models. Turbulent dissipation over continental shelves and in marginal seas is known to be a major mechanism, if not the dominant one, and the interpretation by Mofjeld of his observations consequently involved a model in which the role of dissipation and its variation across the shelf are important factors. But there is another potential dissipation mechanism that is, even in principle, poorly understood; conversion of barotropic tidal energy to turbulence by baroclinic tides.

New data on baroclinic tides was presented by Wunsch. For the first time, a baroclinic tide signal having phase coherence with the barotropic tide was identified. The observations were made at Woods Hole Oceanographic Institution's Site *D*, with moored current meters; the coherent signal was, surprisingly, detectable only in the upper layers. This is presumably a focusing effect, concentrating energy generated at the shelf slope near the surface further seaward. A subsequent array of current meter moorings on the continental slope south of Nantucket shoals showed a concentration of tidal kinetic energy just above the bottom boundary layer, in agreement with theoretical prediction. Over 90% of the tidal energy appeared as very short wavelength baroclinic tides. Extrapolated to the entire length of the world's continental shelves, the estimated internal wave energy flux could account for as much as half of the astronomically determined total tidal dissipation. In a related discussion, C.N.K. Mooers (Univ. Miami) suggested that the observed low frequency modulation of baroclinic tidal seiches in the Florida straits might provide a sensitive measure fluctuation of the Florida current. Also, since the straits are nearly spatially resonant for baroclinic tides, i.e., cross-stream seiche conditions are nearly satisfied, the conversion of barotropic to baroclinic tidal energy may be particularly efficient there.

It is also possible to approach the problem of dissipation in a more indirect manner. The amount of information about the frequency response and damping of ocean tides to be learned by comparison of ocean response relative to driving forces (tidal admittances) was illustrated by Garrett in a study of tides in the Bay of Fundy.

The response of the bay at three semidiurnal frequencies (M_2, S_2, N_2), taking into account the effect of nonlinear friction, suggests that the resonant period is about 13½ hours, with a Q of about 5 for the present M_2. Moreover, the resonant system encompasses all of the Gulf of Maine and is not confined to the Bay of Fundy. All this suggests that construction of dams for tidal power generation might bring the resonant period closer to the semidiurnal one and increase tidal ranges slightly over the whole Gulf of Maine.

R.M. Gallet (ERL/NOAA) reported on an application of this response method to the deep-sea tides measurements obtained in the Northeast Pacific Ocean basin by Jean Filloux. A resonance period of 18.3 hours is well determined using the admittances at *eight* frequencies, four diurnal (Q_1, O_1, P_1, K_1) and four semidiurnal (N_2, M_2, S_2, K_2). This result can be obtained using only the diurnal components; but it is stable and remains essentially unaltered if one combines all the eight frequencies in one and the same resonance curve. There was general agreement about the basic utility of the approach, but the extent to which diurnal and semidiurnal admittances could be combined to make a single estimate of the admittance-frequency curve was debated.

Closely related to these discussions was Platzman's application to the North Atlantic Ocean of his previously published general method for the determination of free modes of ocean oscillation. He had found three modes having one, two, and three amphidromes with periods of 21.2, 14.0, and 11.5 hours, respectively. These results are the first of their kind for an ocean basin of global size and of realistic shape and relief; the near coincidence of the second free period with that recently suggested by Wunsch on the basis of an analysis of tidal admittance at Bermuda and the Azores is striking.

Increases in sensitivity and stability of solid-earth tide measurements are beginning to make long-period tides accessible to earth tidalists, and it was therefore quite appropriate that a portion of the discussion was devoted to the properties of long-period ocean tides. Conflicting results of geodetic and oceanographic 'leveling' were discussed by Montgomery and by Sturges. Land-based surveys suggest that mean sea level rises toward the north by over 50 cm in 20° of latitude on either side of the continental United States. This result is in conflict with steric level determination of ocean surface slope as derived from the measured field of ocean density, which suggests that sea level falls from south to north. The origin of the discrepancy is not understood. Larsen discussed the application of electromagnetic methods to measurement of ocean currents, especially tidal currents. His method is especially well suited for the study of long-period tides because it responds to horizontal flow rather than to surface elevation, which is relatively small in long-period tides.

Some discussion of tidal models had been anticipated, but Grijalva was prevented by illness from discussing details of his numerical studies of tides in the Gulf of California and elsewhere. J.B. Matthews (Univ. Alaska) noted briefly that Mungall (Ph.D. Thesis, Univ. Alaska, Sept. 1972) had been successful in constructing a variable mesh predictive numerical model for Cook Inlet, Alaska, and the Irish Sea.

Throughout the session, the question of an optimal set of observations for the development of global ocean tidal models was raised repeatedly. The most recent discussion of this question from the oceanic point of view had been made by the IAPSO/SCOR/Unesco Working Group No. 27. Developments in earth tide measurements and theory now offer new prospects for such a program and for the resolution of the ocean tide problem.

Second Geodesy/Solid-Earth and Ocean Physics (GEOP) Research Conference

The Rotation of the Earth and Polar Motion

Keynote Speaker: M.G. Rochester, Memorial University of Newfoundland

FAWCETT CENTER FOR TOMORROW
THE OHIO STATE UNIVERSITY
COLUMBUS, OHIO

FEBRUARY 8–9, 1973

Sponsored by: **American Geophysical Union**
National Aeronautics and Space Administration
National Oceanic and Atmospheric Administration
Ohio State University, Department of Geodetic Science
U.S. Geological Survey

The theme for the Second GEOP Research Conference will be set by an introductory review relating to the earth's rotation. The conference will be divided into the following sub-topics, each introduced by an invited moderator and discussed by a panel:

1. Observations and Coordinate Systems; Chairman: William Markowitz, Nova University
2. Meteorological and Seismic Effects; Chairman: Kurt Lambeck, Paris Observatory
3. Core-Mantle Interactions; Chairman: D.E. Smylie, York University
4. Long-Term Variations; Chairman: W.M. Kaula, UCLA

Individuals interested in attending the conference are requested to send their applications on the standard application form available from the American Geophysical Union, 1707 L Street, N.W., Washington, D.C. 20036. Information on the membership in the GEOP Research Conferences may be found on page 305 of the April 1972 issue of EOS.

Further details on the program, accommodations, and registration will be sent to those applicants selected by the committee to attend the conference by December 15.

Applications for attendance must be received by December 8, 1972

American Geophysical Union ★ 1707 L Street, N.W. ★ Washington, D.C. 20036

D2

N76-20568

The Earth's Rotation

M. G. Rochester

The most ancient and fundamental concern of astronomy is the orientation and motion of a terrestrial observer relative to the stars. Its geophysical aspects date from the time of Newton and Halley, and its mathematical foundations were laid by Euler 200 years ago. Despite this honorable antiquity, the subject is far from moribund and today presents a rich and fascinating array of challenges to observation, experiment, data analysis, and theory. The many-faceted problems of the three-dimensional rotation of the earth about its center of mass now attract astronomers and paleontologists, solid earth geophysicists and electrical engineers, general relativists and oceanographers, and applied mathematicians and scholars of classical texts.

In this review I attempt to summarize, as briefly as possible, the current state of knowledge in a field that is complex, extensive, and resurgent under the impact of late 20th century technology. I shall begin with a survey of the appropriate reference frames and problems involved in defining them and then outline the accuracy with which the earth's rotation can be measured relative to these frames by techniques already in use or on the threshold of realization. Following that, I shall discuss in turn the various spectral features of changes in the axis orientation and spin rate of the so-called 'solid' earth (Table 1) and the physical mechanisms known or likely to effect and affect them (Table 2). Copious references are given for deeper study. I shall concentrate almost exclusively on developments in the past decade or so since the appearance of the now-classic monograph by *Munk and MacDonald* [1960], the standard reference for most aspects of the subject.

This article was taken from the keynote address presented at the second GEOP Research Conference on The Rotation of the Earth and Polar Motion, which was held at The Ohio State University, Columbus, February 8–9, 1973.

Reference Frames

The earth is not a rigid body, and so the selection of a reference frame suitable for describing its rotation is not a completely straightforward matter. Strictly speaking, the phrase 'rotation of the earth' is shorthand for the rotation in space of a certain reference frame fixed in some prescribed way to a set of astronomical observatories distributed over the earth's crust. The difficulty of defining a reference frame is increased by the fact that the observatories are located on different crustal 'plates' that are in relative motion [*Vicente*, 1968; *Markowitz*, 1970; *Arur and Mueller*, 1971; *Tanner*, 1972]. The current choice of astronomers and geodesists is a 'geographic' frame whose origin lies at the earth's center of mass, whose z axis points to the Conventional International Origin (CIO)—corresponding very nearly to the mean position of the rotation pole from 1900 to 1905 determined by the International Latitude Service (ILS)—and whose x axis points at right angles to this in the plane of the Greenwich meridian as determined by the Bureau Internationale de l'Heure (BIH) in Paris. At the y axis the astronomers and geophysicists part company, the former choosing a left-handed set and heading 90°W of Greenwich and the latter going 90°E (Figure 1).

Polar motion, which may be either irregular or periodic (in which case it is called 'wobble'), is the displacement of the instantaneous rotation axis relative to this frame, on a small scale ($a \leq 0''.3$, $|x|, |y| \leq 10$ meters). The term 'polar wander' is reserved for the large departure of the rotation pole from its mean position at any one epoch, achieved only on the geologic time scale. Polar motion has been measured for over 70 years by the ILS and its successor, the International Polar Motion Ser-

TABLE 1. Spectrum of Changes in Earth's Rotation

A. Inertial Orientation of Spin Axis	B. Terrestrial Orientation of Spin Axis (Polar Motion)	C. Instantaneous Spin Rate ω about Axis
1. Steady precession: amplitude 23°.5; period ≃25,700 years.	1. Secular motion of pole: irregular, ≃0″.2 in 70 years.	1. Secular acceleration: $\dot{\omega}/\omega \simeq -5 \times 10^{-10}$/yr.
2. Principal nutation: amplitude 9″.20 (obliquity); period 18.6 years.	2. 'Markowitz' wobble: amplitude ≃0″.02(?); period 24–40 years(?).	2. Irregular changes: (*a*) over centuries, $\dot{\omega}/\omega \leqslant \pm 5 \times 10^{-10}$/yr; (*b*) over 1–10 years, $\dot{\omega}/\omega \leqslant \pm 80 \times 10^{-10}$/yr; (*c*) over a few weeks or months ('abrupt'), $\dot{\omega}/\omega \leqslant \pm 500 \times 10^{-10}$/yr.
3. Other periodic contributions to nutation in obliquity and longitude: amplitudes <1″; periods 9.3 years, annual, semiannual, and fortnightly.	3. Chandler wobble: amplitude (variable) ≃0″.15; period 425–440 days; damping time 10–70 years(?).	3. Short-period variations: (*a*) biennial, amplitude ≃9 msec; (*b*) annual, amplitude ≃20–25 msec; (*c*) semiannual, amplitude ≃9 msec; (*d*) monthly and fortnightly, amplitudes ≃1 msec.
4. Discrepancy in secular decrease in obliquity: 0″.1/century(?).	4. Seasonal wobbles: annual, amplitude ≃0″.09; semiannual, amplitude ≃0″.01.	
	5. Monthly and fortnightly wobbles: (theoretical) amplitudes ≃0″.001.	
	6. Nearly diurnal free wobble: amplitude ⩽0″.02(?); period(s) within a few minutes of a sidereal day.	
	7. Oppolzer terms: amplitudes ≃0″.02; periods as for nutations.	

vice (IPMS). The five ILS observatories are spaced out along the same parallel of latitude (39°8′N), and thus the effects of any systematic errors in star catalogs are eliminated. Both the IPMS and the BIH publish determinations of the pole path about the CIO (Figure 2). The IPMS pole path is based on observations at the five ILS stations, whereas the BIH pole path currently incorporates data on latitude variation from some 50 stations, and thus the effects of star catalog errors are statistically reduced. The difference between the two pole paths, which can amount to ≃0″.1, is a measure of the effects of errors due to local motions of the vertical, plate motions, refraction, instrumental peculiarities, and systematic differences in data reduction techniques. It is worth noting that the individual observations scatter much more widely than the published curves suggest. The IPMS and BIH both claim errors of only ±0″.01 in their published 0.5-year and 5-day means. Certainly, this sets a limit to the precision of which the basic instruments of optical astronomy, the photographic zenith tube (PZT) and the astrolabe, are presently capable.

New techniques, such as Doppler tracking of artificial earth satellites [*Anderle*, 1972], which provides pole positions at 2-day intervals, have already achieved an accuracy comparable to that of the BIH [*Feissel et al.*, 1972]. In fact, the BIH recently began to include in its data set the observations made by the Dahlgren Polar Monitoring Service (DPMS). Laser ranging to artificial satellites offers even greater accuracy together with pole positions determined at more frequent time intervals. *Smith et al.* [1972] report a sequence of

TABLE 2. Mechanisms with Effects Now Distinguishable on the Earth's Rotation

Mechanism	Effect*
Sun	
Gravitational torque	A, B7, C1, C3*c*
Solar wind torque	C2*c*(?)
Moon	
Gravitational torque	A, B7, C1, C3*d*
Mantle	
Elasticity	B1, B3–4, C1–2*a*, C3*c*–*d*
Earthquakes	B1, B3
Solid friction	B3(?), C1
Viscosity	C2*a*
Liquid core	
Inertial coupling	A2–3, B2, B6
Topographic coupling	C2*b*–*c*(?)
Electromagnetic coupling	A4(?), B3, C2
Solid inner core	
Inertial coupling	B2(?)
Oceans	
Loading and inertia	B1, B3, B5, C2*a*
Friction	B3(?), C1
Groundwater	
Loading and inertia	B4
Atmosphere	
Loading and inertia	B4
Wind stress	C2*c*, C3*a*–*c*
Atmospheric tide	C1

*Numbers refer to Table 1.

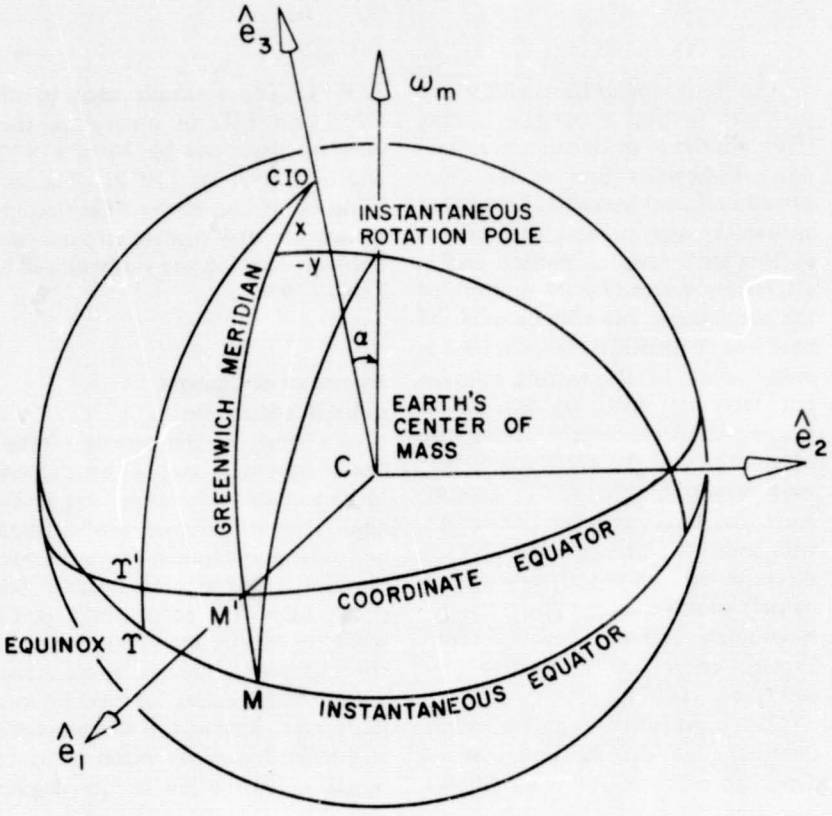

Fig. 1. Time and polar motion.

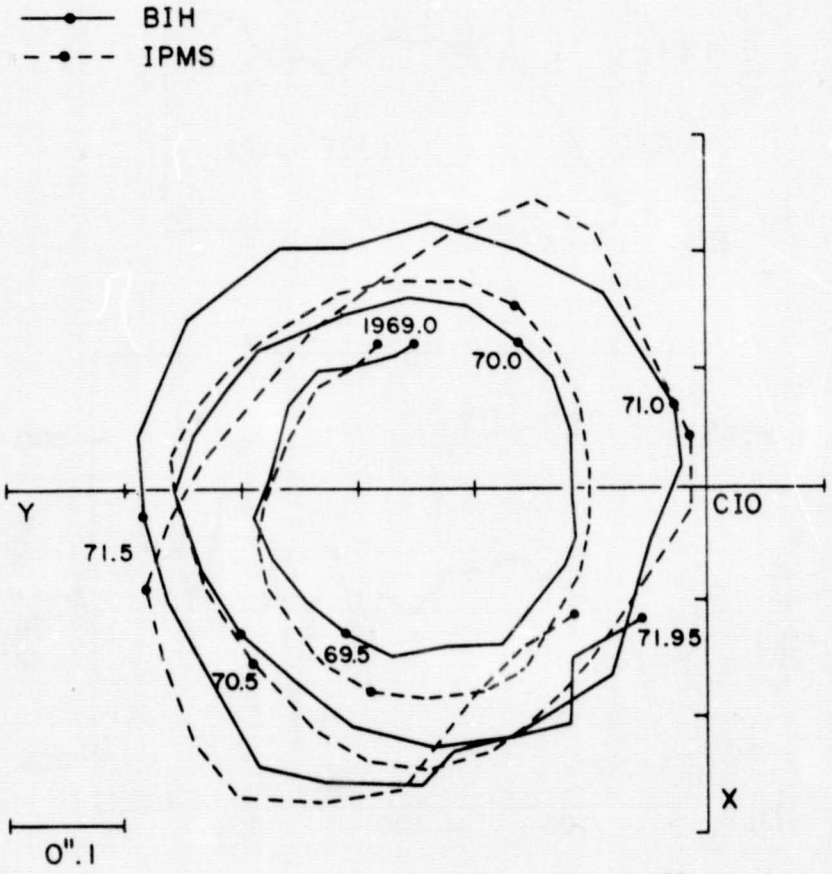

Fig. 2. Pole paths 1969.0–1971.95.

6-hour mean pole positions within ±0".03 of the BIH path from a single laser tracking system operated over 5 months. Accurate tracking of artificial satellites should also permit checking that the geographic axes of reference do pass through the earth's center of mass [*Lambeck*, 1971; *Melchior*, 1972]. *Gold* [1967] and *MacDonald* [1967] first pointed out that very long base line interferometry (VLBI) would make possible very precise measurement of changes in the earth's rotation (see also *Burke* [1969]). Laser ranging to corner cube reflectors on the moon should enable polar motion and spin rate to be measured with an accuracy nearly comparable to that expected from VLBI [*Alley and Bender*, 1968; *Faller and Wampler*, 1970; *Chollet*, 1970; *Rösch*, 1972]. Although the newer techniques will eventually largely replace optical astronomy, it will be important to continue the PZT observations for years to come to provide consistency and a standard of comparison during the transition period.

Orientation of the instantaneous rotation axis in space requires the selection of an inertial frame based on a catalog of fundamental stars, with due allowance for such things as proper motions and galactic rotation [*Woolard and Clemence*, 1966]. The best catalog in current use is FK4, based on over 1500 well-studied stars, but it contains systematic errors of the order of 0".1. Although these could be detected and corrected by a sustained program of laser tracking and photographic observation of artificial satellites [*Williams*, 1972], the development of VLBI seems to promise a better solution in the long run. The ultimate resolution of the order of 0".001 expected to be obtained with VLBI raises the possibility of using radio sources at enormous distances (with negligible proper motions) as a fundamental catalog, if a sufficiently dense distribution of quasars can be found over the celestial sphere.

The orbital motion of the moon and changes in the obliquity of the earth's equator to the ecliptic are connected to problems of the earth's

rotation, and so it is useful to define an intermediate reference system tied to the ecliptic and vernal equinox at some epoch. Lunar laser ranging (LLR) will in the course of time greatly improve the determination of the moon's orbit, the lunar ephemeris [*Faller and Wampler*, 1970; *Rösch*, 1972]. The VLBI tracking of spacecraft or artificial satellites placed in orbit around other planets could at some future date tie the ecliptic frame to an inertial frame constructed from the quasar sources [*Preston et al.*, 1972].

Time

Essentially three different kinds of time are required to discuss the earth's rotation. Sidereal and universal time (UT) are both based on the earth's diurnal rotation. Sidereal time is defined by the angle through which the Greenwich meridian has turned past the vernal equinox (Figure 1). Universal time is related to sidereal time by an adopted formula (whose origins are now of purely historical interest) and is therefore an equivalent direct measure of the earth's axial spin. In practice, UT is determined by meridian transits of stars, and so the PZT provides simultaneous determinations of time and latitude. Universal time corrected for polar motion (Figure 1) is called UT1. Since the earth's axial spin shows periodic, irregular, and secular changes, UT1 does not provide a uniform measure of time. Such a uniform reproducible time scale, called atomic time (AT), has been made available since 1955 by atomic frequency standards accurate to 1 part in 10^{13}. These atomic 'clocks,' now widely distributed at astronomical observatories, are presently synchronized by transport and side-by-side comparison, or less accurately by radio signals from quartz crystal oscillators carried in artificial satellites, but remote synchronization using VLBI techniques should soon be feasible. The PZT observations, coupled with atomic timekeeping, from the participating stations are processed and disseminated by the BIH as UT1-AT. Changes in the earth's axial spin rate are therefore obtained by differentiating UT1-AT with respect to (atomic) time.

The third kind of time with which we have to deal is ephemeris time (ET), the basis of dynamical astronomy. Ephemeris time is the (presumed uniform) measure of time that appears as the independent variable in Newton's laws of motion and is effectively defined by the motions of the sun, moon, and planets over the past few centuries. Ephemeris time is independent of the earth's rotation but rests implicitly on Newtonian theory. Until the advent of AT, the irregularities in the earth's spin rate were measured by ET-UT (Figure 3). Any divergences between ET and AT will indicate hitherto unsuspected shortcomings in the theory of the moon's motion and/or possible non-Newtonian effects [*Sadler*, 1968; *Shapiro et al.*, 1971; *Oesterwinter and Cohen*, 1972].

The most recent comprehensive treatment of the measurement of time and polar motion is by *Mueller* [1969]. The methods used by the IPMS and BIH in processing their data are described by *Yumi* [1972] and *Guinot et al.* [1972]. The possibilities of the newer observational techniques now coming into use have been explored in the study edited by *Kaula* [1970].

Dynamics of Changes in Earth's Rotation

A change in the earth's rotation can be brought about (1) by a change in its angular momentum due to the application of external torques (lunar and solar gravitational torques on the equatorial bulge, the bodily and ocean tides, the solar wind) or (2) while its angular momentum remains constant, by a change in its inertia tensor (earthquakes, sea level fluctuations, rearrangement of the geographic distribution of air mass) or by internal redistribution of its angular

Fig. 3. Changes in length of day. (a) After Guinot *[1970]. (b) After* Stoyko *[1970].*

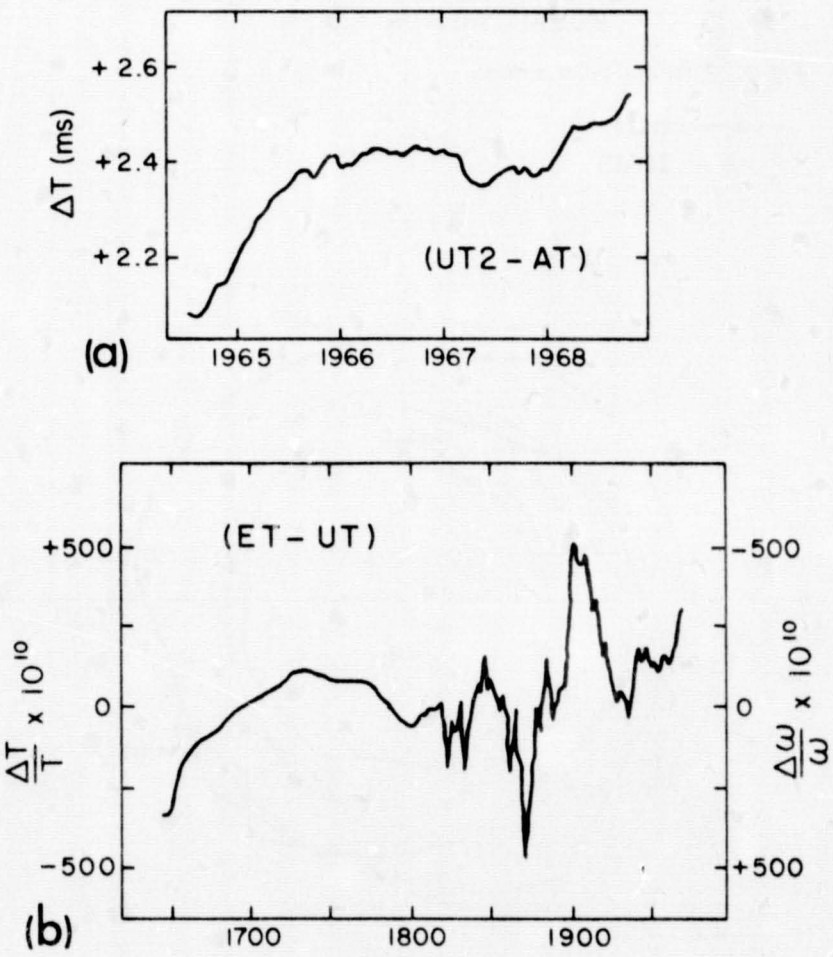

momentum (winds, core-mantle coupling).

The role of the core, almost completely enigmatic at the time when Munk and MacDonald wrote their book, has since become much more prominent. During the past decade a number of features of the earth's rotation spectrum, directly affected by the existence of the liquid core, have been identified with varying degrees of certainty [*Rochester*, 1970]. The principal effective mechanisms by which angular momentum can be transferred between the core and mantle are:

(1) inertial coupling due to the hydrodynamic pressure forces that act over the ellipsoidal core-mantle boundary when internal flow is induced in the liquid core by any shift in the earth's rotation axis [*Toomre*, 1966];

(2) electromagnetic coupling due to the operation of Lenz's law consequent upon leakage of geomagnetic secular variation (GSV) into the electrically conducting lower mantle [*Rochester*, 1960, 1968]. The GSV in turn is associated with internal motions of the highly conducting core, driven by mechanisms appropriately examined in the context of geomagnetic dynamo theory but closely connected with the earth's rotation.

Although there is as yet no seismic evidence for (or against) small-scale (not more than a few kilometers high) topography on the core-mantle interface, *Hide* [1969] has for other reasons proposed a coupling mechanism that may be comparable to or even stronger than the electromagnetic:

(3) topographic coupling, in which a stress on the mantle is produced by the flow of the rotating core over any 'bumps' or depressions on the core-mantle boundary.

Significant viscous friction at the core-mantle interface now seems most unlikely because of the very low molecular viscosity of the core estimated by *Gans* [1972] and the apparent ineffectiveness of turbulent (eddy) friction [*Toomre*, 1966; *Rochester*, 1970].

Precession

The combination of dynamical ellipticity (the equatorial bulge), obliquity, and spin causes the earth to respond to the gravitational attraction of the moon and sun by a steady precession of its rotation axis in space at a rate of 5037″/century (Figure 4). The earth is treated as a rigid body to deduce from this rate the value of one of the fundamental geophysical constants, its dynamical ellipticity $H = (C - A)/C$, where C and A are its axial and equatorial moments of inertia, respectively. The effect of a liquid core, first treated imperfectly by Hopkins in 1839 and then elegantly by Poincaré in 1910, has been discussed most recently by *Stewartson and Roberts* [1963], *Busse* [1968], *Gans* [1969], and *Suess* [1970]. Even if VLBI can reduce the error in the measured lunisolar precession rate to ±0″.1/century in the next decade [*Shapiro and Knight*, 1970], the effect of the liquid core (4 parts in 10^6) would remain undetectable. However, Shapiro and Knight point out that a more immediate result of this refinement will be the observational isolation of the general relativistic contribution to precession (≃1″.9/century).

Nutation

The orbital motions of the earth and moon give rise to ripples on the precessional cone (Figure 4), the

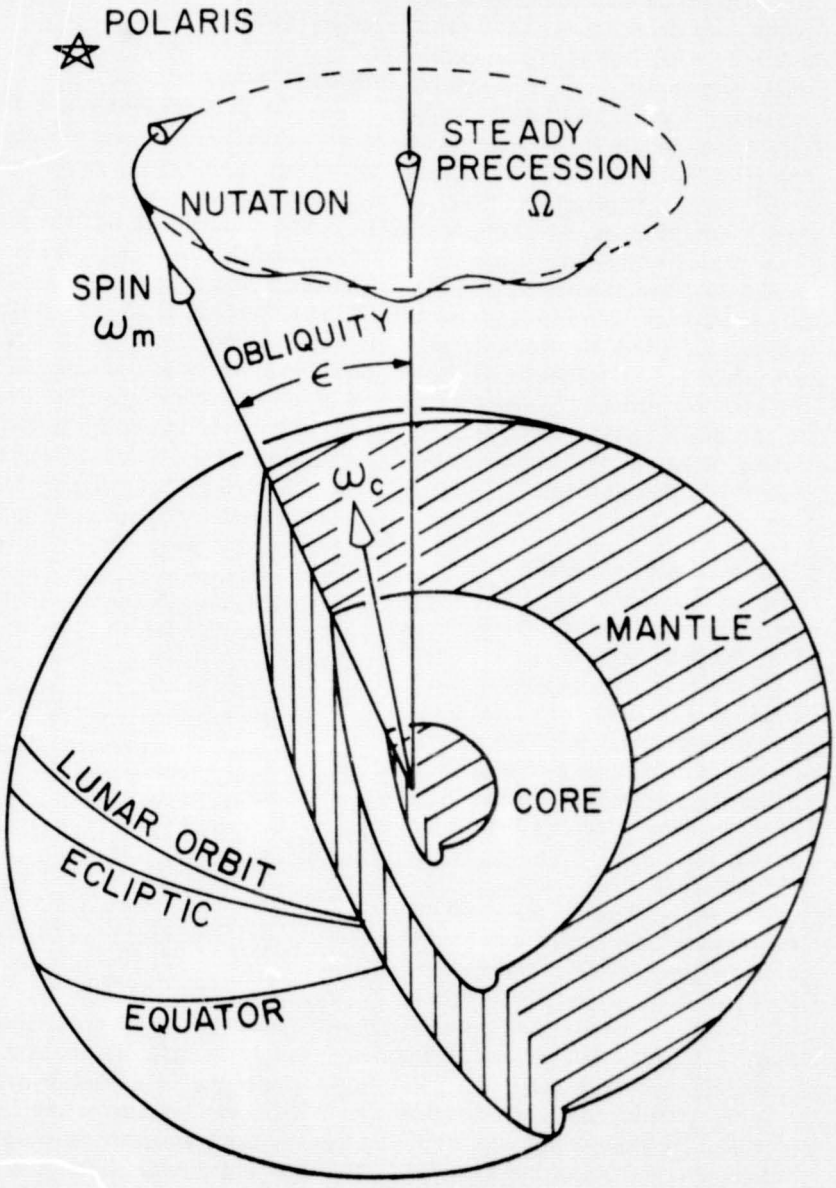

Fig. 4. Precession and nutation.

largest of which, the principal nutation, is associated with the regression of the lunar orbit's line of nodes with a period of 18.6 years. It is an elliptical motion of the rotation axis, the semimajor axis (nutation in obliquity) having an amplitude of 9".20. Independently, *Jeffreys and Vicente* [1957] and *Molodenskii* [1961] showed that allowing for mantle elasticity and the liquid core (inertially coupled to the mantle) removed the discrepancy of 0".02 between the observed amplitude and that derived from theory assuming the earth to be rigid.

Melchior [1971] has recently reviewed the dynamical effects of the liquid core on the long-period (18.6 and 9.3 years) and short-period (annual, semiannual, and fortnightly) nutations. Annual nutation in obliquity is due entirely to the presence of the core but is of small amplitude (≃0".006). Satisfactory observational confirmation of the corrections required by a deformable earth model has already been obtained by conventional astronomical techniques, according to Melchior (see also *Wako* [1970]). Clearly, the new methods of VLBI and laser ranging to the moon promise more discriminating tests of the earth models adopted by theoreticians.

'Secular' Decrease in Obliquity

The observed 'secular' (≃40,000-year period) decrease in the obliquity (Figure 4), at a rate ≃47"/century, can be almost, if not entirely, accounted for by the gravitational perturbations of the ecliptic by the other planets. Earlier analyses indicating a difference of ≃0".3/century between calculated and observed rates have been questioned [*Lieske*, 1970; *Fricke*, 1971], and it now appears unlikely that any real discrepancy can exceed ≃0".1/century [*Fricke*, 1972]. *Shapiro and Knight* [1970] suggest that a decade of VLBI and timing pulsar signals might suffice to determine whether such a discrepancy is real.

Aoki [1969] has proposed that frictional coupling of the core to the precessing mantle can cause a rotation of the equator in space, in the sense of reducing the obliquity, at approximately the rate indicated by the above possible discrepancy. *Kakuta and Aoki* [1972] claim to have removed certain objectionable features of Aoki's earlier model by taking into account electromagnetic coupling of the mantle to a liquid core, but the problem is complex and far from being satisfactorily solved. It is, in fact, part of a much larger problem of absorbing interest in connection with the possible operation of the geomagnetic dynamo by stirring up the core by the differential precessional torque arising from the 25% difference between the ellipticities of the earth's outer surface and the core-mantle boundary [*Malkus*, 1963; *Gans*, 1969; *Busse*, 1971; *Stacey*, 1973].

Chandler Wobble

The 70 years of systematic latitude observations using optical astronomy have not yet proved adequate to resolve unambiguously the spectrum of polar motion. The principal features are the 14-month (Chandler) and annual wobbles. The Chandler wobble is the torque-free Eulerian wobble for a uniaxial rigid earth with the period lengthened to ≃435 days by allowing for the liquid core, elastic mantle, and the mobility and loading of the oceans. The spectral peak at the Chandler frequency is broad and conventionally interpreted as indicating a more or less randomly excited oscillation damped with a relaxation time of the order of 10–25 years [*Jeffreys*, 1968; *Mandelbrot and McCamy*, 1970]. The value of Q (≃30–60) thus indicated has seemed anomalously low if the damping is to be attributed entirely to anelasticity of the mantle and if Q is rather independent of frequency [*Stacey*, 1967]. *Rochester and Smylie* [1965] showed that electromagnetic core-mantle coupling failed by a factor of at least 10^4 to provide the necessary damping.

Colombo and Shapiro [1968] have argued that the variable amplitude of the Chandler wobble is strikingly suggestive of a beat between two resonant periods within the Chandler band separated by roughly 10 days and having much sharper peaks, so as to remove the apparent problem with Q. It is difficult to see how two such close frequencies could exist near the Chandler peak for any reasonable model of the earth's interior. The ILS data are sufficiently inhomogeneous and the record length short enough that ordinary spectral analysis cannot with confidence resolve the question of whether they exist [*Pedersen and Rochester*, 1972]. When they are analyzed by Burg's maximum entropy method, neither the ILS data [*Claerbout*, 1969] nor the BIH data [*Smylie et al.*, 1973] yield any evidence for splitting of the Chandler peak. The trouble with Q may not be real, anyway, since the oceans have not been eliminated as a possible sink for wobble energy [*Munk and MacDonald*, 1960; *Lagus and Anderson*, 1968; *Miller*, 1973]. It may be worth noting that *Hendershott* [1972] gets $Q \simeq 35$ for the oceans at the semidiurnal period.

Continued observation of the Chandler wobble, even at increasing amplitude from time to time, in the presence of such strong damping, points to an efficient excitation mechanism. Amplification of the Chandler resonance by sidebands of the annual variation in atmospheric mass distribution is far too small [*Munk and Hassan*, 1961]. Earthquakes, dismissed by Munk and MacDonald, have been revived in a series of papers beginning with the one by *Mansinha and Smylie* [1967]. The far-field displacements accompanying a major earthquake, calculated by the elasticity theory of dislocations in a spherical earth, change the off-diagonal components of the inertia tensor and thus shift the earth's pole of figure (mean pole of epoch). Independent formulations of the theory for a self-gravitating earth model with liquid core and realistic distributions of density and elastic properties in the mantle have been given by *Smylie and Mansinha* [1971], *Dahlen* [1971, 1973], and *Israel et al.* [1973]. Their theoretical treatments differ in detail and have given rise to a small controversy over the physical principles governing static deformation of the liquid core (see also *Jeffreys and Vicente* [1966] and *Pekeris and Accad* [1972]). However, the effect of differing prescriptions of boundary conditions at the core-mantle interface is

likely to be small, and the authors generally agree in concluding that a major earthquake can produce a polar shift of the order of 0″.1. However, *Mansinha and Smylie* [1970] and *Dahlen* [1971] disagree on whether the cumulative effect of all earthquakes is enough to sustain the Chandler wobble. The sources of disagreement have not yet been conclusively identified but probably lie primarily in the different ways in which the authors relate the excitation due to a particular earthquake to its seismic character.

Ideally, one would like to test the hypothesis by matching a change in the pole path with the occurrence of a major earthquake and the shift in the pole of figure predicted by elastic dislocation theory from the earthquake's location and associated fault geometry [*Smylie and Mansinha*, 1968]. However, the data are so noisy that such attempts have so far been inconclusive [*Haubrich*, 1970; *Dahlen*, 1971], and we must await a great improvement in the accuracy with which wobble is monitored.

Modeling of seismic effects on the inertia tensor by sudden dislocations leaves so far unexamined the possible effects of creep on polar motion [*Chinnery*, 1970].

During the past decade, excitation of mantle wobble by electromagnetic coupling to the core has been shown to be utterly inadequate by *Rochester and Smylie* [1965], who took step function torques to be sufficiently optimistic, and has been resuscitated, on quite different grounds, by Runcorn and Stacey. *Runcorn* [1970*a*] contends that high-frequency GSV creates the core equivalent of sunspots at the core-mantle boundary and thus supplies an impulsive torque to the mantle that can transfer angular momentum rapidly enough to sustain the Chandler wobble. Earthquakes leave the instantaneous rotation pole unchanged but shift the axis of figure, so that the pole path experiences a discontinuous change in direction. Impulsive torques, on the other hand, leave the axis of figure unchanged and shift the rotation pole, so that the radius of the pole path is changed discontinuously. There is some support for the latter phenomenon in the observations: a change of the order of 0″.1 in arc radius taking place in a year or two [*Guinot*, 1972]. The details of electromagnetic coupling on such a short time scale have not been fully worked out, partly because the high-frequency GSV is screened from our observation by the electrical conductivity in the lower mantle that provides the coupling. But *Kakuta* [1965] concluded that magnetohydrodynamic oscillations in the core could not excite detectable wobble. *Stacey* [1970] uses a quasi-dynamical argument to estimate how much energy could be fed into the mantle wobble from the differential precession torque on the core through a nonlinear electromagnetic coupling mechanism. The proposal is intriguing but needs to be given a more rigorous formulation.

In an interesting translation of geophysics into an astronomical context, starquakes have been offered as an explanation of pulsar wobble [*Pines and Shaham*, 1973], and its damping has been discussed in terms of various mechanisms in the core and mantle of a neutron star [*Chau and Henriksen*, 1971].

Seasonal Wobbles

The amplitude of the annual (and much smaller semiannual) wobble can be sufficiently well explained by the seasonal variation in the geographic distribution of the mass of the atmosphere [*Munk and Hassan*, 1961], although the observed phase requires some additional excitation (snowfall, groundwater), according to *Jeffreys* [1972].

It has been customary to separate the Chandler wobble from the latitude data by removing an annual wobble that is constant in amplitude and phase from year to year, determined by a least squares fit. The suspicion that changing weather patterns from year to year would differentially drive the annual wobble is confirmed by the analysis of *Chollet and Débarbat* [1972], who find its amplitude to vary between 0″.04 and 0″.10 over a 14-year series of observations at Paris. The point is reinforced by *Wells and Chinnery* [1972], who find the annual wobble to be but poorly determined from the IPMS latitude data and conclude that it cannot be well separated from the Chandler wobble by the customary method. *Guinot* [1972], however, finds 'quiet' intervals of a few years over which the annual wobble is nearly constant.

Other short-period terms in the ILS data with very small amplitudes are probably forced wobbles of meteorological origin [*Sugawa et al.*, 1972].

Secular Motion of the Pole

The ILS data also reveal an irregular drift of the pole from its mean position 70 years ago in a rather sluggish sort of 'Brownian' motion that has carried it altogether ≃0″.2 towards Newfoundland in that time [*Yumi and Wako*, 1970; *Mandelbrot and McCamy*, 1970; *Mikhailov*, 1972]. The observed secular motion of the pole may be contaminated by as yet unresolved nonpolar latitude variations due to continental drift [*Arur and Mueller*, 1971]. There seems little reason to doubt that this secular motion is the cumulative result of changes in the inertia tensor due to sea level fluctuations [*Munk and MacDonald*, 1960] and tectonic processes [*Mansinha and Smylie*, 1970]. *Batrakov* [1972] estimates that a gigantic engineering project proposed to turn the flow of Siberian rivers southward will, through a redistribution of groundwater, shift the pole by no more than 0″.014.

Long-Period Wobbles

Markowitz [1970] adduces empirical evidence from the ILS data for a 24-year period wobble, which *Busse* [1970] has suggested may represent the response of the mantle to wobble of the solid inner core inertially coupled to the mantle via the liquid core. *Rykhlova* [1969], using a longer but less homogeneous record, finds evidence for a 40-year period instead. This may be the 'Markowitz wobble' with the period poorly determined because of contamination from the secular motion. But *McCarthy* [1972] also finds from latitude observations at Washington a 'period' somewhat longer than Markowitz's. If it is real, the phenomenon may well be the only observable manifestation of the presence of the

solid inner core in the entire spectrum of changes in the earth's rotation.

Nearly Diurnal Free Wobble

Perhaps the most intriguing wobble mode is the torque-free nearly diurnal polar motion made possible in principle by the presence of the liquid core inertially coupled to the mantle, first predicted in 1896 independently by both Hough and Sludskii. The predicted motion is retrograde about the axis of figure with a period about 3 min short of a sidereal day, according to the (slightly different) earth models of *Jeffreys and Vicente* [1957] and *Molodenskii* [1961]. Besides giving a resonance amplification to the nearly diurnal tides, this wobble mode will appear in observations of latitude and time (UT) as a period (relative to the stars) of 464 sidereal days or 204 mean solar days, according to Molodenskii's models. The most recent discussions of the observational evidence are those by *Sugawa and Ooe* [1970], *Popov and Yatskiv* [1971], and *Débarbat* [1971]. If this wobble could be unambiguously identified, its period would serve as a fairly stringent filter for earth models. However, its amplitude ($\simeq 0''.02$, according to Popov) is at noise level, and there is reason to be suspicious of this value, since it must be accompanied by a nutation hundreds of times larger (A. Toomre, private communication, 1973).

Other small ($\simeq 0''.02$) wobbles are forced by the sun and moon. These are the Oppolzer terms due to departure of the axis of rotation from the figure axis during nutation (discussed by *Takagi and Murakami* [1968]).

Short-Period Changes in Length of Day

Although the seasonal variations in the length of day were detected by Stoyko during the 1930's by pendulum clocks, the short-period changes naturally show up much better in UT1-AT, available since 1955. The annual variation (amplitude $\simeq 20$–25 msec) is primarily explained by winds and the semiannual variation (amplitude $\simeq 9$ msec) by the solar bodily tide, small additions to changes in the axial moment of inertia being contributed by the seasonal redistribution of air mass, ocean load, groundwater, snow, and vegetation [*Munk and MacDonald*, 1960]. The discrepancies in amplitude and phase between the seasonal fluctuations deduced by different workers [*Fliegel and Hawkins*, 1967; *Challinor*, 1971] reflect the year-to-year variability in the excitation mechanisms. *Frostman et al.* [1967] concluded that there are still large unexplained differences in phase between theoretical and observed seasonal variations. This objection appears to have been entirely removed by *Lambeck and Cazenave* [1973], who use much better meteorological data to calculate the seasonal fluctuations in atmospheric angular momentum.

Nordtvedt and Will [1972] point out that theories of gravitation involving a preferred reference frame predict anisotropies in the gravitational constant that change the earth's moment of inertia during its orbital motion and give rise to small annual and semiannual changes in the length of day. These effects are likely to be indistinguishable from the meteorological effects at the level of accuracy with which the latter are known. At present, all one can do is use the uncertainty in the extent to which the known meteorological and hydrological excitations can account for the observed seasonal variations in the length of day to set upper limits on the relevant parameters in nongeneral relativistic theories.

A 9-msec amplitude biennial term in the length of day was first reported by Iijima and Okazaki in 1966 and is presumably related to the 26-month atmospheric oscillation. For reports of other short-period variations (of possibly meteorological origin) see the papers by *Korsun' and Sidorenkov* [1971] and *Iijima and Okazaki* [1972].

Atomic timekeeping now permits unequivocal observation of the small (<1-msec amplitude) fortnightly and monthly lunar tidal variations in the length of day [*Guinot*, 1970].

Irregular Fluctuations in Axial Spin Rate

Subtracting from UT1 an adopted value for the seasonal variation in the length of day gives UT2. It is important to note that UT2 will still contain some small meteorological effects, since the seasonal fluctuations change in amplitude and phase from year to year. Irregular changes in the length of day show up in UT2-AT since 1955 and in ET-UT over the last three centuries (Figure 3). The corresponding rotational accelerations have been reviewed by *Markowitz* [1970, 1972]. A change of 1 msec in the length of day is about 1 part in 10^8, so that the data from Figure 3 divide roughly into three categories: (1) changes of a few milliseconds over several decades or longer (accelerations in the spin rate of $\leqslant 5 \times 10^{-10}$/yr), (2) changes of a few milliseconds over a few years to a decade (accelerations $\leqslant 80 \times 10^{-10}$/yr), the so-called 'decade fluctuations,' and (3) changes of a substantial fraction of a millisecond over a few weeks or months (accelerations $\leqslant 500 \times 10^{-10}$/yr), the most rapid of these being the 'abrupt' changes [*Guinot*, 1970].

Changes in this last category were not registered in UT until the atomic clocks came into use. Presumably, VLBI and laser ranging to the moon will enable the time intervals over which such changes can be detected to be whittled down to a fraction of a day, and improved global meteorological data will be used to test whether any appeal to the core must be made to explain such short-term irregularities.

Electromagnetic torques have been shown to be just barely adequate to transfer angular momentum between the core and the mantle at the rate necessary to account for the accelerations characteristic of the decade fluctuations [*Rochester*, 1960; *Roden*, 1963; *Kakuta*, 1965; *Roberts*, 1972]. *Vestine and Kahle* [1968] cite evidence for this mechanism in the correlation of changes in the length of day with changes in the westward drift of a prominent geomagnetic field constituent during the last 80 years.

The more rapid and abrupt changes in the length of day are much more likely to be explained by winds. They cannot be explained by electromagnetic coupling unless the electrical conductivity approaches 10^3 mhos/m at the very bottom of

the mantle and there is sufficient power in the GSV at high frequencies, say, ≥ 1 cycle/yr. Topographic coupling may play some role. After a checkered history of claims for detectable effects from the solar wind torque, it appears that this source can be neglected [*Coleman*, 1971; *Hirshberg*, 1972].

The slower changes, of type 1, are readily accounted for by electromagnetic coupling to the long-period GSV in the core [*Rochester*, 1970]. *Braginskii* [1970] and *Wilhelm* [1970] have calculated the long-term changes in the length of day associated with particular features of the GSV. *Munk and MacDonald* [1960] argue that changes in sea level do not contribute significantly to fluctuations in the spin rate on this time scale because there is no indication of the concomitant polar motion over the last 70 years. The same will not be true of sea level changes on a time scale of many centuries or millenia.

Secular Acceleration of Earth's Rotation

The major contributor to secular change in the length of day is tidal friction, which transfers earth's spin angular momentum to the lunar orbit and thus gives the moon an angular acceleration $\dot{n}$ in space. Until recently, the accepted value for the present era was $\dot{n} \simeq -22''/\text{century}^2$, determined over 30 years ago by Spencer Jones from telescopic observations of the sun, moon, and planets over the previous 2½ centuries (ET-UT). It now appears that errors in the poorly determined early observations could change his value by ±100%. More recent values were determined by (1) *Newton* [1968], who found $\dot{n} \simeq -20 \pm 3''/\text{century}^2$ from a few years' tidal perturbations of artificial earth satellite orbits (according to *Newton* [1972*a*], the systematic errors here may be much larger than indicated), (2) *Van Flandern* [1970], who obtained $\dot{n} \simeq -52 \pm 16''/\text{century}^2$ from 15 years of lunar occultations timed against AT and made unusually generous allowances for systematic error, and (3) *Oesterwinter and Cohen* [1972], who arrived at $\dot{n} \simeq -38 \pm 8''/\text{century}^2$ by fitting the last 60 years of lunar and planetary observations against UT and AT.

If the sun's tide on the earth is taken into account, the total gravitational tidal acceleration of the earth's spin is given by $\dot{\omega}/\omega \simeq 1.16\dot{n} \times 10^{-9}$/century, where the coefficient is uncertain to within a few percent owing to uncertainty in the knowledge of the ratio of the lunar to the solar tidal torque (various models range from 3.5 to 4.7). Thus the 'modern' rate of secular deceleration due to tidal friction is probably close to twice the value used by *Munk and MacDonald* [1960]. This in turn nearly doubles the problem of accounting for the accompanying energy dissipation ($\simeq 3.5 \times 10^{12}$ watts, according to Munk and MacDonald).

The shallow seas have long been regarded as the chief sink for tidal energy. *Miller* [1966] found that they could dissipate 1.7×10^{12} watts (±50%). Degradation by scattering into internal modes in the ocean is probably $\leq 0.5 \times 10^{12}$ watts [*Cox and Sandstrom*, 1962; *Munk*, 1966]. The contribution by bodily tides in the solid earth is probably not more than a few percent of the whole [*Munk*, 1968]. More recently, *Hendershott* [1972] and *Pariiskii et al.* [1972] have used cotidal charts and, taking ocean loading into account, estimated dissipation in the world ocean and thus obtained values roughly double Miller's (see also *Brosche and Sundermann* [1972]). An overall dissipation rate of $\simeq 3$–5×10^{12} watts can be inferred from the rough estimate of average (oceanic and bodily) tidal phase lag from gravimetry [*Smith and Jungels*, 1970]. The position appears to be that there are large uncertainties, but ocean tidal friction appears likely to meet the bulk of the dissipation requirements posed by the lunar acceleration.

Records of positions and times of ancient eclipses and of other events involving celestial bodies provide information on the average values of $\dot{\omega}$ and $\dot{n}$ over large segments of historical time. The best determined quantity is an epochal average of $\dot{\omega} - 0.622\dot{n}$, obtained from discrepancies between recorded locations of solar eclipses and those predicted by assuming zero accelerations between then and now. Other kinds of data, even less trustworthy, are used to separate $\dot{n}$ and $\dot{\omega}$. The necessary interpretation of sources, almost always at second- or third-hand, has given rise to energetic controversy. Until recently, a rather limited body of data, much of it of dubious reliability, was worked over by different investigators in as many different ways with varying weightings according to their individual assessments, so that even essentially the same data could be used to give widely divergent results. *Curott* [1966] and *Dicke* [1966] both assumed Spencer Jones's value for $\dot{n}$ to be valid over the last 3000 years in order to deduce values for $\dot{\omega}$ from eclipse data. A major contribution to the subject has been made by *Newton* [1970, 1972*b*], who amassed and extensively discussed the reliability of a much larger body of data and found $\dot{n} \simeq -42 \pm 6''/\text{century}^2$ over the last 2000 years, in agreement with the more recent 'modern' observations cited above.

Newton's analysis gives a nontidal acceleration of the earth's spin $\dot{\omega}/\omega \simeq 20 \times 10^{-9}$/century over the last 2000 years or so. *Dicke* [1966] investigated most of the presently conceivable mechanisms for explaining the acceleration of about half this amount given by his analysis and found that the largest contribution was from the postglacial rise in sea level and the accompanying isostatic adjustment. After other geophysical mechanisms were examined and dismissed as much smaller, the bulk of the remaining acceleration was attributed to the effect (on ET and on the earth's axial moment of inertia) of a decrease in the gravitational constant G with time predicted by certain theories of gravitation. The upper limit to $|\dot{G}|$ set by this reasoning is an order of magnitude smaller than that obtained by *Shapiro et al.* [1971] from radar and optical observations of planets since the advent of AT. Later, *Dicke* [1969] reversed his argument, assumed a contribution due to G and inferred the average viscosity in the deep mantle by at-

tributing the rest of the nontidal $\dot{\omega}$ to the rise in sea level and isostatic recovery following deglaciation. *O'Connell* [1971] has estimated the viscosity profile in the mantle by regarding the entire nontidal acceleration as due to the latter processes.

The rise in sea level assumed by these authors is within the limits set by *Walcott's* [1972] recent study of postglacial eustatic changes. But their interpretations neglect the possibility of substantial contributions from other geophysical effects. The long-period GSV indicates that the core should be able to store or provide angular momentum on a millenial time scale [*Sekiguchi*, 1956; *Rochester*, 1970]. Electromagnetic core-mantle coupling, limited by *Dicke* [1966] to much smaller effects by inadequate arguments and rather cavalierly dismissed by *Newton* [1970, 1972*a*], was studied in detail by *Yukutake* [1972]. He found that the 8000-year period change in the geomagnetic dipole moment (revealed by archeomagnetism) would give rise to an average $\dot{\omega}/\omega \simeq 5 \times 10^{-9}$/century over the past 2000 years. Also, *Gjevik* [1972] has argued that surface readjustments due to subcrustal phase transitions may mimic postglacial rebound in amplitude and relaxation time.

During the past decade, beginning with the work of *Wells* [1963], efforts have been made to extend estimates of $\dot{\omega}$ and $\dot{n}$ back over geologic time by using the fossil clocks provided by marine organisms whose shell structures show daily, monthly, and annual ridge patterns. The data tend to support an increase in the length of day since the Precambrian at an average rate more compatible with Spencer Jones's value for $\dot{n}$ than with more recent astronomical determinations of the 'modern' value [*Runcorn*, 1970*b*]. There is some evidence for changes in the tidal deceleration rate [*Pannella et al.*, 1968; *Pannella*, 1972]. In view of the possibility that the distribution of shallow seas was very different in the past, such changes would hardly be surprising. However, the uncertainties in the determinants of ridge growth are so great that it seems premature to draw any detailed conclusions from paleontological data regarding the history of the length of day. The most recent review is by *Scrutton and Hipkin* [1973].

Conclusion

This survey of current knowledge and problems of the earth's rotation is necessarily rough and superficial, and I can only hope that it conveys something of the compelling attraction that this global subject exerts on its devotees. There seems little doubt that the coming decade will eclipse even the enormous strides that were taken during the 1960's in the acquisition, accuracy, and analysis of data and bring much closer to resolution several of the tantalizing questions still presented by the rotation of the earth.

Acknowledgment

Financial support of this work from a National Research Council of Canada operating grant is gratefully acknowledged.

References

Alley, C.O., and P.L. Bender, Information obtainable from laser range measurements to a lunar corner reflector, in *Continental Drift, Secular Motion of the Pole, and Rotation of the Earth*, edited by W. Markowitz and B. Guinot, pp. 86–90, D. Reidel, Dordrecht, Netherlands, 1968.

Anderle, R.J., Pole position for 1971 based on Doppler satellite observations, *Rep. TR-2734*, 97 pp., U.S. Naval Weapons Lab., Dahlgren, Va., 1972.

Aoki, S., Friction between mantle and core of the earth as a cause of the secular change in obliquity, *Astron. J.*, *74*, 284–291, 1969.

Arur, M.G., and I.I. Mueller, Latitude observations and the detection of continental drift, *J. Geophys. Res.*, *76*, 2071–2076, 1971.

Batrakov, Yu.V., Effect of diverting the flow of Siberian rivers upon the rotation of the earth, *Sov. Astron. AJ*, *15*, 853–857, 1972.

Braginskii, S.I., Torsional magnetohydrodynamic vibrations in the earth's core and variations in day length, *Geomagn. Aeron.*, *10*, 1–8, 1970.

Brosche, P., and J. Sündermann, On the torques due to tidal friction of the oceans and adjacent seas, in *Rotation of the Earth*, edited by P. Melchior and S. Yumi, pp. 235–239, D. Reidel, Dordrecht, Netherlands, 1972.

Burke, B.F., Long-baseline interferometry, *Phys. Today*, *22*(7), 54–63, 1969.

Busse, F.H., Steady fluid flow in a precessing spheroidal shell, *J. Fluid Mech.*, *33*, 739–751, 1968.

Busse, F.H., The dynamical coupling between inner core and mantle of the earth and the 24-year libration of the pole, in *Earthquake Displacement Fields and the Rotation of the Earth*, edited by L. Mansinha, D.E. Smylie, and A.E. Beck, pp. 88–98, D. Reidel, Dordrecht, Netherlands, 1970.

Busse, F.H., Bewegungen im Kern der Erde, *Z. Geophys.*, *37*, 153–177, 1971.

Challinor, R.A., Variations in the rate of rotation of the earth, *Science*, *172*, 1022–1025, 1971.

Chau, W.Y., and R.N. Henriksen, Pulsar wobble, *Astrophys. Lett.*, *8*, 49–52, 1971.

Chinnery, M.A., Earthquake displacement fields, in *Earthquake Displacement Fields and the Rotation of the Earth*, edited by L. Mansinha, D.E. Smylie, and A.E. Beck, pp. 17–38, D. Reidel, Dordrecht, Netherlands, 1970.

Chollet, F.C., Mouvements de l'axe instantané de rotation de la terre déduits des mesures laser de distance terre–lune, *Astron. Astrophys.*, *9*, 110–124, 1970.

Chollet, F.C., and S. Débarbat, Analyse des observations de latitude effectuées à l'astrolabe Danjon de l'Observatoire de Paris de 1956.5 à 1970.8, *Astron. Astrophys.*, *18*, 133–142, 1972.

Claerbout, J., Frequency mixing in Chandler wobble data (abstract), *Eos Trans. AGU*, *50*, 119, 1969.

Coleman, P.J., Solar wind torque on the geomagnetic cavity, *J. Geophys. Res.*, *76*, 3800–3805, 1971.

Colombo, G., and I.I. Shapiro, Theoretical model for the Chandler wobble, *Nature*, *217*, 156–157, 1968.

Cox, C.S., and H. Sandstrom, Coupling of internal and surface waves in water of variable depth, *J. Oceanogr. Soc. Jap.*, *20*, 499–513, 1962.

Curott, D.R., Earth deceleration from ancient solar eclipses, *Astron. J.*, *71*, 264–269, 1966.

Dahlen, F.A., The excitation of the Chandler wobble by earthquake, *Geophys. J.*, *25*, 157–206, 1971.

Dahlen, F.A., A correction to the excitation of the Chandler wobble by earthquakes, *Geophys. J.*, *32*, 203–217, 1973.

Débarbat, S., Nearly diurnal nutation from time measurements, *Astron. Astrophys.*, *14*, 306–310, 1971.

Dicke, R.H., The secular acceleration of the earth's rotation and cosmology, in *The Earth–Moon System*, edited by B.G. Marsden and A.G.W. Cameron, pp.

98–164, Plenum, New York, 1966.

Dicke, R.H., Average acceleration of the earth's rotation and the viscosity of the deep mantle, *J. Geophys. Res., 74,* 5895–5902, 1969.

Faller, J.E., and E.J. Wampler, The lunar laser reflector, *Sci. Amer., 222*(3), 38–49, 1970.

Feissel, M., B. Guinot, and N. Taton, Comparison of the coordinates of the pole as obtained by classical astrometry (IPMS, BIH) and as obtained by Doppler measurements on artificial satellites (Dahlgren Polar Monitoring Service), in *Rotation of the Earth,* edited by P. Melchior and S. Yumi, pp. 104–111, D. Reidel, Dordrecht, Netherlands, 1972.

Fliegel, H.F., and T.P. Hawkins, Analysis of variations in the rotation of the Earth, *Astron. J., 72,* 544–550, 1967.

Fricke, W., Determinations of precession, *Celestial Mech., 4,* 150–162, 1971.

Fricke, W., On the motion of the equator and the ecliptic, in *Rotation of the Earth,* edited by P. Melchior and S. Yumi, p. 196, D. Reidel, Dordrecht, Netherlands, 1972.

Frostman, T.O., D.W. Martin, and W. Schwerdtfeger, Annual and semiannual variations in the length of day, related to geophysical effects, *J. Geophys. Res., 72,* 5065–5075, 1967.

Gans, R.F., The steady-state response of a contained, rotating, electrically conducting, viscous fluid subject to precessional and Lorentz forces, and its implications regarding geomagnetism, Ph.D. thesis, 94 pp., Univ. of Calif., Los Angeles, 1969.

Gans, R.F., Viscosity of the earth's core, *J. Geophys. Res., 77,* 360–366, 1972.

Gjevik, B., Surface readjustment owing to a subcrustal phase transition, *Phys. Earth Planet. Interiors, 5,* 403–408, 1972.

Gold, T., Radio method for the precise measurement of the rotation period of the earth, *Science, 157,* 302–304, 1967.

Guinot, B., Short-period terms in universal time, *Astron. Astrophys., 8,* 26–28, 1970.

Guinot, B., The Chandlerian wobble from 1900 to 1970, *Astron. Astrophys., 19,* 207–214, 1972.

Guinot, B., M. Feissel, and M. Granveaud, *Rapport Annuel pour 1971,* 183 pp., Bureau International de l'Heure, Paris, 1972.

Haubrich, R.A., An examination of the data relating pole motion to earthquakes, in *Earthquake Displacement Fields and the Rotation of the Earth,* edited by L. Mansinha, D.E. Smylie, and A.E. Beck, pp. 149–158, D. Reidel, Dordrecht, Netherlands, 1970.

Hendershott, M.C., The effects of solid earth deformation on global ocean tides, *Geophys. J., 29,* 389–402, 1972.

Hide, R., Interaction between the earth's liquid core and solid mantle, *Nature, 222,* 1055–1056, 1969.

Hirshberg, J., Upper limit of the torque of the solar wind on the earth, *J. Geophys. Res., 77,* 4855–4857, 1972.

Iijima, S., and S. Okazaki, Short period terms in the rate of rotation and in the polar motion of the earth, *Publ. Astron. Soc. Jap., 24,* 109–125, 1972.

Israel, M., A. Ben-Menahem, and S.J. Singh, Residual deformation of real earth models with application to the Chandler wobble, *Geophys. J., 32,* 219–247, 1973.

Jeffreys, H., The variation of latitude, *Mon. Notic. Roy. Astron. Soc., 141,* 255–268, 1968.

Jeffreys, H., The variation of latitude, in *Rotation of the Earth,* edited by P. Melchior and S. Yumi, pp. 39–42, D. Reidel, Dordrecht, Netherlands, 1972.

Jeffreys, H., and R.O. Vicente, The theory of nutation and the variation of latitude, *Mon. Notic. Roy. Astron. Soc., 117,* 142–161, 162–173, 1957.

Jeffreys, H., and R.O. Vicente, Comparison of forms of the elastic equations for the earth, *Mem. Acad. Roy. Belg., 37*(3), 1–31, 1966.

Kakuta, C., Magnetohydrodynamic oscillation within the fluid core and irregularities in the rotational motion of the earth, *Publ. Int. Latitude Observ. Mizusawa, 5,* 17–42, 1965.

Kakuta, C., and S. Aoki, The excess secular change in the obliquity of the ecliptic and its relation to the internal motion of the earth, in *Rotation of the Earth,* edited by P. Melchior and S. Yumi, pp. 192–195, D. Reidel, Dordrecht, Netherlands, 1972.

Kaula, W. (Ed.), *The Terrestrial Environment: Solid-Earth and Ocean Physics, NASA Contract. Rep. 1579,* chaps. 2 and 4, 1970.

Korsun', A.A., and N.S. Sidorenkov, A spectral analysis of the pulsations in the earth's rotational velocity, *Sov. Astron. AJ, 14,* 896–900, 1971.

Lagus, P.L., and D.L. Anderson, Tidal dissipation in the earth and planets, *Phys. Earth Planet. Interiors, 1,* 505–510, 1968.

Lambeck, K., Determination of the earth's pole of rotation from laser range observations to satellites, *Bull. Geod., 101,* 263–281, 1971.

Lambeck, K., and A. Cazenave, The earth's rotation and atmospheric circulation, 1, Seasonal variations, *Geophys. J., 32,* 79–93, 1973.

Lieske, J.H., On the secular change of the obliquity of the ecliptic, *Astron. Astrophys., 5,* 90–101, 1970.

MacDonald, G.J.F., Implications for geophysics of the precise measurement of the earth's rotation, *Science, 157,* 304–305, 1967.

Malkus, W.V.R., Precessional torques as the cause of geomagnetism, *J. Geophys. Res., 68,* 2871–2886, 1963.

Mandelbrot, B.B., and K. McCamy, On the secular pole motion and the Chandler wobble, *Geophys. J., 21,* 217–232, 1970.

Mansinha, L., and D.E. Smylie, Effect of earthquakes on the Chandler wobble and the secular polar shift, *J. Geophys. Res., 72,* 4731–4743, 1967.

Mansinha, L., and D.E. Smylie, Seismic excitation of the Chandler wobble, in *Earthquake Displacement Fields and the Rotation of the Earth,* edited by L. Mansinha, D.E. Smylie, and A.E. Beck, pp. 122–135, D. Reidel, Dordrecht, Netherlands, 1970.

Markowitz, W., Sudden changes in rotational acceleration of the earth and secular motion of the pole, in *Earthquake Displacement Fields and the Rotation of the Earth,* edited by L. Mansinha, D.E. Smylie, and A.E. Beck, pp. 69–81, D. Reidel, Dordrecht, Netherlands, 1970.

Markowitz, W., Rotational accelerations, in *Rotation of the Earth,* edited by P. Melchior and S. Yumi, pp. 162–164, D. Reidel, Dordrecht, Netherlands, 1972.

McCarthy, D.D., Secular and nonpolar variation of Washington latitude, in *Rotation of the Earth,* edited by P. Melchior and S. Yumi, pp. 86–96, D. Reidel, Dordrecht, Netherlands, 1972.

Melchior, P., Precession-nutations and tidal potential, *Celestial Mech., 4,* 190–212, 1971.

Melchior, P., Earth tides and polar motions, *Tectonophysics, 13,* 361–372, 1972.

Mikhailov, A.A., The polar motion of the earth, *Sov. Astron. AJ, 15,* 1035–1038, 1972.

Miller, G.R., The flux of tidal energy out of the deep oceans, *J. Geophys. Res., 71,* 2485–2489, 1966.

Miller, S.P., Observations and interpretation of the pole tide, M.S. thesis, 97 pp., Mass. Inst. of Technol., Cambridge, 1973.

Molodenskii, M.S., The theory of nutation and diurnal earth tides, *Commun. Observ. Roy. Belg., 188,* 25–56, 1961.

Mueller, I.I., *Spherical and Practical Astronomy with Application to Geodesy,* Frederick Ungar, New York, 1969.

Munk, W.H., Abyssal recipes, *Deep Sea Res., 13,* 707–730, 1966.

Munk, W.H., Once again—tidal friction, *Quart. J. Roy. Astron. Soc., 9,* 352–375, 1968.

Munk, W.H., and E.S.M. Hassan, Atmospheric excitation of the earth's wobble, *Geophys. J., 4,* 339–358, 1961.

Munk, W.H., and G.J.F. MacDonald, *The Rotation of the Earth,* Cambridge University Press, London, 1960.

Newton, R.R., A satellite determination of tidal parameters and earth deceleration, *Geophys. J., 14,* 505–539, 1968.

Newton, R.R., *Ancient Astronomical Observations and the Accelerations of the Earth and Moon,* Johns Hopkins Press, Baltimore, Md., 1970.

Newton, R.R., Astronomical evidence concerning non-gravitational forces in the earth-moon system, *Astrophys. Space Sci., 16,* 179–200, 1972*a*.

Newton, R.R., *Medieval Chronicles and the Rotation of the Earth,* Johns Hopkins Press, Baltimore, Md., 1972*b*.

Nordtvedt, K., and C.M. Will, Conservation laws and preferred frames in relativistic gravity, 2, *Astrophys. J., 177,* 775–792, 1972.

O'Connell, R.J., Pleistocene glaciation and the viscosity of the lower mantle, *Geophys. J., 23,* 299–327, 1971.

Oesterwinter, C., and C.J. Cohen, New orbital elements for moon and planets, *Celestial Mech., 5,* 317–395, 1972.

Pannella, G., Paleontological evidence on the earth's rotational history since early Precambrian, *Astrophys. Space Sci., 16,* 212–237, 1972.

Pannella, G., C. MacClintock, and M.N. Thompson, Paleontological evidence of variations in length of synodic month since Late Cambrian, *Science, 162,* 792–796, 1968.

Pariiskii, N.N., M.V. Kuznetsov, and L.V. Kuznetsova, The effect of oceanic tides on the secular deceleration of the earth's rotation, *Izv. Acad. Sci. USSR Phys. Solid Earth, 10,* 65–70, 1972.

Pedersen, G.P.H., and M.G. Rochester, Spectral analyses of the Chandler wobble, in *Rotation of the Earth,* edited by P. Melchior and S. Yumi, pp. 33–38, D. Reidel, Dordrecht, Netherlands, 1972.

Pekeris, C.L., and Y. Accad, Dynamics of the liquid core of the earth, *Phil. Trans. Roy. Soc. London, Ser. A, 273,* 237–260, 1972.

Pines, D., and J. Shaham, The elastic energy and character of quakes in solid stars and planets, *Phys. Earth Planet. Interiors, 6,* in press, 1973.

Popov, N.A., and Ya.S. Yatskiv, Amplitude variations in the free diurnal nutation of the earth, *Sov. Astron. AJ, 14,* 1057–1059, 1971.

Preston, R.A., R. Ergas, H.F. Hinteregger, C.A. Knight, D.S. Robertson, I.I. Shapiro, A.R. Whitney, A.E.E. Rogers, and T.A. Clark, Interferometric observations of an artificial satellite, *Science, 178,* 407–409, 1972.

Roberts, P.H., Electromagnetic core-mantle coupling, *J. Geomagn. Geoelec., 24,* 231–259, 1972.

Rochester, M.G., Geomagnetic westward drift and irregularities in the earth's rotation, *Phil. Trans. Roy. Soc. London, Ser. A, 252,* 531–555, 1960.

Rochester, M.G., Perturbations in the earth's rotation and geomagnetic core-mantle coupling, *J. Geomagn. Geoelec., 20,* 387–402, 1968.

Rochester, M.G., Core-mantle interactions: Geophysical and astronomical consequences, in *Earthquake Displacement Fields and the Rotation of the Earth,* edited by L. Mansinha, D.E. Smylie, and A.E. Beck, pp. 136–148, D. Reidel, Dordrecht, Netherlands, 1970.

Rochester, M.G., and D.E. Smylie, Geomagnetic core-mantle coupling and the Chandler wobble, *Geophys. J., 10,* 289–315, 1965.

Roden, R.B., Electromagnetic core-mantle coupling, *Geophys. J., 7,* 361–374, 1963.

Rosch, J., Laser measurements of earth-moon distances, *Moon, 3,* 448–455, 1972.

Runcorn, S.K., A possible cause of the correlation between earthquakes and polar motions, in *Earthquake Displacement Fields and the Rotation of the Earth,* edited by L. Mansinha, D.E. Smylie, and A.E. Beck, pp. 181-187, D. Reidel, Dordrecht, Netherlands, 1970*a*.

Runcorn, S.K., Palaeontological measurements of the changes in the rotation rates of earth and moon and of the rate of retreat of the moon from the earth, in *Palaeogeophysics,* edited by S.K. Runcorn, pp. 17–23, Academic, New York, 1970*b*.

Rykhlova, L.V., Evaluation of the earth's free nutation parameters from 119 years of observations, *Sov. Astron. AJ, 13,* 544–545, 1969.

Sadler, D.H., Astronomical measures of time, *Quart. J. Roy. Astron. Soc., 9,* 281–293, 1968.

Scrutton, C.T., and R.G. Hipkin, Changes in the rotation of the earth, *Earth Sci. Rev., 9,* in press, 1973.

Sekiguchi, N., On the secular accelerations in the mean longitudes of the moon and the sun, *Publ. Astron. Soc. Jap., 8,* 163–172, 1956.

Shapiro, I.I., and C.A. Knight, Geophysical applications of long-baseline radio interferometry, in *Earthquake Displacement Fields and the Rotation of the Earth,* edited by L. Mansinha, D.E. Smylie, and A.E. Beck, pp. 284–301, D. Reidel, Dordrecht, Netherlands 1970.

Shapiro, I.I., W.B. Smith, M.E. Ash, R.P. Ingalls, and G.H. Pettengill, Gravitational constant: Experimental bound on its time variation, *Phys. Rev. Lett., 26,* 27–30, 1971.

Smith, D.E., R. Kolenkiewicz, P.J. Dunn, H.H. Plotkin, and T.S. Johnson, Polar motion from laser tracking of artificial satellites, *Science, 178,* 405–406, 1972.

Smith, S.W., and P. Jungels, Phase delay of the solid earth tide, *Phys. Earth Planet. Interiors, 2,* 233–238, 1970.

Smylie, D.E., and L. Mansinha, Earthquakes and the observed motion of the rotation pole, *J. Geophys. Res., 73,* 7661–7673, 1968.

Smylie, D.E., and L. Mansinha, The elasticity theory of dislocations in real earth models and changes in the rotation of the earth, *Geophys. J., 23,* 329–354, 1971.

Smylie, D.E., G.K.C. Clarke, and T.J. Ulrych, Analysis of irregularities in the earth's rotation, *Methods Comput. Phys., 13,* in press, 1973.

Stacey, F.D., Consequences of energy dissipation by creep in the mantle, *Geophys. J., 14,* 433–438, 1967.

Stacey, F.D., A re-examination of core-mantle coupling as the cause of the wobble, in *Earthquake Displacement Fields and the Rotation of the Earth,* edited by L. Mansinha, D.E. Smylie, and A.E. Beck, pp. 176–180, D. Reidel, Dordrecht, Netherlands, 1970.

Stacey, F.D., The coupling of the core to the precession of the earth, *Geophys. J.,* in press, 1973.

Stewartson, K., and P.H. Roberts, On the motion of a liquid in a spheroidal cavity of a precessing rigid body, *J. Fluid Mech., 17,* 1–20, 1963.

Stoyko, A., La variation séculaire de la rotation de la terre et des problèmes connexes, *Ann. Guebhard, 46,* 293–316, 1970.

Suess, S.T., Some effects of gravitational tides on a model earth's core, *J. Geophys. Res., 75,* 6650–6661, 1970.

Sugawa, C., and M. Ooe, On the nearly diurnal nutation term derived from the ILS *z* term, *Publ. Int. Latitude Observ. Mizusawa, 7,* 123–147, 1970.

Sugawa, C., H. Ishii, and G. Teleki, On the relation between the ILS mean closing error and the ILS *z* term, *Proc. Int. Latitude Observ. Mizusawa, 12,* 176–199, 1972.

Takagi, S., and G. Murakami, Numerical analysis of the Oppolzer terms, *Publ. Int. Latitude Observ. Mizusawa, 6,* 225–229, 1968.

Tanner, R.W., The estimation of plate motions by astronomical methods, *Can. J. Earth Sci., 9,* 1052–1054, 1972.

Toomre, A., On the coupling of the earth's core and mantle during the 26,000-year precession, in *The Earth-Moon System,* edited by B.G. Marsden and A.G.W. Cameron, pp. 33–45, Plenum, New York, 1966.

Van Flandern, T.C., The secular acceleration of the moon, *Astron. J., 75,* 657–658, 1970.

Vestine, E.H., and A. Kahle, The westward drift and geomagnetic secular change, *Geophys. J., 15,* 29–37, 1968.

Vicente, R.O., The possibilities of detecting motions of the crust, *Geophys. J., 14,* 475–478, 1968.

Wako, Y., Interpretation of Kimura's annual *z*-term, *Publ. Astron. Soc. Jap., 22,* 525–544, 1970.

Walcott, R.I., Late Quaternary vertical movements in eastern North America: Quantitative evidence of glacio-isostatic rebound, *Rev. Geophys. Space Phys., 10,* 849–884, 1972.

Wells, F.J., and M.A. Chinnery, Variations in the annual component of polar motion at individual observatories (abstract), *Eos Trans. AGU, 53,* 345, 1972.

Wells, J.W., Coral growth and geochronometry, *Nature, 197,* 948–950, 1963.

Wilhelm, H., Eine sakulare Schwingung des erdmagnetischen Quadrupolfelds als Ursache einer Anderung der Erdrotation, *Z. Geophys., 36,* 697–723, 1970.

Williams, C.A., Corrections to star catalogues from satellite observations *Mon. Notic. Roy. Astron. Soc., 158,* 125–149, 1972.

Woolard, E.W., and G.M. Clemence, *Spherical Astronomy,* pp. 418–440, Academic, New York, 1966.

Yukutake, T., The effect of change in the geomagnetic dipole moment on the rate of the earth's rotation, *J. Geomagn. Geoelec., 24,* 19–47, 1972.

Yumi, S., *Annual Report of the IPMS for the Year 1970,* International Polar Motion Service, Mizusawa, 1972.

Yumi, S., and Y. Wako, Secular motion of the pole, in *Earthquake Displacement Fields and the Rotation of the Earth,* edited by L. Mansinha, D.E. Smylie, and A.E. Beck, pp. 82–87, D. Reidel, Dordrecht, Netherlands, 1970.

Michael G. Rochester is Professor of Physics at the Memorial University of Newfoundland, St. John's, Newfoundland, Canada. He received his B.A. in applied mathematics from the University of Toronto in 1954, his M.A. in physics from Toronto in 1956, and his Ph.D. in physics from the University of Utah in 1959. He has held faculty appointments at the University of Toronto and the University of Waterloo, and has been at Memorial since 1967. He is a member of Canada's National Research Council Associate Committee on Geodesy and Geophysics, and of the International Geodynamics Project's Working Group on Physical Processes in the Earth's Interior.

OMIT

The Rotation of the Earth and Polar Motion

REPORT ON THE SECOND GEOP RESEARCH CONFERENCE

The Second GEOP Research Conference was attended by about 80 persons, 34 invited and 46 observers. The conference was opened by W.H. Munk, general chairman of the conference, followed by M.G. Rochester of the University of Newfoundland, who delivered the keynote address. The keynote address in its entirety is printed on page 769 of this issue. This address and the following summaries of the sessions constitute a report on this conference.

This report was prepared by W.M. Kaula, Kurt Lambeck, Wm. Markowitz, Ivan I. Mueller, and D.E. Smylie. Material contained herein should not be cited.

First Session

Panel on Observations and Coordinate Systems

Chairman: Wm. Markowitz (Nova University)

Members: R. Anderle (U.S. Naval Weapons Laboratory), P. Bender (Joint Institute for Laboratory Astrophysics), C. Counselman (MIT), B. Guinot (BIH), P. Melchior (Observatoire de Belgique), J. Ramasastry (NASA, Goddard), D.E. Smith (NASA, Goddard), T.C. Van Flandern (U.S. Naval Observatory), G.M.R. Winkler (U.S. Naval Observatory)

The opening session was concerned with observational methods used to determine variations in speed of rotation of the earth and polar motion. The chairman, Wm. Markowitz, remarked that, in addition to the classical optical methods (e.g., use of the photographic zenith tube (PZT), astrolabe, and zenith telescope), techniques had been developed that use Doppler shift, laser ranging of the moon and of artificial satellites, and very long base line radio interferometry (VLBI). Since all these methods had been described during the past few years at symposiums and in journals, the session would be devoted mainly to giving accuracies of measurements recently obtained or expected shortly. He noted that the fundamental polar path, to which other pole paths are referred, has been determined since 1900 by a few stations on a common latitude, designated the International Latitude Service (ILS). Reductions are currently made by the International Polar Motion Service (IPMS) at Mizusawa. The results are free systematically of errors such as those in star positions or in reduction constants. The pole path determined by the Bureau de l'Heure (BIH) at Paris is based on time and latitude observations of a large number of stations.

B. Guinot reported on the accuracy of measurements of the coordinates of the pole and of universal time as obtained by the classical astronomical methods. Two international services are involved in the determination of the rotation vector of the earth, the IPMS and the BIH. Table 1 lists their chief areas of activity in 1973. Table 2 lists the error budgets in the coordinates of the pole, x and y. Table 3 lists the error budget in UT1.

G.M.R. Winkler reported that a new PZT with a 65-cm aperture (20 cm is usual) is scheduled for completion in 1974. The instrument will allow numerous experiments to be performed that will improve the accuracy of PZT observations.

R. Anderle reported on the path of the pole obtained from analysis of Doppler observations made since 1969 of Navy navigational satellites. Sporadic results had been obtained for the period 1965–1969. Currently, pole position is computed on the basis of observations made on at least one satellite during each 48-hour interval. The random error in the range difference (from Doppler integration) is typically 10 cm, which yields a theoretical precision of 50 cm in the latitude of a receiver observing a polar satellite at an elevation greater than 10°. However, uncertainties in the evaluation of the earth's gravity field produce errors in the computed satellite position of 3 meters amplitude. The fundamental period of the error is about 2

TABLE 1. Time and Polar Motion Services

	IPMS/ILS	BIH
Sources of observational data	5 stations	50 instruments, latitude; 60 instruments, UTO-UTC
Raw results	x, y*	x, y; UT1−UTC‡
Smoothed results	x, y†	x, y; UT1-UTC‡
Program	Same stars observed: no systematic error due to star position errors.	Different stars observed; errors due to star position errors statistically reduced.
Common sources of error	Local drifts of the vertical; instrumental errors; random errors.	Local drifts of the vertical; instrumental errors; random errors.

The BIH uses the data of new techniques, but a purely classical solution is maintained for comparison purposes. The subsequent data were obtained with the latter.

*Monthly values.

†Values every 0.05 year.

‡5-day values.

TABLE 2. Error Budget in x or y

Error Source	Error (One Sigma)	
	IPMS/ILS	BIH
Systematic errors in drift		
Errors of the proper motion of stars, cm/yr	0	} 3 (combined)
Local drifts, cm/yr	2	
Annual errors		
Errors of star positions, refraction, cm	30	30
Random errors (instrument, refraction, observers, etc.)		
5-day mean, cm		40
1-month mean, cm	100	30
1-year mean, cm	60	20

The above values were obtained in most cases by a study of the residuals of each series of latitude relative to the evaluated results. Data are given in centimeters at the surface of the earth; 1 arc second ≈ 30 meters. The effect of local drifts on IPMS/ILS data is subject to controversy. Note that the random errors are not a white noise. They are not likely to be reduced by averaging errors more than 1 year.

TABLE 3. B¹H Error Budget in UT1

Error Source	Error (One Sigma)
Systematic errors in drift	
Motion of equinox, sec/yr	?
Local drifts and random errors in proper motion, sec/yr	0.0003
Annual errors	
Errors in star positions, refraction, sec	0.0013
Random errors	
5-day mean, sec	0.0020
1-month mean, sec	0.0014
1-year mean, sec	0.0010

Estimates were made as for Table 2. A constant error results from the adopted values for the conventional longitudes.

hours, but the error includes many superimposed periods of $24/m$ hours (m = 1, 2, · · ·). Therefore the actual error in the latitude determination of a receiver based on a single satellite pass is no better than 3 meters. However, since 20 receivers are used and since each receiver observes 4–12 satellite passes per day, the pole position is determined to an accuracy of 60 cm on the basis of each 48 hours of data. During the latter half of 1972, pole position was computed on the basis of observations of three satellites, the standard error of the mean being 22 cm for a 5-day average.

D.E. Smith described preliminary results on variation of latitude obtained from satellite laser ranging. Observations made at several stations well distributed in longitude would provide the motion of the pole. He reported that the present capability of laser ranging to satellites for the determination of polar motions is 1 meter in an interval of 6 hours, as demonstrated in an experiment in 1970 conducted by NASA Goddard Space Flight Center. A single laser tracking station observed the variation in its latitude arising from polar motion over an interval of 5 months, described in *Science (178,* 405–406, 1972). In essence, the technique uses the orbit of a satellite as its external reference system from which the variation in latitude is determined.

Current limitations of this technique lie in our ability to account for the observed perturbations of the orbit (the reference system). These perturbations are due principally to the higher harmonics of the earth's gravitational field and to a lesser extent to the earth tides. Present (1972) instrumental capabilities probably limit the technique to about 25 cm from 6 hours of data. However, with the use of future satellites in higher orbits the problem of the gravity will largely be removed, and the limitation will then probably lie with the earth tides (particularly the oceans) and our ability to compute the perturbations of earth albedo radiation pressure. Instrumentation capability, which will be 10 cm in range accuracy in July 1973 and about 3 cm in 1974–1975, is not expected to be a major factor. Consequently, it is anticipated that by 1975 laser ranging to satellites will permit the variation in latitude of a tracking station to be determined to about 10 cm in about 6 hours. By 1978, this value will probably be reduced to 2–3 cm.

Peter L. Bender reported on the use of lunar range measurements for determining polar motion. Measurements with an accuracy of 15 cm are currently being made by the McDonald Observatory of the University of Texas three times per day on about three quarters of the days during the month, weather permitting. A lunar ephemeris and a set of topocentric correction parameters for the problem now exist that fit the observations within about 4 meters over a period of 2.5 years. The lack of a better fit is believed to be due to uncertainties in the lunar libration angles; improved calculations that should remove this problem will be completed before the end of 1973.

A new lunar ranging station in Hawaii with an accuracy goal of 2–3 cm is being constructed by the Institute for Astronomy of the University of Hawaii. The use of a Nd-YAG laser with a 200 psec pulse length is planned. Four to six additional stations should be in regular operation in other countries by 1975. It should then be possible to begin the regular determination of polar motion and fluctuation in the earth's rotation rate at intervals down to 1 or 2 days. The accuracy expected is about that of the basic range measurements.

Charles C. Counselman III reported on the use of VLBI as a potentially important technique for measuring the speed of rotation of the earth, polar motion, and also precession and nutation. Measurements are made with respect to extragalactic objects that define an excellent inertial frame. Technical improvements expected during the next 2 years should enable measurement uncertainties to be obtained in all three coordinates equivalent to a few centimeters of displacement at the earth's surface. Delay measurements between stations 5000 km apart performed by the MIT-Haystack VLBI group with a group from NASA Goddard Space Flight Center and the University of Maryland gave a scatter of 0.1 nsec rms, equivalent to 3 cm of displacement, over 6 hours of observations on August 29, 1972.

Separate determinations of UT1 and pole position have not yet been made. However, from four experiments made in 1969 and 1972 it is deduced that the errors in value published by the U.S. Naval Observatory must be smaller than 3 meters, or 0.1 arc second.

Methods are available to enable the effect of the earth's ionosphere (about 10 cm) and neutral atmosphere (variable by 40 cm) to be eliminated with an estimated uncertainty of less than 5 cm.

J. Ramasastry gave a report on VLBI experiments carried out by NASA Goddard Space Flight Center and the Smithsonian Astrophysical Observatory (SAO), which included the first measurement of the rotation of the earth through use of VLBI. This was made possible through the availability of (1) hydrogen masers with a frequency stability of 1 part in 10^{14}, (2) a catalog of quasar positions with an accuracy of 0.5 arc second, and (3) reasonably accurate estimates of tropospheric and ionospheric effects. The stations at Agassiz, Massachusetts (SAO, 84-ft dish), and Owens Valley, California (Cal Tech, 130-ft dish), operated in the *C* bands (4995 MHz) during February and March of 1972.

The mean residual in the time determined, essentially UT1-AT, for 24 hours, was 2.8 msec (to be regarded as a zero point correction) over an interval of 12 days. This interval was too short to detect any variation in speed of rotation. The rms deviation was 500μ which should be reduced as the technique is refined. It is planned to measure both UT1 and polar motion from observations of both quasar sources (at *S* and *C* bands) and water vapor sources (at *KU* band).

T.C. Van Flandern discussed modern determinations of the secular acceleration of the earth (and moon). The secular decelerations of the moon's orbital motion and of the earth's rate of rotation are closely linked. The accelerations obtained have been changed by large amounts several times in the last 200 years. The earliest

derived value for $\dot{n}_M$, the centennial rate of change of the moon's mean motion per century, was +20″/century², determined about 1780, before it was realized that the earth's rotation was also varying. Modern determination began with H. Spencer Jones's 1939 value for $\dot{n}_M$ which is −22″.44/century². Attempts to account for this variation in terms of tidal exchange of angular momentum from earth to moon have not yet succeeded. All determinations of $\dot{n}_M$ during the last 5 years are nearly twice Spencer Jones's value: −52″/century² by Van Flandern, −40″ by L.V. Morrison (using both occultations and the atomic time scale for about 15 years), −38″ by C.J. Cohen and C. Oesterwinter (Spencer Jones's method, but modern observations), and R.R. Newton's values for ancient observations of −42″ at 200 B.C. and −44″ at 1000 A.D. Hence, if we assume Spencer Jones's value to be ruled out by the more recent determination, there is no evidence for any change in $\dot{n}_M$ over the past 30 centuries.

Second Session

Panel on Seismic and Meteorologic Effects on the Earth's Rotation

Chairman: K. Lambeck (Groupe de Recherches de Géodesie Spatiale, Observatoire de Paris)

Members: K. Aki (MIT), M.A. Chinnery (Brown University), F.A. Dahlen (Princeton University), R.A. Haubrich (University of California, San Diego)

One of the outstanding problems of the earth's rotation concerns the nature of the Chandler wobble, the earth's free nutation with a frequency of 0.85 cycle/yr. As the earth is not a perfect elastic body, any such nutation will be damped and will cease to exist after a suitable time interval. Evidence of damping of the Chandler motion comes directly from the broadening of the spectral peaks centered at the Chandler frequency. However, the Chandler motion has been observed now for more than 70 years, longer than the generally accepted damping time, and there must be some mechanism regenerating the motion. Two such mechanisms that have been variously proposed are of meteorological and seismic origins.

If the changes in the atmospheric inertia tensor are not purely seasonal, there could be sufficient power in the annual line in the inertia frequency spectrum to sustain the Chandler wobble, as was first suggested by Volterra in 1895 and further detailed by Jeffreys in 1940. The study of Munk and Hassan (*Geophysical Journal, 4*, 339, 1960), however, indicated that this mechanism failed by 1 or 2 orders of magnitude. At present there is no evidence for revising these conclusions.

The alternative and attractive hypothesis that seismic activity is responsible has a long history. Kelvin in 1876 (*Mathematical and Physical Papers, 3*, 332, 1890) speculated what the effect of sudden changes in mass distribution would be on the as then still unobserved polar motion. Munk and MacDonald (*The Rotation of the Earth*, Cambridge University Press, 1960) ruled out this possibility as being too small by several orders of magnitude. Press's work (*Journal of Geophysical Research, 70*, 2395, 1965), however, indicated that the dislocation fields associated with earthquakes were much more extensive than had previously been recognized. Mansinha and Smylie (*Journal of Geophysical Research, 72*, 4781, 1967) recognized that the changes in the earth's inertia tensor would in consequence also be much larger. Using a simple earth model, they indicated that earthquakes could indeed excite the Chandler motion, and in a later paper (*Journal of Geophysical Research, 73*, 7661, 1968) they indicated that there was some evidence to support this hypothesis in the astronomical data. Since these important studies were made, a number of detailed investigations have been published with conflicting results. One of the objectives of the panel, then, if not to resolve the existing differences, is at least to determine where the differences lie.

Both F.A. Dahlen and R.A. Haubrich argue that the astronomically derived polar motion data are too noisy to show any correlation with earthquakes. Dahlen argues that one must instead compute the excitation functions from the seismic evidence and determine whether earthquakes suffice to drive the Chandler motion. This computation was in fact done by Smylie and Mansinha (EOS, *Transactions of the American Geophysical Union, 50*, 645, 1969; *Geophysical Journal, 23*, 329, 1971), using realistic earth models, and they again answered in the affirmative. Dahlen and Chinnery indicated that recent unpublished studies by Israel, Ben-Menahem, and Singh, by Saito, and by Dahlen argue that available excitation is too small by an order of magnitude and that these solutions agree with one another and with the earlier Smylie-Mansinha calculations to within 10%, except for a special case in the latter. Dahlen then considers that the mathematical problem of estimating the changes in the inertia tensor resulting from earthquakes is solved, although a number of interesting problems remain.

M.A. Chinnery stated that he had estimated the polar shift that Dahlen's calculations would give for a vertical fault model for the 1964 Alaskan earthquake and found it to be an order of magnitude smaller than the polar shifts deduced by the above authors for dipping faults. He suggested the following possible causes for the differences: (1) the nature of the core-mantle boundary conditions assumed, (2) the choice of the equations of state in the fluid core, (3) the analytical representation of the seismic source, (4) the earth model used, (5) the methods used for estimating the cumulative earthquake effect, and (6) a numerical error.

D.E. Smylie and L. Mansinha in their 1971 paper give the first static treatment of the core-mantle boundary conditions, which do not require the Adams-Williamson law to hold throughout the core. Certain aspects of this treatment now appear to be generally accepted, but in any case both Dahlen and Chinnery doubt that the inertia tensor is sensitive to the treatment of the core, since the inertia of the core as a whole is small in comparison with the inertia of the total earth. Smylie thinks that the anomalous result that Chinnery finds for vertical faults might be due to Dahlen's use of dynamic boundary conditions at the core-mantle boundary. Chinnery doubts whether the free oscillation variable y_6 is continuous at the core-mantle boundary in the Smylie-Mansinha model, but Smylie indicated that it must be in order for the normal component of the solenoidal vector (of which y_6 is the radial coefficient) to be continuous across the boundary.

According to Chinnery, the Smylie-Mansinha excitation is larger than that computed by others using the same set of fault parameters for the 1964 Alaskan earthquake; this statement, according to Smylie, is correct only for vertical faults. The results are, however, in agreement for the 1960 Chilean event and the 1964 Alaskan event for a dipping fault model.

Smylie has some doubts whether Chinnery in fact used exactly the same parameters in his comparison and indicated that the solutions can be very sensitive to the source parameters.

Smylie pointed out that the solution is sensitive to the choice of mantle model (Chinnery was uncertain to what degree). In particular, he reported calculations that showed that the inclusions of thin soft layers in the upper mantle could increase the calculated excitation by nearly an order of magnitude.

The pole shift produced by a point earthquake is proportional to the earthquake moment, and the largest dynamic moment ever measured is that of the 1964 Alaskan earthquake. If it is presumed that there are no thin soft layers in the mantle, Dahlen's new results show that this event caused a pole shift of 0″.0073 and that for a Q as large as 200 at least 10 such earthquakes are required per year to account for the observed Chandler power. This value is an order of magnitude larger than the actual observed level of seismic activity.

To estimate the cumulative effect of seismic activity on the Chandler motion, we need information on the seismic records of past earthquakes. K. Aki stressed that an accurate determination of the seismic moment of an earthquake is possible only when observations on seismic spectra are available for wavelengths much longer than the source dimension. For most old earthquakes we know only the magnitudes as determined by Gutenberg and Richter. Semiempirical relations between the surface wave magnitude M_s and the seismic moment have been established by using dislocation models of earthquakes by

Brune, based on a ω^{-1} dependence of the source spectra, and by Aki, who assumes a ω^{-2} dependence. According to Aki, recent comparisons of these models with accurate determination of seismic moment appear to support the ω^{-2} model, although there are some discrepancies when this model is applied to the magnitudes given by Gutenberg and Richter. In some cases this discrepancy appears to be due to an overestimation of the Gutenberg-Richter magnitudes. Aki emphasizes the necessity of reinvestigating old seismic records to obtain more reliable estimates of seismic moment for the largest earthquakes. This need is well illustrated by the Sanriku earthquake of 1933, whose correct magnitude is 8.3, equal to that of the 1964 Alaskan event. According to Kanamori, however, the observed seismic moment of the latter is about 10 times greater than that estimated for the Sanriku event. Aki also mentioned the recent results obtained by Brune and colleagues from studying the mantle wave magnitudes M_m of old earthquakes. These results indicate that the Alaskan earthquake had the largest M_m and that the Sanriku earthquake of 1933 had the ninth largest M_m during the interval 1923–1964. Aki's results, combined with Dahlen's observation that at least 10 Alaskan-sized earthquakes per year are required, do not support the theory of seismic excitation of the Chandler motion. Smylie disagrees with this last statement.

Mansinha and Smylie in their 1967 paper presented a study of cumulative effects based on the theory of random walks and using the Tocher-Press fault length–magnitude relation. In their 1971 paper they used this theory to estimate cumulative effects based on their calculations for the 1960 Chilean and the 1964 Alaskan earthquakes. The Tocher-Press law and Aki's law give comparable cumulative effects, but Brune's law gives effects about an order of magnitude smaller, as pointed out by Dahlen. Dahlen in 1973 performed Monte Carlo random walk experiments using Brune's moment-magnitude relation and Aki's ω^{-2} relation and the Gutenberg-Richter seismic magnitudes updated by Duda. These experiments did not alter his basic conclusions.

R.A. Haubrich discussed his reexamination of the latitude data for the likely times of occurrence, the size, and the direction of steps or pulses in the Chandler excitation. The time series of the astronomically estimated excitation function is noisy. Filtering of the excitation removed frequencies outside a band near the Chandler frequency, and this filtered function was examined for steps or pulses by a combined method of least squares and exhaustive search using dynamic programing. Using four different models of fitting, Haubrich arrives at the times of occurrence of the 10 most likely instants at which breaks occurred in the pole paths as determined by the ILS for 70 years and by the BIH for 10 years. He concludes that there is no correlation between the events determined from two data sets and that neither data set correlates highly with the times of the largest earthquakes, the largest events as deduced from the pole paths appearing to be unassociated with earthquakes. Smylie pointed out that he had done a similar study several years ago and that the polar motion measurements did not seem to be good enough to draw conclusions either way.

In summing up the question of seismic excitation of the Chandler motion, W.H. Munk asked four questions. (1) Are the results of Smylie and Mansinha and of Dahlen in agreement or disagreement? (2) If there is disagreement, can it be due to the difference in treatment of the core? (3) Is the use of Aki's ω^{-2} model for the seismic moment a cause for disagreement? (4) What is the situation on the data analysis with respect to the correlation of the pole path with earthquakes?

The answer to the first question is that there is disagreement. Dahlen says earthquakes cannot excite the Chandler motion, whereas Smylie and Mansinha maintain that earthquakes can excite the motion. The differences in the conclusions are largely dependent on whether one uses Brune's moment-magnitude law or the Tocher-Press fault length–magnitude relation. Aki's law, mentioned earlier, gives results similar to those of the Tocher-Press law, but this relation predicts earthquake moments at least a factor of ten larger than the moment for the Alaskan earthquake.

In response to the second question, Chinnery, Dahlen, and Smylie agree that the different treatment of the core and core-mantle boundary is unimportant. Dahlen indicated that, when he adopted the Smylie-Mansinha conditions, his results changed by only a few percent. Smylie indicated that the core treatment could become important if one were to accept the sludgelike core model proposed recently by Higgins and Kennedy.

Concerning the third question, Chinnery stresses that the cumulative seismic effects have been treated in different ways and that this may be the real reason for the disagreement, although there exists a factor of 10 disagreement in the calculation for an individual earthquake. Dahlen mentioned some computer studies using both Aki's and Brune's moment-magnitude relationships and stated that his conclusions do not change.

There is general agreement between Dahlen, Haubrich, and Smylie that the astronomical data are too noisy to excite a high correlation with earthquakes. At the time of Smylie and Mansinha's 1968 correlation study, only highly smoothed pole paths had been published. It later became apparent in examining the unpublished raw polar motion data that the noise level was substantially higher than was claimed. Mansinha argues that the correlations exist but that the significance of the correlations in the presence of noise is in question. The decisive proof will be the detection of continuing correlation.

If earthquakes do not excite the Chandler motion, what does? Chinnery, Dahlen, and others have at various times speculated on a related hypothesis that the lithospheric motions that are aseismic but 'jerky' on a 14-month time scale are more common than earthquakes themselves and that they could provide the excitation mechanism. Mansinha and Smylie made the same suggestion in an earlier paper (*Science, 161*, 1127, 1968).

Meteorological effects on the earth's rotation were discussed by K. Lambeck. Their influences take two forms: variations in the inertia tensor due to periodic distributions in the atmospheric mass and variations in the relative angular moments due to the movement of air mass with respect to the earth's surface. The changes in the inertia tensor affect mainly the polar motion, and this is the principal contribution to the annual period. The inertia changes are of minor importance for the earth's rate of rotation about the instantaneous rotation axis because the principal transport of air mass is east-west and does not contribute significantly to the product of inertia about the rotation axis. Winds affect the polar motion only if they are ageostrophic. Departures from geostrophic motion are, however, small. Winds do modify very significantly the earth's rate of rotation. Lambeck showed that the zonal winds explained completely the periodic variations in the earth's rotation that are not of tidal origin. In particular, the variable quasi-biennial wind oscillation is very clearly reflected in the astronomical data, and thus some conclusions can be drawn about the period and the variable extent of the downward propagation of these winds (Lambeck and A. Cazenave in *Geophysical Journal, 32*, 79, 1973). A month-by-month computation of the wind excitation function by Lambeck and Cazenave (*Geophysical Journal*, in press, 1973) also showed a very high correlation with the short-period variations in the length of day, and there is no need to invoke an interior mechanism to explain these. The wind excitation function has a typical time scale of a few days. Analysis of the variations in the length of day for short-period tidal terms will therefore be distorted by the wind contribution. There is also evidence for long-period variations in the excitation function. For the 5-year period of analysis, 1958–1963, the long-period variation found in the excitation is of the same magnitude and sign as the long-period variation in the change of length of day. Thus not all long-term fluctuations such as the decade variations can be attributed to core-mantle coupling.

Third Session

Panel on Core-Mantle Interactions

Chairman: D.E. Smylie (York University)

Members: M. D. Fuller (University of Pittsburgh), D. Gubbins (CIRES/NOAA), M.G. Rochester (University of Newfoundland), A. Toomre (MIT)

The subject was introduced by a brief review presented by D.E. Smylie, the

panel chairman. The review included discussions of the possible implications of 1972 results on the viscosity of the core by Gans and *PnKP* seismic phases by Bolt and a comparison of topographic and electromagnetic coupling by Roberts.

Alar Toomre spoke on the general features of the fluid motions in the liquid core. He pointed out that at precessional frequencies inertial coupling is dominant and that the core ought to exhibit the flow features common to all rotating fluids. By citing a result known to classic workers such as Poincaré and Kelvin, Toomre demonstrated that the reported observations of a diurnal wobble of 0″.02 amplitude must surely be wrong because it must be accompanied by a nutation of the rotation axis in space of amplitude comparable to that of the principal nutation and this has not been observed.

M.G. Rochester reviewed the energetics of core-mantle coupling and some 1973 work by Stacey on the transfer of energy to the core from precession. Whether this mechanism provides enough power to drive the geomagnetic dynamo depends critically on the strength of the dissipative fraction of the total coupling; a factor of 10^5 is in question. The conclusion expressed was that more detailed study of the dynamics of core-mantle interaction models is required.

David Gubbins pointed out that the dynamics of the earth's core is not as well understood as was once supposed. The evidence for a large (50 gauss) toroidal magnetic field in the core is very weak because the estimates for it are based on the numerical dynamos of Bullard and Gellman, which have been shown to diverge. This divergence affects the electromagnetic coupling between the core and mantle. Also, if one accepts the ideas of Malkus, Busse, and Elsasser that the core is an iron slurry, the viscosity may be much larger than the usual estimates, and the viscous coupling would thus be raised.

M.D. Fuller commented on some recent archeomagnetic results. With improved descriptions of the geomagnetic field reversals that have come about in the last few years, it appears that associated with the reversal of field direction on a time scale of the order of 10^3 years there is a longer fluctuation in field intensity of 10^4-year time scale. The observations are consistent with a much reduced dipole field with little change in the magnitude of the higher-order harmonics that dominate the nondipole field.

The implications of recent results in archeomagnetism for core-mantle coupling were discussed by members of the panel. The principal result is that, as the main dipole field weakens, the coupling weakens, and the role of westward drift of the main field increases.

Fourth Session

Panel on Long-Term Variations

Chairman: W.M. Kaula (UCLA)

Members: R.H. Dicke (Princeton), C.G.A. Harrison (Miami), P.M. Muller (Jet Propulsion Laboratory), W.H. Munk (University of California, San Diego), H.C. Noltimier (Ohio State), R.J. O'Connell (Harvard), G. Pannella (Puerto Rico), and S.J. Peale (University of California, Santa Barbara)

In an introductory statement W.M. Kaula divided the subject into two parts, observational and theoretical. Extrapolation of polar wander and spin into times before systematic astronomic observations requires special techniques: paleomagnetism for pole locations with respect to continents, chronicle analysis for spin in historic times, and fossil growth bands for spin in geologic times. Attempts to explain the inferred variations include (1) motions in the solid earth for the nontidal acceleration of spin (on a 1000-year time scale) and for polar wander and (2) tidal dissipation in the oceans and resonances with Venus for the tidal deceleration of spin throughout geologic time. Oddly, the original causes of the earth's spin rate and obliquity are not customarily included as part of the subject.

H.C. Noltimier summarized the results for virtual paleomagnetic poles. Data now exist for all periods back to Cambrian for North America, South America, northern Europe, Africa, Australia, and India. Rocks of all periods from these continents are radiometrically dated, save for some Mesozoic and Paleozoic sequences in South America and India. Fewer data are known for west Antarctica, Russia, Siberia, and China.

These data indicate major breakups between continents since Triassic, 200 m.y. ago. In Paleozoic there was apparently also some coming together of separate Russian, Siberian platform, and China plates. The pattern of virtual pole movement is mainly one of gradual motion with occasional rapid motions such as those in Devonian, Carboniferous, and Cretaceous. Of these rapid motions all but the late Triassic-Jurassic and Cretaceous are in common between the continents, and thus a motion of the pole of about 0.3°/m.y. rather than tectonic motion is indicated. The Cretaceous pole path, for example, differs between South America and Africa; this difference indicates the rifting that created the South Atlantic. In Cambrian the continents were clumped together in Pangaea, the south pole being in what is now North Africa.

Detailed data for Precambrian exist only in North America. In a study by Irving, rapid excursions of the apparent pole, of the order of 60°, occurred 1100, 1300, 1950, and 2500 m.y. ago. Data from other continents or tectonic plates are insufficient to determine whether this motion was in common.

Paul H. Muller discussed the analysis of medieval and ancient records of eclipses and other astronomical observations to determine variations of the spin. He concludes, contrary to Newton, the principal recent writer on the subject, that the data supplementary to solar eclipses are insufficient to separate tidal and nontidal decelerations. Assuming the modern rate for tidal deceleration of about $-45''/\text{century}^2$ in lunar motion leads to a historical mean nontidal rotational acceleration of about $22 \times 10^{-9}\omega_E/\text{century}^2$, plus a strong oscillation to negative values in the years 700–1000 A.D.

W.H. Munk presented an analysis by Cartwright of tidal records at Brest, France, back to 1711. They appear to indicate significant changes in amplitude and phase of the M_2 and O_1 components that cannot be attributed to harbor modifications.

G. Pannella reviewed his work on fossil evidence of days per month and days per year. For most of Phanerozoic there are quite reliable results from molluscan bivalves, some specimens showing daily growth increments for more than 40 months. From recent specimens the systematic error is only 1%. The results for Cenozoic indicate excellent agreement with the new higher determinations of tidal deceleration in modern times. The rate appears to have been much lower in Mesozoic, but the data are sparse. In Paleozoic back to 450 m.y. B.P. the average rate was almost as high as that in Cenozoic.

For Precambrian times the only data are stromatolites, daily laminas of algae and sediments. These appear to be much more subject to interruption and hence to giving too few days per month. However, tides appear to have existed back to at least 2800 m.y. B.P., a systematic increase occurring in the number of bands per group back in time. The best estimates are those for Gunflint time (1750 m.y. B.P.), at least 445 days/yr and 36 days/month.

R.J. O'Connell discussed the effects of motions in the solid earth and mass transfers between ice caps and the oceans. Postglacial data indicate a viscous relaxation time of the mantle as low as 1000 years for the oblateness. The isostatic backsurge from the major glacial melting 7900 years B.P. seems sufficient to account for the mean nontidal acceleration in historical time but not for the modern observed polar drift of about 10 cm/yr toward Greenland. Changes in sea level of about 1.5 meters in the years 700–1000 A.D. would be required to account for the oscillation in nontidal acceleration inferred by Muller.

The short viscous relaxation time τ indicates that on the much longer time scale of tectonic activity the earth can be treated as a sphere: the rate of polar wander is proportionate to $I_{13}/[\tau(C'-A')]$, where I_{13} is the maximum product of inertia and $C'-A'$ represents the differences of the principal moments of inertia from those for a fluid earth. Hence, as was emphasized by Goldreich and Toomre, rapid excursions of the pole may not require major tectonic activity to increase I_{13} but may only entail a passage of $C'-A'$ through zero.

W.H. Munk reviewed tidal dissipation in the oceans. The recent solution of the

global tides by Hendershott obtained a total tidal energy twice that for an equilibrium tide. Integration of the lunar and solar work rates over this tidal surface obtains 3.0×10^{19} ergs/sec as the estimated mean dissipation rate, about 50% of that required to account for the recent determinations of lunar acceleration. An additional increment may come from internal tides. The present arrangement of continents could plausibly lead to a tidal energy anomalously high by a factor of 2; the further factor of 2.7 needed to stretch the moon's orbital lifetime to 4.6×10^9 years must come from more limited shallow seas in the past.

S.J. Peale discussed the proposal of Hipkin that resonances between the moon's orbit and Venus may have delayed the tidal evolution. Independent detailed examinations by Hipkin and by Yoder conclude that resonances not dependent on lunar orbit eccentricity are at best marginally stable against tidal disruption and have negligible capture probabilities. Yoder further found that lunar eccentricity dependent resonances are an order of magnitude more stable against tidal disruption but are definitely unstable against variations in planetary orbit eccentricities on a 10^5-year time scale.

W.M. Kaula summarized the integration backward in time of the tidal evolution of the earth-moon system to the early state of a higher lunar orbit inclination, a lower obliquity, and an earth rotation rate half that for instability. The angular momentum, inclination, and obliquity are all compatible with models of planetesimal infall in the later stages of the planetary system formation.

R.H. Dicke reviewed briefly current ideas on $\dot{G}$ change in the gravitational constant, and reaffirmed the unlikelihood of its detection in earth rotation phenomena.

Third Geodesy/Solid-Earth and Ocean Physics (GEOP) Research Conference

Vertical Crustal Motions and Their Causes

Keynote Speaker: Henry W. Menard, Scripps Institute of Oceanography, LaJolla, California

FAWCETT CENTER FOR TOMORROW
THE OHIO STATE UNIVERSITY
COLUMBUS, OHIO

MAY 31–JUNE 1, 1973

Sponsored by: **American Geophysical Union**
National Aeronautics and Space Administration
National Oceanic and Atmospheric Administration
Ohio State University, Department of Geodetic Science
U.S. Geological Survey

The theme for the Third GEOP Research Conference will be set by an introductory review relating to vertical crustal motions and their causes. The conference will be divided into the following sub-topics, each introduced by an invited moderator and discussed by a panel:

1. **Slow Vertical Displacements of Continental Interiors; Chairman: R I. Walcott, Department of Energy, Mines and Resources**
2. **Vertical Motions along Active Continental Margins and Island Arcs; Chairman: Bryan L. Isacks, Cornell University**
3. **Vertical Motions within Oceanic Regions; Chairman: Manik Talwani, Lamont-Doherty Geological Observatory**

Individuals interested in attending the conference are requested to send their applications on the standard application form available from the American Geophysical Union, 1707 L Street, N.W., Washington, D.C. 20036. Information on the membership in the GEOP Research Conferences may be found on page 305 of the April 1972 issue of EOS. Please note that the topics of Conferences 3 and 4 have been interchanged.

Further details on the program, accommodations, and registration will be sent to those applicants selected by the committee to attend the conference by April 15.

Applications for attendance must be received by April 7, 1973.

American Geophysical Union ★ 1707 L Street, N.W. ★ Washington, D.C. 20036

D3

Epeirogeny and Plate Tectonics

H. W. Menard

This review is generated by an intensification of interest in a classical subject of geology, vertical motions of the crust and their causes. The subject was examined qualitatively for more than a century within a paradigm of a mainly static earth that merely moved up and down. The new interest derives from the fact that some aspects of vertical motion can now be explained semiquantitatively and also from the realization that, in the paradigm of a dynamic earth, some vertical motions are related to horizontal drifting.

The fact that large regions of the earth are warped vertically has been known since the beginnings of modern geology. *Lyell* [1835] cites Playfair and Von Buch among others who recognized the uplift of Scandinavia. Likewise, *Darwin* [1842] observed that the distribution of atolls and elevated islands establishes regional warping of ocean basins. The term 'epeirogeny' was coined by *Gilbert* [1890] to describe this broad, gentle warping, which is such a common feature of the history of the whole earth.

Concerning its causes, *Lyell* [1835, vol. 2, p. 349] wrote of the evidences of uplift of Sweden, 'Whether we ascribe these to the expansion of solid matter by continually increased heat, or to the liquification of rock or to the crystallization of a dense fluid, or the accumulation of pent-up gases, in whatever conjectures we indulge, we can never doubt for a moment, that at some unknown depth the structure of the globe is in our time becoming changed from day to day, throughout a space probably more than a thousand miles in length and several hundred in breadth.'

Evidence of the existence of epeirogenic warping accumulated from many sources during the century that followed. Broad plateaus have been elevated and eroded, and broad basins depressed and filled with sediment without significant crustal deformation. Peneplanes and shorelines have been similarly warped. Despite the prevalence of these phenomena, their causes remain conjectural.

At present it appears that the causes of epeirogeny may be divided into four useful classes and the results into two. The causes are external loading or unloading, bending of tectonic plates plunging into subduction zones, internal density changes, and dynamic effects of mantle motion. The results depend on whether the cause is in the lithosphere or below and whether the lithosphere is in motion relative to the asthenosphere. The results are vertical or radial from the center of uplift if drifting is not occurring or if the cause is within the lithosphere. If the cause is in the asthenosphere or deeper and the lithosphere is drifting, the cause may remain fixed or migrate at a different velocity. Thus the expression of epeirogenesis may move across the surface of a plate. Some of the effects may reflect the lateral motion. Visualize the lithosphere riding over a bumpy asthenosphere. Different phenomena may occur on the updrift and downdrift slopes of bumps.

This brief review attempts to span the range of the more important epeirogenic phenomena and their causes but focuses on the most recent developments, which have more immediate implications for further research.

External Loading and Unloading

Loading of the crust may occur by localized accumulation of sediment, volcanic rock, water, or ice; unloading by erosion, evaporation, or melting. These ordinary geological phenomena depress or elevate the underlying and surrounding crust by amounts that depend on the mass and dimensions of the loads. As small a feature as Lake Mead depressed the

This article was taken from the keynote address presented at the third GEOP Research Conference on Vertical Crustal Motions and Their Causes, which was held at The Ohio State University, Columbus, May 31–June 1, 1973.

crust as much as 18 cm in 15 years merely by elastic compression [*Raphael*, 1954]. Larger features also produce epeirogenic effects by elastic bending, plastic flow, and phase changes [*Broecker*, 1962].

The volcanoes of the Hawaiian-Emperor line formed one by one as the lithosphere drifted over a hot spot in the mantle [*Wilson*, 1963]. Each enormous growing volcano has depressed the crust below and also deformed the surrounding sea floor into a moat and arch [*Dietz and Menard*, 1953; *Hamilton*, 1957]. This gentle warping, 500–1000 meters high and extending 500 km from the islands (Figure 1), wraps around the end of the archipelago and thus develops updrift from the active hot spot. It still persists on each side of the Emperor seamounts [*Menard*, 1964], which are more than 40×10^6 years old [*Clague and Jarrard*, 1973].

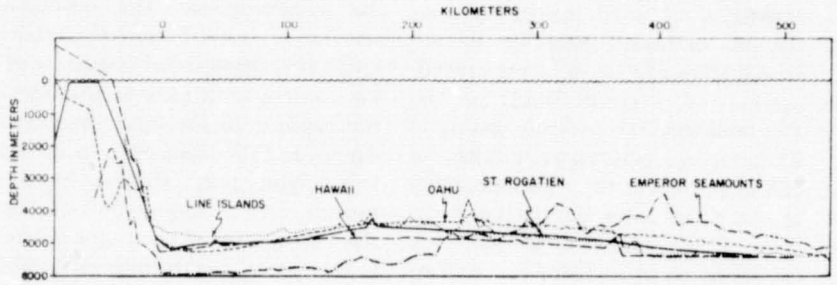

Fig. 1. Bathymetric profiles across moats and arches produced by the load of oceanic volcanoes [from Menard, *1964].*

Transient effects of loading can be studied at the sites of Pleistocene lakes and ice sheets. It was *Gilbert*'s [1890] recognition of the elevation of the crust after the evaporation of Lake Bonneville that caused him to create the term 'epeirogeny.' Subsequent study [*Crittenden*, 1963] confirms that the crust subsided under an average load of 145 meters of water 15,000–25,000 years ago; shoreline features developed, and these have been elevated as much as 64 meters since the load was removed.

The effects of loading and unloading associated with Pleistocene ice sheets were much greater. Scandinavia has recoiled 275 meters since the ice melted [*Daly*, 1934]. The elevation still continues at more than 11 mm/yr in the northern Baltic Sea, the obvious results being noted by Lyell. At the former margins of the ice the crust is sinking 1 mm/yr. Similar epeirogenic phenomena have occurred in eastern North America [*Walcott*, 1972]. In the last 6000 years the crust under the former center of the ice sheet has risen 138 meters and is rising now at 20 ± 5 mm/yr. A free air gravity anomaly of −35 mgal suggests 300 ± 120 meters of further rebound before isostatic compensation is restored. Around this and all other regions of post-glacial rebound is a belt of peripheral submergence about 2000 km wide. At present the coast of Virginia is sinking 4 mm/yr, and tens of meters of subsidence have occurred in some places.

Epeirogenic warping that is the reverse of the glacial sequence presumably occurred in the Mediterranean area. The sea evaporated until it became a desert 3 km below sea level about 6×10^6 years ago [*Hsu*, 1972]. Thus the crust in the center of the basin was first warped upward by unloading and was later depressed by reloading. Presumably, a wide belt of peripheral sinking and then elevation also formed. The occurrence of salt basins around the margins of Africa and elsewhere suggests that evaporation and flooding may be more frequent causes of epeirogenic warping than glaciation is.

Bending at Subduction Zones

The lithosphere bends upward and breaks in tension at the surface as it curves over to plunge into a subduction zone [*Stauder*, 1968]. This action produces fault scarps, tectonic benches, and small grabens [*Ludwig et al.*, 1966]. The upward bend is 200–300 km wide and 300–500 meters high and is accompanied by a free air gravity anomaly of up to +50 mgal [*Talwani*, 1971].

This epeirogenic warp is a permanent dynamic feature during subduction and elevates atolls and volcanic islands. However, they speedily are subducted; thus ancient evidence of this phenomenon is inherently rare.

Density Changes

As *Lyell* [1835] so briefly indicated, there are many ways in which the density may change in the interior of the earth and cause epeirogenic warping at the surface. The reader is referred to *Beloussov* [1962] for a critical review of the extensive geological literature on this subject. Much of the older literature is concerned primarily with relating horizontal thrusting and folding in orogenic belts to sliding or spreading away from epeirogenic elevations [*van Bemmelen*, 1935, 1966; *Rich*, 1937; *Willis*, 1929]. In contrast, the more recent literature focuses on epeirogeny itself as an effect of cooling of the lithosphere or phase changes at various depths.

The lithosphere that is created at spreading centers is elevated to form midocean ridge crests, and it sinks as it ages and spreads to the ridge flanks [*Menard*, 1969]. Several factors in the asthenosphere influence the depth at a ridge crest [*Anderson et al.*, 1973] (Figure 2). Likewise, overriding of asthenospheric bumps introduces variations in the history of sinking of the flanks. Nonetheless the average rate of sinking is quite uniform for crust of a given age (Figure 3). It averages 90 m/10^6 yr for the first 10 m.y., 33 m/10^6 yr for the period from 10–40 m.y., and 20 m/10^6 yr from 40–70 m.y. Although it varies regionally, in any given region the depth is relatively uniform for crust of a given age [*Sclater et al.*, 1971; *McKenzie and Sclater*, 1971]. The regional depth-age curve can be used as a standard to prepare a depth anomaly map after correcting for sediment loading [*Menard*, 1973*a*]. Anomalies in the eastern Pacific have a relief of +700 to −200 meters and wavelengths of 500–2000 km. They continue across fracture zones and thus are independent of age (Figure 4). These anomalies obscure the depth-age curve where the crust is more than 70 m.y. old. The observed heat flow and sink-

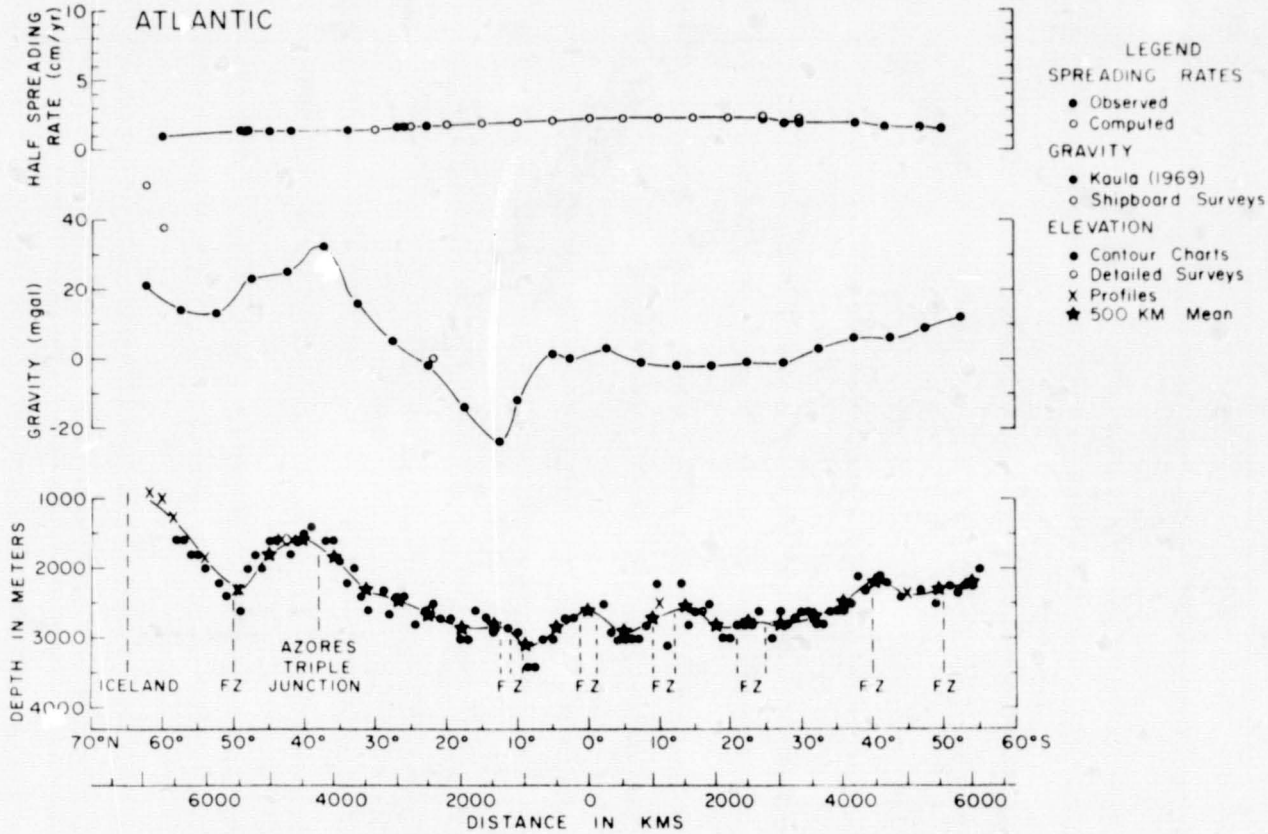

Fig. 2. The close correlation between free air gravity and depth of the crest of the mid-Atlantic ridge [from Anderson et al., *1973]. The large positive gravity anomalies probably are caused by upward convection in the mantle.*

ing of the oceanic lithosphere for 70 m.y. can be explained to a reasonable approximation by the cooling of the lithosphere after it solidifies at a spreading center [*Sclater and Francheteau,* 1970; *Parker and Oldenburg,* 1973]. The depth anomalies are a consequence of the overriding of asthenospheric bumps [*Menard,* 1973*a*] or other epeirogenic phenomena.

Among the other phenomena the most important probably are the phase changes that occur because the crust and mantle consist of silicate minerals that assume different atomic configurations according to the temperature and pressure. The major phase changes of interest have been summarized by *Knopoff* [1969]. Many of the typical silicates of continental crust are transformed to denser phases at about 30-km depth; the feldspars, for example, become garnets. The basalt of the oceanic crust is transformed to eclogite at about the same depth in subduction zones. The pressure on a mineral at depth can readily be

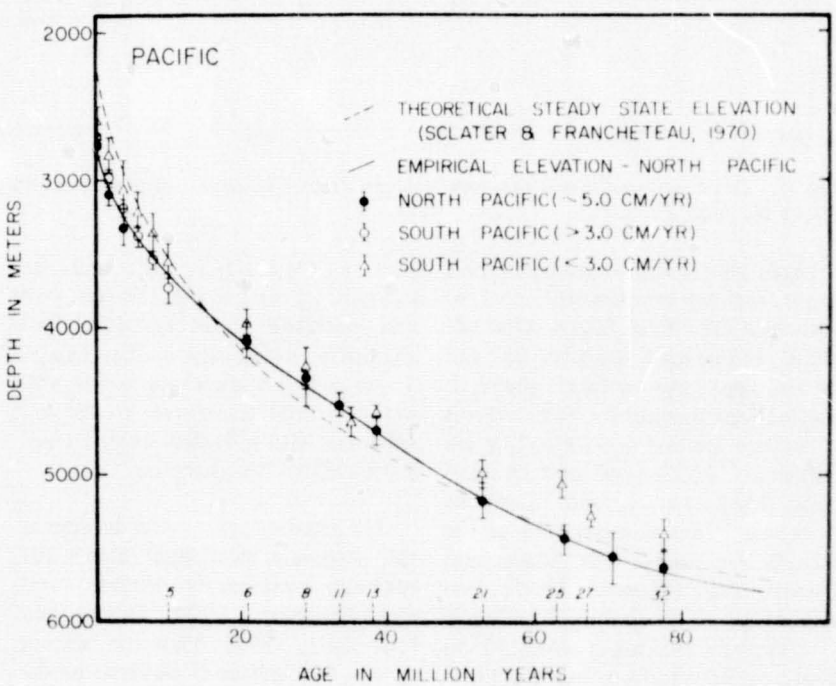

Fig. 3. The correlation of depth and age of oceanic crust in the north Pacific compared with a steady state model of subsidence due to cooling of the lithosphere [from Sclater et al., *1971].*

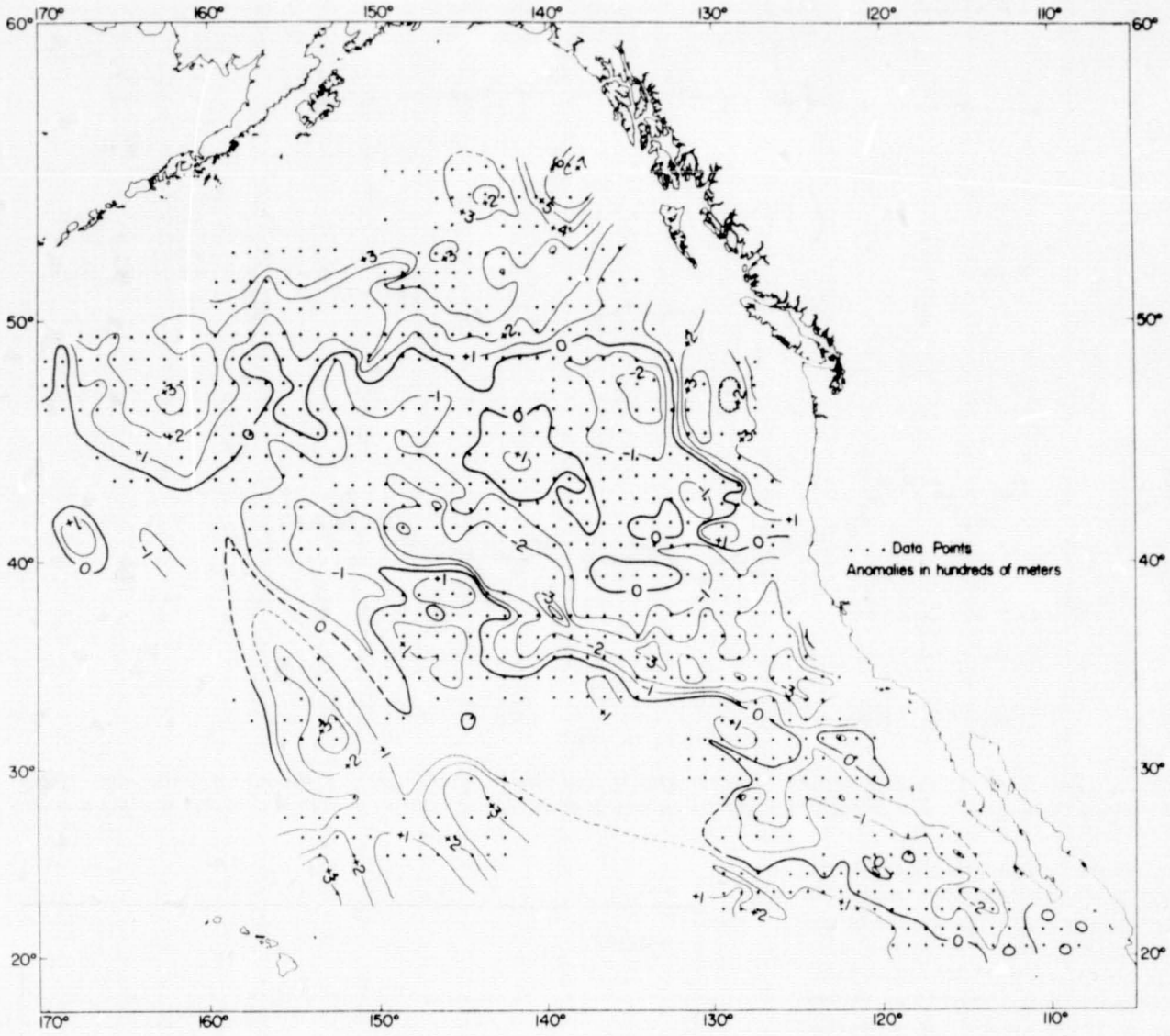

Fig. 4. Depth anomalies in the northeastern Pacific relative to the empirical age-depth relationship shown in Figure 3 [from Menard, *1973a].*

changed by erosion or sedimentation above, and the temperature can vary with heat flow from below. Thus the phase boundaries migrate up and down, and the surface above is warped epeirogenically. The effects of surface loading and unloading are reinforced [*O'Connell and Wasserburg,* 1967, 1972], and enormous thicknesses of sediment, such as the 10–20 km under the Black and Caspian Seas [*Menard,* 1967], can accumulate in basins only 5 km deep.

The phase changes at about 30-km depth occur mainly within the lithosphere and thus drift with it. Phase changes deeper than 100 km do not. Two minerals that are probably common in the upper mantle are enstatite ($MgSiO_3$) and forsterite (Mg_2SiO_4). At a depth of about 400 km, enstatite alters to spinel and stishovite; its density increases from 3.1 to 3.4–3.5 g/cm^3. At about 600 km, forsterite transforms to the spinel form with a density change from 3.2 g/cm^3 to 3.5–3.6 g/cm^3.

The lithosphere may be defined as the relatively rigid layer above the melting temperature [*Sclater and Francheteau,* 1970; *Parker and Oldenburg,* 1973]. Thus the bottom of the lithosphere is elevated or depressed by any deep phase changes that may occur. However, the prevalence or importance of this phenomenon is at present unknown.

Mantle Motion

Free air gravity anomalies with amplitudes of tens of milligals and wavelengths of thousands of kilometers (Figure 5) have been discovered by analysis of perturbations in satellite orbits [*Gaposchkin and Lambeck,* 1971]. The rigid lithosphere is too weak to sustain such broad anomalies, and the asthenosphere below is even weaker. It follows that the anomalies are the consequences of convection in the mantle [*McKenzie,* 1967; *Kaula,* 1972], which causes a relief to form on the upper surface of the asthenosphere. Upward convection causes positive gravity anomalies and anomalously shallow depths [*Morgan,* 1972;

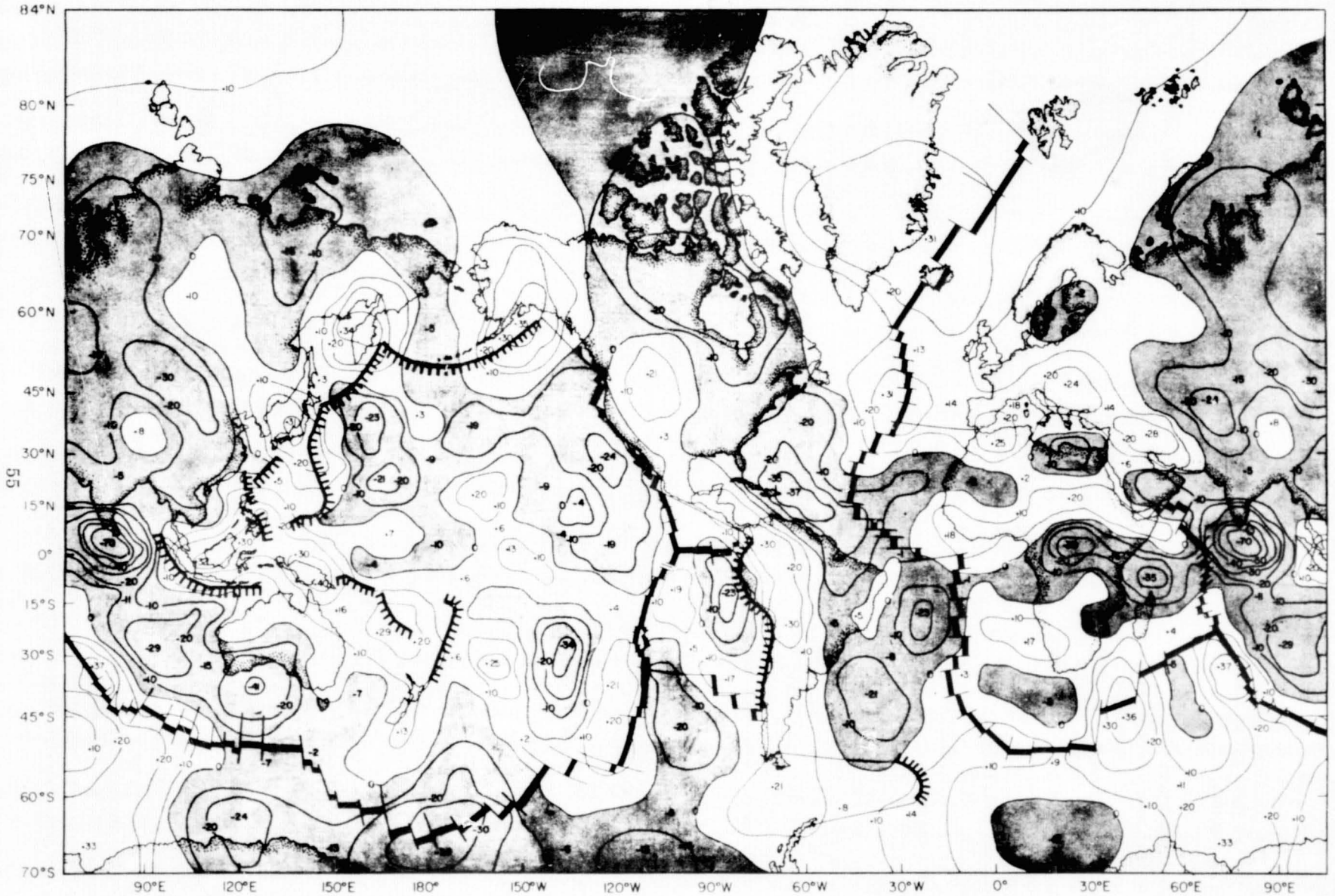

Fig. 5. Free air gravity anomalies and major tectonic plate boundaries [from Anderson et al., *1973].*

Anderson et al., 1973; *Menard*, 1973*a*].

Epeirogenic warping of a kilometer or more occurs as the lithosphere drifts over asthenospheric bumps. The question of the persistence of the bumps will be examined in the next section.

Epeirogeny and Drift

The relationship between epeirogeny and drift can readily be visualized in terms of rates of motion of the lithosphere relative to the asthenosphere. The type of epeirogeny observed in the Russian platform is probably typical of a motionless lithosphere. Lithofacies maps show the shoreline drifting across the platform during Paleozoic and Mesozoic time, but the main loci of deposition move hardly at all [*Beloussov*, 1962]. Where thick sandstone accumulates at one time, thick shale accumulates at another. In this way a few kilometers of sediment is deposited in basins a few hundred kilometers in diameter during a period of more than 10^8 years. Epeirogeny had geological effects, but they are visible mainly because the platform environment was otherwise stable.

A more active stage of epeirogeny has formed great domes in East Africa, the Rhine region, the Baikal region, and elsewhere. The domes are 1–2 km high and 10^2–10^3 km in diameter and persist for 10^7–10^8 years. The Rhine region is an example of a small but otherwise typical feature [*Cloos*, 1939]. An area about 300 km in diameter was warped upward during Mesozoic and early Tertiary time. In the Oligocene a graben formed along what are now the upper and lower Rhine valleys, with a branch into Hesse. Tertiary and Quaternary vulcanism accompanied the faulting.

The great grabens that form on epeirogenic domes are 50–200 km wide and 200–2000 km long and are bounded by steep fault systems 1–2 km high. They characteristically occur in groups of three, radiating from a point near the center of the uplift, but other patterns occur (Figure 6). *Wilson* [1972] has proposed that the initial fracturing of immobilized lithosphere occurs along such grabens. Domes may form anywhere without regard to the distribution of continents or ocean basins. As the doming continues, rifts extend outward and eventually intersect. At this stage the lithosphere is broken into plates, which may become mobilized by the same mantle convection that causes the initial doming [*Wilson and Burke*, 1973]. Heat intrusion along the rifts causes thermal expansion and uplift of mountains such as those that border the Red Sea [*Kinsman*, 1973]. Cooling subsequently causes subsidence and produces the continental shelf [*Sleep*, 1971].

This hypothesis has been strengthened by incorporating the related origin of aulacogens, which are sediment-filled grabens that trend at steep angles to other structures in many continental shields [*Shatsky*, 1955]. They are 100–300 km wide, and many are more than 1000 km long. They die out in the interiors of platforms but are deep enough to accumulate geosynclinal thicknesses of sediment at the edges [*Salop and Scheinmann*, 1969]. Aulacogens may be viewed as 'failed arms' of triple junctions with regard to plate tectonics [*Dewey and Burke*, 1973]. They occur at reentrants in shields because the other two arms became spreading centers. The Benue trough of the Gulf of Guinea is an example of a failed arm that can be related to the opening of the Atlantic basin [*King*, 1950; *McConnell*, 1969]. It contains 4–8 km of Cretaceous and Cenozoic rock, beginning with a marine sequence of Early Cretaceous sediments that have been broadly folded [*King*, 1962]. The two buried troughs of the Argentine continental shelf [*Ewing et al.*, 1963] probably are similar aulacogens. They are 150–200 km wide, at least 700 km long, and 6–8 km deep (Figure 7). They occur near the point where the change in trend of the southwest tip of Africa formerly rested against South America [*Bullard et al.*, 1965].

Gondwanaland may have fractured along rifts connecting triple junctions over hot rising mantle plumes [*Morgan*, 1972; *Wilson*, 1972]. Indeed the plumes or lines of divergent convection that caused the separation of India may still persist

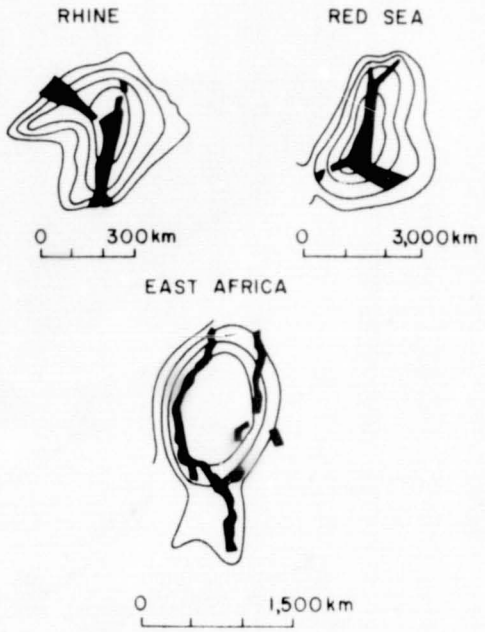

Fig. 6. Rifting over broad low continental domes. The contours indicate the shape of the epeirogenic uplift [after Beloussov, *1962].*

in the southwestern Indian Ocean [*Menard*, 1973*b*], where they cause a complex pattern of intense positive gravity anomalies. India, which has a roughly equivalent shape and size, was over the present location of

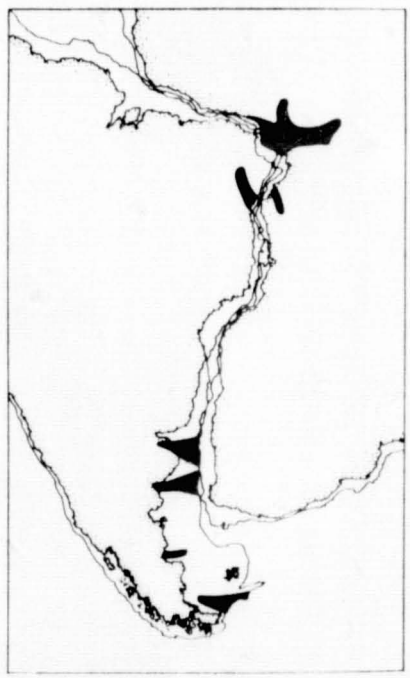

Fig. 7. Aulacogens and probable aulacogens that formed when the Atlantic began to open [after Bullard et al., *1965;* King, *1950;* Ewing et al., *1963].*

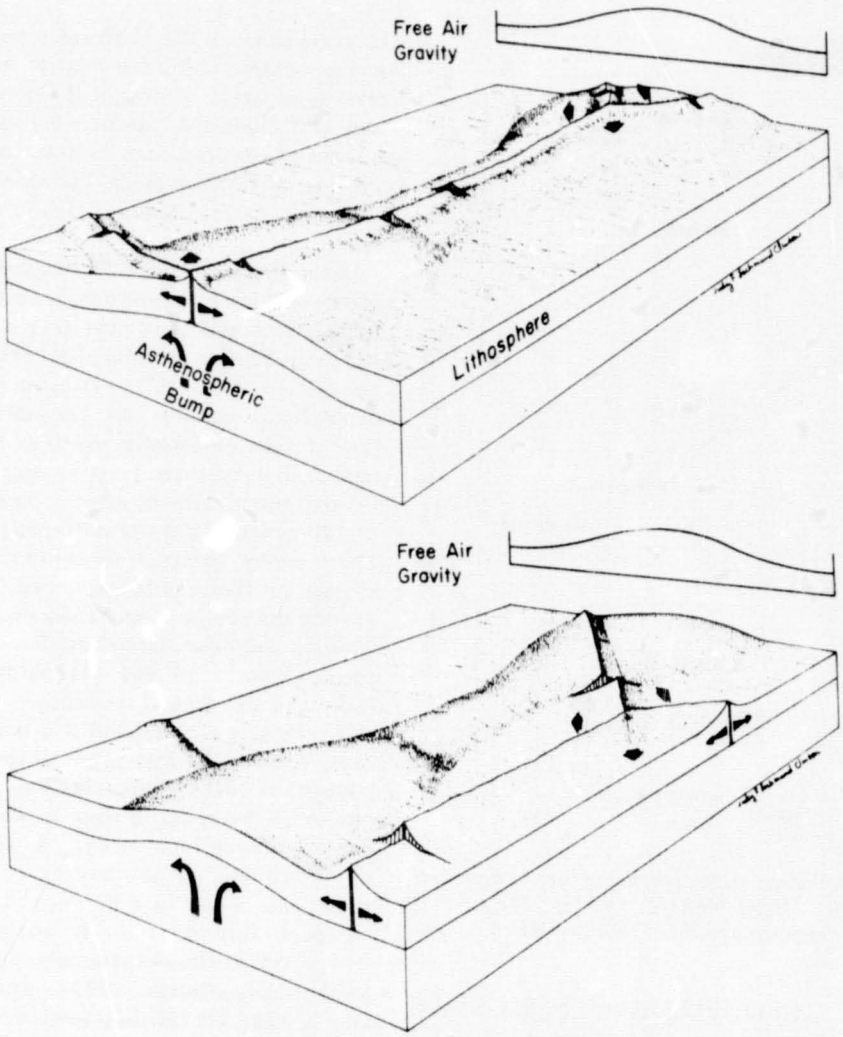

Fig. 8. (Top) Formation of plate boundaries. Rifting produces incipient triple junctions over asthenospheric bumps that are elevated by mantle plumes. The triple junctions are connected by extending rifts that tend to follow less intense lines of upward convection. (Bottom) Drift of plate boundaries. The tectonic plates and the boundaries between them drift according to the rules of plate tectonics. The mantle plumes, asthenospheric bumps, and associated gravity anomalies may remain fixed relative to the spin axis, as was proposed by Morgan *[1972], or they may also drift or decay.*

these anomalies when it separated from Gondwanaland 180 m.y. ago [*Dietz and Holden*, 1970].

A new epeirogenic regime arises when an episode of drifting begins. In addition to the opening of rifts and vulcanism the lithosphere begins to ride over asthenospheric bumps, and epeirogenic phenomena migrate (Figure 8). *Faure* [1971, 1972] has identified epeirogenic waves moving through Africa by their effects of slowly alternating erosion and deposition. They have the following characteristics: height, 1–10 km; wavelength, 10^2-10^3 km; period, 10^7-10^8 years. The speed, 0.1–10 cm/yr, is not determined accurately enough for the present purposes by the sedimentary record. However, the fixed hot spot hypothesis indicates very slow motion of Africa over the mantle [*Burke and Wilson*, 1972] and thus slow epeirogenic warping.

Another example of the effects of slow drift over an asthenospheric bump can be seen in western North America. At present a large positive gravity anomaly of the type attributed to rising mantle convection exists in the region. 'The continent has thus been riding over a substructure of considerable relief' [*Gilluly*, 1973, p. 509]. The asthenospheric bump, and thus the convection, apparently has persisted since early Mesozoic time. Gilluly suggests that flow away from the asthenospheric bump may have contributed to the variations in crustal thickness and to the formation of the Uinta and Owl Creek ranges, which are parallel to the dominant drift direction. Drifting over the bump may also have triggered the 'orogenic wave' that migrated across the region from west to east from Jurassic to Paleocene time at an average rate of about 2 cm/yr for roughly 10^8 years.

Some effects of faster drift over asthenospheric bumps can be seen in the Pacific plate, which is drifting past hot spots presumably fixed in the mantle at roughly 10 cm/yr [*Morgan*, 1972, 1973; *Clague and Jarrard*, 1973] in the central Pacific. In the Atlantic, the Azores, and Iceland, hot spots lie relatively near the center of asthenospheric bumps over mantle plumes. In the Pacific, however, the hot spots are shifted from the centers of the bumps to the updrift sides [*Menard*, 1973*a*]. The active hot spots associated with the Hawaiian and Austral islands and the recently active ones associated with the Society and Marquesas islands all lie on the updrift sides of broad positive gravity anomalies (Figure 9). The Pratt-Welker chain of seamounts in the Gulf of Alaska is on the updrift side of a large depth anomaly, but the gravity anomaly is unknown. Some of the hot spots have been active for more than 40 m.y.; the association suggests that the bumps and gravity anomalies have been equally persistent.

The uplift of atolls can also be related to overriding of asthenospheric bumps, and it is probable that both carbonate deposition and the locus of turbidites are affected by overriding, but, if so, these effects have not been detected.

In sum a wide range of geological phenomena can be explained by differences in the rates of epeirogeny and drift. Most of the relationships imply that the present regions of broad uplift have been such for 10^7-10^8 years.

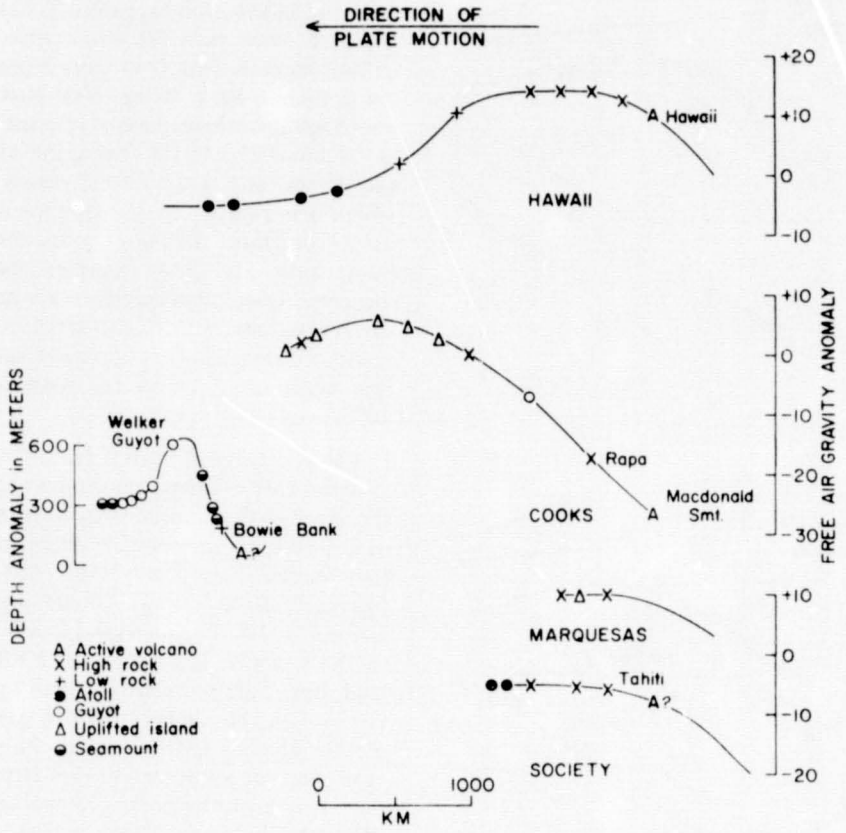

Fig. 9. The association of Pacific hot spots with asthenospheric bumps indicated by gravity and depth anomalies [from Menard, *1973a]. The lines of sections are in the direction of plate motion assuming that the Hawaiian and Macdonald seamount hot spots are fixed.*

Oceanic Epeirogeny

Epeirogenic warping in ocean basins depends on a combination of lithospheric cooling and overriding of asthenospheric relief that is amenable to semiquantitative analysis. With due consideration to the direction and intensity of vertical motions the ocean basins can be divided into several epeirogenic realms, which are characterized by different aspects of marine geology.

A few numbers must be developed before discussing the epeirogenic realms; among them are the rates of vertical motion caused by overriding. *Anderson et al.* [1973] have found a relationship between gravity anomalies and the depth of midocean ridge crests, which indicates that very broad asthenospheric bumps have slopes of as much as 1.3 m/km. In the eastern Pacific, depth anomalies have slopes as great as 5 m/km for 100 km [*Menard,* 1973*a*], and they probably are widespread. Drift rates are in the range of 1–10 cm/yr, and this means that overriding of very broad asthenospheric bumps can produce vertical motions of 13–130 m/10^6 yr. Overriding of local bumps can result in vertical motion of 50–500 m/10^6 yr.

Another number that is useful is the rate of truncation of volcanic islands because it can indicate the time during which a drowned ancient island was at sea level and therefore neither sinking nor rising. The width of the insular shelf was measured on published charts of dated islands in the Canary group [*Bosshard and Macfarlane,* 1970] and the Hawaiian group [*Jackson et al.,* 1972; *Clague and Jarrard,* 1973]. It ranges from about 2 to 8 km around the Hawaiian Islands, aged 1–6 m.y., and also ranges from 2 to 8 km around three of the Canary Islands, aged 12–16 m.y. The rate of shelf widening can be approximated by a simple model in which wave erosion at a constant sea level removes rock at a constant rate from a straight coast; it is independent of the slope. It appears that it requires tens of millions of years to cut a flat platform across a large oceanic volcano if relative sea level is constant or even if it fluctuates as it did in the Pleistocene. Even a series of terraces, such as occur on the top of Horizon guyot [*Lonsdale et al.,* 1972], may require 10 m.y. to cut.

The first of three epeirogenic realms of the ocean basins consists of ridge crests and crust less than 10 m.y. old. This crust sinks at an average rate of 90 m/10^6 yr because of lithospheric cooling. At the same time it rises or sinks as much as 13 meters if it drifts at 1 cm/yr over a normal broad asthenospheric bump or 130 meters if it drifts at 10 cm/yr. The observed spectrum of depth versus age profiles can be explained by drifting up bumps at speeds to about 7 cm/yr and down bumps at about 3 cm/yr (Figures 10 and 11). Within this realm the normal tendency is to sink relatively rapidly, and it is not a likely site for the truncation of large guyots. If lithospheric cooling is reinforced by rapid drifting down a bump, sinking can occur at 200 m/10^6 yr. The circumstances on the west flank of the Juan de Fuca ridge approach this situation. It appears that sinking has been extremely rapid [*Melson and Simkin,* 1972], which may account for the deep terraces on the flanks of Cobb seamount on this ridge [*Schwartz,* 1972].

The second epeirogenic realm consists of the flanks of ridges with crust aged 10–70 m.y. Lithospheric cooling causes a tendency to sink at 20–30 m/10^6 yr. This can be balanced by riding up a broad steep bump at only 2–3 cm/yr or gentle bumps at faster speeds; thus it is hardly surprising that sea floor profiles show reversals in the depth-age curve in many places [*Menard,* 1969].

This second realm is the ideal locus for the truncation of guyots, provided that the lithosphere is drifting rapidly relative to the asthenosphere. Most guyots are in the central western Pacific [*Hess,* 1946; *Menard,* 1964]; they are large volcanoes that were truncated (or conceivably constructed) in water that was commonly only 3.5–4.0 km deep. The Darwin rise was a broad epeirogenic upwarp whose existence about 100

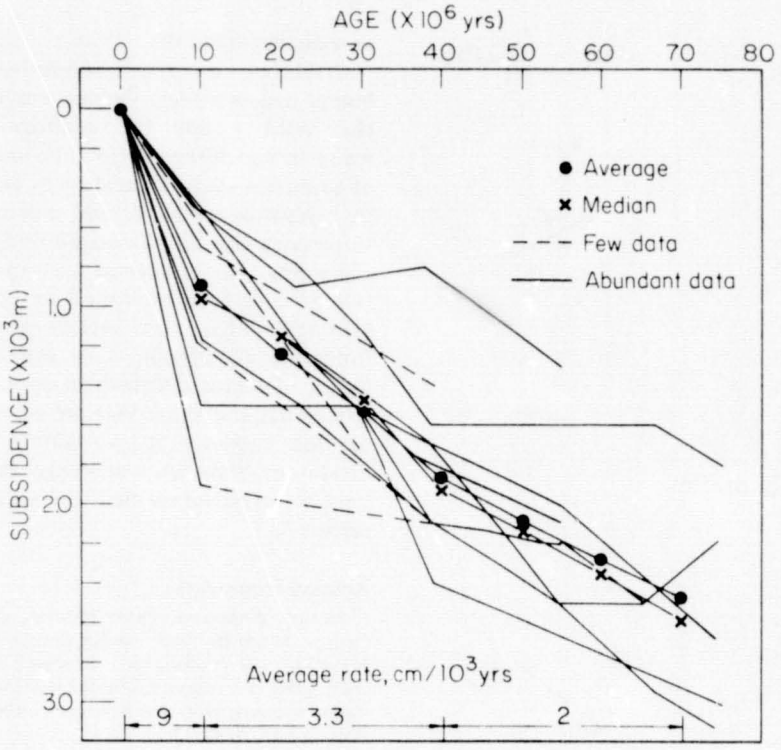

Fig. 10. Profiles of subsidence versus age of the sea floor [from Menard, *1969]. Depth profiles have been normalized to the same depth at zero age in order to eliminate variations shown in Figure 2. Individual profiles show elevation instead of subsidence and also subsidence at accelerated rates at various times. They correspond to profiles of the depth anomalies shown in Figure 4 and probably are produced by overriding asthenospheric relief at different rates as indicated in Figure 11.*

m.y. ago was postulated on the fact that the guyots were truncated in water typical of midocean ridges [*Menard,* 1964]. It is now known that the postulated ridge was not a center of spreading [*Larson and Chase,* 1972], but that fact in no way invalidates the evidence of shallow water. The Darwin rise may be considered to be evidence of an ancient asthenospheric bump.

The exact age of the crust under the central Pacific guyots and atolls remains uncertain, but drilling and magnetic mapping provide adequate dating for the present purposes [*Larson and Chase,* 1972]. The mid-Pacific mountains rest on crust aged about 110–140 m.y., but many of them were truncated volcanic platforms at sea level during the period 100–110 m.y. B.P. [*Hamilton,* 1956]. If they had formed at the ridge crest, they would have sunk too fast to be truncated unless they were riding up an asthenospheric bump. If they had formed on crust 30–40 m.y. old, they would have been in deeper water unless they were on a bump. Drilling at Eniwetok [*Kulp,* 1963] and Horizon guyot [*Winterer et al.,* 1971] indicates that emplacement of shallow water fossils occurred during the period 50–65 m.y. B.P., when the crust was already 60–70 m.y. old. It should have been more than 5 km deep but was only about 3.5 km deep, and therefore it was again passing over an asthenospheric bump.

The third realm consists of the main ocean basins with crust older than 70 m.y. Lithospheric cooling is either complete or so slow that it produces little continuing subsidence. The vertical motions caused by overriding mantle relief, however, are as intense as ever and therefore exert a dominant influence on the depth. In this realm, hot spots may generate volcanoes where the lithosphere is moving very rapidly over asthenospheric bumps. However, few of them, at least in the Hawaiian and Austral islands, seem destined to become guyots. In the Hawaiian group they are still active when they reach the crest of the bump, and they ride down the downdrift side of the bump too fast to be truncated [*Menard,* 1973*a*]. In the Australs and Cooks the volcanoes generally continue to ride upward and thus to be elevated until they disappear into the Tonga trench.

'Midplate rises' are distinctive elevations that occur in the third realm, persist for long periods, and drift with the plate [*Menard,* 1969]. Typical midplate rises are the Shatsky rise in the northwestern Pacific and the Manihiki and Solomons rises in the southwestern Pacific. The Shatsky rise has an area of about 5×10^5 km^2, a relief of about 2500 meters, and a depth above 3000 meters. The sedimentary cover is 800–1000 meters thick [*Ewing et al.,* 1966] and consists of Cretaceous and younger calcareous ooze and clay [*Fischer and Heezen,* 1971]. The Manihiki rise is very similar with regard to area, elevation, relief, thickness of sediment, and age [*Heezen et al.,* 1966]. The Solomons rise is also similar, but the sedimentary cover is cut by normal faulting [*Woollard et al.,* 1967].

It appears that midplate rises originate within plates, and it is certain that they are actively elevated in the second or third epeirogenic realm [*Menard,* 1969]. The fact that some, at least, existed as the shallow sites of carbonate sediment more than 10^8 years ago and are still shallow indicates that they drift with the plate. Seismic refraction measurements of the Shatsky rise show an exceptional thickness of roughly 4 km of volcanic rock, a relatively normal oceanic layer, and an apparent lens of low velocity mantle as much as 10 km thick. The thick volcanic rock would produce some shoaling, and the low velocity lens may be the locus of a phase change [*Den et al.,* 1969]. The Eauripik–New Guinea rise, another midplate rise, has a volcanic layer like the surrounding basins, but an oceanic layer, or low velocity root, 12–15 km thick [*Den et al.,* 1971]. It probably is this root that has caused the uplift of about 2 km, which has persisted about 35 m.y. [*Winterer and Riedel,* 1971].

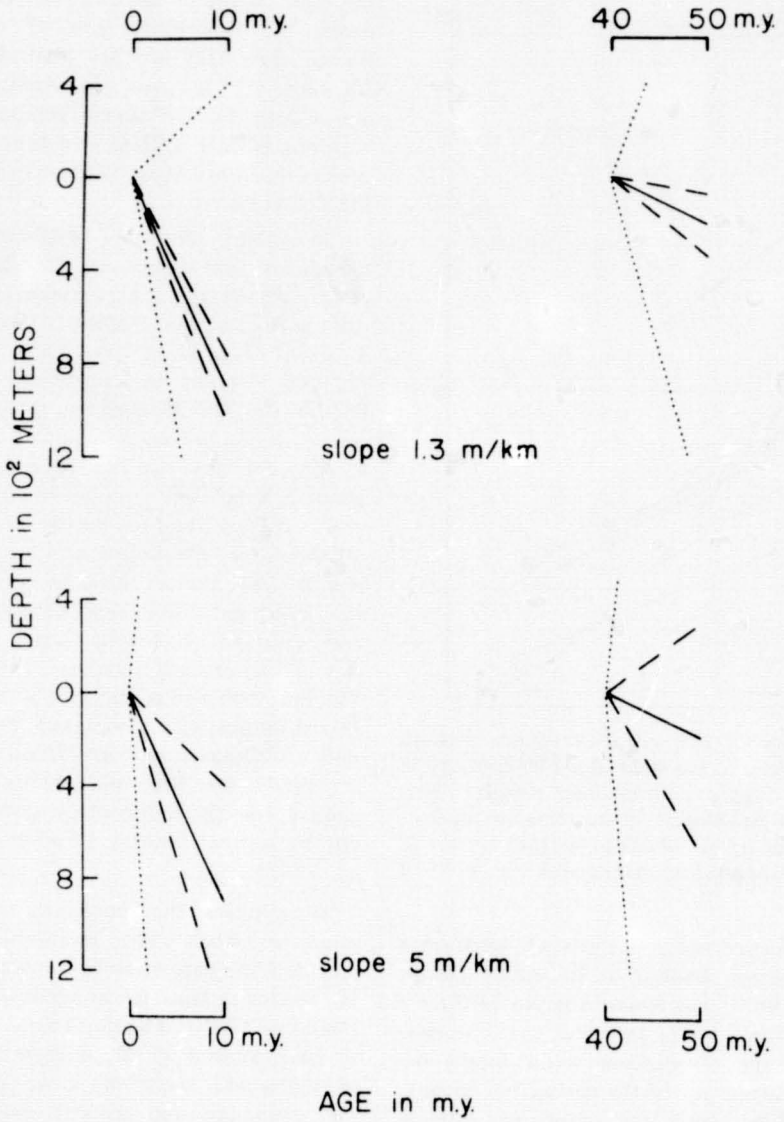

Fig. 11. The combined effects of lithospheric cooling and overriding of asthenospheric relief at different speeds upon normalized profiles of depth versus age of oceanic crust. The solid line indicates the effect of lithospheric cooling alone; the dashed line, cooling plus overriding up or down slope at 1 cm/yr; and the dotted line, cooling plus overriding up or down slope at 10 cm/yr. Note that very fast drifting up even a gentle slope produces elevation of crust of any age. Slow drifting produces elevation only if the crust is old and moves up a steep slope.

The cause of midplate rises is certainly within the lithosphere and long persistent; the most probable causes are phase changes near the top of the mantle and thermal expansion due to heating over hot spots.

Conclusions

Epeirogenic warping has important geological effects on continents and ocean basins. Some effects are transient; some persist for 10^8 years or more. Epeirogeny has various causes: some are within the lithosphere and drift with it; some are below and do not.

One type of epeirogenic doming occurs over asthenospheric bumps, which apparently are caused by rising plumes or limbs of mantle convection. It is possible that the initial disruption of lithospheric plates tends to occur over such domes and the tensional rifts that spread out from them. The rifts become spreading centers, radiating from a triple junction. Frequently, one spreading center fails and becomes an aulacogen, or sediment-filled rift.

Drifting over asthenospheric bumps causes effects that depend on the velocity and the epeirogenic realm in which they occur. The locus of some hot spots, truncation of guyots, elevation of atolls, and possibly subsidence can all be related to fast overriding. No effects of fast overriding have been identified in continents. This may reflect some fundamental difference in the behavior of tectonic plates that contain continents and those that are wholly oceanic. However, it may merely indicate the state of knowledge in a field of investigation that is changing rapidly.

Acknowledgments

Roger Anderson, Peter Molnar, and George Sharman made useful comments regarding the manuscript. Research on epeirogeny was supported by the Oceanography Section, National Science Foundation, grant GA-39219.

References

Anderson, R.N., D.P. McKenzie, and J.G. Sclater, Gravity, bathymetry, and convection in the earth, *Earth Planet. Sci. Lett., 18*, 391–407, 1973.

Beloussov, V.V., *Basic Problems in Geotectonics*, McGraw-Hill, New York, 1962.

Bosshard, E., and D.J. Macfarlane, Crustal structure of the western Canary Islands from seismic refraction and gravity data, *J. Geophys. Res., 75*, 4901–4919, 1970.

Broecker, W.S., The contribution of pressure induced phase changes to glacial rebound, *J. Geophys. Res., 67*, 4837–4842, 1962.

Bullard, E.C., J.E. Everett, and A.G. Smith, The fit of the continents around the Atlantic, in a Symposium on Continental Drift, *Phil. Trans. Roy. Soc. London, Ser. A, 258*, 41–59, 1965.

Burke, K., and J.T. Wilson, Is the African plate stationary?, *Nature, 239*, 387–390, 1972.

Clague, D.A., and R.D. Jarrard, Tertiary plate motion deduced from the Hawaiian-Emperor chain, *Geol. Soc. Amer. Bull., 84*, 1135–1154, 1973.

Cloos, H., Hebung, Spaltung, Vulcanismus, *Geol. Rundsch., 30*, 406–527, 1939.

Crittenden, M.D., Jr., Effective viscosity of the earth derived from isostatic loading of Pleistocene Lake Bonneville, *J. Geophys. Res., 68*, 5517–5530, 1963.

Daly, R.A., *The Changing World of the Ice Age*, Yale University Press, New Haven, Conn., 1934.

Darwin, C., *The Structure and Distribution of Coral Reefs*, Smith, Elder, London, 1842.

Den, N., W.J. Ludwig, S. Murauchi, J.I. Ewing, H. Hotta, N.T. Edgar, T. Yoshii,

T. Asanuma, K. Hagiwara, T. Sato, and S. Ando, Seismic-refraction measurements in the northward Pacific basin, *J. Geophys. Res., 74,* 1421–1434, 1969.

Den, N., W.J. Ludwig, S. Murauchi, M. Ewing, H. Hotta, T. Asanuma, T. Yoshii, A. Kubotera, and K. Hagiwara, Sediments and structure of the Eauripik–New Guinea rise, *J. Geophys. Res., 76,* 4711–4723, 1971.

Dewey, J.F., and K. Burke, Plume generated triple junctions (abstract), *Eos Trans. AGU, 54,* 239, 1973.

Dietz, R.S., and J.C. Holden, The breakup of Panagea, *Sci. Amer., 223,* 30–41, 1970.

Dietz, R.S., and H.W. Menard, Hawaiian swell, deep, and arch, and subsidence of the Hawaiian Islands, *J. Geol., 61,* 99–113, 1953.

Ewing, M., W.J. Ludwig, and J.I. Ewing, Geophysical investigations in the submerged Argentine coastal plain, 1, *Geol. Soc. Amer. Bull., 74,* 275–292, 1963.

Ewing, M., T. Saito, J. Ewing, and L.H. Burckle, Lower Cretaceous sediments from the northwest Pacific, *Science, 152,* 751–755, 1966.

Faure, H., Relations dynamiques entre la croûte et le manteau d'après l'étude de l'évolution paléogéographique des bassins sedimentaires, *C. R. Acad. Sci., Ser. D, 265*(11), 3239–3242, 1971.

Faure, H. Paléodynamique du craton africain, *Proc. Int. Geol. Cong. 24th, Sect. 3,* 44–50, 1972.

Fischer, A.G., and B.C. Heezen, Introduction, in *Initial Reports of the Deep Sea Drilling Project,* vol. 6, pp. 3–16, U.S. Government Printing Office, Washington, D.C., 1971.

Gaposchkin, E.M., and K. Lambeck, Earth's gravity field to the sixteenth degree and station coordinates from satellite and terrestrial data, *J. Geophys. Res., 76,* 4855–4883, 1971.

Gilbert, G.K., *Lake Bonneville, Monogr. 1,* 438 pp., U.S. Geological Survey, Washington, D.C., 1890.

Gilluly, J., Steady plate motion and episodic orogeny and magmatism, *Geol. Soc. Amer. Bull., 84,* 499–514, 1973.

Hamilton, E.L., Sunken islands of the mid-Pacific mountains, *Geol. Soc. Amer. Mem., 64,* 1956.

Hamilton, E.L., Marine geology of the southern Hawaiian ridge, *Geol. Soc. Amer. Bull., 68,* 1011–1026, 1957.

Heezen, B.C., B. Glass, and H.W. Menard, The Manihiki plateau, *Deep Sea Res. Oceanogr. Abstr., 13,* 445–458, 1966.

Hess, H.H., Drowned ancient islands of the Pacific basin, *Amer. J. Sci., 244,* 772–791, 1946.

Hsu, K.J., When the Mediterranean dried up, *Sci. Amer., 227,* 26–36, 1972.

Jackson, E.D., E.A. Silver, and G.B. Dalrymple, Hawaiian-Emperor chain and its relation to Cenozoic circum-Pacific tectonics, *Geol. Soc. Amer. Bull., 83,* 601–618, 1972.

Kaula, W.M., Global and gravity tectonics, in *The Nature of the Solid Earth,* edited by E.C. Robertson, pp. 385–405, McGraw-Hill, New York, 1972.

King, L.C., Speculations upon the outline and mode of disruption of Gondwanaland, *Geol. Mag., 87,* 353–359, 1950.

King, L.C., *The Morphology of the Earth,* Hafner, New York, 1962.

Kinsman, D.J., Rift valley basins and sedimentary history of trailing continental margins, in *Petroleum and Global Tectonics,* edited by S. Judson and A.G. Fischer, Princeton University Press, Princeton, N.J., in press, 1973.

Knopoff, L., The upper mantle of the earth, *Science, 163,* 1277–1287, 1969.

Kulp, J.L., Potassium-argon dating of volcanic rocks, *Bull. Volcanol., 26,* 247–258, 1963.

Larson, R.L., and C.G. Chase, Late Mesozoic evolution of the western Pacific Ocean, *Geol. Soc. Amer. Bull., 83,* 3627–3644, 1972.

Lonsdale, P., W.R. Normark, and W.A. Newman, Sedimentation and erosion on Horizon guyot, *Geol. Soc. Amer. Bull., 83,* 289–315, 1972.

Ludwig W.J., J.I. Ewing, M. Ewing, S. Murauchi, N. Den, S. Asano, H. Hotta, M. Hayakawa, T. Asanuma, K. Ichikawa, and I. Noguchi, Sediments and structure of the Japan trench, *J. Geophys. Res., 71,* 2121–2137, 1966.

Lyell, C., *Principles of Geology,* 4th ed., 4 vol., John Murray, London, 1835.

McConnell, R.B., Fundamental fault zones in the Guiana and West African shields in relation to presumed axes of Atlantic spreading, *Geol. Soc. Amer. Bull., 80,* 1775–1782, 1969.

McKenzie, D.P., Some remarks on heat flow and gravity anomalies, *J. Geophys. Res., 72,* 6261–6273, 1967.

McKenzie, D., and J.G. Sclater, The evolution of the Indian Ocean since the Late Cretaceous, *Geophys. J. Roy. Astron. Soc., 25,* 437–528, 1971.

Melson, W.G., and T. Simkin, Vulcanism and bathymetric symmetry on actively spreading ridges and rises, paper presented at Fall Annual Meeting, AGU, San Francisco, Calif., Dec. 4–7, 1972.

Menard, H.W., *Marine Geology of the Pacific,* McGraw-Hill, New York, 1964.

Menard, H.W., Transitional types of crust under small ocean basins, *J. Geophys. Res., 72,* 3061–3073, 1967.

Menard, H.W., Elevation and subsidence of oceanic crust, *Earth Planet. Sci. Lett., 6,* 275–284, 1969.

Menard, H.W., Depth anomalies and the bobbing motion of drifting islands, *J. Geophys. Res., 78,* 5128–5137, 1973*a*.

Menard, H.W., Does Mesozoic mantle convection still persist?, *Earth Planet. Sci. Lett.,* in press, 1973*b*.

Morgan, W.J., Deep mantle convection plumes and plate motions, *Bull. Amer. Ass. Petrol. Geol., 56,* 203–213, 1972.

Morgan, W.J., Plate motions and deep mantle convection, in Studies in Earth and Space Sciences, *Geol. Soc. Amer. Mem., 132,* 7–22, 1973.

O'Connell, R.J., and G.J. Wasserburg, Dynamics of the motion of a phase change boundary to changes in pressure, *Rev. Geophys. Space Phys., 5,* 329–410, 1967.

O'Connell, R.J., and G.J. Wasserburg, Dynamics of submergence and uplift of a sedimentary basin underlain by a phase change boundary, *Rev. Geophys. Space Phys., 10,* 335–368, 1972.

Parker, R.L., and D.W. Oldenberg, A thermal model for oceanic ridges, *Nature, 242,* 137–139, 1973.

Raphael, J.M., Crustal disturbances in the Lake Mead area, *Monogr. 21,* 14 pp., U.S. Bur. Reclam., Washington, D.C., 1954.

Rich, J.L., Radioactive heating as a cause of mountain building, *Proc. Vol. Geol. Soc. Amer., 1936,* 97, 1937.

Salop, L.I., and Yu.M. Scheinmann, Tectonic history and structures of platforms and shields, *Tectonophysics, 7,* 565–599, 1969.

Schwartz, M.L., Seamounts as sea-level indicators, *Geol. Soc. Amer. Bull., 83,* 2975–2980, 1972.

Sclater, J.G., and J. Francheteau, The implications of terrestrial heat flow observations on current tectonic and geochemical models of the crust and upper mantle of the earth, *Geophys. J. Roy. Astron. Soc., 20,* 509–542, 1970.

Sclater, J.G., R.N. Anderson, and M.L. Bell, The elevation of ridges and evolution of the Central Eastern Pacific, *J. Geophys. Res., 71,* 7888–7915, 1971.

Shatsky, N.S., On the origin of the Pachelma trough, *Byull. Mosk. Obshchest. Lyubiteley Prir. Otd. Geol., 5,* 5–26, 1955.

Sleep, N.H., Thermal effects of the formation of Atlantic continental margins by continental breakup, *Geophys. J. Roy. Astron. Soc., 24,* 325–350, 1971.

Stauder, W., Mechanism of the Rat Island earthquake sequence of February 4, 1965, with relation to island arcs and sea floor spreading, *J. Geophys. Res., 73,* 3847–3859, 1968.

Talwani, M., Gravity, in *The Sea,* vol. 4, part 1, edited by A.E. Maxwell, pp. 251–298, Interscience, New York, 1971.

van Bemmelen, R.W., The undation theory on the development of the earth's crust, *Proc. Int. Geol. Cong. 16th, Sect. 2,* 965–982, 1935.

van Bemmelen, R.W., On mega-undations: A new model for the earth's evolution, *Tectonophysics, 2,* 83–127, 1966.

Walcott, R.I., Late Quaternary vertical movements in eastern North America: Quantitative evidence of glacio-isostatic rebound, *Rev. Geophys. Space Phys., 10,* 849–884, 1972.

Willis, B., Continental genesis, *Geol. Soc. Amer. Bull., 40,* 281–336, 1929.

Wilson, J.T., A possible origin of the Hawaiian Islands, *Can. J. Phys., 41,* 863–870, 1963.

Wilson, J.T., New insights into old shields, *Tectonophysics, 13,* 73–94, 1972.

Wilson, J.T., and K. Burke, Plate tectonics and plume mechanics (abstract), *Eos Trans. AGU, 54,* 238, 1973.

Winterer, E.L., and W.R. Riedel, Introduction, in *Initial Reports of the Deep Sea Drilling Project,* vol. 7, pp. 3–9, U.S. Government Printing Office, Washington, D.C., 1971.

Winterer, E.L., J. Ewing, S.O. Schlanger, R.M. Moberly, Y. Lancelot, R.D. Jarrard, R.G. Douglas, T.C. Moore, and P. Roth, Deep Sea Drilling Project: Leg 17, *Geotimes, 16*, 12–14, 1971.

Woollard, G.P., A.S. Furomoto, J.C. Rose, G.H. Sutton, A. Malahoff, and L. Kroenke, Cruise report on 1966 seismic refraction expedition to the Solomon Sea, *Rep. HIG-67-3*, 31 pp., Hawaii Inst. of Geophys., Honolulu, 1967.

H.W. Menard is a professor of marine geology at the Institute of Marine Resources and Scripps Institution of Oceanography. He received his B.S. and M.S. degrees from the California Institute of Technology and his Ph.D. from Harvard University. Before coming to his present position he was an oceanographer with the Navy Electronics Laboratory.

OMIT

AGU

Vertical Crustal Motions and Their Causes

REPORT ON THE THIRD GEOP RESEARCH CONFERENCE

The Third GEOP Research Conference on Vertical Crustal Motions and Their Causes was attended by 65 persons. On behalf of the GEOP Steering Committee the conference was opened by Neville Carter and Charles H. Whitten, followed by Henry W. Menard, who delivered the introductory lecture. The lecture in its entirety is printed in this issue.

First Session

Slow Vertical Movements in Continental Interiors

Chairman: R.I. Walcott (Earth Physics Branch, Department of Energy and Mines, Ottawa)

Members: K. Burke (University of Toronto), G.H. Cabaniss (AFCRL), L. Cathles (Kennecott), C. Feldscher (NOAA, Detroit), S. Holdahl (NOAA, Washington), R. McConnell (Earth Science Research Inc.), E. Nyland (University of Alberta), B. Parsons (MIT), N. Sleep (MIT), and P. Vanicek (University of New Brunswick)

The evidence of rates and amounts of vertical movement in the phanerozoic was reviewed by Burke. Platforms, the normal environment of the continents, show aggregate movements of less than 0.001 mm/yr over much of their area; in Canada red beds, volcanics and dolomites deposited near sea level about 1700 to 1200 m.y. B.P. remain horizontal and within a few hundred meters of present sea level. The subsidence of the large basins of western Canada and the Soviet Union shows average movements of 0.01 mm/yr. Some more restricted basins like the Michigan and Williston basins show an exponentially decreasing rate of subsidence from their initiation with a time constant of about 50 m.y. Abnormal environments within the continents include those of the collision orogens. Himalayan summits now at about 6 km involve average rates of vertical movement of about 0.3 mm/yr. Burke summarized vertical movements of the phanerozoic as shown in Table 1.

Vertical movements of the late Quaternary were reviewed by Walcott by using data largely from North America. The basic data consist of radiocarbon-dated marine shells and terrestrial peats, some of which were deposited close to the sea level of their time and are now found above or below sea level. These indicate a continent-wide upward doming of the land centered on Hudson Bay with dimensions of about 4000 × 2700 km. The amount of movement in the center in the last 6000 years is 140 m, and the present rate of movement is about 2 cm/yr. Along the Atlantic seaboard of the United States, submerged terrestrial peats indicate a broad zone of submergence peripheral to the rising region. The greatest submergence occurs in the vicinity of Chesapeake Bay, involving 13 m over the last 6000 years. The present rates of movement shown by trends on marigraph records have a pattern and magnitude broadly consistent with the late Quaternary movements.

The panel then considered some of the techniques available for the study of vertical movements within continents. Holdahl gave a statement of the work of the National Geodetic Survey. The interest of the NGS in studies of vertical movements arises because of the requirement of maintaining and developing the U.S. network of geodetic elevations. Mappings of elevation changes based on repeated precise levelings and tide gage records show significant subsidence in the Chesapeake Bay and along portions of the Gulf Coast. A data bank consisting of relative vertical movement values along leveling lines has been created by the Vertical Network Division of the NGS, but at the present time processed data exist only in the Gulf Coast and mid-Atlantic zones.

In the Great Lakes, water level gages have been operating since 1860, and records are available at about 200 locations for varying periods of time. Feldscher reported on some results of the work of the Lake Survey. Over a period of time the gages at each site record progressively different elevations attributed to relative vertical crustal movements. Rates of crustal movement have been determined by computing the trends of the differences between pairs of stations. In the Michigan-Huron system the trends indicate a relative rise of the land to the north with a movement at Thessalon in Canada relative to Milwaukee of about 4 mm/yr.

In answer to a question on the systematic errors in leveling, Vanicek identified several possible sources of systematic error including anomalies in the gravity field. He concluded that although irregularities in the gravity field are recognized to have an effect on heights determined by leveling, they do not have an effect on the crustal movements derived from releveling provided the releveling follows the same paths as the original leveling. The distortion in graduation of the leveling rods, known as rod errors, can be revealed by

This report was prepared by Bryan Isacks, Ivan I. Mueller, R.I. Walcott, and Manik Talwani.

TABLE 1. Tentative Subdivision of the Continental Environment according to Styles of Vertical Movement Relative to Sea Level

	Characteristics	Characteristic Amounts, km	Characteristic Rates, mm/yr
Platforms	Form about one half of continental area and are underwater during episodes of global flooding.	±1	±0.01
Collision orogens	Occur in Himalayan and Tibetan environments, and high areas persist for tens of millions of years.	+5	+0.2
Exogeosynclines or foreland basins	Rapid initial downward movements reach −3 km, and a complementary 1-km uplift occurs further in toward the continent.	−3	−0.2
Uplifts	Seem well developed in Africa now.	+1	0.1
Swells	North America in Paleozoic.	+2	0.1
Basins		−2	−0.1
Rifts	Rift shoulders continue to go up after rifting.	−2	−0.3
Failed arms and aulacogens	Have a successively up-down-up movement.		
Up		1	
Down		−4	
Up		1	

correlation between computed movement and topography. Other known errors due to differential refraction, periodic movements of the ground (earth tides), do not generally contribute errors to any significant degree. Holdahl added that discrepancies between the local mean sea level and the geoid as defined by precise leveling do not necessarily imply systematic errors in the leveling, since the sea surface at the shore is not an equipotential surface. He agreed with Vanicek that gravity anomalies have an insignificant influence on the computation of relative vertical movements by repeated leveling.

Other techniques for the measurement of vertical movements were briefly discussed by McConnell and Cabaniss. Vertical movement of 1 cm implies a change in free air anomaly of 3 μGal or in Bouguer anomaly of 2 μGal, and present-day gravimeters and absolute gravity apparatus have a sensitivity of this order. Cabaniss discussed the problems of measuring secular and tidal changes in tilt by using borehole tiltmeters. The observations from three biaxial tiltmeters show a coherency at tidal frequencies within the uncertainties of calibration and orientation. At longer periods there is a pronounced annual term with a total range of 30×10^{-6} rad from instruments at 20-m and 7-m depth with little overburden that is not, however, directly in phase with either surface or down-hole temperature. It appears that the annual variation is sufficiently consistent from year to year to permit its prediction to a precision of the order of 10^{-8} rad for each particular installation. The measured tilt in boreholes is manifestly sensitive to the nature of instrument coupling to the rock, water level and temperature variations, the nature of the rock (particularly fractures), overburden thickness, topography, and so forth.

The last part of the session was devoted to a discussion of the causes and methods of physical analysis of vertical movements. It is possible to interpret the surface vertical movements as caused by forces that can be deduced by inversion techniques. Nyland gave an example in which the Lac-Saint-Jean vertical movement anomaly was explained by two force vectors at depth in an isotropic elastic half space. The solution was uncertain, owing to limited data. The mid-continent basins, Sleep argued, have a history similar to that of the Atlantic continental margins. The cause of the subsidence is likely to be thermal contraction on a 50 m.y. time scale. The effect of regional isostatic coupling and its relaxation is to cause the exterior part of the basin to move upward relative to the interior during later stages of deposition.

With regard to the late Quaternary movements of Fennoscandia and North America, Cathles suggested that most could be related to isostatic adjustment to post-Pleistocene load distribution. The uplift in central Canada and Fennoscandia might be modeled approximately by a low-viscosity channel of variable thickness and/or viscosity, but the load cycle would have to be taken into account. If this is done, substantial uplift (200 m) cannot remain in Fennoscandia and probably not in Canada. The uplift behavior of areas peripheral to the Canadian glaciation revealed by strandline and tide gage measurements down the East Coast of the United States shows a general uplift (immediately following deglaciation) followed by sinking. This requires deep flow and a reasonably uniform Newtonian mantle viscosity of about 10^{22} P. Smaller-scale unloadings indicate a thin (75-km) low-viscosity channel (4×10^{20} P) beneath the lithosphere in the uppermost mantle. Detailed studies of the direction of migration of the zero uplift isobase in Fennoscandia and of the amount of peripheral depression could place limits on the thickness of the low-viscosity channel. Data accuracy, radiocarbon time scale corrections, and detailed knowledge of eustatic sea level will become important to second-order (but probably not first-order) refinements in the mantle viscosity structure. The low-viscosity channel may be highly variable from one location to another, as the seismic low-velocity zone is.

Parsons gave a review of the general problem of analysis of vertical displacements with emphasis on three major considerations.

1. The choice of a physical model determined many of the steps in an analysis. At present, theoretical understanding is limited to spherically symmetric, linearly viscoelastic self-gravitating earth models. Problems are posed by the fact that this may not be a good model for the earth's rheological behavior. The question of whether creep obeys a linear or nonlinear stress-strain rate relation is still open. If it obeys a nonlinear stress-strain rate relation, many difficult theoretical problems will be posed. A problem more immediately troublesome is that the earth may not be even close to spherical symmetry in its rheological properties. It depends exponentially on whether temperature causes large spherical variations. It would seem to follow from the contradictory conclusions of Walcott and O'Connell that continental and oceanic areas may give different long-term responses to surface loads. The analyses of these workers gave different weights to continental and oceanic regions.

2. Problems are also posed by the distribution of data, which tend to be grouped along coastlines. The numerical calculations naturally make use of a representation in terms of spherical harmonic functions. A choice must be made between extracting spherical harmonic coefficients from the oddly distributed data with the implicit errors that this involves and adding a large number of calculated spherical harmonic coefficients for comparison with the data at given points. The addition of a large number of calculated spherical harmonic coefficients is perhaps

to be preferred, especially considering the importance of small wavelength components of the deformation due to the fact that the data are located in the region between loading in opposite senses.

3. Once the direct problem is understood, i.e., once one can calculate the response for the chosen physical model, it would seem to be a straightforward step to adapt the methods developed in seismology, e.g., the method of Backus and Gilbert, to give a rigorous inversion of the data. The application of these methods to this particular problem has been demonstrated recently by Parsons, who used McConnell's data for Fennoscandia.

Second Session

Vertical Motions along Active Continental Margins and Island Arcs

Chairman: B.L. Isacks (Cornell)

Members: A.L. Bloom (Cornell), J.M. Buchanan-Banks (USGS), D.E. Karig (UCSB), C. Scholz (Lamont-Doherty), and J.C. Stepp (USAEC)

Observations of vertical motions that occur during relatively short periods of time (geodetic and instrumental observations for periods of up to about 100 years) have provided key evidence for the process of underthrusting and lithospheric subduction in such regions of plate convergence as Japan, Alaska, and Chile. As the discussions of Scholz and Stepp showed, these types of observations promise important new information about the detailed process of plate slippage, the generation of large earthquakes, and, consequently, the prediction of earthquakes and also probably offer unique information about the system of applied forces acting to produce lithospheric subduction. Analyses of geodetic and instrumental measurements in the region of the transverse ranges of southern California (Stepp and Buchanan-Banks) are yielding valuable information about the tectonics of that unusual area of crustal compression within the San Andreas transform fault system.

Observations of vertical motions for periods of time of hundreds to millions of years generally rely upon accurate dating of coastal material with a known relationship to an ancient sea level. Entangled with this, of course, is the problem of the eustatic variation of sea level during the past.

In a discussion of the uplift of the Huon Peninsula in New Guinea, which is an interesting area of probable collision between an island arc and a continent, Bloom showed how the tectonic and eustatic variations may eventually be separated. Karig used marine geological and geophysical data to discuss aspects of the longer-term evolution of vertical motions in island arcs. He concentrated the additional mass to the arc in the form of sediments scraped off in various ways from the subducted oceanic plate.

Third Session

Vertical Motions within Oceanic Regions

Chairman: M. Talwani (Lamont-Doherty)

Members: A. Bally (Shell Oil), H.C. Noltimier (OSU), W.C. Pitman III (Lamont-Doherty), J.C. Sclater (MIT), and N. Sleep (MIT)

In his introductory remarks Talwani called attention to the fact that although horizontal motions in the oceans have been the subject of great interest, much less attention has been paid to vertical motions in oceanic areas.

In their remarks Sleep and Bally discussed the problem of subsidence associated with passive continental margins. Sleep presented a model in which he attributed the subsidence of the margin to thermal contraction of the lithosphere. His model is based on the observation that vertical movements on older Atlantic continental margins are gradual subsidences and that a 50 m.y. exponential decay of the subsidence rate is observed that is similar to the subsidence on the midoceanic ridges due to thermal cooling. The effect of regional isostatic compensation and later creep that decouples adjacent areas is evident from the distribution of sediments. Sleep maintained that coupling of the subsidence of the shelf to sedimentation on the continental rise and seaward spreading of the continental crust like oil over water are not important on the East Coast of the United States.

In Bally's view, subsidence may not necessarily be associated with thermal phenomena. Thus the Gulf of Mexico has subsided even though it has not been subjected to the thermal effects of the proximity to a spreading center. Bally stressed that in order to arrive at a more realistic model of the earth, oceanic observations have to be made compatible with observations in ancient geosynclines, which in many respects are comparable to recent passive margins. Bally called attention to the following geological observations.

1. The process occurs whether or not it is obviously associated with a spreading center (e.g., the Gulf of Mexico).

2. A scan-type survey shows that subsidence in excess of 10,000 feet is nearly ubiquitous for the Mesozoic but exceptional for the Tertiary. Exceptions are major depocenters (e.g., Mississippi and the Niger delta).

3. Reconstruction of the Cape May section suggests massive crustal rearrangements accompanied by corresponding modification of paleohypsographic curves.

4. Modifications of paleohypsographic curves are registered with great sensitivity in transgressive and regressive cycles on continental shelves. It has been observed that transgressions are short-lived events, whereas regressive foresetting (offlap) is longer lasting. Examples of short widespread transgressions are Upper Jurassic, mid-Cretaceous, and Upper Cretaceous. Very precise correlations are needed to confirm these impressions.

5. In the Atlantic realm the Tertiary is conspicuous by an overall regression, whereas in the active margins of the Pacific, clear transgressions occur in mid-Eocene and mid-Miocene in associated basins.

Sclater and Pitman considered a different aspect of the subsidence of the ocean basins. Both started from the premise that Sclater and his co-workers have postulated, that all active mid-oceanic ridges have a uniform relation between depth and age of the oceanic crust, a relation that can be accounted for by the creation of oceanic plates. By using the knowledge of the past separation of South American and African plates and the depth-age relationships, Sclater constructed paleobathymetric charts of the South Atlantic. These charts yield models of the sedimentary process on the ocean floor as a function of time. It is possible to test these models directly by Joides deep-sea drilling.

By using Sclater's age-depth relationships, Pitman and Hays demonstrated how rapid sea floor spreading causes the ridges to expand horizontally and hence reduces the volumetric capacity of the ocean basins and gives subsequent rise to transgressions. Pitman was thus able to attribute the worldwide Upper Cretaceous transgression to a contemporaneous pulse of rapid spreading at most of the mid-oceanic ridges between −110 m.y. and −85 m.y. The general regression continued until −9 m.y. because spreading rates continued at a low rate and in some instances were further reduced. During the transgressive phase, sedimentation in the inland seas may have kept pace with the rises of the seas that were leveling and filling interior basins. Hence when the regression occurred, the lowering of sea level by 100 to 200 m would have drained vast land areas rapidly. His calculations indicate that by −10 m.y. the regression had caused the sea level to be reduced to about 40 m above the present level. This calculation does not take into account the quantities of water locked up in ice sheets. Pitman and Hays suggested that as the regression progressed through the Tertiary, continentality increased, hence climates cooled, climatic contrast increased, and circulation with the Arctic Ocean decreased, conditions necessary for the initiation of the Northern Hemisphere continental glaciation thus occurring.

Noltimier proposed a model to explain the puzzling observation of why some mid-oceanic ridge crests are characterized by horst and others by grabens. Briefly, his model suggests that when material is intruded at the ridge crest over a distance greater than that required to accelerate the crestal material from zero horizontal velocity to the spreading velocity, a central graben forms. When material is intruded over a narrower distance than that required to accelerate to spreading velocity, a central horst forms.

Fourth Session

Modern Geodetic Technology in Service of Detecting Vertical Crustal Displacements

Chairman: I.I. Mueller (OSU)

Members: C.C. Counselman III (MIT), J.E. Faller (JILA), R.S. Mather (GSFC), and J.W. Siry (GSFC)

Virtually all our understanding today of vertical crustal movements, Faller noted, rests on long-term evidence or on incremental evidence developed from the more precipitous displacements of the crust. Significant measurement capabilities, however, now exist that would permit 'real-time' observation of vertical displacements at the 1 cm/yr level, that is, direct measurement of these motions in the time scale of a few years.

The first technique, the absolute measurement of gravity made with portable instruments using high-speed laser interferometry, is sensitive to both height changes and mass redistribution inside the earth. Work is presently in progress on a new instrument patterned on an earlier instrument of Faller and Hammond that was used to measure gravity with an accuracy of between 4 and 5 parts in 10^8 at strategic locations around the world to provide bench mark values. The new instrument, which incorporates improvements in both the mechanical design and the data processing techniques, should ultimately be capable of accuracies of 1 part in 10^9, corresponding to a height sensitivity of about 3 mm. Such an instrument (or instruments) could be used to monitor strain fields and would open up an important new parameter for possible use in the prediction of earthquak[illegible]. Use of gravity variations would requi[illegible] superficial geological effects suc[illegible] changing water tables be subtracted on t[illegible] basis of direct measurement, differential gravitational measurements, or differing characteristic frequencies.

The second new type of measurement capability involves the methods of satellite ranging, very long base line radio interferometry (VLBI), and lunar ranging. With reference to lunar ranging, a regular program is being carried out from the McDonald Observatory to the Apollo retroreflectors on the moon with a point-to-point measurement accuracy of 15 cm. Plans are under way to upgrade this station to the ranging accuracy of the station under construction in Hawaii, i.e., from 2 to 3 cm. Vertical height information at about the measurement accuracy will be derivable from the data. The LURE (Lunar Ranging Experiment) team is presently looking into the possibility of a relatively small and transportable lunar ranging station that would be used to occupy twenty or so carefully selected sites on approximately a 2-year interval with the aim of checking for possible site variations (in x, y, and z) at the several centimeter level.

The two data types, direct height variations obtained by using satellite and/or lunar ranging and/or VLBI and information regarding variations in gravity, are highly complementary. Although both yield height information, in combination they yield separable information on vertical movements and internal mass motions as well.

Counselman gave a tutorial paper on progress and prospects in three-dimensional geodesy by means of VLBI. All three components of the position vector of one site relative to another, where the two sites may be separated by thousands of kilometers, are determined by comparing tape recordings of radio signals received simultaneously at the separate sites from extragalactic radio sources. Observed differences between the reception times at the two sites of signals from four sources distributed reasonably well in the sky allow all three components of the intersite 'base line' vector, plus the site clock synchronization error, to be determined. Unknown source directions, as well as polar motion, UT1, precession, and nutation, can also be determined if observations are continued for a major portion of a day.

The state of the art of VLBI geodesy, as demonstrated by the MIT-Haystack Observatory group in cooperation with others from NASA/GSFC, University of Maryland, and JPL, is such that five independent determinations during 1972 of [illegible] length of a 4000-km base line from [illegible]husetts to California were scattered by 10 [illegible] scatter in the direction of the base l[illegible] vector corresponded to 1–3 m, principally in a north-south sense, indicating possible uncertainty in the pole positions assumed in these experiments. Known error sources include the troposphere (40-cm uncertainty), ionosphere (15 cm), instrumental drift (possibly 1 m), and radio noise (3 cm). Means exist to reduce each of these to less than 3 cm. It is reasonable to expect that a portable VLBI terminal with a 1-m-diameter antenna capable of 3-cm uncertainty geodetic measurements will be developed. Such a terminal could be assembled from presently available electronic components.

Siry spoke on vertical crustal motion measurement by means of satellite techniques, noting that vertical crustal motions of the order of several centimeters have been observed to precede earthquakes. Scholz, Sykes, and Aggarwal have proposed a model that relates these and other precursory phenomena to dilatancy (C. Scholz, L. Sykes, and Y. Aggarwal, The physical basis for earthquake prediction, paper presented at AGU Meeting, Washington, D.C., April 1973). They presented evidence linking the precursor time interval with the earthquake magnitude and the length of the aftershock zone. Dilatant regions of the order of a few tens of kilometers in scale and precursor time intervals ranging from roughly half a year to a year and a half are expected to be of interest in connection with earthquakes of magnitude 6, for example. The dilatancy mechanism seems to be operative in the case of thrust faults and probably also in the case of at least some strike-slip events. A system for sensing precursory crustal motions should thus have the capability for determining site positions with an accuracy of the order of a couple of centimeters in a time interval of approximately a quarter of a year at spacings of roughly 10 km in a region of interest such as a fault zone. Several hundred such locations are needed to cover the fault systems in the California area.

A system for monitoring such precursory crustal motions was presented. It involved a set of automated corner reflector stations tracked by means of a laser operating in the Geopause satellite. It should be possible to range some 3 times during every Geopause pass to each of the sites in such an ensemble, weather permitting. One-centimeter range data gathered during a quarter of a year should yield position component accuracies of the order of a couple of centimeters. A laser beam 0.1 mrad in diameter would, in general, illuminate a single station in such an array. A broader beam would generate reflections from several sites, overlapping data thus being produced. A chain or pattern of such overlapping regions can strengthen the solution for site positions. Pressure, temperature, and humidity gages can provide refraction correction' data. Turnaround transponders interrogated by the Geopause radio tracking system can furnish corresponding data in excessively cloudy regions. This concept offers the prospect of a practical approach to the problem of monitoring precursory vertical crustal motions.

Fourth Geodesy/Solid-Earth and Ocean Physics (GEOP) Research Conference

The Geoid and Ocean Surface

ENGINEERING CENTER
UNIVERSITY OF COLORADO
BOULDER, COLORADO

AUGUST 16–17, 1973

Sponsored by: **American Geophysical Union**
National Aeronautics and Space Administration
National Oceanic and Atmospheric Administration
Ohio State University, Department of Geodetic Science
U.S. Geological Survey

The theme for the Fourth GEOP Research Conference will be set by an introductory review relating to the geoid and ocean surface. The conference will be divided into the following sub-topics, each introduced by an invited moderator and discussed by a panel:

1. **Reference Surfaces and Height Systems: Ocean and Earth; Chairman: Richard H. Rapp, OSU**
2. **Departures of Sea Surface from the Geoid; Chairman: Wilton Sturges, Florida State University**
3. **Instrumentation and Data Acquisition; Chairman: George C. Weiffenbach, Smithsonian Astrophysical Observatory**
4. **Analysis Techniques for Determining the Geoid and Ocean Surface Topography; Bernard H. Chovitz, NOS/NOAA**

Individuals interested in attending the conference are requested to send their applications on the standard application form available from the American Geophysical Union, 1707 L Street, N.W., Washington, D.C. 20036. Information on the membership in the GEOP Research Conferences may be found on page 305 of the April 1972 issue of EOS. Please note that the topics of Conferences 3 and 4 have been interchanged.

Further details on the program, accommodations, and registration will be sent to those applicants selected by the committee to attend the conference by June 20.

Applications for attendance must be received by June 16, 1973.

American Geophysical Union ★ 1707 L Street, N.W. ★ Washington, D.C., 20036

D4

The Geoid: Definition and Determination

Richard H. Rapp

THE determination of the geoid has been one of the prime goals of geodesy. Knowledge of geoid undulations with respect to some reference surface was needed for the determination of the figure of the earth, for the precise reduction of distance measurements to a reference ellipsoid, and for the determination of the geocentric location of points on the surface of the earth. Currently and in the future, undulation information can also be used in geophysical studies related to crustal structures and in oceanographic studies related to sea surface topography. The actual determination of global geoids has been carried out by using gravimetric data, satellite-derived information related to the gravitational field of the earth, or a combination of the two techniques. Regional geoid determinations have been made by astrogeodetic techniques. For some applications of undulation information, undulation standard deviations of the order of ±5 m would be sufficient. Such an accuracy can be obtained by using data currently available. In the past few years, renewed interest in the geoid arose when the concept of satellite altimetry was proposed to measure the distance from the satellite to some area on the ocean surface.

The use of precise satellite altimetry data at the ±10-cm level requires a thorough examination of our definitions and theoretical models so that advantage can be taken of such satellite altimetry data. This is especially important in the oceanographic area, where it may be possible to determine the separation between the actual sea surface topography and some equipotential surface (which may be the geoid). This re-

This article was taken from the keynote address presented at the Fourth GEOP Research Conference on The Geoid and Ocean Surface, which was held at the University of Colorado, Boulder, August 16 and 17, 1973.

view discusses the problems connected with geoid determinations and some definitions that may be needed for the precise work of the future.

The Geoid—Definition

We start by characterizing the gravity field of the earth by a set of equipotential surfaces. These surfaces are determined primarily by the mass distribution of the earth and the rotation of the earth. In reality, the effect of the attraction of the sun and moon, both direct and indirect, and the attraction of the atmosphere will affect the equipotential surface surrounding and interior to the earth. The potential W at any point can be written

$$W = W_g + W_a + W_t \qquad (1)$$

where W_g is the potential of gravity, W_a is the potential of the atmosphere, and W_t is the tidal potential. It is usual practice in gravimetric geodesy to ignore the W_a and W_t terms, since they may be accurately computed. In this paper, however, we shall not disregard W_a but, following *Mather* [1973], shall include it in our definition of the potential at a point on the earth. We now define a geop as an equipotential surface on which $W_g + W_a$ is a constant. The geop that corresponds to mean sea level is called the geoid. In this context, the geodetic community generally considers mean sea level as dependent only on the gravitational attraction of the earth and atmosphere and the rotation of the earth and therefore motionless, so that disturbances caused by tidal movements, winds, and ocean currents are not considered [*Helmert*, 1884]. Alternate definitions of mean sea level considering oceanographic information may be needed for future work. The term geoid was first introduced by the German geodesist *Listing* [1872]. The potential on the geoid (excluding the tidal potential) is usually designated by W_0.

We next introduce a biaxial rotational ellipsoid whose surface is equipotential as a figure of reference. The parameters of this ellipsoid include its geocentric gravitational constant kM_0, its rotational velocity ω, its flattening f, and the potential U_0 on its surface. With properly chosen values of these constants the reference ellipsoid is termed a 'mean earth ellipsoid' [*Heiskanen and Moritz*, 1967]. For further discussion we assume that the center of this ellipsoid is at the center of mass of the solid earth, which should be close to the center of mass of the solid earth plus the atmosphere. The separation between the geoid and the ellipsoid is the geoid undulation. The elevation h of a point above the ellipsoid is the sum of the geoid undulation plus the orthometric height H of the point above mean sea level, as shown in Figure 1.

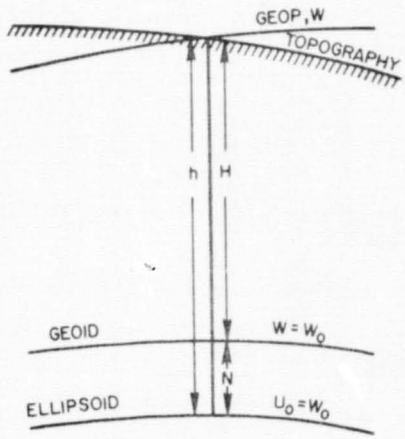

Fig. 1. The relationship between the geop through a point, the geoid, and the ellipsoid.

The Geoid—Determination

The determination of the geoid is primarily the task of determining the undulations of the geoid. A procedure for such determination was given by *Stokes* [1849]. In his work, Stokes assumed a spherical reference surface with no masses external to the geoid. The Stokes equation (generalized for reference to an arbitrary ellipsoid is [*Heiskanen and Mortiz*, 1967, p. 101]

$$N = N_0 + \frac{R}{4\pi G} \iint_{\sigma} \Delta g\, S(\psi) d\sigma \qquad (2)$$

where R is a mean earth radius (6371 km) and G is a mean value of gravity (979.8 Gals), $S(\psi)$ is the Stokes function, and ψ is the spherical distance between the point at which N is being computed and the place where the Δg values are given. N_0 is the zero order undulation [*Rapp*, 1967] given by

$$N_0 = \frac{(kM - kM_0)}{RG} - \frac{(W_0 - U_0)}{G} \qquad (3)$$

In many cases, N_0 is considered to be zero, so that the resultant values from the integral expression in (2) are referred to an ellipsoid, whose mass is the same as that of the earth and whose surface potential is the same as that of the geoid. The integration in (2) is to be taken over the whole world. The Δg values are the gravity anomalies representing the difference between gravity on the geoid (with no external masses) and the gravity implied by the reference ellipsoid or reference gravity formula.

The accuracy of the Stokes equation (which is really taken as the integral component of equation 2) is dependent on several factors. First is the spherical approximation made by Stokes for the reference surface. The error (with respect to a better choice being the reference ellipsoid) is of the order of Nf. Additional work has been done to derive formulas analogous to the Stokes equation but eliminating a spherical approximation. Solutions are due to *Sagrebin* [1956] (which contained an error), *Bjerhammar* [1962], *Molodenskii et al.* [1962, p. 53], and *Lelgemann* [1970]. Lelgemann gives a map showing on a global scale the error caused by the spherical approximation of the Stokes equation. The maximum error was -0.5 m with a root mean square error of ±0.2 m.

The second problem relates to the determination of gravity on the geoid. Since our gravity observations are generally not made on the geoid, it is necessary to reduce them to this surface. To do this, we need to know the elevation of the points with respect to the geoid and the density of the masses between the geoid and the observation point. This latter requirement cannot be precisely met, so that some approximation will always be made in reducing gravity from the observation point to the geoid. This problem can be reduced by using the concepts of modern gravimetric geodesy that attempt to define the gravimetric boundary value problem at the surface of the earth instead of at the geoid. These procedures will be discussed in a subsequent section of this paper.

A third problem exists in forming our model so that no masses are external to the geoid, as is required by Stokes's equation. Many types of reductions can be made to try to do this. However, all but one type of reduction (the Rudski) will change the position of the geoid so that what is in reality computed is a cogeoid. There are as many types of cogeoids as there are types of procedures to incorporate the mass external to the geoid into the earth. If we let δN be the separation between the geoid and cogeoid, we can write

$$N = N_0 + \frac{R}{4\pi G} \iint_{\sigma} (\Delta g' + 0.3086\, \delta N) S(\psi)\, d\sigma + \delta N \qquad (4)$$

where $\Delta g'$ is the gravity anomaly after some reduction technique has been applied. The type of reduction of the gravity observations and thus the type of anomaly used in undulation determination should be one where the indirect effect (i.e., the δN term) is small, and it should be such that the Δg values can be used for purposes other than just undulation computations. Such an anomaly is a free-air anomaly, where the indirect effect is about 1 m per 3 km of average elevation (*Heiskanen and Moritz*, 1967, p.145). Thus, for undulation determinations at sea, the use of a free-air anomaly should yield almost directly the geoid undulations, excluding the contribution of the indirect effect in the anomaly term in areas distant from the computation point.

The fourth problem relates to the accuracy of the geoid undulations obtained when global gravity coverage does not exist or when the anomalies used in the stokes equation are assumed to have some standard deviation. Work in this area has been done by *deGraff-Hunter* [1935], *Hirvonen* [1956], *Kaula* [1957], *Paul and Nagy* [1973] and *Groten and Moritz* [1964], the latter paper being summarized in *Heiskanen and Moritz* [1967, p. 274]. From the Groten and Moritz paper, the standard deviation to be expected of geoid undulations computed from 1° X 1° anomalies with a point anomaly in every 1° block is ±1.5 m, or ±1.2 m if a centered anomaly profile exists in each block. For 5° X 5° blocks the corresponding undulation standard deviations are ±13 and ±7 m, respectively.

Another way to look at the accuracy problem is to assume perfect gravity coverage out to some spherical radius ψ_0 with no other gravity material being used. Procedures and results can be found in *Kaula* [1957], *Molodenskii et al.* [1962, p. 164], *Heiskanen and Moritz* [1967, p. 259], and *Wong and Gore* [1969]. Current estimates of the undulation standard deviation (assuming a true equatorial gravity) as a function of ψ_0 are shown in Figure 2.

Geoid undulations can also be computed by techniques other than just terrestrial gravity data. If $\bar{C}_{lm}$, $\bar{S}_{lm}$ are fully normalized potential coefficients of the earth's gravitational potential with respect to those implied by the reference ellipsoid, then we can write (for example) [*Rapp*, 1971]

$$N = N_0 + R \sum_{l=2}^{l_{max}} (\bar{C}_{lm} \cos m\lambda + \bar{S}_{lm} \sin m\lambda)\, \bar{P}_{lm}(\sin \varphi) \qquad (5)$$

where φ and λ are the latitude and longitude of the point at which N is being evaluated and $\bar{P}_{lm}$ are the fully normalized associated Legendre functions. The geometric errors associated with (5) are the same as with Stokes's equation. A more critical question relates to the convergence of (5) at the geoid owing to masses being outside the geoid. *Levallois* [1970, 1972] has considered this question and concludes that errors that can reach 4 or 5 m are associated with (5) owing to the topography external to the geoid. This error is not restricted to land areas but, for spherical harmonic developments to deg 20, can also reach several meters in the ocean areas.

The undulations of the geoid as computed from (5), with $N_0 = 0$ and using a set of potential coefficients [*Rapp*, 1973*a*] complete to deg 20, are shown in Figure 3. The root mean square undulation is ±30 m with the largest (in absolute value) undulation −110 m just to the south of India.

The first application of the Stokes integral for undulation computations was made by *Hirvonen* [1934] using approximately 1500 1° X 1° free-air anomalies. *Tanni* [1948] computed a geoid based on 4380 1° X 1° isostatic anomalies meaned into 5° X 5° anomalies and later [*Tanni*, 1949] computed a detailed geoid in Europe by using the 1° X 1° data. *Zhonogolovich* [1952] carried out a spherical harmonic analysis to deg 8 by using 4378 1° (roughly equal area) blocks that were formed into 10° equal area blocks. Geoid undulations were computed essentially on the basis of (5). *Heiskanen* [1957] gave geoid undulation maps based on 6679 1° X 1° free-air anomalies. *Uotila* [1962] reported a geoid computed through a spherical harmonic analysis to deg 4 by using 11,294 1° X 1° free-air anomalies.

Because the maximum degree to which we have potential coefficients

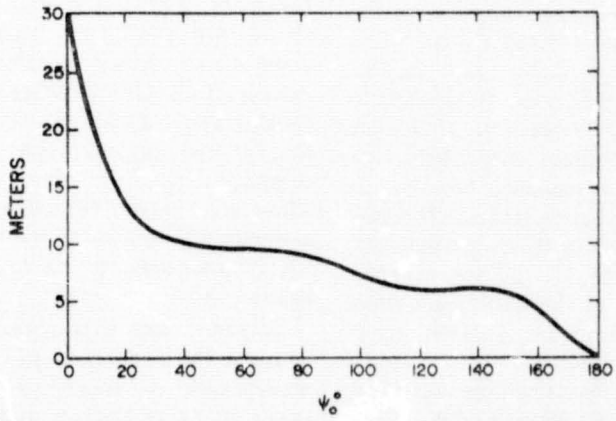

Fig. 2. Undulation standard deviation assuming perfect gravity material out to a spherical radius of ψ_0°.

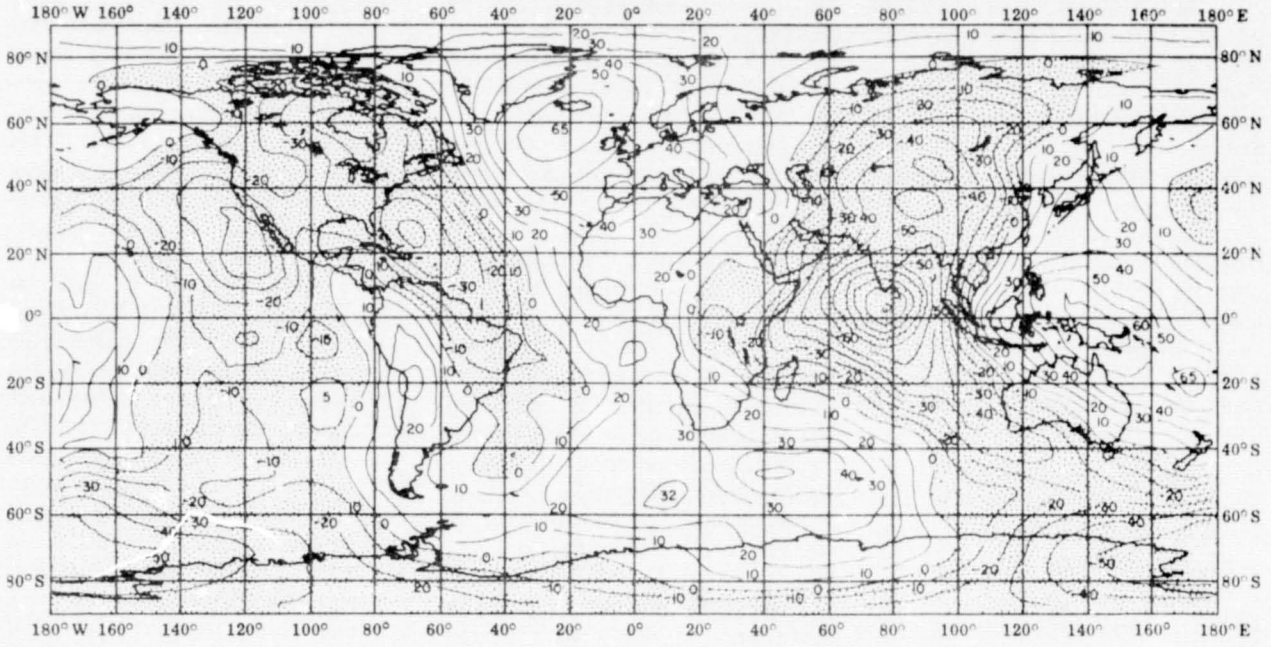

Fig. 3. Geoid undulations as computed from a set of potential coefficients of Rapp [1973a] complete to deg 20. Countour interval, 10 m; reference flattening, 1/298.256.

is of the order of 16°–20°, the shorter wavelength undulations are missing from the results of (5). Consequently, it is convenient to combine potential coefficient information with gravity information to obtain more detailed geoids. This is done by representing the undulation as the sum of two terms N_1 and N_2. N_1 is given by (5). N_2 is computed through the Stokes integral, where the anomalies used are the difference between the terrestrial anomalies and the anomalies implied by the potential coefficients used in computing (5), and the integration is carried out over a limited cap approximately to a ψ_0 of 7°–10°. Results from such computations have been given by *Talwani et al.* [1972] for the North Atlantic, by *Kahle and Talwani* [1973] for the Indian Ocean, and by *Vincent and Marsh* [1973] for the globe; the Vincent and Marsh paper culminates a sequence of local detailed geoid computations. The gravity data used in these computations were generally 1° × 1° values except for an area in the Caribbean, which was computed by *Talwani et al.* [1972] by using 10′ × 10′ values to obtain the fine structure associated with the Puerto Rican trench.

The accuracy of an undulation computed by using the procedures of the above paragraph will depend on several factors, which include the accuracy of the potential coefficients, the accuracy of the gravity material, the value of ψ_0 chosen for the integration cap, the accuracy of the equatorial value of gravity, and the size of the smallest anomaly block used in the computations. Considering these error sources, *Rapp* [1973*b*] estimated the standard deviation of an undulation as a function of ψ_0. At $\psi_0 = 0°$ the standard deviation was ±6.5 m, whereas at $\psi_0 = 10°$ it was ±3.3 m, exclusive of model errors connected with the Stokes equation and using the Smithsonian Astronomical Observatory Standard Earth II [*Gaposchkin and Lambe* ., 1971] potential coefficients. For certain ψ_0 values, the undulation error is dominated by the inaccuracy in the knowledge of equatorial gravity. These results indicate that at the present time we can compute a geoid undulation in areas where good gravity coverage exists to a standard deviation of the order of ±3 m exclusive of N_0 or model errors.

In some cases it is convenient to consider the undulation in terms of wavelength or frequency components. In *Rapp* [1972], undulations were broken into long wavelength (l = 2 to 10), intermediate wavelengths (l = 11 to 100), short wavelengths (l = 101 to 1000), and very short wavelengths (l = 1001 to ∞). The undulation information in these wavelengths was ±29.5 m, ±6.0 m, ±0.6 m, and ±0.06 m, respectively. The amount of undulation information above degree l can be represented in an integral expression given by *Pellinen* [1970] or by the simple expression 64/l (meters) by *Chovitz* [1972]. Using the detailed undulations of *Vincent et al.* [1971], *Brown and Vincent* [1972] carried out a spectral analysis of geoid profiles by computing power spectral density values using a discrete Fourier transform of autocorrelation values of the undulations. Plots of the energy versus frequency can be used to reveal information about the behavior of high-degree potential coefficients.

The geoid can also be determined on a relative basis with respect to some arbitrary datum by astrogeodetic techniques [*Heiskanen and Moritz*, 1967, p. 1971; [*Bomford*, 1971, p. 361]. The accuracy of astrogeodetic geoid determinations is a function of the spacing of the astronomic observations and the length of the profile. Detailed astrogeodetic maps for the North American Datum, 1927, have been given by *Fischer* [1967], for the European Datum, 1950, by *Bomford* [1971]

and in *Mather et al.* [1971] for Australia. Although astrogeodetic geoid determinations are primarily made on land, *von Arx* [1966] has described the determination of the astrogeodetic geoid in the Puerto Rican trench area. The use of deflections of the vertical at sea by using inertial navigation equipment yields data from which astrogeodetic geoids or geoid slopes can be computed [*Butera et al.*, [1970]. And *Schwarz* [1972] has proposed that geocentric station positions, as determined with the geoceiver, and orthometric heights could be used for land undulation determinations to an accuracy of a few meters.

Theoretical Refinements

As was pointed out previously, the use of Stokes's equation for computing the undulation of the geoid involves several assumptions that make the precise determination of the undulation impossible. An alternate formulation of the problem by M.S. Molodensky in 1945 led to a more precise solution of the problem of determining the physical surface of the earth. An introduction to the so-called modern methods for determining the figure of the earth can be found in *Heiskanen and Moritz* [1967, chap. 8]. In the new method a surface called the telluroid is introduced. This nonequipotential surface is defined as having the same potential difference C between it and the reference ellipsoid as does the point on the surface of the earth and the geoid. The distance between the ellipsoid and the telluroid is called the normal height H^*, and the distance between the telluroid and the surface point is the height anomaly ζ. If the height anomaly were measured from the reference ellipsoid, the quasi-geoid surface (which is not an equipotential surface) would be formed. The geometric height of the surface point above the ellipsoid is $H^* + \zeta$, as is shown in Figure 4. The value of C is found from leveling, with gravity measurements being made so that accurate potential differences can be computed. The determination of ζ has been the subject of much work. For solutions computed by using the sphere as a reference surface, see *Heiskanen and Moritz* [1967] and *Moritz* [1966, 1968*b*]. For results where an ellipsoidal reference surface is used, for example, see *Mather* [1973]. In one type of linear solution *[Heiskanen and Moritz*, 1967, p. 310] we write

$$\zeta = \zeta_0 + \frac{R}{4\pi G} \iint_\sigma (\Delta g + G_1) \cdot S(\psi)\, d\sigma \qquad (6)$$

where G_1 is a correction term very similar to the terrain effect. The anomaly Δg is called the surface free-air anomaly and is the difference between observed gravity at the earth's surface and normal gravity (due to the reference ellipsoid) at the telluroid. Although G_1 may be negligible in some areas, it does not follow that the global effect of G_1 is negligible because of the global summation required in (6). A considerably more elaborate solution for ζ is given in *Mather* [1973], where a complete determination for ζ is carried out by an iterative procedure.

The geoid undulation can be related to the height anomaly through the following expression:

$$N = \zeta + \frac{\bar{g} - \bar{\gamma}}{\bar{\gamma}} H \qquad (7)$$

where $\bar{g}$ is the average value of gravity between the geoid and the surface point and $\bar{\gamma}$ is the average value of normal gravity between the ellipsoid and telluroid. In the ocean areas, H is essentially zero, so that the geoid undulations and height anomalies should be virtually identical in such areas.

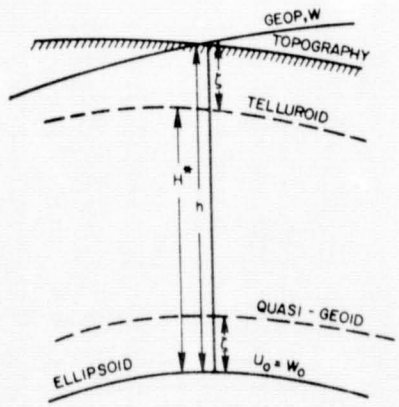

Fig. 4. The relationship between the telluroid, quasi geoid, ellipsoid, and the geop through a point.

Gravity Data Requirements for a Precise Geoid

The determination of accurate undulations of the geoid requires good gravity material. The precise statement of gravity material requirements is not clear at this time. The hypothetical studies of *Groten and Moritz* [1964] yield some ideas of undulation accuracy to be expected with uniform gravity coverage. The best undulation standard deviation there was ±1.2 m (profile measurements in $1^\circ \times 1^\circ$ blocks). *Rapp* [1973*b*] indicates that the contribution of the inaccuracy of the $1^\circ \times 1^\circ$ data to the undulation error is of the order of ±0.5 m for a cap size of 10° in well-surveyed areas such as might be found in the United States. This error is dominated by errors from other sources. *Mather* [1973] argues that for geoid determination to ±10 cm it is necessary to be able to accurately determine anomalies on at least a tenth of a degree grid so that $1^\circ \times 1^\circ$ anomalies are determined to ±0.3 mGal and that the anomalies have systematic errors below ±0.05 mGal. Current gravity material falls far from meeting the needs of precise undulation determinations. A summary of available data to June of 1972 is given by *Decker* [1972]. Currently (July 1973) we have approximately 26,000 $1^\circ \times 1^\circ$ values out of the 64,800 blocks on the earth. This amounts to an area coverage of about 38%. Large gaps exist in the Pacific Ocean area as well as in the politically inaccessable areas. The accuracies of the known $1^\circ \times 1^\circ$ anomalies vary from ±1 to ±23 mGals. At sea the standard deviation of $1^\circ \times 1^\circ$ data estimated from ship data depends on the accuracy of the ship's measurements as well as on the number and distribution of measurements in the $1^\circ \times 1^\circ$ blocks. Standard deviations of the order of ±10 mGals are probably somewhat optimistic [*LePichon and Talwani*, 1969].

It appears that additional effort is needed to clarify the data requirements for precise gravimetric undulation determinations using current or future computational procedures and to estimate the feasibility of obtaining the data needed for such computations.

Mean Sea Level and the Geoid

The geoid has been loosely defined as an equipotential surface that corresponds to an idealized sea surface. To a certain degree of approximation this idealized sea surface coincides with mean sea level. Consequently, tidal gages have been used to define mean sea level at various points along coast lines. Averaging of the levels observed at the tidal stations over periods of time (1 to 19 years) will remove periodic effects. The resultant mean sea level is usually thought of as the geoid. Now the orthometric heights, or the geopotential number of points on land are determined by using leveling (and gravity) information starting from a sea level datum that hopefully could correspond to the geoid. Unfortunately the mean sea level at one location may not coincide (i.e., the two mean sea level surfaces do not lie on the same equipotential surface) with mean sea level at another location. This may be due to systematic winds, currents, and temperature and salinity differences of the water, in the areas of the tidal gages. These factors give rise to the problem of the slope of sea level. This slope can be detected by leveling [*Braaten and McCombs*, 1963] or by oceanographic computations [*Sturges*, 1967], although there is disagreement between the leveling and oceanographic determinations of sea slope measurements in a north-south direction [*Sturges*, 1967, 1972; *Hamon and Greig*, 1972].

The noncoincidence of mean sea level and the geoid creates a problem for the geodesist who is attempting to determine accurate undulations of the geoid. This problem stems from the fact that the elevation (or potential difference) of a point needed for the determination of gravity anomalies is defined to be with respect to the geoid. Since we cannot uniquely define the geoid through mean sea level determination, our global anomalies can be referred to different level surfaces, such surfaces being defined by the vertical datum in each country or region where a vertical control net is defined or referenced. Since the deviation between the geoid and mean sea level is of the order of 1 m, the errors caused by datum inconsistency have been small relative to other error sources connected with undulation computations. The actual effect of inconsistent heights on the undulations has not been precisely computed. *Mather* [1973] suggests that such effects could be of the order of 15–60 cm. Further work needs to be done in this area.

In the future, if we are going to try to determine undulations at the ±10-cm level, it is going to be necessary to improve our height datums. This may not be a difficult problem for land datums, but for gravity measurements made at sea it may be quite difficult to determine the height of the ship gravity meter relative to the geoid to an accuracy of the order of 15 cm.

Some possible help in reconciling the height datums may come from oceanography, where attempts are made to determine the dynamic topography of the sea surface with respect to some level surface. Basically, there are two methods of carrying out such computations [*Sturges*, 1968]. The first method, used by *Stommel* [1964] and *Lisitzin* [1965] uses the hydrostatic equation and observed density values along with an assumption of a reference isobaric surface as an equipotential surface. *Sturges* [1968] uses the geostrophic equation and observed surface currents.

Stommel [1964] and *Lisitzin* [1965] present global maps of, in essence, the elevation of the physical sea surface (exclusive of such factors as random winds and tides) above some arbitrary level surface. In the Stommel computation the 1000 dbar surface was used as a reference level surface, whereas Lisitzin used a 4000 dbar surface. The Listizin 'elevations' (Figure 5) are approximately 1.5 dynamic meters greater than those of Stommel. The average elevation on

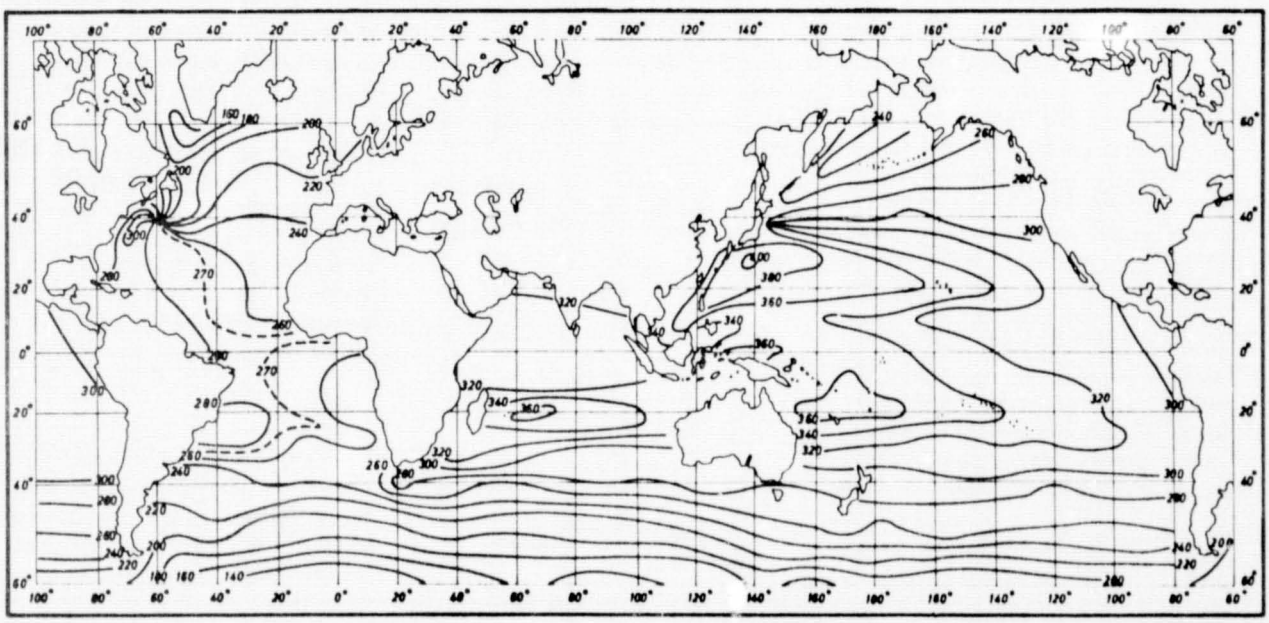

Fig. 5. Dynamic elevation (in dynamic centimeters) of the sea surface above an arbitrary level surface [from Lisitzin, 1965].

the Lisitzin map is about 2.8 dynamic meters, which could be taken as the definition of the geoid level. The corresponding level on the Stommel reference would be 1.3 dynamic meters, as estimated by *Montgomery* [1969] for the Stommel map. The time variations of mean sea level have recently been discussed by *Lisitzin* [1970] and others.

If the sea surface topography maps were valid for coastal areas, geodesists could use such information to determine a global elevation datum. Since a global datum is probably impractical, the simplest procedure would be to convert existing gravity anomalies to a common datum using the sea surface topography information.

Satellite Altimetry

The renewed interest in the geoid has primarily been brought about by the potentialities of satellite altimetry. In essence, satellite altimetry is the measurement of a distance from a satellite to the ocean surface. If the orbit of the satellite were known, it would be possible to determine the geocentric radius vector to points on the geoid. Satellite altimetry measurements have application in two areas, physical oceanography and the determination of the gravity field of the earth. The oceanographic application conceptually consists of the determination of the gravity field of the earth. The oceanographic application conceptually consists of the determination of the sea surface topography. If the accuracy is sufficient, it would be possible to determine information relative to tides, storm surges, ocean currents, sea slope etc. The gravity field information results from the inclusion of the altimeter data in orbit determination programs, by determination of potential coefficients through equation 5 or determination of anomalies (for example) through equation 2 using geoid undulations determined from the altimeter measurements.

The initial suggestion for the use of altimetry data was reported by *Moore* [1965] and *Godbey* [1965]. *Greewood et al.* [1967, 1969*a*, 1969*b*] discussed the information to be gained from satellite altimetry data. The verification of altimeter measurements was discussed by *Weiss* [1970*a*, *b*]. Hudson [1970] and *Stanley et al.* [1972] discuss geoid determinations from altimetry. *Hudson* [1971] presents an overview of the goals of the satellite altimetry project. A set of papers relating altimetry data to sea surface topography can be found in a two-volume set edited by *Apel* [1972].

Studies giving in detail some of the benefits of altimeter data in conjunction with other data sources include the Williamstown report [*Kaula, 1970a, b*] and a Jet Propulsion Laboratory study [*Loomis,* 1972]. JPL [*Gardner,* 1972] has also prepared a study on the feasibility of a radar altimetry project and has carried out analysis of the altimetry systems from launch to tracking to data recovery.

The geodetic applications have been adddressed in several ways. *Koch* [1970*a, b*] discusses the determination of surface density values from the geoid heights obtained from time-averaged altimeter data. This work was extended by *Isner* [1972], who discusses the determination of global 5° and local 1° surface density values under the assumption of geoid undulations given from altimeter data and terrestrial gravity data given with respect to a reference set of spherical harmonic coefficients. *Lundquist* [1967], *Brown* [1973], and others have suggested the incorporation of the altimeter data into the orbit determination program for improvement of the geopotential, with Lundquist working with long orbit arcs and Brown working with short orbit arcs. *Rapp* [1971*b*] carried out simulation studies to determine the degree to which potential coefficients could be found with altimeter and other data. With ocean undulations determined to ±1 m and land undulations to ±5 m, it was concluded that potential coefficients to deg 82 could be found.

Brown and Fury [1972] discuss the detailed procedure for handling altimeter data and the various error sources involved. They describe various models for the gravitational potential for use with the altimeter data in a long-arc reduction model. *Strange* [1972] uses the Stokes equation for simulation studies to determine anomalies, given geoid undulations that would be obtained from the altimeter data. *Arnold* [1972] proposes a procedure where the gravitational field is represented by geoid undulations. He suggests an iterative solution where a set of 15° × 15° undulations are found first considering their influence on the satellite orbit. Then the 1° × 1° anomalies within the 15° compartment are found under the assumption that the orbit is partially independent of the influence of any 1° × 1° undulations. In this way the solution of a system of equations containing approximately 30,000 unknowns can be carried out efficiently.

Closing Remarks

In this paper I have attempted to outline some of the principles and problems relative to the determination of the geoid. In this area we found that currently we can expect to determine geoid undulations on a global basis to ±3 m and somewhat better on a relative basis. More accurate determinations, especially at the ±10-cm level will require extensive recasting of our analytical procedures and data collection. A unification of regional height datums will be needed and hopefully will be obtained from oceanographic data. The impending acquisition of satellite altimeter data will improve our knowledge of the earth's gravity field and, with an altimeter of high accuracy, will help the oceanographer in his studies of the ocean surface, provided he can get the geodesist to provide him with sufficiently accurate geoid information. The scheduled July 1974, launch of the Geos-C satellite, with an altimeter whose precision is ±1 m with a total satellite to sea level distance accuracy of the order of ±5 m, will be the first step in a direct study of the geoid and ocean surface using satellite data.

References

Apel, J., Ed., Sea surface topography from space, *Tech. Rep. ERL 228-AOM: 7,* Nat. Oceanic Atmos. Admin., 1972.

Arnold, K., Das Geoid aus Beobachtungen der Satellitenallemetrie, *Veroeff. Zentralenst. Phys. Erde,* no. 7, Potsdam Germany, 1972.

Bjerhammar, A., On an explicit solution of the gravimetric boundary value problem for an ellipsoidal surface of reference

Rep. AD296827, Roy. Inst. of Technol., Stockholm, 1962.

Bomford, G., *Geodesy*, 3rd ed., 731 pp., Oxford University Press, New York, 1971.

Bomford, G., The astro-geodetic geoid in Europe and connected areas, in *Travaux de l' Association Internationale de Géodésie*, vol. 24, pp. 357–371, Paris, 1972.

Braaten, N.F., and C.E. McCombs, Mean sea level variations as indicated by a 1963 adjustment of first-order leveling in the United States, paper presented at IUGG General Assembly, Berkeley, Calif., 1963.

Brown, D.C., Determination of oceanic geoid from short arc reduction of satellite altimetry, paper presented at 1st International Symposium on Use of Artificial Satellites for Geodesy and Geodynamics, Athens, May 14–21, 1973.

Brown, R.D., and R.J. Fury, Determination of the geoid from satellite altimeter data, *Rep. 5035-21000-OITM*, Contr. NAS5-11790, Comput. Sci. Corp., May 1972.

Brown, R.D. and S. Vincent, Power spectra of geoid undulations (abstract), *Eos Trans. AGU, 53*, 969, 1972.

Butera, A., J. DeMatteo, and S. Goclowski, Direct measurement of deflection of the vertical using a ship's inertial navigation systems (SINS), in *Marine Geodesy, A Practical View*, pp. 129–138, Marine Technology Society, Washington, D.C., 1970.

Chovitz, B., Downward continuation of the potential from satellite altitudes, paper presented at 5th Symposium on Mathematical Geodesy, Italian Geod. Comm., Florence, Italy, Oct. 1972.

Decker, B.L., Present day accuracy of the earth's gravity field (abstract), *Eos Trans., AGU, 53*, 891, 1972.

deGraaf-Hunter, J., The figure of the earth from gravity observations and the precision obtainable, *Phil. Trans. Roy. Soc. London, Ser. A., 234*, 377–431, 1935.

Fischer, I., Geoid charts of North and Central America, *Tech. Rep. 62*, Army Map Service, Washington, D.C., 1967.

Gaposchkin, E.M., and K. Lambeck, Earth's gravity field to the sixteenth degree and station coordinates from satellite and terrestrial data, *J. Geophys. Res., 76*, 4855–4883, 1971.

Gardner, J., Earth physics satellite radar altimeter study, *Tech. Rep. 760-73*, Jet Propul. Lab., Pasadena, Calif., 1972.

Godbey, T., Oceanographic satellite radar altimetry and wind sea sensor, in Oceanography from Space, *Rep. 65-10*, Woods Hole Oceanogr. Inst., Woods Hole, Mass., 1965.

Greenwood, A.J., A. Nathan, G. Neumann, W. Pierson, F. Jackson, and T. Pease, Radar altimetry from a space craft and its potential application to geodesy and oceanography, *Rep. TR-67-3*, Dep. of Meteorol., N.Y. Univ., New York, 1967.

Greenwood, A.J., A. Nathan, G. Neumann, W. Pierson, F. Jackson, and T. Pease, Radar altimetry from a spacraft and its potential applications to geodesy, *Remote Sensing Environ., 1*, 59–70, 1969*a*.

Greenwood, A.J., A. Nathan, G. Neumann, W. Pierson, F. Jackson, and T. Pease, Oceanographic applications of radar altimetry from a spacecraft, *Remote Sensing Environ., 1*, 71–80, 1969*b*.

Groten, E., and H. Moritz, On the accuracy of geoid heights and deflections of the vertical, *Rep. 38*, Dep. of Geod. Sci. Ohio State Univ., Columbus, 1964.

Hamon, B.V., and M.A. Greig, Mean sea level in relation to geodetic land leveling around Australia, *J. Geophys. Res., 77*, 7157–7162, 1972.

Heiskanen, W.A., The Columbus geoid *Eos Trans. AGU, 38*, 841–848, 1957.

Heiskanen, W., and H. Moritz, *Physical Geodesy*, W.H. Freeman, San Francisco, 1967.

Helmert, F.R., *Mathematischen und Physikalischen Theorem der Hoheren Geodäsie*, p. 5, Teubner, Leipzig, 1884.

Hirvonen, R.A., The continental undulations of the geoid, *Publ. 19*, Finn. Geod. Inst., 1934.

Hirvonen, R., On the precision of the gravimetric determination of the geoid, *Eos Trans. AGU, 37*, 1–8, 1956.

Hudson, E., Determining the geometric shape of the geoid in the ocean-covered areas of the world by satellite radar altimetry (abstract), *Eos Trans. AGU, 51*, 263, 1970.

Hudson, E., A geodetic and oceanographic satellite altimeter system, paper presented at Space Systems Meeting, Amer. Inst. Aeronaut. Astronaut., Denver, Colo., 1971.

Isner, J., Determination of surface densities from a combination of gravimetry and satellite altimetry, *Rep. 186*, p. 61, Dep. of Geod. Sci., Ohio State Univ., Columbus, 1972.

Kahle, H.G., and M. Talwani, Gravimetric Indian Ocean geoid, *Z. Geophys., 39*, 167, 1973.

Kaula, W.M., Accuracy of gravimetrically computed deflections of the vertical, *Eos Trans. AGU, 38*, 297–305, 1957.

Kaula, W.M., Ed., The terrestrial environment: Solid earth and ocean physics, (Williamstown report), *NASA Contract. Rep. CR-1579*, p. 153, 1970*a*.

Kaula, W., Application of space and astronomic techniques to solid earth and ocean physics, in *Advances in Dynamic Gravimetry*, pp. 130–135, Instrument Society of America, Pittsburg, Pa., 1970*b*.

Koch, K., Gravity anomalies for ocean areas from satellite altimetry, in *Marine Geodesy, A Practical View*, pp. 301–308, Marine Technology Society, Washington, D.C., 1970*a*.

Koch, K., Gravity values for continental shelf areas from satellite altimetry, Report on the Symposium on Coastal Geodesy, July 1970, edited by R. Sigl, Tech. Univ., Munich, 1970*b*.

Lelgemann, D., Untersuch ungen zu einer genaueren Lösung des Problems von Stokes, dissertation, *ser. C, no.* 155, Deut. Geod. Komm., Munich, 1970.

LePichon, X. and M. Talwani, Regional gravity anomalies in the Indian Ocean, *Deep Sea Res., 16*, 263–274, 1969.

Levallois, J.J., Note sur la convergence du développement du potentiel en harmoniques, *Proceedings, Fourth Symposium on Mathematical Geodesy, 1969*, pp. 71–80, Italian Geod. Comm., Bologna, Italy, 1970.

Levallois, J.J., Remarques générales sur la convergence du développement du potentiel terrestre en harmoniques sphériques, paper presented at 5th Symposium on Mathematical Geodesy, Italian Geod. Comm., Florence, Italy, Oct. 1972.

Lisitzin, E., The mean sea level of the world ocean, *Soc. Sci, Fenn., Commentat. Phys. Math., 30*, 35 pp., 1965.

Lisitzin, E., The mean sea level and its changes in time and space in the North Atlantic Ocean, in *Report on the Symposium on Coastal Geodesy*, edited by R. Sigal, pp. 279–283, Institute for Astronomical and Physical Geodesy, Technical University, Munich, 1970.

Listing, Regarding our present knowledge of the figure and size of the earth, *Rep. Roy. Soc. Sci. Gottingen*, 66 pp., 1872.

Loomis, A., Earth and ocean physics applications planning study, *Rep. 760-72*, Jet Propul. Lab., Pasadena, Calif., 1972.

Lundquist, C., Satellite altimetry and orbit determination, *Spec. Rep. 248*, Smithson. Astron. Observ., Cambridge, Mass., 1967.

Mather, R., A solution of the geodetic boundary value problem to order e^2, *NASA Doc. X-592-73-11*, Goddard Space Flight Center, Greenbelt, Md., 1973.

Mather, R.S., B.C. Barlow, and J.G. Fryer, A study of the earth's gravitational field in the Australian region, paper presented at 15th Annual Assembly of IUGG, Moscow, Aug. 2–14, 1971.

Molodenskii, M.S., V. Eremeev, and M. I. Yurkina, *Methods for Study of the External Gravitational Field and Figure of the Earth, OTS 61–31207*, translated from Russian, Israel Program for Scientific Translations, Jerusalem, 1962.

Montgomery, R.B., Comments on oceanic leveling, *Deep Sea Res., 16*, suppl., 147–152, 1969.

Moore, R., Satellite radar oceanography, An introduction, Oceanography from Space, *Rep. 65-10*, Woods Hole Oceanogr. Inst., Woods Hole, Mass., 1965.

Moritz, H., Linear solutions of the geodetic boundary value problem, *Rep. 79*, Dep. of Geod. Sci., Ohio State Univ., Columbus, 1966.

Moritz, H., On the use of the terrain correction in solving Molodensky's problem, *Rep. 108*, Dep. of Geod. Sci., Ohio State Univ., Columbus, 1968.

Moritz, H., Nonlinear solutions of the geodetic boundary value problem, *Rep. 126*, Dep. of Geod. Sci., Ohio State Univ., Columbus, 1969.

Paul, M.K., and D. Nagy, The accuracy of geoidal height obtainable from gravity

data alone, *Can. Surv., 27,* 149–156, June 1973.

Pellinen, L. P., Estimation and application of degree variances of gravity, *Stud. Geophys. Geod., 14,* 168–173, 1970.

Rapp, R.H., The equatorial radius of the earth and the zero-order undulation of the geoid, *J. Geophys. Res., 72,* 589–593, 1967.

Rapp, R.H., Methods for the computation of geoid undulations from potential coefficients, *Bull. Geod.* no. 101, 283–297, 1971*a*.

Rapp, R.H., Accuracy of potential coefficient determinations from satellite altimetry and terrestrial gravity, *Rep. 166,* 27 pp., Dep. of Geod. Sci. Ohio State Univ., Columbus, 1972.

Rapp, R.H., Geopotential coefficient behavior to high degree and geoid information by wavelength, *Rep. 180,* 22 pp., Dep. of Geod. Sci., Ohio State Univ., Columbus, 1972.

Rapp, R.H., Numerical results from the combination of gravimetric and satellite data using the principles of least squares collocation, *Rep. 200,* Dep. of Geod. Sci., Ohio State Univ., Columbus, 1973*a*.

Rapp, R.H., Accuracy of geoid undulation computations, *J. Geophys. Res., 78,* 7589–7595, 1973*b*.

Sagrebin, D.W., Die theorie des regularisierten geoids, *Veroeff. Geod. Inst. Potsdam,* no. 9, Akademie, Berlin, 1956.

Schwarz, C.R., Direct determination of geoid undulations with the geoceiver (abstract), *Eos Trans. AGU, 53,* 893, 1972.

Stanley, H.R., N.A. Roy, and C.F. Martin, Rapid global geoid mapping with satellite altimetry, in *The Use of Artificial Satellites for Geodesy, Geophys. Monogr. Ser.,* vol. 15, edited by S.W. Henriksen, A. Mancini, and B.H. Chovitz, pp. 209–216, AGU, Washington, D.C., 1972.

Stokes, G., On the variation of gravity at the surface of the earth, *Trans. Cambridge Phil. Soc., 8,* part 5, 672–695, 1849.

Stommel, H., Summary charts of the mean dynamic topography and current field at the surface of the ocean, and related functions of the mean wind-stress, in *Studies on Oceanography,* pp. 53–58, University of Tokyo Press, Tokyo, 1964. (English translation, University of Washington Press, Seattle, 1965.)

Strange, W., Numerical testing of an altimeter reduction method (abstract), *Eos Trans. AGU, 53,* 968, 1972.

Sturges, W., Slope of sea level along the Pacific coast of the United States, *J. Geophys. Res., 72,* 3627–3637, 1967.

Sturges, W., Sea-surface topography near the Gulf Stream, *Deep Sea Res., 15,* 149–156, 1968.

Sturges, W., Comments on ocean circulation with regard to satellite altimetry, Sea Surface Topography from Space, vol. 2, *Tech. Rep. ERL 228-AOML 7-2,* Nat. Oceanic Atmos. Admin., Boulder, Colo., 1972.

Talwani, M., H. Poppe, and P. Rabinowitz, Gravimetrically determined geoid in the western north Atlantic, Sea Surface Topography from Space, vol. 2., *Tech. Rep. ERL 228-AOML 7-2,* Nat. Oceanic Atmos. Admin., Boulder, Colo., 1972.

Tanni, L., On the continental undulations of the geoid as determined from the present gravity material, *Publ. 18, Isostatic Inst.,* pp. 791, Int. Ass. of Geod., Helsinki, 1948.

Tanni, L., The regional rise of the geoid in central Europe, *Publ. 22, Isostatic Inst.,* 19 pp., Int. Ass. of Geod., Helsinki, 1949.

Uotila, U.A., Harmonic analysis of worldwide gravity material, *Ann. Acad. Sci. Fenn., Ser. A,* 67, Helsinki, 1962.

Vincent, S., and J. Marsh, Global detailed gravimetric geoid, paper presented at 1st International Symposium on Use of Artificial Satellites for Geodesy and Geodynamics, Athens, May, 14–21, 1973.

Vincent, S., W. Strange, and J.G. Marsh, A detailed gravimetric geoid from North American to Europe (abstract), *Eos Trans. AGU, 52,* 817, 1971.

von Arx, W.S., Level-surface profiles across the Puerto Rico trench, *Science, 154,* 1651–1653, 1966.

Weiss, E., Space geodesy altimetry verification experiment design study, *Rep. SR70-4108,* Raytheon Co., Sudbury, Mass., 1970*a*.

Weiss, E., Satellite altimeter verifications (abstract), *Eos Trans. AGU, 51,* 739, 1970*b*.

Wong, L., and R. Gore, Accuracy of geoid heights from modified Stokes kernals, *Geophys. J. Roy. Astron. Soc., 18,* 81–91, 1969.

Zhongolvich, I.D., *The Outer Gravitational Field of the Earth and the Fundamental Constants Related to It* (in Russian), vol. 3, 129 pp., Institute of Theoretical Astronomy, Academy of Science, Moscow, 1952. (English translation, *AD-733840,* Defense Mapping Agency/Aerospace Center, St. Louis, Mo., 1971.)

Richard H. Rapp is professor of geodetic science at the Ohio University in Columbus, where he has been a faculty member since 1964. He received his B.S. degree in physics from Rensselaer Polytechnic Institute and his M.S. and Ph.D. degrees in geodetic science from Ohio State. He is a member of several study groups of the International Association of Geodesy and chairman of a special study group on earth models. He is chairman of the Scientific Papers Committee of the Section of Geodesy, AGU.

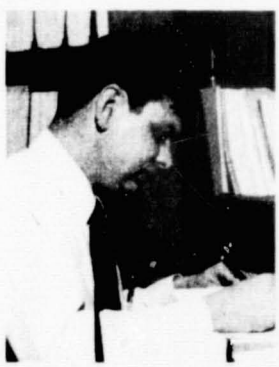

OMIT

AGU

The Geoid and Ocean Surface

REPORT ON THE FOURTH GEOP RESEARCH CONFERENCE

THE Fourth Geodesy/Earth and Ocean Physics (GEOP) Research Conference was held on August 16 and 17, 1973, at the University of Colorado, Boulder. It was attended by about 65 persons. John Apel, general chairman, opened the conference, followed by Richard H. Rapp of the Ohio State University, who delivered the keynote address. The keynote address in its entirety is printed elsewhere in this issue. This address and the following summaries of the sessions constitute a report on this conference.

First Session

Panel on Reference Surfaces and Height Systems: Ocean and Earth

Chairman: Richard H. Rapp (Ohio State University)

Members: S. Holdahl (National Geodetic Survey), E. Balazs (National Geodetic Survey), I. Fischer (Defense Mapping Agency Topographic Center)

In discussing the geoid and the ocean surface it is necessary to define as precisely as possible the reference surfaces and height systems. In addition, quantities that are measured must be related to the geoid and/or ocean surface. One such quantity is our system of heights that are viewed as being approximately determined by classical leveling procedures. Holdahl reviewed different aspects of heights and their implementation in the leveling network of the United States. In essence, height determinations consist of determining a distance between a reference equipotential surface of the earth's gravity field and the corresponding surface passing through the point whose height is to be determined. To precisely determine this distance, it is necessary to determine the potential difference between the two surfaces, or the geopotential number of the points. The geopotential number can be estimated from leveling data and values of gravity computed from some normal gravity formula or by measuring actual gravity values along a leveling line. Holdahl pointed out that the error in using normal gravity will not generally cause an error of more than 0.1 kGal m (in the geopotential number). However, a true geopotential number can deviate as much as 0.08 kGal m from the normal geopotential number over short distances owing to rapidly changing gravity anomalies. To convert geopotential numbers to rigorous heights, real gravity values are required. Not using such values in height computations introduces an error accumulation that exceeds 1 m in the most mountainous regions of the United States.

The current height system in operational use in the United States was based on a 1929 adjustment at which the elevation at 26 mean sea level stations was forced to be zero. It is clear that such a procedure would not be followed now. Holdahl indicates that a future national network will incorporate actual gravity data in geopotential number and height determinations and will also recognize the fact that the mean sea level surfaces generally lie on different equipotential surface.

Balazs described a set of new adjustments of leveling data in the United States whose purpose was to determine local mean sea level in relation to geodetic leveling along the coastlines. The nets described by Balazs were two independent first-order level nets, one at the Atlantic and Gulf coastal area and the other in the California coastal area. On the east coast, 18,600 km of leveling was used. An adjustment was made to determine free adjusted elevations whereby only one elevation was fixed in the adjustment. The adjusted elevations represent the height above an equipotential surface that coincides with the 1966.9 mean sea level (MSL) at Portland, Maine, for the east coast and with the 1969.3 MSL at Neah Bay, Washington, for the Pacific coast. Using this information Balazs computed the departure of local MSL from a reference equipotential surface that in turn permitted him to compute the slope of mean sea level along each coast. On the Atlantic coast he found a slope of 13 mm/deg latitude and on the Pacific coast a slope of 62 mm/deg latitude, both cases indicating a rise in mean sea level from South to North. Although they agree on the general slope, the new results given by Balazs differ considerably from the results reported in 1963 by N.F. Braaten and C.E. McCombs, who found a slope of 30 mm/deg latitude on the Atlantic coast and 26 mm/deg latitude on the Pacific coast. Some of the questions that the work of Balazs raised were also discussed in the second panel session.

Irene Fischer discussed the principles of astrogeodetic geoid determinations and some of the current results. Such discussions helped to define the concept of pre-

This report was prepared by B. Chovitz, Ivan A. Mueller, R.H. Rapp, W. Sturges, and G. Weiffenbach. Material contained herein should not be cited.

cisely what is meant by an astrogeodetic geoid in contrast to other types of geoids, such as a geoid determined gravimetrically. The question arose as to whether astrogeodetic techniques could be helpful in resolving the separation between mean sea level and the geoid. Because of the nature of astrogeodetic techniques, they would not appear to be helpful for the separation determination.

Second Session

Panel on Departures of Sea Surface from the Geoid

Chairman: W. Sturges (Florida State University)

Members: R.B. Montgomery (Johns Hopkins University), J.L. Reid (Scripps)

In the work of this panel we excluded departures of the sea surface caused by sea, swell, and tides. It was pointed out that normal seasonal variations in the density field lead to surface height variations of ±10–15 cm at middle latitudes. Nearly random wavelike phenomena with periods of a few months have similar amplitudes. Atmospheric pressure changes give rise to surface amplitudes of about ±20 cm at high latitudes. The largest signals are across strong boundary currents (e.g., the Gulf Stream and Kuroshio), where the change in level is about 100 cm. Changes in position of these currents can produce the largest changes in surface elevation at a given position. The horizontal scale of strong boundary currents and eddies (or Gulf Stream rings) is about 100–150 km. A sampling problem arises, as a result of this scale, when satellite altimetry is discussed in terms of the number of times a given 1° rectangle is sampled per unit time. If a track line is obtained only about once per month in a given 1° rectangle, it may be very difficult to resolve time changes at a fixed point from horizontal variability of the sampling position. This lack of resolution is usually called 'aliasing'; it may be severe, and it requires further study.

Most maps of sea surface topography are based on calculations of geopotential anomaly (or 'dynamic height'). R.B. Montgomery discussed the assumptions and methods that oceanographers use in calculations of geopotential. Variations of sea level, as calculated from the density field ('steric level'), have been shown to follow the variations observed at nearby tide gauges. For maps of steric sea level, the 2000-dbar reference surface, which lies near a depth of 2000 m, is optimum for worldwide studies. This surface may not be sufficiently level in the Antarctic Circumpolar Current, the Gulf Stream, or regions where strong currents extend to the bottom. In other regions, these maps may be interpreted as the time-averaged 'absolute topography' (with the addition of an atmospheric pressure correction) if an error of about ±10 cm is acceptable. In regions of strong currents, however, direct current measurements plus geostrophic leveling can be used to compute surface slopes that could provide results accurate to ±10 cm.

J.L. Reid presented maps of topography of the Atlantic and Pacific Oceans; the reference surface is 2000 dbar. The range is about 2½ m; the highest area is near Japan, and the lowest is in the Antarctic. The major features of the maps are well understood in terms of the major circulation patterns and the wind field. Seasonal maps are in preparation. Variations in near-shore (~500-m depth) currents are clearly apparent in the density field off California, where a seasonal range of some 15 cm in surface elevation is observed. Across the Antarctic Circumpolar Current the slope of the 2000-dbar surface, relative to the 3000-dbar surface, is about 25 cm.

Sturges discussed recent work concerning the slope of sea level along continental boundaries. The oceanographic results, on both the Pacific and Atlantic coasts of the United States, indicate a slope downward to the north, with the magnitude being larger on the Atlantic coast. The dominant dynamical effect is the variation of the Coriolis parameter on the meridional flow of boundary currents. The latest results are greatly at variance with the results of geodetic leveling on land. The discrepancy is about 1 m on both coasts. It has been suggested that there is an urgent need for a critical study of leveling results to try to locate a source of systematic errors, but this suggestion has not been greeted warmly by the leveling community.

An additional source of information is the numerical modeling of wind-driven ocean circulation. Although no member of this area was able to attend, very recent results were kindly provided by Kirk Bryan, Jr. His maps of the wind-driven sea surface agree well with those derived from the density field, except in the areas where, on fundamental grounds, agreement is not expected, as was already mentioned.

In the lively discussion that followed, four main points emerged. First, for purposes of physical oceanography, to interpret the results of a satellite altimeter, it is necessary to know the absolute shape of a level surface (i.e., relative to the ellipsoid) near mean sea level, although this surface need not be 'the geoid.' Second, except for interpreting the results of a satellite altimeter, it is not necessary in most applications for physical oceanographers to know the absolute shape of a level surface. Third, there was an apparent lack of agreement about some details in the definition of the geoid. Fourth, the discrepancy between the results of land leveling and oceanic leveling near the coasts is important and requires serious examination.

Finally, it should be stressed that a much larger and more difficult set of problems deals with the instantaneous sea surface, which is disturbed by wind waves, by tides, and by the complicated interactions of weather and oceanic perturbations, as well as by normal seasonal changes, changes in currents, or the motion of eddies. When sufficiently accurate satellite altitudes become available, their interpretation will depend on taking all these factors into account.

Third Session

Panel on Instrumentation and Data Acquisition

Chairman: G.C. Weiffenbach (Smithsonian Astrophysical Observatory)

Members: W.E. Brown (Jet Propulsion Laboratory), G.B. Bush (Applied Physics Laboratory, Johns Hopkins University), T.W. Godbey (General Electric Co.), F. Nathanson (Technology Serivce Corp.)

After Weiffenbach's introduction to problems in data acquisition due to atmospheric and ionospheric propagation, Bush summarized the basic principles of Satellite altimetry. Nathanson and Brown discussed the two main techniques, namely, the techniques of pulse compression and coherent radars. Godbey showed recent results from the Skylab 1 altimetry. During the discussion attention was called to the fact that earth resources data from Skylab will be placed in the public domain and will thus be available to anyone (for a price). The Earth Resources Experiment Package (EREP) flown on Skylab includes the S190 multispectral photography, S191 IR spectrometer, S192 multispectral scanner, S193 microwave radiometer/scatterometer/altimeter (KuBand), and S194 L-band radiometer.

Photographic data products from Skylab 2 are now in the public domain and can be obtained from the U.S. Geological Survey, Department of Interior, EROS, Sioux Falls, S. Dak. 57198 (telephone 605-339-2270).

Electronic data products are not yet in the public domain. To obtain data when they are placed in the public domain, requests should be addressed to NASA, Skylab Program Office, Johnson Space Center, Houston, Texas (Attention of K. S. Kleinknecht).

Data products potentially available for the S-193 altimeter are the following:

1. Altitude: tabulations S072-1, S072-2; plots S073-7.
2. AGC (backscatter information): tabs S072-8, S072-9; plots S073-2, S073-3, S073-11, S073-12.
3. Sample and hold data (sea state information): tabs S072-4; plots S073-4, S073-5.
4. Housekeeping data (internal engineering, operational mode status, and malfunction data): tabs S072-3, S072-6; plots S073-10, S073-6, S073-1.
5. Attitude, altitude, and sensor field of view, etc.: tabs S072-7; plots S073-8.

For a more detailed description of the data products listed above, see *document PHO-TR524.*

S-193 altimeter calibration information is available as follows:

1. S-193 Microwave Radiometer/Scatterometer/Altimeter, Calibration Data Report, Flight Hardware, vol. 1B, Reid, *Doc. 72SD4207,* General Electric Co., Space Systems Organization, Philadelphia, Pa. 19101. (These same data are available in a document published by the Johnson Space Center.)
2. Skylab Program, Earth Resources Experiment Package, Sensor Performance Report, vol. 5 (S193 Altimeter), (Preflight Engineering Baseline), *Doc. MSC-05528,* Martin Marietta Corp., Denver, Colo. (Note: This document will be updated to include a flight sensor performance evaluation following each Skylab flight (SL2, SL3, and SL4).

The second calibration data reference above has been prepared for each EREP sensor: S190, vol. 1; S191, vol. 2; S192, vol. 3; S193, vol. 4 (radiometer/scatterometer); S193, vol. 5 (altimeter); S194, vol. 6. Those who have questions concerning data products, calibration data, geographical area of coverage, or data usage should write R.W. Smith, Mail Stop 8392, P.O. 179, Martin Marietta Corp., Denver, Colo. 80201 (telephone 303-794-5211).

Fourth Session

Panel on Analysis Techniques for Determining the Geoid and Ocean Surface Topography

Chairman: B. Chovitz (National Oceanic and Atmospheric Administration, National Ocean Survey)

Members: P. Argentiero (NASA, Goddard), J. Berbert (NASA, Goddard), R. Brown (Computer Sciences Corp.), J. Buglia (NASA, Langley), T. Davis (Naval Oceanographic Office), S. Jordan (Analytic Sciences Corp.), W. Kahn (NASA, Goddard), J. Marsh (NASA, Goddard), F. Morrison (NOAA, NOS), W. Strange (Computer Sciences Corp.), S. Yionoulis (Applied Physics Laboratory, Johns Hopkins University)

B. Chovitz began with remarks on the close interconnection between progress in analysis techniques and the type of data available. For example, Stokes's formula, published in 1849, languished unused for many years because of lack of gravity data. Now it is the method 'par excellence' for the determination of the geoid, mainly because of the availability of gravity measurements. The intense effort over the past fifteen years in analysis of satellite orbits for the determination of the gravitation field has obviously been due to the acquisition of measurements of direction, distance, and velocity of artificial satellites, from which perturbations could be inferred. In this spirit, the analysis techniques of greatest interest at this conference are centered on a new anticipated data source: satellite altimetry.

In considering the impact on analysis techniques of various types of data, the most important factor is not the quality or nature of the data, or even the raw quantity, but the distribution. What is desired is worldwide continuous coverage, and this is true (though in a qualified sense) even if the geoid determination is wanted not worldwide but only over a local area. In the past, such coverage has generally been lacking, and the exercise of ingenuity in devising analysis techniques has been directed toward the statistical prediction of gravity. On the other hand, the anticipated influx of dense and widely distributed altimetry data is expected to lead to techniques of amalgamation and smoothing and the application of approximations and shortcuts that will achieve the accuracy desired and yet leave the problem amenable to solution on present-day computers. As an example of an analysis technique devised to handle altimetry data, Chovitz mentioned a recent publication of K. Arnold in which the parameters of the solution are geoid heights over 40,000 1-deg squares. Because the effect of the gravity field on the satellite orbit is of much lower frequency than what is obtained from direct altimetry, the two effects can be separated in a first approximation, leading to an initial solution that can be improved by iteration, so that the largest full matrix inversion involves many fewer unknowns.

W. Strange reviewed the methods of combining surface gravity and satellite data that have been applied by him and a number of collaborators in obtaining both regional and worldwide geoids. The method capitalizes on the fact that surface gravity provides the high-frequency contribution and satellite data the low frequency contribution to the field and, furthermore, that the former is irregularly and the latter regularly distributed. At any point the contribution to the geoid from available gravity data for a 20° radius about that point is obtained by Stokes's formula and then suitably combined with the best available satellite geoid. The most recent example of this method of analysis was presented by J. Marsh in the form of a detailed geoid for the Atlantic and northeast Pacific Ocean areas. As part of this work a number of satellite-derived gravity models were evaluated to establish the one that best represented the long-wavelength features of the geoid in the above area. Comparisons with astrogeodetic data and dynamically derived tracking station heights show agreement of the order of 2 m or better.

It has been realized for some time that the techniques applied by N. Wiener to time series have a ready application to spatial series of gravity and astrogeodetic data for the purpose of obtaining the geoid and deflections of the vertical. T. Davis discussed means of obtaining accurate estimates of the spatial frequency content of these in the short-wavelength range of 3–150 km. The basic problem involved is determining the accuracy of the algorithms employed for evaluating the Stokes and Vening-Meinesz integrals. Two such algorithms that have the most desirable frequency responses were presented.

In addition, Davis addressed the problem of inherent spectral leakage associated with computing the numerical Fourier transform for a finite data sample. This particular problem is of primary importance in computing sample spectra or autocorrelation functions for fields where most of the energy is concentrated in wavelengths longer than the available record. A comparison was made between two methods for minimizing leakage: classical window modification with a cosine taper and space domain prewhitening with subsequent frequency domain correction by means of the convolution theorem. Analysis of the undulation spectra indicates that the expected rms amplitude of geoidal undulations over ocean areas for wavelengths below 20 km is less than 3 cm.

The subject of statistical analysis of data was continued by S. Jordan. He pointed out that this approach involves two steps, first, to develop self-consistent statistical models for all signals and noises based on theory and data, and second, to apply standard techniques (least-squares, collocation, or Wiener or Kalmer filtering) to separate the signal and noise. Jordan and his collaborators have employed this approach for the estimation and direct recovery of vertical deflections. Future applications are envisioned for satellite altimetry and gravity gradiometry.

Further emphasis was placed by the next three speakers on the impact of the availability of data that yield high-frequency information regarding the gravitational field. Methods of coping with this type of data (especially altimetry) lead to the problem of how to best represent the field, or to put the question another way: given a certain type of data, what is the most expeditious form of the parameters of the solution?

F. Morrison described the method in which the gravity field is represented by a simple surface density layer and the parameters of the solution are the values of the density, usually discretized over a grid on the surface. This representation has been used successfully with satellite perturbation data and is planned to be employed with altimetry. The primary difficulty with the method is that the integral that computes the geopotential is improper, going to infinity if the point at which the potential is required is directly on the surface. Close to the surface the numerical quadrature formulas do not work well, and these difficulties are amplified in computing the gradient of the potential. Morrison has been experimenting with variable grid sizes and analytic representations for the density instead of a fixed mesh of constant density cells, which is equivalent to an array of surface mass points. Techniques of this nature have improved the present lower practical

limit of these formulas to an altitude of 200–300 km, instead of the 1000-km altitude for the fixed mesh. It is hoped that further experimentation will make them valid even at the surface. A related problem is that of speeding the calculations, since the computing time increases with the fineness of the mesh. Possible approaches include reducing the order of numerical quadrature, or substituting an analytic or series approach for quadrature.

Just as Stokes's formula provides a direct method for obtaining geoid heights from gravity data, an inverse of this formula will yield gravity from geoid heights. J. Buglia showed how these two formulas can be combined into an algorithm to handle a combination of gravimetry and altimetry. The earth's surface is partitioned into cells; it is assumed that there is a gravity observation for each land cell, and an altimetry (i.e., geoid height) observation for each water cell. One can begin with the direct formula, assign gravity values from some model for the cells that have no gravity observations, compute geoid heights, assign these to cells with no geoid height observations in the inverse formula, and continue the iteration until suitable convergence is reached. Geoid heights obtained in a test case for 30° cells, using an eighth-degree field to generate the simulated data, checked to within 3 m.

The spherical harmonic representation of the geopotential is acknowledged to be the best and most efficient way of handling satellite orbits, but it becomes deficient when tackling localized, irregularly distributed data like altimetry. C.A. Lundquist and G.E.O. Giacaglia have set forth a linear transformation representation of spherical harmonics, which they have termed 'sampling functions,' and which passes the property of mirroring local effects very efficiently. These functions were discussed by R. Brown. He pointed out that spherical harmoinc sampling functions are just one example of many such types, each type being derived from a different set of orthogonal functions. Investigations into the common properties of this larger set give an insight into the limitations as well as the advantages of spherical harmonic sampling functions.

Altimetry measures to the sea level surface. Then the geocentric radius vector to the satellite is (roughly) the sum of the altimetric reading, the geocentric ellipsoidal radius, the geoid height, and departure of sea level from the geoid. To separate out these last two quantities, which are the ones of geophysical interest and are of the order of 10 m and 1 m, respectively, it is necessary to obtain the position of the satellite to a comparable precision. P. Argentiero reported on test runs based on simulated laser station data for GEOS-C for long (more than 1 day) arcs. The data reflected the presence of 10-cm noise and bias in the laser measurements, a 5-m error in each tracking station coordinate, and a 5% error in the dominant geopotential terms. The tracking stations were concentrated in the west Atlantic of the U.S. coast. Using arcs up to 7 days in length, the average orbital height error was 1.4 m over the aforementioned area and up to 8 m over each entire arc. It is believed that the primary source of error is due to the geopotential uncertainty.

J. Berbert attacked the same problem from the point of view of short arc (less than 10 min) determination. The simulations were based on tracking from 4 neighboring stations. The most crucial factor in orbital height recovery was the limitation on the number of stations that could track, owing to weather conditions. To obtain a 2-m height accuracy for 10 min, the experiment showed that all 4 lasers are required.

W. Kahn gave an overall summary of geopotential recovery from altimetry data, discussing the form of the observation equations, the possible parametric representations of the geopotential, and the errors resulting from the necessary limitations on the size of the parametric set.

S. Yionoulis proposed the two-satellite system as a future source of improved data for the geopotential. The continuous tracking advantages of a pair (both high-low and low-low configurations) provide resolutions of the field up to degree 90 and can yield useful estimates of the deflection of the vertical from data obtained for a single pass.

A contributed paper not presented was 'Computation Techniques for Various Gravity Anomaly Correction Terms,' by H. Emrick. The paper deals with the procedure for reduction to the level surface passing through the computation point, the integration requirement for the inner most area, methods for computation of outer areas using various approaches, and tests to determine whether to use linear, nonlinear, or iterative solutions.

Fifth Geodesy/Solid-Earth and Ocean Physics (GEOP) Research Conference

Planetary Dynamics and Geodesy

Keynote Speaker: John D. Anderson, Jet Propulsion Laboratory

FAWCETT CENTER FOR TOMORROW
THE OHIO STATE UNIVERSITY
COLUMBUS, OHIO

OCTOBER 8–9, 1973

Sponsored by: **American Geophysical Union**
Defense Mapping Agency
National Aeronautics and Space Administration
National Oceanic and Atmospheric Administration
Ohio State University, Department of Geodetic Science
U.S. Geological Survey

The theme for the Fifth GEOP Research Conference will be set by an introductory review. The conference will be divided into the following sub-topics, each introduced by an invited moderator and discussed by a panel:

1. Interior Structure as Inferred from Geodetic Data; Chairman: Wendell C. DeMarcus, University of Kentucky
2. Shape and Topography; Chairman: Charles C. Counselman III, Massachusetts Institute of Technology
3. Gravity Field; Chairman: Robert H. Tolson, Langley Research Center, NASA
4. Rotation and Spin Orbit Coupling; Chairman: S.J. Peale, University of California, Santa Barbara

Further details on the program, accommodations, and registration will be sent to those applicants selected by the committee to attend the conference by September 7.

Individuals interested in attending the conference are requested to send their applications on the standard application form available from the American Geophysical Union, 1707 L Street, N.W., Washington, D.C. 20036

Applications for attendance must be received by August 31, 1973

American Geophysical Union ★ 1707 L Street, N.W. ★ Washington, D.C. 20036

D5

N76-20571

Geodetic and Dynamical Properties of Planets

J. D. Anderson

The work presented in this paper represents one phase of research at the Jet Propulsion Laboratory, California Institute of Technology, under Contract NAS 7-100, sponsored by the National Aeronautics and Space Administration.

THE study of planetary dynamics and geodesy is a difficult subject. This is so, not simply because of the complexity of the interactions between several scientific disciplines, including geophysics, geology, geochemistry, seismology, celestial mechanics, radar astronomy, and meteoritics, but perhaps more fundamentally, because of a lack of data.

Although it is true that the space age has brought about important new observational techniques, which are responsible in large part for the rapid developments in planetary science over the past decade, and although we should expect to see significant progress in the field over the next few years, it is still a sad fact that data will be severely limited for an indefinite period of time in the future. The basic problem is that we can observe and study, at present, only one planetary system in the universe. This system, our solar system, contains only four major planets, five terrestrial planets, where we are inclined to include the moon but exclude Pluto, and a fairly limited collection of debris, presumably left over from some inadequately understood formation process. Thus it is impossible to base the study of planets on a significant statistical sample.

When a peculiarity is observed—for example, the slow retrograde rotation of Venus—there exists no empirical guide to whether this is really a peculiarity or whether it is instead a common occurence in planetary systems in general. It is very unsatisfying to develop an explanation for an observed planetary phenomenon without the opportunity to test that explanation against many planets with similar characteristics. Nevertheless, the best that can be done for now is to gather as many data as possible on the accessible planets and then to rely on theories developed from these data to attempt to achieve an understanding of planetary formation and evolution. This is a difficult task, but no other alternatives are evident.

By far the largest body of planetary data exists for the earth. Its gravity field has been probed in detail by artificial satellites, its surface structure is known, its interior has been explored by seismic measurements, the chemistry of its crust has been specified, and its rotation rate is measured daily. These data and more are invaluable to an understanding of other planets, particularly the terrestrial planets. It is fashionable these days to justify space exploration on the basis of what can be learned about our own planet. Yet, from the viewpoint of a general understanding of the human conditon, it is perhaps more reasonable to justify expenditures in earth physics on the basis of what can be learned about the origin and evolution of the whole solar system. At the present time it is considerably less expensive to study the earth at first hand rather than to explore the moon and planets. For this reason alone, sources of data in the near future are likely to be confined to detailed measurements of the earth and to earth-based observations of the planets, with crucial supplemental information provided by carefully selected experiments on space probes and planetary orbiters. The primary task of the planetary scientist is to learn as much as possible from these data.

The purpose of this paper is to discuss the sources of planetary data and to present a general review of the current knowledge of planetary dynamics and geodesy. The scope of the paper is limited to Mercury, Venus, Mars, and the four major planets. Future expectations in some areas are discussed briefly.

Gravity Fields

Because all planets in the solar system can be treated as spheres to a

---

This article was taken from the keynote address presented at the Fifth GEOP Research Conference on Planetary Dynamics and Geodesy, which was held at the Ohio State University, Columbus, October 8–9, 1973.

zero order approximation, their external gravity fields are usually expressed in terms of spherical harmonics. The gravitational potential is given by

$$U = \frac{GM}{r}\left[1 - \sum_{l=2}^{\infty} J_l \left(\frac{R}{r}\right)^l P_l(\sin\phi) + \sum_{l=2}^{\infty}\sum_{m=1}^{l}\left(\frac{R}{r}\right)^l P_{lm}(\sin\phi) \cdot (C_{lm}\cos m\lambda + S_{lm}\sin m\lambda)\right] \quad (1)$$

where M is the total mass of the planet, R is its equatorial radius, and the spherical coordinates (r, ϕ, λ) are identified with the radius, latitude, and longitude, respectively. The harmonic coefficients (J_l, C_{lm}, and S_{lm}) are determined empirically from the orbital motions of artificial and natural bodies and are related to the density distribution $\rho(r, \phi, \lambda)$ within the planet. *Herrick* [1972] derives the following:

$$J_l = -\frac{1}{MR^l}\int_V \rho(r, \phi, \lambda) r^l P_l(\sin\phi)\, dV \quad (2)$$

$$\begin{Bmatrix} C_{lm} \\ S_{lm} \end{Bmatrix} = \frac{2}{MR^l}\frac{(l-m)!}{(l+m)!}\int_V \rho(r, \phi, \lambda) \cdot r^l P_{lm}(\sin\phi)\begin{Bmatrix} \cos m\lambda \\ \sin m\lambda \end{Bmatrix} dV$$

where the integration is carried out over the entire volume V of the planet.

For a rotating planet in hydrostatic equilibrium, all the harmonic coefficients except the even zonals (J_2, J_4, J_6, ···) will be zero. The terrestrial planets posses significant values for the odd zonal coefficients as well as the tesseral coefficients (C_{lm}, S_{lm}), which indicates that they can support deviations from hydrostatic equilibrium, at least in their outer layers. The accurate determination of the gravity fields for these planets has its greatest value in helping to define and understand the distribution of mass in the upper levels of the planet. An outstanding example of this is provided by the discovery by *Muller and Sjogren* [1968] that the lunar maria are sources of large mass concentrations. By contrast, the value of determining the harmonic coefficients for the major planets is that they provide significant constraints on the allowable density distributions within the planets. However, these are integral constraints as given by (2), and hence it is not possible to determine a unique density distribution from a finite number of gravity coefficients. In this sense the observed coefficients impose necessary but not sufficient conditions on the validity of any proposed planetary model.

The most easily determined parameter in the gravity field of a planet is the zero-order coefficient GM, which represents the total mass. The procedure for determining this quantity for any planet is to observe the orbital motions of other bodies that are perturbed significantly by the planet.

In the case of Mercury a determination is difficult because the perturbations that Mercury exerts on the orbits of Venus and earth are small. Probably the most reliable determination of the mass is provided by radar tracking of the inner planets. Least squares analyses of radar data have been carried out by experimenters at the Massachusetts Institute of Technology and the Jet Propulsion Laboratory. Both groups express their results in terms of the inverse mass ratio $M_M^{-1} = GM_S/GM_M$. The inverse mass has the same accuracy as GM_M because the value of GM for the sun is known to much higher accuracy than any value of GM for the planets. *Ash et al.* [1971] at MIT give a value for M_M^{-1} of 6,025,000 ± 15,000, whereas *Melbourne et al.* [1968*b*] at JPL give a value of 5,983,000 ± 37,000.

There is a difference of 42,000 between the JPL and MIT values of the inverse mass. We adopt a mean value between the two determinations

$$M_M^{-1} = 6{,}004{,}000 \pm 37{,}000$$

With an error of 0.6%, the mass ratio for Mercury is the poorest known of any terrestrial planet's. The reason for this is simple. The masses of the other planets have been determined to high accuracies by means of the Doppler tracking of flyby spacecraft. No spacecraft have flown by Mercury at this time. However, if the Mariner Venus-Mercury spacecraft provides good Doppler data during its scheduled flyby of Mercury in late March of 1974, a very precise determination of the mass of Mercury will be available from the postflight analysis of those data. This analysis will be conducted jointly by experimenters at JPL and MIT and should result in a determination of the mass to at least 1 part in 10^4, or to about ±600 in the inverse mass.

Two spacecraft, Mariner 2 and Mariner 5, have flown by Venus. An analysis of data from both spacecraft by *Anderson and Efron* [1969] has resulted in a value of the inverse mass of

$$M_V^{-1} = 408{,}521.8 \pm 1.0$$

A more recent analysis of the Mariner 5 data, carried out by J.D. Anderson and N.A. Mottinger at JPL (unpublished data, 1973) indicates that this value of M_V^{-1} may be too small by about 1.7 standard deviations. We now prefer a value of

$$M_V^{-1} = 408{,}523.5 \pm 1.0$$

The current Mariner Venus-Mercury mission has the potential of providing more information on the mass of Venus, but the real dynamical significance of any future flyby or orbiter of that planet rests on a specification of the higher-order moments in the gravity field.

A total of four American spacecraft, Mariner 4, 6, 7, and 9, have returned Doppler data from the vicinity of Mars. However, only Mariner 4 has provided usable data during the critical period from a few days before encounter to a few days after encounter with the planet. Mariners 6 and 7 were plagued with significant nongravitational forces during their flybys [*Anderson et al.*, 1970], and Mariner 9, being an orbiting spacecraft, provided mass information only during the approach phase of the mission [*Lorell et al.*, 1973]. A reliable value for the mass of the planet cannot be obtained from orbiter data because strong correlations exist with the orbital elements of the

spacecraft and with the higher moments in the gravity field. This is consistent with the general rule that it is always preferable to determine the mass of a planet from flyby data and then to use this value of the mass along with orbiter data, if it is available, to determine the higher-order moments.

The value for the inverse mass ratio of Mars from the Mariner 4 data is given by *Null* [1969]:

$$M_{\mathrm{Mars}}^{-1} = 3{,}098{,}714 \pm 5$$

The mass of Jupiter has been determined most accurately from its gravitational effect on the orbits of asteroids [*Klepczynski*, 1969; *Scholl*, 1971; *Zielenbach*, 1969] or through its effect on the orbit of Mars as observed in the radar data [*Ash et al.*, 1971; *Lieske et al.*, 1971]. A weighted mean of several determinations has been obtained by *Klepczynski et al.* [1971], and their adopted value is

$$M_J^{-1} = 1047.366 \pm 0.007$$

Two spacecraft, Pioneer 10 and 11, will provide data from flybys of Jupiter in December 1973 and December 1974, respectively. A postflight analysis of the Doppler data will make possible a new determination of the mass of Jupiter to an accuracy of about 0.002 in the inverse mass ratio and in addition will provide a clear discrimination between the mass of the planet and the masses of the Galilean satellites.

The masses of the other major planets have been investigated by *Klepczynski et al.* [1970, 1971]. They used optical observations of Jupiter from 1913 to 1968 to determine the mass of Saturn, optical observations of Saturn from 1913 to 1968 to determine the mass of Uranus, and observations of Uranus from 1781 to 1968 to determine the mass of Neptune. They also evaluated all other independent determinations of the mass and as a result recommended the values given in Table 1.

Surveys of all the determinations of the masses of the planets have been made by *Klepczynski et al.* [1971] and by *Kovalevsky* [1971].

TABLE 1. Masses of Saturn, Uranus, and Neptune

Planet	Reciprocal Mass
Saturn	3498.1 ± 0.4
Uranus	22,800 ± 107
Neptune	19,325 ± 26

After *Klepczynski et al.* [1971].

The higher-order moments in the gravity fields of the planets are best determined from the earth-based tracking of planetary orbiters. At present, only Mars has been studied by this technique and even in this case only one orbit is available (Mariner 9). Nevertheless, *Lorell et al.* [1973] have determined the second- and third-degree harmonics for Mars. Values of the harmonic coefficients for which a significant determination exists have been tabulated by *Jordan and Lorell* [1973]. The second- and third-degree harmonics are listed in Table 2. The fourth-degree harmonics were also included in the fit, but those values tend to be smaller than the standard errors, and they are not listed here.

TABLE 2. Gravity Field of Mars From Mariner 9

Harmonic Coefficient for Mars	Value × 10^5 From Mariner 9
J_2	196.4 ± 0.6
C_{22}	−5.5 ± 0.1
S_{22}	3.1 ± 0.2
J_3	3.6 ± 2.0
C_{31}	0.5 ± 0.4
S_{31}	2.6 ± 0.5
C_{32}	−0.6 ± 0.2
S_{32}	0.3 ± 0.2
C_{33}	0.48 ± 0.03
S_{33}	0.35 ± 0.03

After *Jordan and Lorell* [1973].

The determination of second-degree and higher gravity moments for Mars indicates that the gravity field is closely approximated by the combination of an oblate spheroid and a large concentration of mass in the Tharsis region at a longitude of about 105°W and a latitude of 10°N.

The dynamical flattening that corresponds to the difference in the equatorial and polar axes of a rotating fluid can be obtained from the first-order formula

$$f = \frac{a - b}{a} = \frac{3}{2}J_2 + \frac{1}{2}m + O(J_2^2)$$

where m is the ratio of the centrifugal to gravitational acceleration. *Lorell et al.* [1973] give for Mars

$$m = (4.60 \pm 0.01) \times 10^{-3}$$

and the resulting dynamical flattening is

$$f_{\mathrm{Mars}} = (5.24 \pm 0.02) \times 10^{-3}$$

An idea of the difference in the principal moments of inertia in the equatorial plane can be obtained from

$$(B - A)/MR^2 = 4(C_{22}^2 + S_{22}^2)^{1/2}$$

The gravity coefficients for Mars yield

$$(B - A)/MR^2 = (25.2 \pm 0.5) \times 10^{-5}$$

It is possible to use a close flyby of a planet to determine some higher-order moments in the gravity field. A flyby is in many ways dynamically equivalent to a single revolution of an orbiter in a highly eccentric orbit. Thus repeated close flybys can reveal a considerable amount of information on the gravity field.

Even for a single flyby, solutions have been obtained for J_2 of Mars and Venus from Mariner 4 and Mariner 5, respectively. *Null* [1969] obtained a value for J_2 of Mars of $(187 \pm 7) \times 10^{-5}$, which is in good agreement with the Mariner 9 value, although it is an order of magnitude less accurate. Using Mariner 5 Doppler data, *Anderson and Efron* [1969] obtained a value of $J_2 = (-5 \pm 10) \times 10^{-6}$ for Venus. More recently, J.D. Anderson and N.A. Mottinger (unpublished data, 1973) have reviewed the analysis of the Mariner data and have obtained the second-degree coefficients in Table 3.

TABLE 3. Gravity Field of Venus From Mariner 5

Harmonic Coefficient For Venus	Value × 10^5 From Mariner 5
J_2	2.7 ± 0.9
C_{22}	−0.1 ± 0.6
S_{22}	0.5 ± 0.7

It appears from the analysis of one close flyby that Venus iis more spherical than Mars or earth. The dynamical flattening is

$$f_V = (4.0 \pm 1.4) \times 10^{-5}$$

which corresponds to a difference of only 240 m between the polar and equatorial axes.

The difference in the equatorial moments of inertia is for Venus

$$(B - A)/MR^2 = (2.0 \pm 2.9) \times 10^{-5}$$

The relationship between the gravitational fields of the major planets and their interior models has been reviewed by *Peale* [1973], and the various methods of determining the harmonic coefficients have been evaluated. Our present knowledge of the gravity fields of Jupiter, Saturn, Uranus, and Neptune is based on perturbations in the orbits of the natural satellites. In addition, by assuming hydrostatic equilibrium, various models of the interior can be used to predict unknown coefficients.

The observationally determined values of the coefficients have been discussed by *Brouwer and Clemence* [1961], and theoretical values of the moments J_2, J_4, and J_6 have been calculated from available models for Jupiter and Saturn by *Zharkov et al.* [1973]. They also have estimated J_8 and J_{10}. Theoretical values for J_2, J_4, and J_6 have been computed for all the major planets by *Zharkov and Trubitsyn* [1971] for assumed linear and quadratic density distributions in the interiors.

Recently, *Whitaker and Greenburg* [1973] have remeasured all available plates showing Miranda, the fifth satellite of Uranus, and from a new determination of the nodal and apsidal precession, have concluded that J_2 for Uranus must be in the neighborhood of 0.005. Also, *Garcia* [1972] has determined values of J_2 and J_4 for Saturn from the motions of the satellites Tethys, Dione, Rhea, and Titan. However, the value for J_4 from his determination is equal to 0.0014. A positive value for J_4 would imply that the density of material in Saturn is decreasing with increasing depth below the surface of the planet. Because of the unlikelihood of a decrease in density, we adopt the older value of $J_4 = -0.00103$ from *Brouwer and Clemence* [1961].

A summary of the current knowledge on the gravity fields of the major planets is given in Table 4. Three theoretical models for Jupiter and Saturn are taken from *De Marcus* [1958], *Peebles* [1964], and *Hubbard* [1968], and the coefficients have been calculated by *Zharkov et al.* [1973].

Within the next few years the observed values of the harmonic coefficients for Jupiter and Saturn will be improved considerably by the Pioneer and Mariner Jupiter-Saturn flybys. It is reasonable to expect the two Pioneer flybys of Jupiter to yield values for J_2 and J_4 that are good to the order of 1 part in 10^5.

New determinations of J_4 would be particularly important because at present the observed value ($J_4 = -6.7 \pm 3.8$) depends completely on the analysis of data from Jupiter V, the innermost satellite of Jupiter. Reliable values for J_2 and J_4 from the upcoming flybys would place tighter constraints on the acceptable interior models. This would almost surely result in improvements.

It is also important to determine or bound other harmonic coefficients in the gravity fields of the outer planets because significant values for J_3 or C_{22} and S_{22} would have important implications for interior models. The tracking of spacecraft is the only technique for determining the gravity fields of other planets with enough precision to detect deviations from hydrostatic equilibrium.

Shape and Topography

The general shape of the planets is expressed in terms of their flattening:

$$f = (a - b)/a$$

where a is the measured equatorial radius and b is the polar radius. Optical measurements of planetary diameters have been made by *Dollfus*

TABLE 4. Gravity Fields of the Major Planets

Planet	Model	$J_2 \times 10^3$	$J_4 \times 10^4$	$J_6 \times 10^5$	$J_8 \times 10^6$	$J_{10} \times 10^7$
Jupiter	De Marcus	14.2	−5.9	3.9	−2.8	2.2
	Peebles	15.3	−6.5	4.3	−3.2	2.5
	Hubbard	15.3	−6.3	4.1	−3.0	2.3
	Observed	14.71	−6.7			
		±0.14	±3.8			
	Adopted	14.7	−6.7	4.2	−3.1	2.4
Saturn	De Marcus	16.8	−12.9	15.8	−19	24
	Peebles	17.0	−11.2	12.4	−14	17
	Hubbard	24.9	−16.7	18.3	−21	26
	Observed	16.67	−10.3			
		±0.02	±0.8			
	Adopted	16.7	−10.3	13.0	−16	20
Uranus	Quadratic Law	12.4	−4.0	1.9	...	...
	Linear Law	10.8	−3.2	...	...	...
	Observed	~5				
	Adopted	12	−4	2	...	...
Neptune	Quadratic Law	5.8	−0.86	0.18	...	...
	Linear Law	4.9	−0.66	...	...	...
	Observed	4.9				
		±0.5				
	Adopted	4.9	−0.9	0.2		

TABLE 5. Planetary Shapes

Planet	Equatorial Radius a, km	Geometrical Flattening f
Mercury	2,432 ± 7	...
Venus	6,052 ± 6	...
Mars	3,402 ± 8	0.0103 ± 0.0033
Jupiter	70,850 ± 100	0.0607 ± 0.0020
Saturn	60,000 ± 240	0.1092 ± 0.0057
Uranus	25,400 ± 280	0.028 ± 0.016
Neptune	24,300 ± 450	...

After *Dollfus* [1970*a*, *b*].

[1970*a*, 1972]. *Dollfus* [1970*b*] also has reviewed all the determinations of the equatorial and polar axes for the planets and has adopted what he considers the most likely values along with an estimate of the maximum error. His results are summarized in Table 5 by listing values of a and f. The radius of Venus is derived from radar measurements [*Ash et al.*, 1968; *Melbourne et al.*, 1968*a*].

Any flattening of Mercury or Venus is imperceptible from earth, and not enough precision can be achieved in the optical measurements of Neptune. A new radius of Neptune has been obtained by *Freeman and Lynga* [1970] from a star occultation. They give a larger radius (24,753 ± 59) than that determined from observations of the disk and also obtain a geometrical flattening of 0.0259 ± 0.0051.

The occultation of Beta Scorpii by Jupiter has been used by *Hubbard and Van Flandern* [1972] to obtain a value for the radius of Jupiter of 71,880 ± 30 km at a point in the stratosphere. They estimate that the cloud top on Jupiter is about 300 km below this level. We adopt a value for the equatorial radius at the surface of Jupiter, below the clouds, of 71,400 km, which is somewhat larger than the radius adopted by Dollfus. A value of 0.060 ± 0.001 for the geometrical flattening of Jupiter was also obtained from the Beta Scorpii occultation. This is in good agreement with Dollfus's value in Table 5.

The shape and radius of Mars have been improved significantly by the radio occultation data from Mariner 9. *Cain et al.* [1972] give a mean equatorial radius of 3397.2 ± 1 km and a polar radius of 3375.5 ± 1 km. The geometrical flattening of f = 0.0064 ± 0.0003 from Mariner 9 is consistent with recent values given by *Dollfus* [1972] and *Kliore* [1971] but is not as small as the very accurate dynamical flattening (0.0052 ± 0.00002) determined from the orbital motion of Mariner 9. Mars is supporting stresses that allow a fairly significant difference between the dynamical and geometrical flattening. In addition to a determination of the shape of Mars from the occultation data, *Cain et al.* [1972] find that the center of figure of the planet is displaced almost 3 km south of the center of mass and almost 2 km toward the region of Tharsus (100°W longitude). A similar result has been obtained by *Schubert and Lingenfelter* [1973] from an analysis of radar range residuals.

Measurements of planetary topographies are limited to Mercury, Venus, and Mars. Current information has been obtained primarily from radar and from the Mariner 9 orbiter for Mars. Radar ranging can provide a direct measurement of heights at the subradar point on the planet, but this technique is limited for Mercury and Venus because their spin axes are almost perpendicular to the ecliptic; only an equatorial belt can be explored. The inclination of Mercury's orbit to the plane of the ecliptic reveals a region of about ±7° about the equator, and a similar region is available on Venus because of a combination of an orbital inclination of 3.4° and an obliquity of the equator of Venus to its orbit of 176.5°. On the other hand, the obliquity of Mars is 24.77° and its orbital inclination is 1.85°. Therefore a region of ±26.6° about the Martian equator is available for direct radar topographic measurements from earth. Also, the rapid rotation rate of Mars, as contrasted to the slow rotations of Venus and Mercury, is favorable because the subradar point changes at a rate of about 1° of Martian longitude (60 km) every 4 min. Thus, on any given day of observation it is possible to obtain a strip of radar topography of 100° of arc or more along a particular circle of latitude. The technique is limited at the present time by the power and aperture of existing radar dishes. No observatory can track Mars completely around its orbit, and hence topography is available only for those latitude regions that are viewable at Mars opposition.

A plot of the subradar point on Mars is shown in Figure 1 for a number of years, and the times when Mars is at opposition are shown.

Radar topography around the 22°N parallel of latitude was determined by *Pettengill et al.* [1969] during the 1967 opposition of Mars. During the 1969 opposition, topography was again determined from Haystack to a vertical accuracy of about 100 m and with a horizontal resolution of the order of 1° of arc (60 km). In 1969 a region from 3° to 12°N latitude was mapped. Also, *Goldstein et al.* [1970] reported topographic measurements from Goldstone with a 0°–10°N zone, but resolution was limited and individual peaks or craters were not observable.

Both Haystack and Goldstone were used during the very favorable opposition of 1971 to determine topographic variations between −14° and −22°S. *Pettengill* [1971, 1973] derived surface height variations over this region that are accurate to about 75 m in some favorable cases and that have a resolution of the order of 1.3° (80 km) in latitude and 0.8° (45 km) in longitude. In the region between −14.6° and −17.9°S, where the signal was weaker during the 1971 opposition, a resolution of about 1.7° (100 km) was obtained in both latitude and longitude.

Taking advantage of an increased sensitivity in the Goldstone radar system, *Downs et al.* [1971] obtained surface height variations with an accuracy of 150 m on the average and accuracies of 40 m in regions of strong signal. Resolutions of 0.16° (8 km) were obtained in longitude and 1.33° (80 km) in latitude. This was sufficient to detect the heavy cratering of the Martian surface, and several large craters of 50–100 km in

diameter and 1–2 km deep were particularly conspicuous.

The Mars opposition of 1973 is also being used to obtain surface height variations, but the latitude region is roughly the same as in 1971 (see Figure 1). This is a disadvantage in that no previously inaccessible regions on Mars will be in view, but it is a definite advantage in that closure points, where the same longitude and latitude are at the subradar point at widely separated times, will be available on a two-year baseline. This will impose a very tight constraint on the ephemeris of Mars. In effect, the radial drift in the earth-Mars orbit will be no more than 150 m over two years (0.002 mm/sec), and as a result the separation of orbital effects from topographic effects in the radar data will be achieved to a very high precision.

It is also possible to study the topography of a planet by observing the surface pressure by spectroscopic techniques. This has been done with the Mariner 9 orbiter of Mars in the infrared [*Conrath et al.*, 1973] and in the ultraviolet [*Hord et al.*, 1972, 1974]. The resolution is not as good as with radar ranging, but areas of the planet can be mapped that are inaccessible to radar.

Surface height variations on Venus and Mercury have been obtained by *Smith et al.* [1970] with radar time-delay and Doppler observations. For Venus, heights can be deduced from distortions in the Doppler spectrum or from direct time-delay measurements to the subradar point. Unlike Mars, however, the surface resolution is of the order of hundreds of kilometers, and fine-scale topography is not as easy to observe. Mercury has been investigated by ranging to the subradar point.

Radar data from the inferior conjunction of Venus in November 1970 were combined with earlier data from Arecibo and Haystack [*Campbell et al.*, 1972] to obtain surface height variations over the entire equatorial region on Venus. Surface resolutions of 200–400 km were achieved, and height determinations were repeatable within 200–500 m. Total height variations of the order of 6 km were observed on Venus.

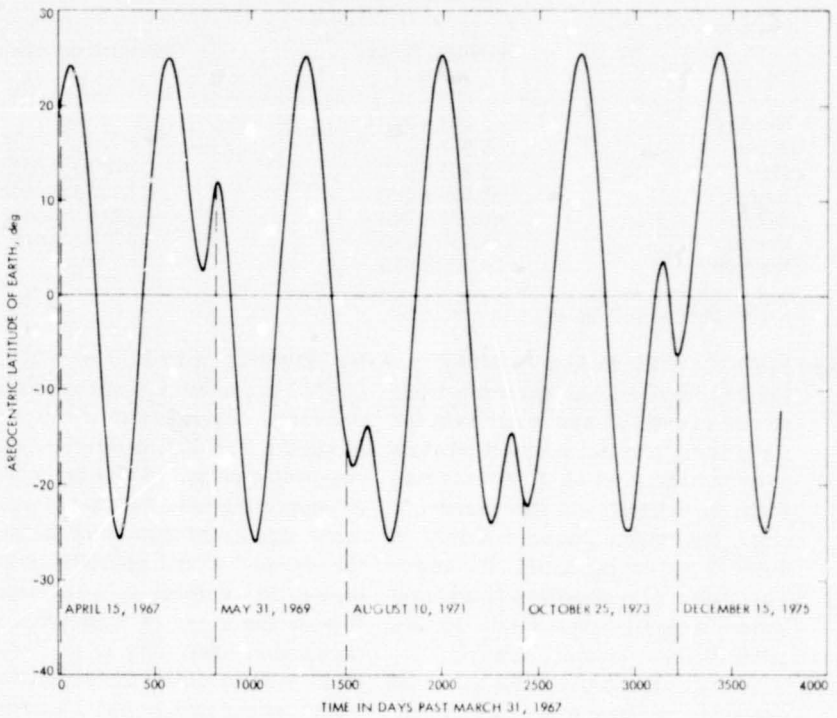

Fig. 1. Variation in latitude of the subradar point on Mars. The Mars oppositions are marked by dotted lines.

Planetary Rotations

Perhaps the most interesting of the planetary rotations, those for Venus and Mercury, were unknown until the advent of radar astronomy. From the April 1965 inferior conjunction of Mercury, *Pettengill and Dyce* [1965] found that its rotation period must be about 59 days in the direct sense. Further radar studies plus a reinterpretation of the visual maps of Mercury [*Chapman*, 1967; *Smith and Reese*, 1968; *Camichel and Dollfus*, 1968] showed that its rotation period was in a spin orbit resonance of 58.65 days. Dynamical justifications for this 2/3 resonance were studied by *Colombo* [1965], by *Colombo and Shapiro* [1966], and by *Goldreich and Peale* [1966*a*, *b*]. They were able to show that the 2/3 resonance is stable and that it can be maintained by solar torques acting on tidal deformations as well as on a permanent asymmetry in Mercury's equatorial plane.

In the early days of planetary radar astronomy, *Muhleman* [1961] demonstrated that the rotation rate of Venus was very slow. Later *Carpenter* [1964, 1966] and *Goldstein* [1964] determined that Venus was rotating in a retrograde sense with a period of about 250 days. Still later, several measurements of the rotation rate were summarized by *Shapiro* [1967], who gave a value of 243.09 ± 0.18 days. Also, the direction of the spin axis was determined to lie within 1° of arc of the negative direction of the orbital angular momentum vector for Venus. The spin rate of Venus was very close to a resonance state with the orbit of the earth, and *Goldreich and Peale* [1966*a*] suggested that the earth might in fact be controlling the rotation of Venus. They called this type of interaction a resonance of the second kind to distinguish it from the case where the rotation rate of a body is determined by its own orbital motion, as in the case of Mercury.

Every synodic period of 583.92 days, Venus apparently makes four complete rotations with respect to the earth. A retrograde rotation period of 243.16 days produces this type of resonance exactly, and hence Venus turns the same face to the earth at every inferior conjunction. However, an earth lock of this type would also occur if Venus had a retrograde rotation of 1454.93 days, in which case it would rotate twice between conjunctions, or of 416.69

days for three rotations, or 171.67 days for five rotations, or 132.67 days for six rotations, and so on. In some ways it seems preferable to assume that the presently observed earth lock is simply a coincidence, rather than to believe that the earth exerts a powerful dynamical control over Venus. If it is simply a coincidence, that the evolution of the spin rate of Venus has just now produced a rather unusual geocentric phenomenon, this does not seem to be any more strange than the fact that the evolution of the orbit of the moon has reached a point where the lunar disk is now almost exactly the same size as the sun. However, in view of the astonishing agreement between the observed value of the rotation rate and the four to one resonance value, attention has been given to a dynamical explanation. A particularly ingenious explanation that relies on a canceling of the solar-induced atmospheric and solid body tidal effects has been proposed by *Gold and Soter* [1969].

Current research on the rotation of planets has concentrated on the evolutionary paths of their spin axes. This is a very interesting problem when the orbital elements of the planet are allowed to vary, and recently *Peale* [1974] has studied this situation by determining the possible evolutionary paths of the spin axis of Mercury.

Planetary Interiors

The specification of a planetary interior is accomplished in all cases by assuming hydrostatic equilibrium and by integrating the differential equation

$$\frac{dp}{ds} = -\frac{G\rho(s)M(s)}{s^2} + \frac{2}{3}\omega^2 s\rho(s)$$

where p is the pressure, ρ is the density, ω is the angular velocity of rotation of the planet, and M is the mass given by

$$M(s) = 4\pi \int_0^s \rho(a)a^2 \, da$$

The independent variable s is associated with the surfaces of constant density within the planet and is related to the radius r and latitude ϕ by

$$r = s[1 + \epsilon_2(s)P_2(\sin\phi) + \epsilon_4(s)P_4(\sin\phi) + \cdots]$$

One more relation between the pressure and density is needed before a solution for the interior can be found. This is the equation of state $p = f(\rho)$.

The basic problem in finding an acceptable model for the planetary interior is to specify the chemical composition with depth and then to find a physically realistic equation of state for the material, often at pressures and densities that are unavailable in the laboratory. In this regard and also with respect to the equation of hydrostatic equilibrium, the problem is quite different for the terrestrial and major planets.

In the case of the terrestrial planets the rotation term in the hydrostatic equilibrium equation is neglected, and spherical models are developed. The assumed materials are taken from earth models. The boundary conditions are the total mass and the radius of [illegible]

Models [illegible] are dominated by [illegible] mean density is of the order of [illegible] g/cm^3, and hence it is composed of relatively dense material with respect to the other terrestrial planets. Modern models for Mercury are very rich in metallic iron, of the order of 60% of the total mass of the planet. *Bullen* [1952*a*, 1973] and *Ringwood* [1966] suggest that the proximity of Mercury to the sun has caused a volatilization of materials with densities less than that of iron. Thus Mercury may be chemically quite different from Venus, earth, and Mars.

Interior models for Venus and Mars follow two very different geochemical assumptions. In the first it is assumed that Venus, earth, and Mars all have the same overall composition and that their cores are composed of hypothetical metallized silicates. The second assumption is that the three planets have cores that are chemically distinct from their mantles, and as a result of this assumption it is usually concluded that the earth, Venus, and Mars do not have the same chemical composition. Arguments that the earth has an iron-rich core are favored by *Wildt* [1961] and *Kovach and Anderson* [1965]. The latter investigators are able to derive models for Venus, earth, and Mars with iron-rich cores and the same overall chemical composition, but it is necessary that the radius of Mars be 3310 km, a value that is now known to be too small by about 85 km.

Models for the major planets are computed in a much different manner than models for the terrestrial planets are. First of all, their low densities imply that they are made up primarily of hydrogen and helium in some unknown ratio. Current models assume that the density ρ of a mixture of x parts of hydrogen by mass and y parts of helium ($x + y = 1$) is given by

$$1/\rho = (x/\rho_1) + (y/\rho_2)$$

where ρ_1 and ρ_2 are the densities of pure hydrogen and of pure helium as derived from their respective equations of state:

$$\rho_1 = g_1(p)$$
$$\rho_2 = g_2(p)$$

When the equation of hydrostatic equilibrium for the major planets is integrated, the rotation term is included, and hence the density distribution within the planet is determined to the first order in the small parameter q ($q = \omega^2 R^3/GM$).

The first-order density distribution can be used to calculate the second-degree zonal harmonic coefficient J_2 to the second order in q and the coefficients J_4 and J_6 to the third order. Formulas for evaluating J_2, J_4, and J_6 from a given density distribution are given by *Zharkov and Trubitsyn* [1970]. These calculated values can be compared with observed values, when they are available, and any model that does not predict the correct external gravity field must be discarded. The harmonic coefficients serve as important boundary conditions on the models of the outer planets.

An inversion of the gravity formulas has recently been performed by W.B. Hubbard (work in preparation, 1974). Under the assumptions

that the planet is in hydrostatic equilibrium and that the density near the surface varies smoothly with depth, assumptions that are probably satisfied by the giant planets but certainly not by the terrestrial planets, it is possible to compute the density distribution in the outer layers of the planets from given values of J_2, J_4, and J_6. Then, by integrating the equation of hydrostatic equilibrium, the variation of pressure with depth in the outer layers can be obtained as well. In this way an empirical equation of state for the planetary material can be obtained to a sounding depth of about 3000 km for Jupiter, 3600 km for Saturn, 1000 km for Uranus, and 500 km for Neptune. It is indeed remarkable that we expect to learn a great deal about the chemistry of the giant planets simply by observing the orbital motions of flyby spacecraft and orbiters, but this happens to be the case. Seismological data will continue to be the chief source of information on the internal structure of the terrestrial planets, but it is expected that the external gravitational fields, as determined from the Doppler tracking of spacecraft, will be the primary source of information on the internal structure of the giant planets.

Theoretical models for Jupiter and Saturn have been calculated by *De Marcus* [1958], *Peebles* [1964], and *Hubbard* [1968, 1969, 1970]. Reviews of this work are available [*Hubbard*, 1973; *Hubbard and Smoluchowski*, 1973]. The main complication in constructing models is to account for the fact that Jupiter and Saturn radiate more energy into space than they receive [*Low*, 1966; *Aumann et al.*, 1969; *Gulkis and Poynter*, 1972]. Radio emissions indicate that Jupiter radiates about 2.7 times more energy than it receives from the sun, and Saturn radiates about 2.4 times more than it receives. This implies that some very high temperatures of the order of thousands of degrees may be reached in the interiors of Jupiter and Saturn. Valid models must take these high temperatures into account and must evaluate the effect of a finite temperature on the equation of state of the hydrogen-helium mixture. This is not an easy problem. Interior models for the outer planets, particularly Jupiter and Saturn, are a subject of active research at the present time, and it is anticipated that upcoming Pioneer and Mariner missions to the planets will provide some very useful information on their gravity fields and atmosphere. Models should become much more definitive within the next few years.

References

Anderson, J.D., and L. Efron, The mass and dynamical oblateness of Venus (abstract), *Bull. Amer. Astron. Soc., 1*, 231–232, 1969.

Anderson, J.D., L. Efron, and S.K. Wong, Martian mass and earth-moon mass ratio from coherent *S* band tracking of Mariners 6 and 7, *Science, 167*, 277–279, 1970.

Ash, M.E., D.B. Campbell, R.B. Dyce, R.P. Ingalls, R. Jurgens, G.H. Pettingill, I.I. Shapiro, M.A. Slade, and T.W. Thompson, The case for the radar radius of Venus, *Science, 160*, 985–987, 1968.

Ash, M.E., I.I. Shapiro, and W.B. Smith, The system of planetary masses, *Science, 174*, 551–556, 1971.

Aumann, H.H., C.M. Gillespie, Jr., and F.J. Low, The internal powers and effective temperatures of Jupiter and Saturn, *Astrophys. J., 157*, L69–L72, 1969.

Brouwer, D., and G.M. Clemence, Orbits and masses of planets and satellites, in *The Solar System*, vol. 3, *Planets and Satellites*, edited by G.P. Kuiper and B.M. Middlehurst, pp. 31–94, University of Chicago Press, Chicago, 1961.

Bullen, K.E., Cores of the terrestrial planets, *Nature, 170*, 363, 1952.

Bullen, K.E., Cores of the terrestrial planets, *Nature, 243*, 68–70, 1973.

Cain, D.L., A.J. Kliore, B.L. Seidel, and M.J. Sykes, The shape of Mars from Mariner 9 occultations, *Icarus, 17*, 517–524, 1972.

Camichel, H., and A. Dollfus, La rotation et la cartographie de la planète Mercure, *Icarus, 8*, 216–226, 1968.

Campbell, D.B., R.B. Dyce, R.P. Ingalls, G.H. Pettengill, and I.I. Shapiro, Venus: Topography revealed by radar data, *Science, 175*, 514–516, 1972.

Carpenter, R.L., Study of Venus by CW radar, *Astron. J., 69*, 2–11, 1964.

Carpenter, R.L., Study of Venus by CW radar–1964 results, *Astron. J., 71*, 142–152, 1966.

Chapman, C.R., Optical evidence on the rotation of Mercury, *Earth Planet. Sci. Lett., 3*, 381–385, 1967.

Colombo, G., Rotational period of the planet Mercury, *Nature, 208*, 575, 1965.

Colombo, G., and I.I. Shapiro, The rotation of the planet Mercury, *Astrophys. J., 145*, 296–307, 1966.

Conrath, B., R. Curran, R. Hanel, V. Kunde, W. Maguire, J. Pearl, J. Pirraglia, and J. Welker, Atmospheric and surface properties of Mars obtained by infrared spectroscopy on Mariner 9, *J. Geophys. Res., 78*, 4267–4278, 1973.

DeMarcus, W.C., The constitution of Jupiter and Saturn, *Astron. J., 63*, 2–28, 1958.

Dollfus, A., New optical measurements of the diameters of Jupiter, Saturn, Uranus, and Neptune, *Icarus, 12*, 101–117, 1970*a*.

Dollfus, A., Diamètres des planètes et satellites, in *Surfaces and Interiors of Planets and Satellites*, edited by A. Dollfus, Academic, New York, 1970*b*.

Dollfus, A., New optical measurements of planetary diameters, 4, Planet Mars, *Icarus, 17*, 525–539, 1972.

Downs, G.S., R.M. Goldstein, R.R. Green, and G.A. Morris, Mars radar observations, A Preliminary report, *Science, 174*, 1324–1327, 1971.

Freeman, K.C., and G. Lynga, Data for Neptune from occultation observations, *Astrophys. J., 160*, 767–780, 1970.

Garcia, H.A., The mass and figure of Saturn by photographic astrometry of its satellites, *Astron. J., 77*, 684–691, 1972.

Gold, T., and S. Soter, Atmospheric tides and the resonant rotation of Venus, *Icarus, 11*, 356–366, 1969.

Goldreich, P., and S.J. Peale, Spin-orbit coupling in the solar system, *Astron. J., 71*, 425–438, 1966*a*.

Goldreich, P., and S.J. Peale, Resonant spin states in the solar system, *Nature, 209*, 1078–1079, 1966*b*.

Goldstein, R.M., Venus characteristics by earth-based radar, *Astron. J., 69*, 12–18, 1964.

Goldstein, R.M., W.G. Melbourne, G.A. Morris, G.S. Downs, and D.A. O'Handley, Preliminary radar results of Mars, *Radio Sci., 5*, 475–478, 1970.

Gulkis, S., and R. Poynter, Thermal radio emission from Jupiter and Saturn, *Phys. Earth Planet. Interiors, 6*, 36, 1972.

Herrick, S., *Astrodynamics*, vol. 2, pp. 160–165, Van Nostrand-Reinhold, Princeton, N.J., 1972.

Hord, C.W., C.A. Barth, A.E. Stewart, and A.L. Lane, Mariner 9 ultraviolet spectrometer experiment: Photometry and topography of Mars, *Icarus, 17*, 443–456, 1972.

Hord, C.W., K.E. Simmons, and L.K. McLaughlin, Mariner 9 ultraviolet spectrometer experiment: Pressure-altitude measurements on Mars, *Icarus*, in press, 1974.

Hubbard, W.B., Thermal structure of Jupiter, *Astrophys. J., 152*, 745–754, 1968.

Hubbard, W.B., Thermal models of Jupiter and Saturn, *Astrophys. J., 155*, 333–344, 1969.

Hubbard, W.B., Structure of Jupiter: Chemical composition, contraction, and rotation, *Astrophys. J., 162*, 687–697, 1970.

Hubbard, W.B., Interior of Jupiter and Saturn, *Annu. Rev. Earth Planet. Sci., 1*, 85–106, 1973.

Hubbard, W.B., and R. Smoluchowski, Structure of Jupiter and Saturn, *Space Sci. Rev., 14*, 599–662, 1973.

Hubbard, W.B., and T.C. Van Flandern, The occultation of beta scorpii by Jupiter and Io, 3, Astrometry, *Astron. J., 77*, 65–74, 1972.

Jordan, J.F., and J. Lorell, Mariner 9, an instrument of dynamical science, paper presented at AAS/AIAA Astrodynamics Conference, Amer. Astronaut. Soc., and Amer. Inst. of Aeronaut. and Astronaut., Vail, Colo., July 16–18, 1973.

Klepczynski, W.J., The mass of Jupiter and the motion of four minor planets, *Astron. J., 74,* 774–775, 1969.

Klepczynski, W.J., P.K. Seidelmann, and R.L. Duncombe, The masses of Saturn and Uranus, *Astron. J., 74,* 739–742, 1970.

Klepczynski, W.J., P.K. Seidelmann, and R.L. Duncombe, The masses of the principal planets, *Celestial Mech., 4,* 253–272, 1971.

Kliore, A., Improved figure of Mars from Mariner radio occultation measurements (abstract), *Bull. Amer. Astron. Soc., 3,* 498, 1971.

Kovach, R.L., and D.L. Anderson, The interiors of the terrestrial planets, *J. Geophys. Res., 70,* 2873–2882, 1965.

Kovalevsky, J., Determination des masses des planètes, *Celestial Mech. 4,* 213–223, 1971.

Lieske, J.H., W.G. Melbourne, D.A. O'Handley, D.B. Holdridge, D.E. Johnson, and W.S. Sinclair, Simultaneous solution for the masses of the principal planets from analysis of optical, radar, and radio tracking data, *Celestial Mech. 4,* 233–245, 1971.

Lorell, J., G.H. Born, E.J. Christensen, P.B. Esposito, J.F. Jordan, P.A. Laing, W.L. Sjogren, S.K. Wong, R.D. Reasenberg, I.I. Shapiro, and G.L. Slater, Gravity field of Mars from Mariner 9 tracking data, *Icarus, 18,* 304–316, 1973.

Low, F.J., Observations of Venus, Jupiter, and Saturn at λ 20 μ, *Astron. J., 71,* 391, 1966.

Melbourne, W.G., D.O. Muhleman, and D.A. O'Handley, Radar determination of the radius of Venus, *Science, 160,* 987–989, 1968*a*.

Melbourne, W.G., J.D. Mulholland, W.L. Sjogren, and F.M. Sturms, Jr., Constants and related information for astrodynamic calculations, 1968, *Tech. Rep. 32-1306,* Jet Propul. Lab., Pasadena, Calif., July 15, 1968*b*.

Muhleman, D.O., Early results of the 1961 JPL Venus radar experiment (abstract), *Astron. J., 66,* 292, 1961.

Muller, P.M., and W.L. Sjogren, Mascons: Lunar mass concentrations, *Science, 161,* 680–684, 1968.

Null, G.W., A solution for the mass and dynamical oblateness of Mars using Mariner-IV Doppler data (abstract), *Bull. Amer. Astron. Soc., 1,* 356, 1969.

Peale, S.J., The gravitational fields of the major planets, *Space Sci. Rev., 14,* 412–423, 1973.

Peale, S.J., Possible histories of the obliquity of Mercury, Submitted to Astron. J., 1974.

Peebles, P.J.E., The structure and composition of Jupiter and Saturn, *Astrophy. J., 140,* 328–347, 1964.

Pettengill, G.H., and R.B. Dyce, A radar determination of the rotation of the planet Mercury, *Nature, 206,* 1240, 1965.

Pettengill, G.H., C.C. Counselman, L.P. Rainville, and I.I. Shapiro, Radar measurements of martian topography, *Astron. J., 74,* 461–482, 1969.

Pettengill, G.H., A.E.E. Rogers, and I.I. Shapiro, Martian craters and a scarp as seen by radar, *Science, 174,* 1321–1324, 1971.

Pettengill, G.H., I.I. Shapiro, and A.E.E. Rogers, Topography and radar scattering properties of Mars, *Icarus, 18,* 22–28, 1973.

Ringwood, A.E., Chemical evolution of the terrestrial planets, *Geochim. Cosmochim. Acta, 30,* 41, 1966.

Scholl, H., Correction to the mass of Jupiter derived from the motion of (143) Hilda, (279) Thule, and (334) Chicago, *Celestial Mech. 4,* 250–252, 1971.

Schubert, G., and R.E. Lingenfelter, Martian centre of mass–Centre of figure offset, *Nature, 242,* 251–252, 1973.

Shapiro, I.I., Resonance rotation of Venus, *Science, 157,* 423–425, 1967.

Smith, B.A., and E.J. Reese, Mercury's rotation period: Photographic confirmation, *Science, 162,* 1275–1277, 1968.

Smith, W.B., R.P. Ingalls, I.I. Shapiro, and M.E. Ash, Surface-height variations on Venus and Mercury, *Radio Sci., 5,* 411–423, 1970.

Whitaker, E.A., and R.J. Greenberg, Eccentricity and inclination of Miranda's orbit, *Mon. Notic. Roy. Astron. Soc., 165,* 15P, 1973.

Wildt, R., Planetary interiors, in *Planets and Satellites,* pp. 159–212, University of Chicago Press, Chicago, 1961.

Zharkov, V.N., and V.P. Trubitsyn, Theory of the figure of rotating planets in hydrostatic equilibrium–A third approximation, *Sov. Phys. Astron., 13,* 981–988, 1970.

Zharkov, V.N., and V.P. Trubitsyn, The gravitational field of the giant planets, *Sov. Astron. AJ, 14,* 465–472, 1971.

Zharkov, V.N., A.B. Makalkin, and V.P. Trubitsyn, Integration of equations of the theory of planetary figures, *Sov. Astron. AJ, 17,* 97–104, 1973.

Zielenbach, J.W., The mass of the Jupiter system from the motion of (48) Doris, *Astron. J., 74,* 567–569, 1969.

John D. Anderson is with the Jet Propulsion Laboratory, California Institute of Technology, Pasadena 91103. He received his Ph.D. in astronomy from the University of California at Los Angeles in 1967. Since he joined JPL in 1960, he has been a principal investigator for several celestial mechanics experiments on Mariner and Pioneer space probes. He is a member of Sigma Xi, the American Institute of Aeronautics and Astronautics, the American Astronomical Society, and the American Geophysical Union.

AGU

OMIT

Planetary Dynamics and Geodesy

REPORT ON THE FIFTH GEOP RESEARCH CONFERENCE

THE Fifth GEOP Research Conference, on Planetary Dynamics and Geodesy, was held October 8–9, 1973, at the Ohio State University and was attended by 55 persons. On behalf of the GEOP steering committee the conference was opened by Ivan I. Mueller, followed by Jack Lorell (JPL), program chairman. The introductory lecture was delivery by John D. Anderson. The lecture in its entirety is printed elsewhere in this issue.

First Session

Panel on Gravity Fields

Chairman: R.H. Tolson (NASA, Langley Research Center)

Members: W.T. Blackshear (NASA, LRC), J.F. Dixon (JPL), P. Esposito (JPL), W.M. Kaula (UCLA), J. Lorell (JPL), R. Reasenberg (MIT)

In his opening remarks, Tolson noted that the keynote address by John Anderson was sufficiently comprehensive that no further review of the status of planetary gravity fields was required. Instead, he addressed his remarks to what he called one of the main problems in planetary gravity field determination, namely, how to extract meaningful and accurate gravity fields from the precise tracking data that is becoming available from planetary orbiters.

There is a tendency on the part of experimenters to try to fit their data to the noise level. This is usually attempted in a planetary gravity field analysis by increasing the degree of the spherical harmonic set being estimated. However, because of the restricted observability associated with planetary missions (e.g., limited range of orbit geometries, occultations, and data spans), increasing the degree of the gravity field usually leads to obvious aliasing in the estimate before all the information is extracted from the data. Thus the analyst suspects that the remaining signal is biasing the estimate, but he also knows that the observability of the system will not support a larger solution set.

Tolson pointed out that the mascon approach of Sjogren and Muller has the advantage of yielding good local fits but permits no extrapolations. On the other hand, spherical harmonics permit extrapolation but provide poorer fits to the tracking data. He proposed that future studies should give consideration to other techniques, such as surface density models, constrained global mascon models, and high-order spherical harmonic models with geophysical constraints. Moritz commented that constrained solutions had been used successfully for many years in the reduction of geodetic data.

Esposito presented a tentative chronology for the Mariner Venus-Mercury mission from the launch in November 1973 to the Venus and Mercury encounters in February and March 1974, respectively. If an 'extended mission' should materialize, the spacecraft will go through superior conjunction in June 1974 and encounter Mercury for a second time in September 1974. He emphasized the celestial mechanics aspects of the Mercury encounter phase of the mission and reported that preflight analysis of simulated data indicates that Mercury's gravitational constant GM will be determined within 0.1 to 1.0 km^3 sec^{-2}. The evaluation of the gravity coefficients J_2, $C_{2,2}$, and $S_{2,2}$ is critically dependent on obtaining high-quality Doppler shift data within encounter ±30 min. The results of the preflight analysis indicate that J_2 will be determined with an accuracy of (1 to 10) × 10^{-5}, and $C_{2,2}$ and $S_{2,2}$ should be evaluated within (0.5 to 5.0) × 10^{-5}. These results represent 2- to 3-order of magnitude improvement in Mercury's mass and the first experimental determination of parameters related to Mercury's gravitational field.

In closing, Esposito mentioned that the Venus flyby will yield an independent evaluation of the planetary mass (previous mass determinations have been deduced from the Mariner 2 and 5 data) as well as refined and independent information on the low-order gravity coefficients J_2, $C_{2,2}$, and $S_{2,2}$ in the potential expansion, as was discussed by Anderson in the keynote address.

Blackshear discussed the gravity field determination problems associated with a Venus orbiter having an orbit geometry similar to that proposed for the Pioneer Venus orbiter. The main problem is associated with the orbit geometry, particularly the fact that a polar orbit is proposed with an apoapse altitude of 61,000.0 km and a periapse altitude of 300.0 km.

Owing to the current preliminary status of the Pioneer Venus 1978 orbiter mission design, Blackshear did not conduct a comprehensive error analysis. Rather, his analysis obtained order of magnitude results on, and insight into, gravitational effects and the anticipated accuracy of estimating gravitational parameters from postflight analysis of such data.

This report was prepared by C.C. Counselman III, W.B. Hubbard, Ivan I. Mueller, S.J. Peale, and R.H. Tolson. Material contained herein should not be cited.

He showed that a direct analysis of Doppler data, spanning a 5-orbit interval, has an ultimate estimation accuracy of 10^{-7} to 10^{-8} for the second-degree spherical harmonic coefficients in the gravitational potential function. However, the biasing effects of unestimated gravitational coefficients through degree 5 degrade this accuracy to the order of 10^{-6}. He estimated that by judicious selection of parameter solution sets and data arc lengths, the direct analysis of Doppler data should yield a postflight estimation accuracy of 10^{-7} for the second-degree harmonic coefficients. On the other hand, Blackshear's results of the analysis of long-period and secular variations in the orbital elements indicates this is not a productive method of analysis for this mission. As illustrations of this point: (1) the ascending node variations due to the second-degree coefficients are, to first order, zero for the nominal mission; and (2) the variation in argument of periapse due to the coefficient $C_{2,0}$ amounts to approximately 0.02 degrees over the complete mission if the current bound of 10^{-5} for $C_{2,0}$ is used.

Dixon reviewed the anticipated results from Jupiter and Saturn gravitational experiments to be performed on the Pioneer and Mariner missions. It is reasonable to assume that these two large, highly spinning, low-density planets will be in hydrostatic equilibrium. Thus the even-order zonal harmonics are expected to dominate their gravity fields. Dixon cited a preflight error analysis that had been performed by George Null at JPL which shows that Doppler tracking of the Pioneer 10 flyby of Jupiter will permit estimates of J_2 and J_4 to better than 10^{-5} and of the Galilean satellite masses to about 1%. The Jupiter mass estimate is expected to be accurate to 300–500 $km^3\ sec^{-2}$, standard deviations. Unfortunately, Mariner Jupiter-Saturn flyby data will not significantly aid in determining planetary coefficients owing to the relatively large encounter distances.

Doppler determinations of the Saturn even zonal coefficients will be complicated by a perfect correlation between these parameters and the mass contained in the rings. Furthermore, if the ring mass is at least 1.5×10^{-6} Saturn masses, as has been suggested by Bobrov, the planetary terms with order greater than 6 will be insignificant compared with ring contributions. Dixon noted that interactions between the rings and Saturn have yet to be considered in planetary interior models.

Lorell presented a summary of and status report on the Mars gravity field analysis at JPL. He pointed out that we know more about the gravity of Mars than that of any other planet, thanks to Mariner 9. Prior to Mariner 9, the mass of Mars and the value of the oblateness coefficient J_2 were well known (on the basis of observations of the natural satellites). Now we have in addition a fairly definitive fourth-degree harmonic representation of the gravity field.

Mars is seen to be an oblate spheroid, with a marked gravitational bulge at about 110°W, in the area known as Tharsis. This bulge dominates the gravity field and is associated with the four large volcanic peaks that identify the Tharsis area.

Several techniques were used by JPL in deriving the fourth-degree gravity model. The two most effective were (1) the direct least-squares fit to the data by using spherical harmonics and (2) the fit to periapsis data over one resonant cycle by using 92 mass points distributed over the surface. These two techniques, which are quite different, yielded remarkably consistent results. This is a considerable achievement in view of the fact that in a comparable comparison for lunar gravity this was never accomplished.

A few of the most important harmonic coefficients from this model are as follows:

	Accuracy, %
$J_2 = 0.00196$	3
$J_{2,2} = 0.63 \times 10^{-4}$	2
$J_{3,1} = 0.27 \times 10^{-4}$	20
$J_{3,3} = 0.60 \times 10^{-5}$	10
$J_{4,4} = 0.26 \times 10^{-6}$	50

The large size of $J_{2,2}$ (4 times that of the corresponding coefficient for the moon) is associated with the Tharsis bulge and was one of the surprises in the Mariner 9 data.

Reasenberg discussed the evolution of the Mars gravity field analysis being performed at MIT. He reviewed the early short-arc analysis of the Mariner 9 tracking data, which yielded a number of sets of spherical harmonic expansion coefficients for the Mars gravity field. These were used successfully in support of the mission navigation effort. When examined for geophysical purposes, however, these navigational models proved to be inconsistent with each other and therefore unusable. It was decided that the data must be used in batches, each of which contain a complete 19-day resonant cycle.

To test this idea, three models were made by combining two 19-day arcs with a total of about 5×10^3 Doppler data: November 16–December 4, 1971, and January 6–25, 1972. These models were of sixth, seventh, and eighth degree. All harmonic coefficients through the indicated degree were estimated, as were two spacecraft states, one for each arc. When these models were represented as equipotential contour maps, it appeared that the sixth- and seventh-degree models were reasonable but that the eighth-degree model contained large nonphysical artifacts. These were assumed to be byproducts of unmodeled effects such as those due to the higher harmonics of Mars and spacecraft gas leaks.

A solution to the artifact problem was sought in the form of a limited memory filter (LMF). The data were broken into four arcs, each 9.5 days long, and the harmonic coefficients were estimated along with the four state vectors. This resulted in a smoothing of all three models. The process was repeated on two additional data sets: December 4–23, 1971, and January 25–February 13, 1972; February 13–March 22, 1972. The complete set of 18 fully converged models can be judged in terms of the internal consistency of the six groups of three, in which members of a group differ only in the choice of data set. It is found that the higher-degree groups are less consistent and that for a given degree the LMF models are more consistent than the unfiltered group.

Reasenberg concluded by saying that, on the basis of their experience with these models, future work will include (1) improvement of the spacecraft motion model, (2) implementation of other filtering techniques, and (3) use of all the data in a single solution.

Kaula presented a general discussion of anticipated gravity field variations based on the M/l^2 rule for the magnitude of normalized gravitational coefficients $\bar{C}_{lm}$, $\bar{S}_{lm}$. He argued that the rule appears to be a consequence of the fact that the characteristic length of phenomena causing density irregularities is small compared with planetary radius. If the size of the irregularities depended solely on the same yield stress for all planets, then the factor M would be proportionate to $1/g^2$. On actual planets, density irregularities depend on an imbalance between dynamic and passive effects—most plausibly, interaction between mobile (asthenospheric) and stiff (lithospheric) parts. The moon (800 km lithosphere) has a factor M that is one-third that predicted from the earth (80 km); the M for Mars (200 km?) is three times that predicted. These results suggest that M for Venus (700°C surface temperature) is smaller by $1/g^2$ than was predicted from the earth; M for Mercury is intermediate between those predicted from Mars and the moon, and the nonhydrostatic variations in the major planets are immeasurably small.

The short characteristic length indicated by the M/l^2 rule means that whether spherical harmonics are the appropriate representation of the gravity field depends much more on the physics of the artificial satellite orbit than on the physics of the planet. For example, high satellite altitude and rapid rotation of the planet favor harmonics. Regardless of the mode of representation, the ill conditioning inherent in tracking an orbit around a distant body makes a priori sigmas for the gravity variations and singular value analysis desirable.

Second Session

Panel on Shape and Topography

Chairman: C.C. Counselman III (MIT)

Members: D.B. Campbell (Arecibo and Haystack), R.M. Goldstein (JPL), C.W. Hord (University of Colorado), R.P. Ingalls (Haystack), H. Masursky (USGS), R.S. Saunders (JPL)

Our current knowledge of the shape and topography of planets other than the

earth and moon is so limited that it is still possible to summarize essentially all this knowledge in one panel session. Our information on Mercury and Venus comes mainly from earth-based radar observations by the Goldstone, Haystack, and Arecibo observatories. Poor signal-to-noise ratio has severely limited the resolution of these observations and has combined with the low spin rates and obliquities to limit the planetary surface coverage. Nevertheless, important characteristics of the topography on these planets have emerged, and a few features such as craters and scarps have been measured in some detail.

Topography on Mars was also first observed by earth-based radar, and such observations continue with ever-improving accuracy and resolution, but the Mariner 9 orbiting spacecraft has given us a much closer look with excellent resolution and planetwide coverage. Five distinct techniques using the spacecraft yield topographic information: (1) ultraviolet spectroscopy, (2) infrared spectroscopy, (3) occultations, (4) television stereogrammetry, and (5) the more qualitative television imaging. The first two of these techniques yield the height of the physical surface of the planet with respect to an isobaric surface of the atmosphere. Combination of these results with those from earth-based radar and spacecraft occultations yields information also on the Martian gravity field. A more direct determination of the gravity field is obtained by tracking the spacecraft's orbital motion. It is important to compare the results of all techniques.

As we attempt to infer from the limited data available what dynamical processes have determined the shape and topography of Mercury, Venus, and Mars, we must not make analogies with terrestrial features without asking whether similar conditions apply. We have seen several times, in the case of Mars, the mistakes one can make by overextending terrestrial analogies. Before Mariner 4, after Mariner 4 but before the first radar measurements of topography, and again after the latter measurements were made but before Mariner 9, false conclusions about Martian topography and dynamical processes were based on terrestrial analogies. We cannot claim to be immune to such errors today.

R.P. Ingalls described surface height profiles near the equator of Mercury measured by the Haystack radar at five interior conjunctions in 1971, 1972, and 1973. The echo from Mercury was resolved in delay and Doppler shift, and the shape of the leading edge of Mercury along the Doppler equator (that is, in the plane passing through the center of mass and normal to the instantaneous apparent rotation axis) was determined by observing the time delay of the first echo returned in each Doppler cell. Resolution was equivalent to 1° in longitude and about 2° in latitude. About 1–2 km of height variation is seen over 10°–20° of longitude, and no more than about 4 km is seen around nearly the entire equator, at least not at this resolution scale. A few relatively sharp features with approximately 1 km of elevation change in a horizontal distance of 40 km have been seen in repeated observations. Overall, Mercury seems to be significantly smoother on horizontal scales greater than a few tens of kilometers than all the other terrestrial planets.

D.B. Campbell reported measurements of topography on Venus by both the Arecibo and Haystack radars and spanning five years. As in the case of Mercury, the Venus measurements are all taken within a few degrees of the equator, but all longitudes on Venus have been well sampled with approximately 1° resolution. The maximum-to-minimum height variation seen on Venus is about 6 km. On Venus as on earth and Mars, the major topographic features extend over thousands of kilometers, but occasionally much sharper relief with a few kilometers of elevation change over 100 km horizontal distance is found. Venus also resembles earth and Mars in having some large portions of its surface significantly smoother than other portions. Such contrast is observed on horizontal scales from 1000 km down to 10 cm. There is a tendency for higher areas on Venus to be rougher.

R.M. Goldstein described observations of Mercury, Venus, and Mars with the 210-ft-diameter Goldstone radar telescope. Delay-Doppler maps of the subearth region on Mercury confirm in more detail the topographic features noted by Ingalls and suggest that some of the sharper features are craters. The first topographic map of Venus made by the technique of delay-Doppler interferometry shows a large crater, 600 km in diameter and 6 km deep with a very flat floor. Earth-based radar profiles of Mars have vertical resolution often better than 100 m, with horizontal resolution of tens of kilometers or better. Detailed elevation profiles have been measured by earth-based radar for many surface features, such as craters, seen in Mariner 9 television pictures. Because Mars rotates rapidly and has been observed over much of its orbit, there is no difficulty in distinguishing orbital effects from surface radius in radar ranging measurements. Thus radar is also useful to establish absolute zero levels and scale factors for some of the spacecraft-based topographic measurements.

C.W. Hord discussed and compared measurements of surface relief on Mars made by Mariner 9 using four different techniques. Both the radius of the physical surface and the atmospheric pressure at the surface were measured by the radio occultation experiment at a number of points forming a coarse grid over the whole planet. Spectroscopic experiments, both ultraviolet and infrared, provided extensive surface pressure measurements south of 20°N latitude. For a few selected features, highly detailed altitude profiles have also been obtained from stereoscopic pairs of television pictures. By using values of the surface radius and pressure measured by radio occultations to calibrate ultraviolet spectrometer (3050 Å) measurements of atmospheric scattering, topographic maps with 10 × 30 km spatial resolution can be obtained for much of the planet. In this way, detailed altitude profiles have been made of the great rift region and the 'middle spot' volcano. Good agreement is found, for most of the planet, between height measurements by the ultraviolet spectrometer and by the infrared spectrometer looking at the optically thin edge of the 15-μ band of CO_2. Comparisons have also been made between the ultraviolet pressure data, converted isothermally to altitude, and ground-based radar data from Haystack and Goldstone. Errors in the pressure-to-altitude conversion and differences in the fields of view of the different measurements are believed to contribute most significantly and approximately equally to the disagreement, generally less than 1 km, between heights measured by the two methods.

R.S. Saunders correlated Martian gravity field results from analysis of Mariner 9 orbit-tracking data with topographic information. Over most of the planet, variations in the gravity field follow closely what would be expected for a homogeneous planet; that is, the surface height variations are not isostatically compensated. However, over Tharsis there is an anomaly of about 500 mGal observed at an altitude of a few hundred kilometers. The height of the topography here is about twice what one would expect from the gravity field on the basis of the relationship between gravity and topography observed over most of the planet. The topographic peak in Tharsis is also much broader than the gravity field peak.

H. Masursky related results from the Mariner 9 television experiment to those of other experiments, both aboard the spacecraft and ground based, and emphasized geologic and geophysical interpretations of these observations.

During the Mariner 9 mission to Mars the entire surface of the planet was photographed at a resolution of 1–3 km, and 1–2% of the surface was sampled with a long focal length camera at a resolution of 100–300 m.

The highest points on the planet, all near the equator, are the great volcanic pile at Nix Olympica and the three volcanoes along the Tharsis ridge. Olympus Mons is 500 km in diameter and rises about 27 km above its base. The peaks along the Tharsis ridge rise about 17 km above the neighboring Amazonis basin. The complex summit calderas and the form of the flank flows indicate that the great volcanoes may be basaltic to andesitic in composition. The crispness in detail of the flows and lack of superposed impact craters indicate that the flows are geologically youthful. The great low-lying plains that occupy most of the northern hemisphere are covered by lobate lava flows and studded with many shield volcanoes, implying a basaltic composition. Extending east from the Tharsis ridge is a little-cratered young plateau underlain by layered, probably volcanic rocks. The

plateau is cut into a mosaic of fault blocks and is transected by a great rift valley that extends 5000 km to the east and is as much as 75 km wide and 6 km deep. The tectonic activity responsible for the faulting and rifting cuts the youngest rocks and may still be continuing.

The southern hemisphere is largely underlain by high-standing, ancient, heavily cratered rocks. The largest impact basin on Mars, Hellas, is almost twice the size of the largest one on the moon, the Imbrium basin. There are ancient heavily cratered volcanic centers in the southern uplands that resemble terrestrial ring dike-cone sheet complexes. On earth these compfexes are composed of highly diversified and, in many cases, highly differentiated silica-rich rocks. Volcanic activity on Mars thus appears to have occurred over a wide interval of time—from the earliest decipherable records until recent times.

The polar regions are underlain by very young glacio-eolian layered deposits that are being actively redistributed by the wind now. They apparently occupy a bowl-shaped depression. If this depression was caused by the weight of the overburden of sediment and ice, it would seem that the Martian crust has responded similarly to the earth's crust, which, in the Hudson Bay region and elsewhere, was depressed by the North American ice sheet during the Pleistocene epoch.

In contrast to the polar regions, the Tharsis ridge with its superincumbent volcanic pile stands high, and the center of mass of the planet is displaced from the center of figure almost 2 km in the direction of this bulge. Furthermore, the center of figure–center of mass displacement is almost 3 km in the direction of the south pole. If the low-density, differentiated early crust was uniformly distributed early in Mars's history, as it apparently was distributed on the moon, it has been stripped from the northern half of the planet and transported to the southern half. Convection within the mantle may have been the driving force. Dynamically, Mars may thus occupy an intermediate position between the earth and moon. The earth has about 75% oceanic crust (basaltic material overlying mantle), Mars about 50%, and the moon about 20%.

Third Session

Panel on Rotation and Spin-Orbit Coupling

Chairman: S. J. Peale (UCSB)

Members: J.A. Burns (Cornell), G. Colombo (Universidad de Padova), R. Goldstein (JPL), R. Greenberg (University of Arizona), W. Ward (Harvard)

Considerable interest and activity in the study of the historical and current rotation of solar system bodies was renewed by the development of planetary radar during the last decade. The anomalous rotations of both Mercury and Venus, which were determined by radar, forced us to reorder our thoughts on possible primordial states of rotation and on the evolutionary paths to the currently observed states.

Several effects alter the primordial spin of a solar system body. Any nonprincipal axis rotation will decay to a rotation about the axis of maximum moment of inertia from internal energy dissipation, unless this dissipation is compensated by some regeneration of the wobble. Tidal friction affords a means of transferring angular momentum in a secular way between the spin and orbital motions, and indirectly, between the orbital motions of the satellites of the major planets. Finally, conservative torques also effect transfers of angular momentum between orbit and spin. The most obvious of these is the tendency for a spin vector to precess uniformly about the orbit normal while maintaining a constant obliquity. An example is the precession of the equinoxes for the earth. Important transfers of angular momentum also result from torques due to the axial asymmetry of a spinning body when the spin is commensurate with the orbital motion. A free libration of the moon leads to a periodic transfer. The maintenance of the spin rate of Mercury at precisely 1.5 times its orbital angular velocity requires that the conservative torque on the axial asymmetry of Mercury have a secular component to counteract the dissipative tidal torque. The unchanging rotation of a planet or satellite at a rate commensurate but not necessarily synchronous with its orbital motion is now referred to as spin-orbit coupling.

The subject of rotation and spin-orbit coupling in the solar system has grown very diverse. The dynamics are for the most part reasonably well understood, but the introduction of more degrees of freedom, which are necessary to describe and explain many of the observations, often leads to surprising bonuses of information. The importance of the study of rotational dynamics in the solar system is emphasized by some of these bonuses of information presented by the panel members. Unfortunately, not all the important topics could be presented, and a time limitation prevented a thorough discussion of many of the subjects that were introduced. This summary contains some details that were mentioned but not thoroughly discussed.

R. Goldstein presented recent radar data on Mercury and Venus that used an improved range-Doppler technique to yield remarkably high resolution of surface features of both planets. With a resolution of about 7 km on Mercury and a little worse on Venus, craters were identified on both planets. Interferometry was used in conjunction with the range-Doppler technique on Venus to eliminate the north-south ambiguity and improve resolution. The radar technique for using the features to determine both the rotation rate and the direction of the spin vector was reviewed. The current determinations of the Venus spin vector of 243.0 ± 0.1 days retrograde magnitude and direction within about 3° of the orbit normal should be improved considerably when the technique is fully utilized. A spin direction for Mercury could eventually be determined to 0.3°.

G. Colombo emphasized the connection of the study of rotation with the history and origin of the solar system as well as a means of constraining the internal physical parameters of the body. Primordial spins, if they are known, establish another initial condition for solar system formation, and the subsequent history of those spins may be limited by current observables. (An example that was not discussed but that illustrates the determination of physical properties is that the retrograde spin of Venus requires either a liquid core or atmospheric thermal tide to stabilize it against disruption by the gravitational tide.) The many cases of spin-orbit coupling (mostly synchronous rotation) and orbit-orbit coupling (commensurability of orbital mean motions of satellites of major planets) cannot be due to chance, and they require secular changes induced by dissipative tides, which bring the various systems to these resonant states. Our understanding of the nonsynchronous spin-orbit commensurabilities, such as that displayed by Mercury, was reviewed. The disruption of such commensurabilities by the tides is easily prevented by torques due to gravitational interaction with a permanent axial asymmetry, which tend to restore the alignment of the axis of minimum moment of inertia with the primary when the body is at the pericenter of an eccentric orbit. The assumption of a fixed orbit and a spin normal to the orbit plane is sufficient for understanding the main features of spin orbit coupling of the type exhibited by Mercury.

R. Greenberg was able to use his detailed study of the establishment of orbit-orbit resonances about Saturn to place rather severe constraints on the dissipative properties of that planet. This is another example of Colombo's statement of learning about physical properties of a planet by studying the evolution of the dynamical system.

Greenberg reviewed the constraints on the specific dissipation function Q near a value of 6×10^4, which was determined by P. Goldreich and S.L. Soter and which was based on the nearness of the satellite Mimas to Saturn. A smaller value of Q would imply a greater transfer of angular momentum to Mimas from Saturn over the age of the solar system. A larger value of Q would not have allowed the tidal origin of the present orbital commensurabilities. Now that a mechanism for tidal evolution into an orbital commensurability is understood, the following additional constraints on the amplitude and frequency dependence of Q are established: (1) tidal evolution of the Titan-Hyperion resonance would have required Q for the tides raised by Titan to be tenfold smaller than the minimum Q for tides raised by Mimas; (2) models of the origin of the Mimas-Tethys and Enceladus-Dione resonances require that in each case the period

ratio have been lowered (by independent tidal evolution of each satellite's orbit) from a previously higher value to its present value of 2; and (3) if the orbital commensurabilities are indeed due to tidal evolution, the amplitude and frequency dependence of the planetary Q must be such as to reproduce the different rates of evolution for the various satellite pairs.

Goldreich's and Soter's estimates of Q for other planets were also briefly reviewed, as was S.F. Dermott's suggestion that Q varied with time as the planets cooled to meet the constraints of orbital evolution. As yet no detailed tidal model has been established for the major planets which attempts to match all the constraints.

W. Ward showed that our ideas of uniform precession of a spin vector about the orbit normal at constant obliquity need to be drastically revised if we relax the constraint of a fixed orbit. This is an example of a bonus of information that was obtained by allowing additional degrees of freedom and that may lead to an understanding of past Martian climatology and the generation of some surface features. D. Brouwer and A.J.J. Van Woerkom found that changes in the inclination and longitude of the ascending node of any orbit on the invariable plane of the solar system could be represented by seven periodic forcing terms. The response of the obliquity to these terms is analogous to a forced harmonic oscillator with its natural frequency identified with the frequency for precession of the equinoxes. If the natural frequency is more rapid than the forcing frequency, the response is suppressed. This corresponds to the earth, which experiences only $\sim 2^\circ$ variation. If the natural and forcing frequencies are close, resonance occurs, producing large oscillations. Mars occupies this state, and obliquity variations approach $\sim 20^\circ$. There are rapid oscillations (1.2×10^5 years) superimposed on a slower variation in the amplitude (1.2×10^6 years). Some implications of these oscillations to the past climate of Mars were briefly discussed.

J.A. Burns summarized the observations of the rotations of 65 asteroids with known properties. All asteroids seem to be in pure rotation with no apparent wobble. The mean rotation period is 8.8 hours. Asteroids that are small or irregular, or both, generally spin faster than this, possibly indicating substantial collisions with other asteroids. The collisional history of the asteroids might be inferred by the persistence of nonprincipal axis rotation and the distribution of obliquities. Nonprincipal axis rotation was shown to damp rapidly owing to internal energy dissipation except perhaps for the very smallest observable asteroids ($r \approx 1$ km), and we would expect to see no remnant wobble at estimated collision rates. Interasteroid collisions should scatter the obliquities of the asteroids except for perhaps the largest ones, which may retain their approximate primordial obliquities.

S.J. Peal discussed the tidal evolution of planetary obliquities in the case where the orbit plane precesses at a uniform angular velocity and maintains constant inclination to the invariable plane. This restriction eliminates the large fluctuations in obliquity due to conservative forces that were discussed by W. Ward. Such a study is an example where constraints on primordial spins can be established or, alternatively, where prejudices about such constraints can be relaxed. The moon, Mercury and the natural satellites of the other planets are examples to which the analysis can be applied.

Colombo, Peale, and V.V. Beletskii have separately discussed the generalization of Cassini's laws (which describe the lunar rotation) to other bodies, most importantly to Mercury. If Cassini's laws are applicable, the spin vector of a body may occupy either one of three positions or one of two positions fixed in the plane defined by the orbit normal and normal to the invariable plane as this plane rotates with the orbital precession. Three positions or spin states are possible if the ratio $\dot{\Omega}_0/\mu \gg 1$ where $\dot{\Omega}_0$ is the precessional angular velocity the planet would have if the orbit were fixed and μ is the angular velocity of orbit precession. State 1 is near the orbit normal (small obliquity) but is opposite the normal to the invariable plane. State 2 is near the orbit plane (obliquity near 90°). State 3 is nearly antiparallel to the orbit normal (obliquity near 180°). This is the situation applicable to Mercury. If $\dot{\Omega}_0/\mu \gg 1$, only two spin states are possible. State 1 no longer exists, and state 2 is now near the normal to the invariable plane but opposite the orbit normal. State 3 remains near an obliquity of 180°. The selection of the Cassini states by the tides is summarized as follows:

1. $\dot{\Omega}_0/\mu \gg 1$: Final position is almost certainly state 1 near the orbit normal. The exception is a negligibly small probability of being trapped near state 2 at an obliquity near 90° at the time of capture into a resonance. State 1 is apparently occupied by Mercury. There is essentially no restriction on primordial obliquity.

2. $\dot{\Omega}_0/\mu \ll 1$: Final position must be state 2 near the invariable plane normal. This state is occupied by the moon. There is no restriction on primordial obliquity.

3. $\dot{\Omega}_0/\mu \approx 1$: Final position is either state 1 or state 2, depending on primordial position of spin vector or on the position at the time of capture into a spin resonance. This case may be appropriate to satellites of major planets.

4. If we relax restrictions on invariance of orbit parameters, the spin remains close to the final Cassini state if the precession of the spin about the Cassini state is rapid compared with the orbital variations. This condition is satisfied by Mercury in state 1, where it probably is, but would not be satisfied if it were in state 2. In the opposite extreme, the spin remains close to the average position of the Cassini state if the orbital parameters vary rapidly compared with the spin precession about that state. This is the condition satisfied by the moon.

Fourth Session

Panel on Interior Structure as Inferred From Geodetic Data

Chairman: W.B. Hubbard (University of Arizona)

Members: M. Podolak (Yeshiva University), R. Smoluchowski (Princeton)

Hubbard began by reviewing the current status of theoretical work on the structure of the giant planets, which exhibit appreciable rotational deformations. For these planets, the classical theory of figures, coupled with data on the higher-order multipole moments J_4, J_6, ..., should prove to be one of the most effective tools for probing their interior structure. Because of their rapid rotation, J_6 for the giant planets is at least an order of magnitude larger than nonhydrostatic terms in the earth's potential. Moreover, a variety of arguments based on observation and high-pressure theory can be made to show that all the giant planets may well be liquid to great depths.

The most important of these points are: (1) tidal dissipation parameters Q for the giant planets that are of the order of $10^4 - 10^5$ and thus are much greater than expected values of Q for solids, and (2) observed net heat fluxes from Jupiter and Saturn that seem to require interior temperatures well above melting temperatures of dense hydrogen or helium. If these conclusions are correct, the giant planets may be in hydrostatic equilibrium to much greater precision than is the case for the terrestrial planets. This will probably require development of the theory of figures to much higher order than has so far been done.

On the basis of the above considerations, V.N. Zharkov and V.P. Trubitsyn in the USSR have calculated planetary models to order J_6 that yield predicted values for Jupiter and Saturn. Although accurate gravitational field data could probably become available for Jupiter and Saturn from orbiters during the next decade, theoretical work available until recently has been inadequate to assess the utility of such data for interior studies.

Recent work carried out by Hubbard, Trubitsyn, and Zharkov in collaboration has been aimed at finding inversion methods for gravity data on planets in hydrostatic equilibrium. One possible scheme discovered by Hubbard was described by him in a second talk. The method proceeds from a theoretical framework used by J.P. Ostriker in stellar rotation problems, i.e., an expansion of the density distribution on a Legendre polynomial basis without carrying out the traditional transformation to level surfaces.

The utility of this approach is that it clearly exhibits the manner in which the basic quadrupole rotational perturbation excites higher multipole response from the planet. The properties of the response, for density distributions appropriate to giant

planets, enables one to solve for the density gradient within the planet at a depth of a few thousand kilometers from a knowledge of J_4. Redundant information, and hence a consistency check, is provided by J_6. The resulting information permits the hydrogen/helium ratio to be determined if these are the main constituents. A different but probably equivalent inversion scheme has been derived by Zharkov and Trubitsyn.

Podolak discussed a series of models for giant planets based on a condensation sequence of compounds from the primitive solar nebula. The hydrogen/helium ratio was fixed to the solar value, but abundances of heavier elements were allowed to increase relative to hydrogen to reflect possible condensation sequences. Dense, rocky cores of considerable size seem to be required for Jupiter and Saturn if one adapts such a picture with adiabatic interior temperatures and fits to available gravitational data. Podolak's models favored a downward revision of J_2 for Jupiter, as seems to be indicated by its optical oblateness. A recent revision downward of J_2 for Uranus is also favored by his models.

Smoluchowski discussed the physical properties of hydrogen and helium within Jupiter and Saturn and their effect on observed parameters including gravitational moments. The usual model of the interiors of Jupiter and Saturn assumes that there is a boundary between the metallic and molecular hydrogen and a miscibility gap in the metallic region. There may be two more boundaries if there is a solid mantle separating a liquid core from a fluid exterior. W.B. Streett's recent experimental studies of the hydrogen-helium system suggest the existence of an additional boundary caused by the immiscibility in the molecular hydrogen region. The stability of these boundaries has been analyzed, and consequences for dynamics of the interior and release of gravitational energy in accord with E.E. Salpeter's mechanism have been investigated. Comparison with the required source of internal heat in Jupiter leads to reasonable results. A progressive change of the moment of inertia of the planet is anticipated.

Sixth Geodesy/Solid-Earth and Ocean Physics (GEOP) Research Conference

Earthquake Mechanism and Displacement Fields Close to Fault Zones

Introductory Speaker: James N. Brune, University of California, San Diego.

INSTITUTE OF GEOPHYSICS AND PLANETARY PHYSICS
UNIVERSITY OF CALIFORNIA, SAN DIEGO
LA JOLLA, CALIFORNIA

FEBRUARY 4–5, 1974

Sponsored by: **American Geophysical Union**
Defense Mapping Agency
National Aeronautics and Space Administration
National Oceanic and Atmospheric Administration
Ohio State University, Department of Geodetic Science
U.S. Geological Survey

The theme for the Sixth GEOP Research Conference will be set by an introductory review. The conference will be divided into the following sub-topics, each introduced by an invited moderator and discussed by a panel:

1. Geologic and Tectonic Aspects; Chairman: Clarence Allen, California Institute of Technology.
2. Observational Data; Chairman: James Savage, National Center for Earthquake Research, USGS.
3. Theoretical Models; Chairman: Johannes Weertman, Northwestern University.
4. Instrumentation and the Future; Chairman: Jon Berger, University of California, San Diego.

Individuals interested in attending the conference are requested to send their applications on the standard application form available from the American Geophysical Union, 1707 L Street, N.W., Washington, D.C. 20036.

Further details on the program, accommodations, and registration will be sent to those applicants selected by the committee to attend the conference by December 28.

Applications for attendance must be received by December 21, 1973.

American Geophysical Union ★ 1707 L Street, N.W. ★ Washington, D.C. 20036

C.2

D6

N76-20572

Current Status of Understanding Quasi-Permanent Fields Associated with Earthquakes

James N. Brune

MANY of the basic concepts relating to displacement fields associated with earthquakes were lucidly described by H.F. Reid in his discussion of the mechanism of the 1906 San Francisco earthquake, originally published in 1910 and recently republished [*Reid*, 1969]. His presentation is a natural beginning point for a modern discussion.

The most important changes since Reid's day concern our increased understanding of the geologic and tectonic setting, the discovery of fault creep, and an extended range of possible models of strain buildup. The plate tectonic model has both strengthened Reid's elastic rebound hypotheses and pointed out modifications to some of his interpretations. Modern problems in tectonic modeling relate to understanding (1) frictional heat generation on faults, (2) the character of stress and strain on faults below the depth of earthquakes, and (3) the predictability of major earthquakes. With modern high-quality data and new techniques we are on the verge of being able to critically limit the range of tectonic models and perhaps to understand the basic physical processes underlying tectonic deformations.

This article was taken from the keynote address presented at the Sixth GEOP Research Conference on Earthquake Mechanism and Displacement, which was held at the University of California, La Jolla, California, February 4–5, 1974.

Excerpts from the Reid Report

The Results of the Surveys

Accurate surveys of a part of the region traversed by the fault-line of 1906 were made by the U.S. Coast and Geodetic Survey at various times and presented by Mssrs. Hayford and Baldwin. Their results may be expressed by Figure 1; they show that the displacements reached a maximum at the fault and were smaller as the distance from the fault was greater, in such a way that a line which, at the time of the second survey, was straight as A′O′C′ had at the time of the third survey been broken at the fault and curved into the form A″B′, D′C″. And, although at a few points there is an indication of a compression or an extension at right angles to the fault, generally the movement was parallel with it. The scale of displacements is 1,000 times that of distances; the curvature of the lines is so very small that it would be imperceptible if the two scales were the same. [*Reid*, 1969, pp. 16–17]

The Nature of the Forces Acting

We know that the displacements which took place near the fault-line occurred suddenly and it is a matter of much interest to determine what was the origin of the forces which could act in this way. Gravity cannot be invoked as the direct cause, for the movements were practically horizontal; the only other forces strong enough to bring about such sudden displacements are elastic forces. These forces could not have been brought into play suddenly and have set up an elastic distortion; but external forces must have produced an elastic strain in the region about the fault-line, and the stresses thus induced were the forces which caused the sudden displacements, or elastic rebounds, when the rupture occurred. The only way in which the indicated strains could have been set up is by a relative displacement of the land on opposite sides of the fault and at some distance from it. We conclude that the strains were set

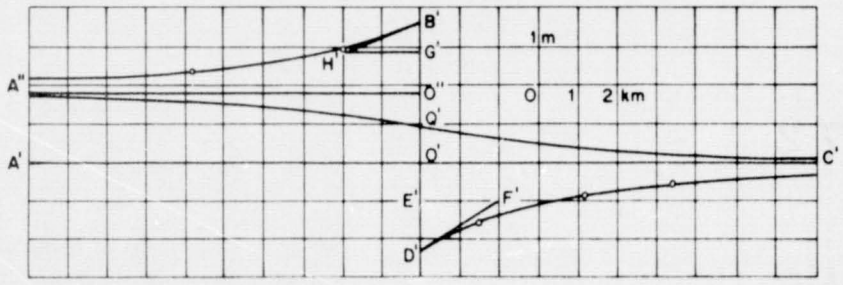

Fig. 1. Diagram illustrating the deformation of surface lines corresponding to the elastic rebound mechanism [*Reid*, 1969].

up by a slow relative displacement of the land on opposite sides of the fault and practically parallel with it; and that these displacements extended to a considerable distance from the fault. It seems not improbable that the strain was accumulating for 100 years, although there is no satisfactory reason to suppose that it accumulated at a uniform rate. [*Reid*, 1969, pp. 17–19]

At this point in the discussion, Reid described an ingenious experiment with gelatin that illustrates the elastic rebound phenomenon.

The Intensity of the Elastic Stresses

The forces which caused the rupture at the fault-plane are measured by the distortion of the rock there, and if we can determine the distortion angles we can estimate these forces. The distortion angle may be as high as 1/1,500. The experiments of Mssrs. Adams and Coker give the value of rigidity for granite as 2×10^{11} dynes per square centimeter (200 kbars); therefore the force necessary to produce the estimated distortion at the fault-plane at a short distance below the surface is 1/1,500 of this, or 1.33×10^{8} dynes per square centimeter (133 bars). [*Reid*, 1969, pp. 20–22]

Reid compares this value for stress drop with some erroneously large values for the strength of granite and concludes that the fault zone must be much weaker than solid granite.

The Work Done by the Elastic Stresses

We can also determine the work done at the time of the rupture; it is given by the product of the force per unit area of the fault-plane multiplied by the area of the plane and by half the slip. If we take the depth of the fault at 20 km, the length at 435 km, the average shift at 4 meters, and the force at 1×10^{8} dynes per square centimeter, we find for the work 1.75×10^{24} ergs. [Using the Gutenberg/Richter energy-magnitude relationship, $\log E = 11.8 + 1.5M$, this corresponds to a magnitude of 8.3.] This energy was stored up in the rock as potential energy of elastic strain immediately before the rupture; when the rupture occurred, it was transformed into the kinetic energy of the moving mass, into heat and into energy of vibrations; the first was soon changed into the other two. When we consider the enormous amount of potential energy suddenly set free, we are not surprised that in spite of the large quantity of heat which must have been developed on the fault-plane, an amount was transformed into elastic vibrations large enough to accomplish the great damage resulting from the earthquake and to shake the whole world so that seismographs almost at the antipodes recorded the shock. [*Reid*, 1969, p. 22]

I omit sections on the distribution of the deforming forces. Reid's ideas here seem to be in part erroneous and in part superseded by recent concepts in plate tectonics. For example, he concludes that the initial deforming forces must have been applied at the base of the crust (lithosphere) near the fault by convection currents forming a closed circuit. He dismisses a suggestion by G.K. Gilbert that the narrow concentration of strain change could be a consequence of the shallow depth of faulting. He mentions the interesting possibility that movements along one fault might trigger movements along another.

The Prediction of Earthquakes

As strains always precede the rupture and as the strains are sufficiently great to be easily detected before the rupture occurs, in order to foresee tectonic earthquakes it is merely necessary to devise a method of determining the existence of the strains, and the rupture will in general occur in the neighborhood of the line where the strains are greatest, or along an older fault-line where the rock is weakest. To measure the growth of strains, we should build a line of piers, say 1 km apart, at right angles to the direction which a geological examination of the region, or past experience, indicates the fault will take when the rupture occurs; a careful determination from time to time of the directions of the lines joining successive piers, their differences of level and the exact distance between them would reveal any strains which might be developing along the region the line of piers crosses.

In the case of vertical, horizontal or oblique shears, if the surface becomes strained through an angle of about 1/2,000, we should expect a strong shock. It would be necessary to start with the rock in an unstrained condition; this could readily be done now in the neighborhood of the San Andreas fault. The monuments set up close to the fault-line were not placed with this object in view, but with the object of measuring actual slips on the old fault-line. Measures of this class described would be extremely useful, not only for the purpose of prediction, but also to reveal the nature of the earth movements taking place and thus, lead to a better understanding of the causes of earthquakes. Less definite, but still valuable information could be obtained by the simpler process of determining from time to time the absolute directions of Farallon Lighthouse and Mount Diablo from Mount Tamalpais; by this means northerly or southerly movements of 1 foot of either of the first two stations relative to the third could be detected; and we should know if strains were being set up in the intermediate region, but we could not tell where the strain was a maximum nor to what extent it may have been relieved by small displacements on intervening fault-planes.

It seems probable that a very long period will elapse before another important earthquake occurs along that part of the San Andreas rift which broke in 1906; for we have seen that the strains causing the slip were probably accumulating for 100 years. There have been no serious earthquakes reported along this part of the rift, except at its southern extremity, since the country has been occupied by white men, although strong earthquakes have occurred in neighboring regions. It seems probable that more consistent results might be obtained regarding the periodicity of earthquakes if only the earthquakes occurring at exactly the same place were considered in the series. [*Reid*, 1969, pp. 31–32]

Reid's concept of the elastic rebound mechanism was remarkably

foresighted. The main modifications that have been added since his time are (1) better understanding of the overall geologic and tectonic picture that gave rise to the forces and processes associated with the earthquake, (2) the discovery of fault creep, and (3) extension of the range of possibilities for the states of stress that could have been responsible for the earthquake.

It was considerably after Reid's time before the first clear evidence for large cumulative displacements along the San Andreas fault was obtained [*Hill and Dibblee*, 1953]. More recently, the development of the theory of plate tectonics has revolutionized our concepts of the deformation of the earth. Cumulative displacements of hundreds of kilometers over millions of years have been established for many fault zones. These motions can be fitted into a rather simple plate model of the lithosphere in which the major tectonic zones are a result of either ridge-type spreading centers where the plates are pulling apart, trench-type subduction zones where plates are crushing together and plunging into the mantle, or transform-fault-type zones where the plates are sliding past one another with more or less horizontal transcurrent motion [*Isacks et al.*, 1968; *McKenzie and Morgan*, 1969].

It is unclear at this time whether the San Andreas fault is a simple boundary between the Pacific plate and the North American plate, or whether a significant amount of the motion between these plates is taken up by offshore or other parallel fault zones, or by compression and rifting of the crust, or by underthrusting of one plate by another; nevertheless, it is clear that the San Andreas fault results from the motion of the Pacific plate relative to the North American plate and contributes a significant amount of this motion. Very convincing data now support an average rate of slip along the San Andreas fault of at least 3 cm per year in recent geologic time and in the last hundred years or so [*Atwater and Molnar*, 1973; J.C. Savage, unpublished data, this conference]. We now know that almost all the earthquakes in California are right lateral and therefore contribute to a net right lateral motion. In Reid's day this was not clear; it might have been possible that left lateral motion could occur and that faulting might result from a complex jumbling of blocks back and forth rather than from cumulative displacement in one direction.

The discovery of fault creep, i.e., continuous or episodic slow movements occurring along the fault without generation of seismic energy, has added a new parameter to our models of fault motion [*Steinbrugge and Zacher*, 1960]. Although this does not change the basic mechanical concepts of Reid, it does suggest new explanations of some phenomena. It suggests the possibility of a large amount of creep occurring below the depth of faulting for large earthquakes. In some areas even shallow parts of the fault are undergoing displacements primarily as creep (R.D. Nason, unpublished data, this conference).

Reid went to some effort to explain how localized stresses at the bottom of the crust could cause slow displacements and strains along the fault. Today we believe that the cumulative slow displacements leading up to earthquakes do not die out with distance from the fault zone and that plates are moving steadily relative to one another.

Although Reid mentions the possibility of weakness of the fault zone concentrating the slip at a particular site or along a particular fault, he does not emphasize this. He attempts to explain the localized slip by localized drag forces. Today it is usually assumed that fault slip along particular faults or plate boundaries is localized by initial weaknesses formed when the plates were created, or by continuing deformation. Stresses might even be higher in the interior of unbroken plates than along the active fault zones [*Sykes and Sbar*, 1973].

Reid did not take into account the difference between stress drop and total stress. He assumed that a stress drop of approximately 100 bars implied that the stresses in the rock prior to the earthquake were also approximately 100 bars. However, if the system is linearly elastic, the stress change is only a lower bound for the initial stress. In laboratory experiments, initial stress can be more than 10 times greater than the stress drop. For the San Francisco earthquake this could imply initial stresses of more than 1 kbar, with consequent energy release (heat plus seismic) 10 times greater than he calculated.

Modern Tectonic Models

A modern model for the San Andreas fault consists of a continental transform fault boundary between the Pacific and North American plates, connecting the spreading centers in the Gulf of California with the spreading centers or a triple junction offshore from Oregon and Washington [*Wilson*, 1965; *McKenzie and Morgan*, 1969; *Atwater*, 1970]. In such a simple system, whenever the fault trace bends to the left, a complication in the fault motion will occur with the two plates tending to thrust over or into one another, and whenever the fault trace bends to the right, a gap or spreading center will occur, with the two plates pulling away from one another and causing intrusion of material into the gap from below (J.C. Crowell, this conference). These features are illustrated in the simplified tectonic fault model of Southern California shown in Figure 2.

There are complications introduced into the system by the structures of the transverse range province and by the existence of parallel faults in the San Andreas system; nevertheless, from a surface point of view, the observations along the San Andreas fault agree well with the plate tectonic theory. Although there is still some controversy concerning this simple theory [*Hill*, 1971; *Baird et al.*, 1974], it is clear that in most recent geologic times the model of progressive right lateral motion is a good approximation.

When we attempt to understand the plate boundary in three dimensions, there are more difficulties and more options in the models. There is no direct way to observe the boundary below the surface. Reid assumed that a lithosphere 10 to 20 km thick (which was equivalent to crust in his day) was subjected to localized viscous convective forces from below.

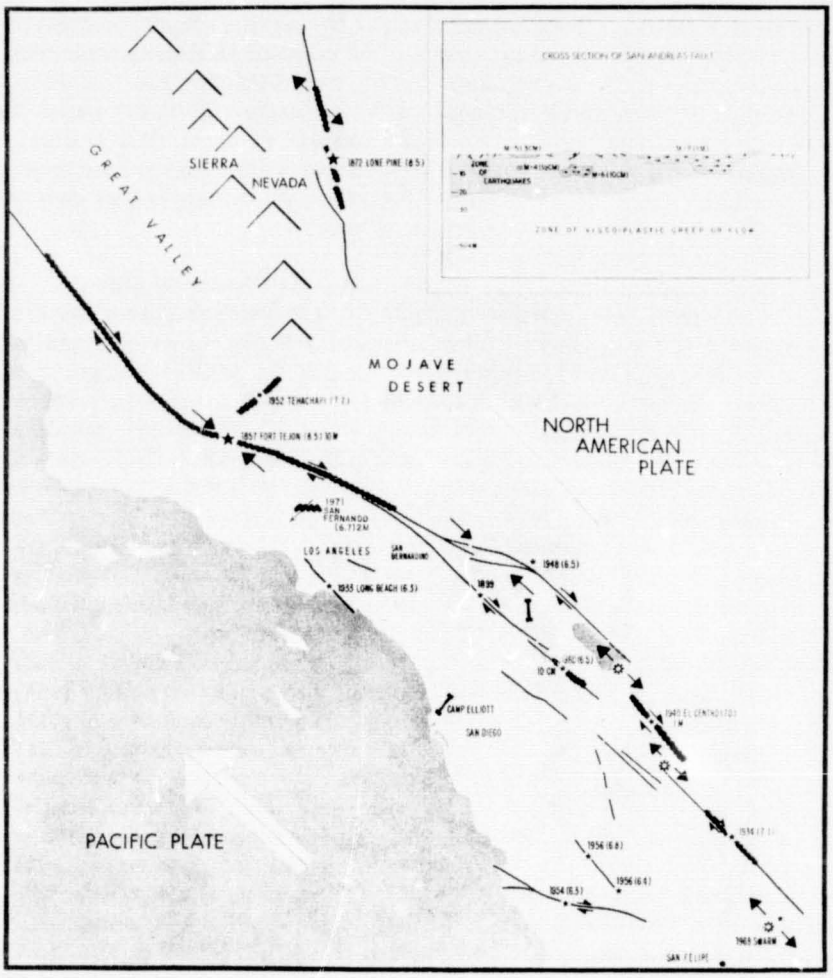

Fig. 2. Diagram of the San Andreas fault system in the neighborhood of southern California. Thick serrated lines represent historical surface breaks, with magnitudes and approximate offsets indicated. Epicenters and dates of selected important earthquakes without known surface faulting are also indicated. Converging arrows indicate zones of crustal compression and thrust faulting; diverging arrows indicate regions of crustal tension and rifting.

Today we believe that the lithosphere consists of large rigid plates moving relative to one another and that the thickness of these plates near their centers is probably of the order of 100 km.

One simple model for the plate boundary along the San Andreas fault consists of two lithospheric plates 100 km thick extending to the fault and separated by a narrow 100-km-deep vertical shear zone. In this model the slip along the fault zone from 20- to 100-km depth is occurring as steady or episodic creep on a time scale too slow to generate observable seismic energy. A model that would include a large amount of slip below 20 km during large earthquakes seems to be excluded by both the geodetic and the seismic data.

Another simple model, which has the lithospheric plates only about 20 km thick, with the motion during earthquakes occurring along the whole fault boundary, also seems to be excluded, since it would imply that the strain drops would extend to distances comparable to the fault length (i.e., of the order of a few hundred kilometers) instead of being concentrated within a few fault depths (i.e., a few tens of kilometers). A more reasonable model might have the plate thickness at approximately 100 km at some distance from the fault but becoming shallower near the fault, with a broad zone of distribution shear possible below the zone of earthquakes.

The simplest plate models assume that there are no stresses applied at the base of the plate. Forces moving the plate are caused either by sinking tension in the plates at subduction zones or by gravity forces sliding the plates off the thermal highs at ridge crests or hot spots, but with the asthenosphere nearly a perfect fluid that does not either drive the plates or resist them. In this case the stresses along the San Andreas fault are all transmitted through the lithosphere, and the pattern of motion in the asthenosphere directly below the fault is irrelevant; it could even be in a local state of left lateral shear while the overlying plate is in a state of right lateral shear. A slight modification of this model would have the plates driven by viscous convective forces in the asthenosphere but with the directions of plate motions determined by the vector sum of many, perhaps random, viscous forces dragging on the plate. Again, there need be no direct correlation between the motion along the plate boundary and the direction of flow in the asthenosphere below.

If we assume that the asthenosphere does apply a significant amount of viscous stress to the base of the lithosphere, then the question arises as to whether, in the neighborhood of the plate boundary, the viscous force acts to resist the right lateral motion or to drive it. If the forces driving the plates are not localized along the transform fault boundaries but originate either at the trenches or spreading centers or from an integrated effect of many different forces acting on the plate as a whole, then it would seem most likely that the local viscous drag in the asthenosphere would be acting to resist the plate motion; that is, the motion of the plates would be shearing the viscous asthenosphere rather than vice versa.

Lachenbruch and Sass [1973] have recently discussed three models they call passive, ductile, and brittle to represent the cases (1) where the shallow part of the crust rides passively over the underlying material (passive), (2) where more or less rigid block motion at depth causes a ductile shearing in the crust (ductile), and (3) where ductile or viscous shear at depth drives rigid or brittle block motion in the crust (brittle).

Their ductile case seems very unlikely, since one would expect the lower temperature and pressure of shallow crust to cause it to be more brittle and since there is strong evidence that most fault slip occurs over a relatively narrow zone. The brittle model would imply that shearing forces at the bottom of the plate in the neighborhood of the fault zone would be acting to resist the plate motion.

A physical model showing a remarkable similarity to oceanic transform faults and spreading centers was described by *Oldenburg and Brune* [1972, 1974, also this conference]. The analogy rests on the peculiar pattern of spreading centers offset at nearly right angles by transform faults. Oldenburg and Brune conclude that this pattern is a result of two conditions: (1) the shear stresses along the transform faults are not great enough to break up or shear the plate; and (2) the stress field in the plate, acting as a stress guide, is nearly uniform. These results strongly suggest that the tectonic plates in the oceans must be in a state of passive tension at least to distances from the ridges comparable to the lengths of transform faults, since it is difficult to conceive of any active forcing mechanism, e.g., convective forces or gravity forces, that would preserve the necessary uniformity in the stress field.

As can be seen from the above discussion, there still exist a large number of possible models for the mechanism of plate motion, and although they have different implications concerning the state of stress, frictional heat generation, and seismic energy release, at present the data are not sufficiently accurate to decide between them. The great challenge brought out by the Sixth GEOP conference is to decide upon and carry out those critical experiments that will allow us to choose between the various models.

Modern Data

Reid based his study of the San Francisco earthquake mainly on the geodetic triangulation results available over a period of less than 100 years. The precision and accuracy of these measurements were about 1 part in 10^5.

Today we have a greatly increased number of data and greatly increased accuracy of measurement, both for triangulation and elevation. We have an extensive array of geodimeter lines distributed along the San Andreas fault. In addition, small geodetic arrays, small creep arrays, and creep meters keep an accurate record of fault slip. We have the possibility of measuring plate motion directly with long-baseline interferometry using satellites, the moon, or extragalactic radio sources. A simple alignment array using astronomical telescopes has been installed by *Vacquier and Whiteman* [1973] along a probable transform fault in the Gulf of California.

In addition to improved instrumental data, we have important information on rates of plate motion from interpretations of the geomagnetic time scale. Eventually the combination of the data on plate motion with a long time sample of fault behavior will allow us to accurately estimate earthquake potential at various parts of the fault.

We have reliable data on the expected in situ strength of rocks, as well as heat flow data in the neighborhood of the fault, that can be used to put constraints on the amount of frictional heat generation over geologic time. Furthermore, an increasing number of data have suggested that an anomalous state of strain, perhaps associated with dilatancy and fluid flow, or microfracturing, may exist over large volumes of rock prior to many earthquakes. Observers in the USSR [*Nersesov and Simbireva*, 1969] reported anomalous changes in the ratio of P wave velocity to S wave velocity (V_p/V_s) preceding large earthquakes in the Garm region of the USSR. *Aggarwal et al.* [1973] observed similar changes preceding small earthquakes in the Blue Mountain region of New York, and *Whitcomb et al.* [1973] reported anomalous velocity changes prior to the San Fernando earthquake of 1971.

Modern Problems

Heat flow, fault friction and strength of rocks. *Brune et al.* [1969] pointed out that the lack of an observable heat flow anomaly along the San Andreas fault gave an upper limit of a few hundred bars for the average stress on the upper 20 km of the fault, averaged over geologic time. When contrasted with the apparent strength of rocks in the laboratory—more than 1 kb—this presented a paradox. It was suggested that low stress along the fault might be explained by a weakened fault zone, possibly because of the presence of fault gouge, the presence of serpentine, the presence of high fluid pore pressures, or a weakening of rocks by relatively high temperatures.

Recently, *Stesky and Brace* [1973] presented extensive data on the strengths of rocks at appropriate temperatures and pressures and found that the paradox could not be explained by the presence of serpentine nor by simple fracturing of rocks along the fault zone. They suggested that the paradox might be explained as a result of (1) actual materials in the fault zone being different from those studied, (2) the existence of high pore pressure that would reduce the effective normal stress and perhaps affect minerals in the fault zone, or (3) a thick gouge zone with unexpected strength properties. They conclude that more data are needed to resolve the paradox and suggest that drilling into a deep fault zone might provide critical data.

Lachenbruch and Sass [1973] recently presented more extensive data on heat flow in the neighborhood of the San Andreas fault in Northern California and confirmed the lack of a localized heat flow anomaly over the trace of the fault. They suggested the existence of a wider (~100 km) zone of high heat flow and presented a thermal model attributing this anomaly to mechanical heat generation in a broad shear zone between the North American and Pacific plates. The model implies that much of the relative plate motion is distributed throughout the broad shear zone, that the right lateral motion of the system is driven by tractions at the edge of the shear zone, and that the motion of the system is resisted at the base of the layer. The model suggests that the (time-averaged)

shear stress for the system may be a minimum at the trace of the fault and that earthquakes may be confined to a superficial layer because of increased ductility at depth.

It is of interest to speculate on the simpler possibility that the broad heat flow anomaly found by *Lachenbruch and Sass* [1973] is directly related to the average shear stress over the whole depth of the fault in the lithosphere. We can easily abstract the results of *Brune et al.* [1969] to apply to this case. Thus a heat flow anomaly of about 1 μcal could result from a rate of slip of 3 cm/yr and a time-averaged stress along the fault of about 500 bars between 20- and 100-km depth.

(This calculation was carried out by several students as a class problem. The result is

$$\dot{q}(x) = \dot{Q}/2\pi \log [(x^2 + b^2)/(x_2 + a^2)]$$

where $\dot{q}$ is the observed surface heat flow, $\dot{Q}$ is the heat generation per unit area on the fault, x is the distance from the fault trace, and a and b are the depths to the top and bottom of the heat generating zone, respectively.)

This would seem to be a straightforward explanation of the broad heat flow anomaly pointed out by Lachenbruch and Sass and would suggest that the time-averaged stress along the fault may increase from less than about 200 bars for the upper 20 km of the fault to about 500 bars for the upper 100 km of the fault. A stress of 500 bars between 20- and 100-km depth is only about a factor of 2 less than the strength estimates of *Stesky and Brace* [1973]. The estimated stress could be increased by reducing the average background heat flow (increasing the anomalous heat flow) or by considering different stress distributions with depth (e.g., stress reaching a maximum at 50 km and decreasing again to near zero at 100-km depth). The fact that the heat flow does not peak sharply over the fault results from the low frictional heat generation on the shallow part of the fault, and this would still have to be explained by some special mechanism.

Is strain buildup and release two-dimensional or three-dimensional? This problem is critical, because it determines the rate of falloff of displacement and strain with distance from the fault. As described by Reid, the displacements at the time of the San Francisco earthquake were three-dimensional because they died off within about 20 km, a distance much less than the fault length. The obvious interpretation is that the faulting only extended to a relatively shallow depth. W.R. Thatcher presented data at the GEOP conference indicating that after the earthquake the zone below 20 km slipped about the same amount. If so, the result of the combined slip during and after the earthquake may have extended to a depth of nearly zero shear strength, thus making the problem two-dimensional; hence the combined strain field would fall off in approximately 1 fault length, i.e., in a few hundred kilometers rather than in a few tens of kilometers as at the time of the earthquake.

J.C. Savage (this conference) presented evidence that part of the San Andreas fault system south of the Bay Area and north of Parkfield is creeping essentially with rigid block motion, indicating that the motion is extending to relatively great depth. Again, the strain release may be two-dimensional and consequently may fall off in a distance comparable to the distance between the Bay Area and Parkfield, i.e., of the order of 100 km. (Of course, the two-dimensional model requires strain concentration at the ends of the section.)

The same situation occurs with strain buildup. For example, if the fault is locked completely down to the depth of the lithosphere and over a section of the fault several hundred kilometers long, the strain buildup will be two-dimensional and will fall off within a few hundred kilometers (length of the locked section) and will be independent of the depth of the locked section. This is one possible explanation of the negative result of *Vacquier and Whiteman* [1973] for fault motion along a transform fault in the Gulf of California. Similarly, the strain buildup prior to the San Francisco earthquake could have been two-dimensional even though the strain release at the time of the earthquake was clearly three-dimensional. Another way of stating this problem is in terms of the time behavior of fault stress below the zone of earthquakes, i.e., does slip along the fault zone below 20 km occur primarily before or after large earthquakes or does it occur more or less continuously between?

Earthquake prediction. Reid suggested that earthquake prediction could be based on understanding the mechanism of strain accumulation: [*Reid*, 1969, p. 31] 'In order to foresee tectonic earthquakes it is merely necessary to devise a method of determining the existence of strains, and the rupture will, in general, occur in the neighborhood of the line where strains are greatest, or along the older fault-line where the rock is weakest.'

This general mechanical model for earthquake prediction is consistent with modern concepts. Unfortunately, it contains within it a possibly severe constraint on the accuracy of any prediction scheme: earthquakes represent a critical-limit phenomenon and might be triggered by a wide variety of effects such as atmospheric loading, tidal strains, nearby small and unpredictable earthquakes, unpredictable creep events in the mantle or shallow crust, or hopefully, by the episodic and observable increase in tectonic strain.

In critical-limit phenomena, the accuracy and reliability of predictions depend on the complexity of the system. Repeated stick-slip events along a smooth saw cut in the laboratory, or in a very small and isolated area of the crust, might be quite predictable, whereas in a complex tectonic situation such as that illustrated by Figure 2, with unknown effects of episodic creep at depth or on adjacent fault zones and with a host of different phenomena causing small perturbations in the strain field, the achievable prediction scheme might be quite probabilistic.

One hope for earthquake prediction is based on finding reliable precursory phenomena. A systematic search for such phenomena associated with large earthquakes is just beginning. Less systematic searches have been carried out for almost 100 years with no reliable result. Some of

the most hopeful precursory phenomena are anomalous changes in elevation, strain, seismic velocities, conductivity, magnetic properties, electric properties, and water flow phenomena (e.g., radon content and well levels).

One recent model used to explain many precursory phenomena is much less probabilistic than Reid's model; this is the dilatancy-fluid flow model [*Nur*, 1972; *Scholz et al.*, 1973; *Anderson and Whitcomb*, 1973]. In this model, increase in strain leads to observable dilatancy and consequent dilatancy strengthening. This is followed by water inflow into the dilatant region that at some point saturates the rock, increases the pore pressure, and triggers the earthquake. Thus the process is relatively causal—if and only if the pore pressure has increased to a certain level will the earthquake be triggered. If it is generally applicable, this model would suggest that relatively reliable predictions could be made by closely monitoring dilatancy and fluid flow. Unfortunately, the applicability of the model is not known at present.

If no generally applicable and reliable precursory phenomena are found, we may have to accept a relatively probabilistic model; i.e., we could specify that a large earthquake is becoming more and more probable in a certain area, but we would not be able to specify its time of occurrence accurately. In such a model all the suggested precursory phenomena could be probabilistically valid in the sense that for a complex system near the failure point any anomalous change is likely to be precursory—e.g., earthquakes occurring in odd places (foreshocks), anomalous changes in strain and related phenomena, and anomalous creep.

A model at the opposite extreme from the causal precursory model is the probabilistic model in which large earthquakes are triggered off by smaller earthquakes; these in turn are triggered by unobservably small and localized strain changes. This model is suggested by the fact that many large earthquakes appear to be multiple events in which the initial events are small compared with later events, e.g., the Alaska earthquake of 1964 [*Wyss and Brune*, 1967]. Distant triggering of small fault slips by moderate earthquakes has been suggested for the Borrego Mountain earthquake of 1968 [*Allen et al.*, 1968] and the Point Mugu earthquake of 1973 [*Ellsworth et al.*, 1973].

In the case of the Alaska earthquake the initial event in the series had a magnitude of only about 6.6 and occurred at the edge of the subsequent rupture zone at considerable depth. Accurate prediction of the Alaska earthquake would have depended on predicting this moderate event as well as knowing that the main rupture zone was in a state of strain that would allow it to be triggered by this particular event and not by the numerous events that preceded it. In such a triggering model, if strain buildup to the critical state is quite slow, the accuracy of prediction could be relatively low. Of course, if buildup to the critical state is relatively rapid, as would be the case if it is caused by a rapid creep episode in the mantle or by a rapid change in pore pressure over the zone of rupture, then more accurate prediction might be possible.

References

Aggarwal, Y.P., L.R. Sykes, J. Armbruster, and M.L. Sbar, Premonitory changes in seismic velocities and prediction of earthquakes, *Nature, 241*, 101–104, 1973.

Allen, C.R., A. Grantz, J.N. Brune, M.M. Clark, R.V. Sharp, T.G. Theodore, E.W. Wolfe, and M. Wyss, The Borrego Mountain, California, earthquake of 9 April 1968: A preliminary report, *Bull. Seismol. Soc. Amer., 58*, 1183–1186, 1968.

Anderson, D.L., and J.H. Whitcomb, The dilatancy-diffusion model of earthquake prediction, in *Proceedings of Conference on Tectonic Problems of the San Andreas Fault System, Geol. Sci. Ser.*, vol. 13, edited by R.L. Kovach and A. Nur, pp. 417–426, Stanford University, Stanford, Calif., 1973.

Atwater, T., Implications of plate tectonics for the Cenozoic tectonic evolution of western North America, *Geol. Soc. Amer. Bull., 81*, 3513–3536, 1970.

Atwater, T., and P. Molnar, Relative motion of the Pacific and North American plates deduced from sea-floor spreading in the Atlantic, Indian, and South Pacific Oceans, in *Proceedings of Conference on Tectonic Problems of the San Andreas Fault System, Geol. Sci. Ser.*, vol. 13, edited by R.L. Kovach and A. Nur, pp. 136–148, Stanford University, Stanford, Calif., 1973.

Baird, A.K., D.M. Morton, K.W. Baird, and A.O. Woodford, Transverse ranges province: A unique structural-petrochemical belt across the San Andreas fault system, *Geol. Soc. Amer. Bull., 85*, 163–174, 1974.

Brune, J.N., T. Henyey, and R. Roy, Heat flow, stress, and rate of slip along the San Andreas fault, California, *J. Geophys. Res., 74*, 3821–3827, 1969.

Ellsworth, W.L., R.H. Campbell, D.P. Hill, R.A. Page, R.W. Alewine, T.C. Hanks, T.H. Heaton, J.A. Hileman, H. Kanamori, B. Minster, and J.H. Whitcomb, Point Mugu, California, earthquake of 21 February 1973 and its aftershocks, *Science, 182*, 1127–1129, 1973.

Hill, M.L., A test of new global tectonics: Comparisons of northeast Pacific and California structures, *Bull. Amer. Ass. Petrol. Geol., 55*, 3–9, 1971.

Hill, M.L., and T.W. Dibblee, San Andreas, Garlock and Big Pine faults, California, *Geol. Soc. Amer. Bull., 64*, 443–458, 1953.

Isacks, B., J. Oliver, and L.R. Sykes, Seismology and the new global tectonics, *J. Geophys. Res., 73*, 5855–5899, 1968.

Lachenbruch, A.H., and J.H. Sass, Thermo-mechanical aspects of the San Andreas fault system, in *Proceedings of Conference on Tectonic Problems of the San Andreas Fault System, Geol. Sci. Ser.*, vol. 13, edited by R.L. Kovach and A. Nur, pp. 192–205, Stanford University, Stanford, Calif., 1973.

McKenzie, D.P., and W.J. Morgan, Evolution of triple junction, *Nature, 224*, 125–133, 1969.

Nersesov, I.L., and I.G. Simbireva, Regularities of distribution of stresses in the foci of weak earthquakes of the Garm region and their relationship to seismicity, in *Acta of the Third All-Union Symposium on the Seismic Regime* (Engl. Transl.), part 1, pp. 147–182, Science Press, Siberian Division, Novosibirsk, USSR, 1969.

Nur, A., Dilatancy, Pore fluids, and premonitory variations of t_s/t_p travel times, *Bull. Seismol. Soc. Amer., 62*, 1217–1222, 1972.

Oldenburg, D.W., and J.N. Brune, Ridge transform fault spreading pattern in freezing wax, *Science, 178*, 301–304, 1972.

Oldenburg, D.W., and J.N. Brune, An explanation for the orthogonality of oceanic ridges and transform faults, *J. Geophys. Res., 79*, in press, 1974.

Reid, H.F., Mechanics of the earthquake, in *The California Earthquake of April 18, 1906*, Carnegie Institution of Washington, Washington, D.C., 1969.

Scholz, C.H., L.R. Sykes, and Y.P. Aggarwal, Earthquake prediction: A physical basis, *Science, 181*, 803–810, 1973.

Steinbrugge, K.V., and E.G. Zacher, Creep on the San Andreas fault—Fault creep and property damage, *Bull. Seismol. Soc. Amer., 50*, 389–396, 1960.

Stesky, R.M., and W.F. Brace, Estimation of frictional stress on the San Andreas fault from laboratory measurements, in *Proceedings of Conference on Tectonic*

Problems of the San Andreas Fault System, Geol. Sci. Ser., vol. 13, edited by R.L. Kovach and A. Nur, pp. 206–214, Stanford University, Stanford, Calif., 1973.

Sykes, L.R., and M.L. Sbar, Intraplate earthquakes, lithospheric stresses and the driving mechanism of plate tectonics, *Nature, 245,* 298–301, 1973.

Vacquier, V., and R.E. Whiteman, Measurements of fault displacement by optical parallax, *J. Geophys. Res., 78,* 858–865, 1973.

Whitcomb, J.H., J.D. Garmany, and D.L. Anderson, Earthquake prediction: Variation of seismic velocities before the San Fernando earthquake, *Science, 180,* 632–635, 1973.

Wilson, J.T., A new class of faults and their bearing on continental drift, *Nature, 207,* 343–347, 1965.

Wyss, M., and J.N. Brune, The Alaska earthquake of 28 March 1964: A complex multiple rupture, *Bull. Seismol. Soc. Amer., 57,* 1017–1023, 1967.

James N. Brune is associate director of the Institute of Geophysics and Planetary Physics at the University of California, San Diego, and chairman of the Geological Research division of Scripps Institute of Oceanography. He was the first recipient (in 1962) of AGU's James B. Macelwane award for outstanding contributions to the geophysical sciences.

AGU

OMIT

Earthquake Mechanism and Displacement Fields Close to Fault Zones

REPORT ON THE SIXTH GEOP RESEARCH CONFERENCE

THE Sixth Geodesy/Solid Earth and Ocean Physics (GEOP) Research Conwas held on February 4–5, 1974, at the Institute of Geophysics and Planetary Physics, University of California, San Diego, in La Jolla, California. It was attended by about 100 persons.

James N. Brune, program chairman, opened the conference and delivered the introductory address, a somewhat extended version of which is printed elsewhere in this issue. Brune's paper and the following summaries of the sessions constitute a report of the conference.

First Session

Panel on Geologic and Tectonic Aspects

Chairman: C.R. Allen (California Institute of Technology)

Members: C.B. Raleigh (U.S. Geological Survey), J.C. Crowell (University of California, Santa Barbara), M.G. Bonilla and G. Plafker (U.S. Geological Survey)

In his brief introductory remarks the chairman stressed the importance of actual field and laboratory measurements in designing realistic models of earthquake mechanisms.

C.B. Raleigh, in the first formal presentation, discussed the implications of recent rock mechanics experiments in the light of the dilatancy model that A. Nur has used to explain the Vp/Vs anomalies preceding earthquakes. Crack propagation stress depends on the internal fluid pressure within the cracks. If the pore pressure is greater than the liquid-vapor equilibrium pressure, opening of cracks will cause the pressure to drop and stabilize the crack. Thus the adjacent cracks will propagate, which will cause the dilatant region to grow, depending primarily on the stresses in the rock. One conclusion is that the pore pressures at the time of earthquakes will be near the liquid-vapor equilibrium pressure. Also, since the total stresses control the dimensions of the dilatant region, thrust faults might be expected to have dilatant volumes that are large compared with those for strike slip faults.

This report was prepared by C.R. Allen, Jon Berger, Ivan I. Mueller, J.C. Savage, and J. Weertman. Material contained herein should not be cited.

J.C. Crowell emphasized that rocks subject to earthquakes in California have been involved in a long and complex history that ought to be kept in mind as we attempt to understand events before, during, and after earthquakes. In looking at the San Andreas system through time, the geologic record discloses that major blocks have moved laterally on near-vertical fault zones, but that these faults are many and are by no means straight or parallel. Blocks along straight faults move easily with pure strike slip, but where the faults curve, two kinds of bends occur, restraining bends and releasing bends. Rocks inside curves of restraining bends have been severely deformed through horizontal shortening for long periods, whereas those outside such bends have been locally stretched. Releasing bends result in the opening of holes, sags, or pull-aparts. The Los Angeles basin was probably formed as a pull-apart depression in Miocene time, and, as in the Salton trough today, volcanics formed the floor as an irregular pull-apart opened and sediments concomitantly poured into it. In the California borderland, fault divergence and convergence, in combination with pull-apart depressions and restraining-bend uplands, provide a simple geometric model of the tectonics. In summary, the boundary between the North American and Pacific plates ought to be envisaged as a broad zone a few hundred kilometers wide that sits astride the present San Andreas fault. This broad zone, through late Cenozoic time, has been active in complex ways that are now being geologically documented.

The detailed description of surface faulting during historic earthquakes was the subject of M.G. Bonilla's remarks. He illustrated these with both photographs and detailed maps of a number of significant historic earthquakes associated with surface faulting. The principal conclusions he drew were the following.

1. There is a poor correlation between magnitude and the surface length of rupture.
2. The correlation between maximum displacement and magnitude is moderately good.
3. Fault zones have appreciable widths, which must be taken into account in engineering considerations.
4. Subsidiary fractures, although usually quite small, can occur many kilometers from the main fault. In the Assam earthquake of 1897, one subsidiary break

was 80 km from the presumed main fault.

5. Contrary to earlier conclusions, the zones affected by the main and subsidiary fractures are as wide for strike slip faults as for other fault types.

6. Map patterns of surface faulting are usually very complex.

The great 1899 earthquake near Yakutat Bay in Alaska was the subject of G. Plafker's paper. On the basis of recent field work, he reinterpreted many of the conclusions contained in the classic 1901 study by Tarr and Martin. Following are his major points.

1. Seismicity and deformation are centered along the south front of the Chugach and St. Elias mountains and probably extend for at least 160 km, and possibly 250 km, west of the Yakutat Bay area.

2. Earthquake-related deformation was primarily uplift relative to sea level and probably involved slip on the complex system of east-trending, north-dipping thrust faults that extend inland from the Gulf of Alaska to the Chugach-St. Elias fault. Absence of an oceanic tsunami suggests that there was probably no significant vertical uplift offshore.

3. Vertical tectonic displacements in the Yakutat Bay area do not define a system of local fault-bounded blocks, as was inferred by Tarr and Martin. Instead, they define a broad regional upwarp 50 km long by 30 km wide, with an average uplift of 2–3 m. Extreme local uplifts of as much as 14.2 m occurred at a small fault-bounded block that is superimposed on the broader upwarp.

4. Swarms of fractures that Tarr and Martin thought to be subsidiary faults at the Nunatak and elsewhere were caused instead by large-scale earthquake-triggered slides.

5. According to this reappraisal, the 1899 earthquake sequence does not fill a possible seismic gap east of the focal region of the 1964 Alaska earthquake. If so, this part of the Alaskan continental margin may have a relatively high potential for a future major earthquake.

Second Session

Panel on Observational Data

Chairman: J.C. Savage (U.S. Geological Survey)

Members: R.O. Castle, R.D. Nason, and M.D. Wood (U.S. Geological Survey)

The phenomenon of fault creep (aseismic fault slip) has been observed directly in Turkey and very recently (according to a comment by G.C.P. King) in Iran. The most extensive observations, however, have been made along the San Andreas fault system in central California, and it was those observations that were reviewed by R.D. Nason. The observed fault creep at some sites is episodic, with several millimeters of fault slip occurring in a period of a few hours, followed by weeks in which very little, if any, slip occurs. At other sites, slip is essentially steady with only minor fluctuations in the creep rate.

Studies of the episodic creep events indicate that the events propagate from site to site at velocities of the order of a few kilometers per day, suggesting spreading surfaces of failure. The observation that rates of fault creep are virtually identical with the observed geodetic deformation across a zone at least 10 km wide suggests that fault creep must extend to appreciable depth (say 20 km or more) on the fault. However, the question of whether creep at depth is eventful or is steady has not been resolved.

J.C. Savage reviewed the geodetic measurements of horizontal deformation. The measured horizontal displacement fields associated with earthquakes are generally consistent with simple dislocation models of faulting, although the detailed agreement is never very good. Two measurements of relative plate motion across the San Andreas fault were contrasted: Astronomic azimuths observed in the vicinity of Hollister, California, indicate a linear-in-time right-lateral motion of 33 mm/yr across a 50-km-wide zone in the period 1884–1962. This motion is almost wholly accounted for by rigid-block motion. Optical parallax measurements in 1970 and 1972 by V. Vacquier and R.E. Whiteman across what is thought to be the fault trace in the Gulf of California suggest no appreciable relative motion other than perhaps uniform rotation across a 25-km-wide zone, although other interpretations are possible. A review of the measurements of the California geodimeter network substantiates the suggestion of R.W. Greensfelder and J.H. Bennett that the measurements of line length versus time generally exhibit a positive curvature (i.e., $d^2L/dt^2 > 0$) throughout the state. It is not yet clear whether this is an artifact of changes in observational procedures or a real physical phenomenon. Although measurements of strain accumulation along the San Andreas fault are individually suspect, taken all together they indicate that the rate of tensor shear strain accumulation is about 0.3 μ strain/yr. W.R. Thatcher discussed the measured strain accumulation near Fort Ross, California, as deduced from triangulation surveys in 1874, 1906, 1930, and 1969. He showed that the data indicated 4 m of slip to a depth of about 10 km at the time of the 1906 earthquake, followed by afterslip of about 3 m in the depth range from 10 km to 20 km or deeper in the period 1906 (postearthquake) to 1930. No significant deformation was detected in the period 1930–1969. Savage suggested that the apparent afterslip might equally well be explained by relaxation of a viscoelastic subcrustal layer, as was proposed by A. Nur and G. Mavko to account for postseismic movements following the 1946 Nankaido earthquake.

Measurements of vertical deformation as detected by geodetic leveling were discussed by R.O. Castle. The vertical deformation observed at the time of an earthquake can be rather precisely reproduced by simple dislocation models. However, the vertical deformation that is known to precede some earthquakes is not understood. Castle reviewed the data that indicated an anomalous 50-mm uplift near Niigata, Japan, five years before the magnitude 7.5 earthquake there. The data would appear to be consistent with the dilatancy theory. New data for vertical deformation near San Fernando, California, in the decade preceding the magnitude 6.5 earthquake there were also presented. Level surveys repeated in 1961, 1964, 1965, 1968, 1969, and 1971 (postearthquake) furnished an exceptionally fine data base for dectection of vertical movement. Several identifiable pulses of anomalous uplift of as much as 80 mm could be detected at various times in the 1961–1971 period, any one of which might be premonitory to the San Fernando earthquake. However, the largest anomaly, about 200 mm, occurred near Palmdale, California, between 1961 and 1964 and appears to be associated with the San Andreas fault. N.L. Morrison discussed the possibility that vertical deformation of the amount associated with these anomalies could be attributed to accumulated error in the level surveys. Random errors in first-order levels accumulate as $aL^{1/2}$ where a is less than 1 mm/km$^{1/2}$ and L is the length of the surveyed section. Observation and computation procedures are such that known causes of systematic error are eliminated by cancellation, calibration, or correction. Existence of significant systematic error is unlikely on these lines of length less than 100 km. Thus the reported anomalies appear to be well above expected errors.

Tide gages along seismically active coasts offer the possibility of obtaining continuous records of preseismic, coseismic, and postseismic vertical deformation. M.D. Wood reviewed these data. Good records of the coseismic elevation changes have been obtained at the time of several great seismic thrusts. The records apparently do not show significant vertical motion immediately preceding (e.g., a few hours before) the earthquakes. Whether premonitory uplift occurs years before the earthquake is difficult to ascertain because of the inherent noise in the tidal record due to changes in water temperature and salinity, prevailing winds, and barometric pressure. The reported abrupt change in sea level at Nezugaseki, Japan, five years before the Niigata earthquake is seen only after corrections for the above parameters are made; the absence of any anomaly on the uncorrected record makes the existence of that reported precursor dubious.

Finally, A.M. Dziewonski reported on compressive deformation at the source that apparently preceded and accompanied two deep-focus earthquakes (Columbia, July 31, 1970, and Peru-Bolivia, August 15, 1963) studied by him and F. Gilbert. The conclusion was based on the low-frequency behavior of the seismic moment tensor determined from several hundred seismograms. The conclusion that the compression was actually precursive was based on extrapolation of the ob-

served Fourier spectrum to the lower frequencies.

Third Session

Panel on Theoretical Models

Chairman: J. Weertman (Northwestern)

Members: J.B. Walsh (Massachusetts Institute of Technology), A. Nur (Stanford), R. Alewine (California Institute of Technology), C.-Y. King (U.S. Geological Survey)

Contributors: D. Turcotte (Cornell), D. Oldenburg (Institute of Geophysics and Planetary Physics, University of California, La Jolla)

In the introduction of the session, J. Weertman noted that changes in displacements around faults can be used to make a rough estimate of the amount of slip on a fault and the size and position of the fault area that has slipped. The estimates are made by comparing observed displacements with displacements calculated from different dislocation models. In only one of the models developed so far can the surface displacements be transformed mathematically to give information such as the dislocation density on a fault. This is the model of an infinitely long, vertical strike slip fault that contains infinitely long screw dislocations that lie parallel to the earth's surface. Let $w(y)$ be the surface displacement, where y is the distance from the fault in a positive direction. Apart from a constant term, the slippage displacement $D(x)$ across the fault at a depth x is equal to 2 Re $[w(ix)]$ and the integrated shear stress $\int \tau(x)\, dx$ that acts across the fault is equal to $-\mu$ Im $[w(ix)]$. The quantity μ is the shear modulus. The dislocation density $B(x)$ is equal to -2 Im $[w'(ix)]$ and the shear stress $\tau(x)$ across the fault is equal to $-\mu$ Re $w'(ix)$, where $w'(y) = dw/dy$. In a practical situation these relationships permit a very rough estimate to be made for $D(x)$ and the integrated shear stress but are virtually useless for obtaining the other quantities.

Weertman also pointed out that the water flow paths around an edge dislocation on a fault in the model of Nur and Booker should be modified if the rock surrounding the fault is impervious to water when it contains no cracks. Such rock will contain cracks and water will flow through the cracks. The water pressure at any point will be the overburden pressure less the most tensile stress (or plus the least compressive stress) component of the dislocation stress field. The effective permeability of fluid flow also will be anisotropic in character because of the nonhydrostatic stress components. If the degree of anisotropy is high, fluid will be forced to flow along the fault plane.

J.B. Walsh showed that surface displacements found by using standard geodetic techniques can be used to estimate parameters such as fault depth and dip angle, energy release, seismic moment, and average stress drop. Direct inversion of the displacement field for the purpose of determining the distribution of the stress change on the fault is not practical because of the uncertainty in the measurements of the surface displacement. Much of this ambiguity in the inversion is inherent in the method. Instead of inverting the surface displacement field, a displacement distribution or stress distribution on the fault is assumed, and the surface displacements are calculated by using elasticity theory. These theoretically calculated surface displacements are fitted to the observed displacements by adjusting a free parameter, usually the fault depth. Values of fault parameters estimated by using different models may differ by a factor of 2.

A. Nur pointed out that there are at least two different time-dependent processes involved in the change of displacement fields near earthquake faults. One of these involves the flow of water and the other the viscoelastic behavior of rock. The postseismic displacement changes that followed the Nankaido earthquake displayed a complicated time behavior for several years at the various observation stations. A simple model of sudden faulting in an elastic lithosphere that rests on viscoelastic asthenosphere can be used to demonstrate that this postseismic deformation is caused by the relaxation in the viscoelastic asthenosphere. Analysis of geodetic, seismic, and gravity data from the Matsushiro earthquake swarm shows remarkable agreement with the features predicted by the theory of dilatancy and water flow. It appears that the (upward) vertical displacements at the surface cannot be explained by the dislocation model that explains the horizontal displacements. The gravity data indicate that during the early stages of the earthquake swarm the vertical displacements were accompanied by a reduction of mass underneath the area that was displaced upward. In the later stages of the swarm the mass in this region increased markedly. Nur believes that these observations prove that dilatancy and fluid flow are responsible for the vertical deformation. He concludes that gravity measurements may be sensitive enough to changes in dilatant expansion to be used as a method for studying the phenomenon of dilatancy at earthquake faults.

R.W. Alewine III described his systematic method for the estimation of fault model parameters. A three-dimensional fault model composed of many appropriately oriented fault elements was used to approximate the faulting of the San Fernando, California, earthquake. The geometry of the fault system was fixed to conform to all the geophysically observable properties of this event. A linear inversion scheme was used to simultaneously estimate in an optimum sense the absolute slip along each of the fault elements given the geometry and a set of observed displacement data. A means of mapping the estimated variance in the observed data into uncertainties in the fault model parameters was given and examples were shown. The displacement function along the fault surface for this earthquake was found to vary considerably with depth, indicating the nonuniformity of the preexisting strain field.

Chi-Yu King summarized observations made on a laboratory model of a seismic strike slip fault. The model consists of spring-connected weights around a circular cylinder. The circular configuration of the model thus eliminates end effects. His model observations suggest that nonuniform friction along a fault is important for the generation of earthquakes of various magnitudes but that the nonuniformity of the friction does not need to be very large. The shear stress drop associated with small and moderate earthquakes is very small in comparison with the total shear stress that exists before the earthquake. That is, the occurrence of small and moderate earthquakes does not perturb greatly the stress level at the fault. The stress drops vary widely in magnitude as a result of a relatively small nonuniformity in the friction; they generally increase in magnitude with the size of the earthquake. King also suggested that ruptures may have a preferred direction of propagation along a curved fault in the earth that has different types of material on either side of the fault. He believes that processes other than frictional sliding that can change the level of the local stresses are required to explain the aftershock and fault creep phenomena. These processes might be viscous sliding and the diffusion of fluids.

D.L. Turcotte presented a cyclical model for the accumulation and release of strain adjacent to a strike slip fault. His model is based on the assumption that the upper 15 km of the plate acts in a brittle manner and that the lithosphere beneath this brittle region is deformed plastically. The model considers a rectangular shaped plate that is bordered on two parallel sides by strike slip faults (transform faults), on one side by a spreading ridge and on the opposite side by a trench. A two-dimensional crack analysis yields the strain field in the lithosphere when the fault is locked to a prescribed depth. The strain field was shown to extend only to a distance of the order of the length of the locked fault away from the fault. The linear increase of stress on the locked fault and the quadratic increase in stored elastic energy was obtained. The results were compared with measurements of strain accumulation, but the scatter in the data makes it difficult to discriminate between alternative models.

D. Oldenburg described and later demonstrated a dynamic laboratory model of oceanic ridges and transform faults. The model uses hot wax that is simultaneously pulled in a horizontal direction and cooled at the upper surface.

Fourth Session

Panel on Instrumentation and the Future

Chairman: Jon Berger (Institute of Geophysics and Planetary Physics, University of California, La Jolla)

Members: S.W. Smith (University of Washington), G.C.P. King (Cambridge), J. Levine (National Bureau of Standards, Boulder), P. Bender (University of Colorado)

Contributors: C. Beaumont (Institute of Geophysics and Planetary Physics, University of California, La Jolla), P.F. MacDoran (Jet Propulsion Laboratory), C.C. Counselman (Massachusetts Institute of Technology), J.P. Murphy and J.W. Siry (NASA), M.J.S. Johnston (U.S. Geological Survey), K.L. Cook (University of Utah)

After introductory remarks by the Chairman, S.W. Smith opened by describing a recent engineering evaluation of several types of conventional quartz tube strain meters. It was shown that the effects of humidity are much larger than might have been expected and that the nonlinear effects of lateral vibrations of the quartz tube are a significant source of long-period noise. Tests were run with quartz strain meters and a laser interferometer on the same piers. Temperature corrections applied to the quartz instruments were adequate to produce a good correspondence between laser and quartz instruments, but changes in humidity between 50% and 100% produced transient strains of 10^{-6} and a time constant of about 20 hours. The strain was recoverable with the same time constant when the humidity was reduced. This observation leads to the conclusion that humidity may be a significant source of apparent seasonal variations observed with quartz strain meters and may be responsible for the large transient strains observed in new installations. Typical deep mine installations are in a constant 100% humidity situation, and hence the effect may not be of significance there.

Smith also described a borehole instrument consisting of five miniature quartz strain meters in a compliant canister that has recently been developed and installed at Mina, Nevada. The installation is in a shallow hole within the mine, which contains conventional quartz strain meters, thus a direct comparison of tidal and secular strains recorded on these different types of instruments will soon be available. The borehole instrument had a drift rate of approximately 10^{-8} per day after 30 days, apparently as a result of the curing of grout used in the installation. Earth tides are clearly visible.

Some very encouraging results from a two-color geodimeter under development at the University of Washington were also reported. Over a 10-km baseline, the standard deviation of distance measurements over several hours' time was 1×10^{-7}. Longer tests that will include a wide variety of meteorological conditions are now under way and will provide an estimate of the absolute accuracy of this instrument. Field tests in which a microwave link was operated simultaneously show that the effects of water vapor on the distance measurement can be significantly reduced. Results to date indicate that this instrument will produce an order of magnitude improvement in distance measurement over a conventional geodimeter.

G.C.P. King reported on results obtained with invar wire strain meters in a variety of configurations. Extensive work at the Queensburg Tunnel in Yorkshire, England, revealed significant effects of the tunnel cavity on the strain measurements. Those instruments aligned along the axis of the tunnel were less affected than those at right angles. King reported on work that the Cambridge group is doing along the Anotolian fault in Iran.

J. Levine reviewed the state of instrumentation of laser strain meters including the I_2 laser system of Cambridge University, the 800-m surface installations of the University of California, San Diego, and his methane-stabilized system installed near Boulder, Colorado. He emphasized that there were several different approaches to the interferometric measurement of strain made possible through the use of lasers, and that if care were taken, they would work equally well. He described the results of an intercomparison of the observations of laser strain meters of different design at three different sites and showed that the measured noise levels agreed to within 10 dB over a frequency range of 10^{-8} to 10^{2} Hz. These observations were free of spurious strain steps, large strain episodes, and other such anomalous behavior. In conclusion, Levine conceived with Smith that the advantages of laser interferometric strain measurements over more conventional types more than compensated for their higher cost. Further, he said that the construction of these instruments, which once involved 'state of the art' complexity, had now become a routine matter.

Extraterrestrial methods for determining crustal movements in seismic zones and for directly measuring the relative motions of tectonic plates were discussed by P.L. Bender. Independent station radio interferometry, laser distance measurements to artificial satellites, and laser measurements to the moon all appear capable of achieving 1- to 3-cm accuracy for determining the three-dimensional location of points on the earth's surface. Observations from a movable station over a period of from a few days to a month would be used with those from already existing fixed stations to determine the movable station location. All three techniques appear desirable for providing a basic framework of control points around and within seismic zones, and intercomparisons at these points would provide accurate cross-checks between the methods. A coarse grid of points within the framework at spacings of down to perhaps 100 km could be remeasured each year by radio interferometry or satellite ranging, provided that the costs can be kept low enough. In regions of particular interest, more closely spaced points would be tied into the grid by ground survey techniques.

The extraterrestrial methods also appear capable of accurately measuring the relative motions of 2 or 3 points on each of the major tectonic plates within a fairly short period of time. This would provide a valuable check on the plate motion models used in trying to understand strain accumulation in seismic zones and would indicate whether appreciable strain accumulation is taking place away from the main seismic zones. In addition, information on whether large aseismic motions accompany some major earthquakes can be obtained from the extraterrestrial methods by accurately observing changes in the polar motion of the earth.

There were seven contributors to this session, beginning with C. Beaumont, who presented the results of work by himself and Berger that examined the changes in the earth tide admittance to be expected to accompany dilatancy. Numerical solutions for the earth tide on a model earth with dilatant crustal inclusions indicate that up to 60% changes in the strain tide and 100% changes in the tilt tide will result from a 15 to 20% reduction in the ratio Vp/Vs, the seismic p to s velocity in the inclusion. Further, detectable changes will occur up to a distance of 1.5 times the typical dimension of the dilatant inclusion. Monitoring of the earth tide was therefore suggested as a sensitive and continuous method of earthquake prediction if such dilatancy precedes earthquakes. The time dependence of the tidal signal due to dilatancy is identical to that of the Vp/Vs ratio, because both depend on changes of the elastic moduli in the dilatant zone. A search of the tidal strain data for the past three years from the laser strain meters at the Piñon Flat Geophysical Observatory yields no existence of anomalous changes in the tidal signal, nor have there been any earthquakes in the vicinity of the observatory. The practical limits of detectability for the method are about ±2% change in strain tide admittance for a one-month period.

P.F. MacDoran reviewed the progress his lab has made in very long baseline radio interferometry (VLBI). He pointed out some advantages that this technique has over the other extraterrestrial ranging methods and outlined plans for a Southern California network of such stations. Feasibility experiments conducted over a 10-km path have demonstrated an accuracy of a few centimeters for three-dimensional determinations of relative position. Operation on longer baselines will require calibration for atmospheric earth rotational, and astronomical effects, but MacDoran indicated that studies have shown that three-dimensional separation of antennas up to several hundred kilometers may be determined to a few centimeters' accuracy.

C.C. Counselman presented some results of VLBI experiments performed between April 1972 and March 1973 with the Haystack Observatory in Massachusetts and the Goldstone Tracking Station in California. Results for the baseline length of 3900 km yielded an rms spread of under 25 cm. The corresponding fractional uncertainty of about 6 parts in 10^{8} is one of the lowest ever achieved in geod-

Seventh Geodesy/Solid-Earth and Ocean Physics (GEOP) Research Conference

Coastal Problems Related to Water Level

FAWCETT CENTER FOR TOMORROW
THE OHIO STATE UNIVERSITY
COLUMBUS, OHIO

JUNE 6--7, 1974

Sponsored by: **American Geophysical Union**
Defense Mapping Agency
National Aeronautics and Space Administration
National Oceanic and Atmospheric Administration
Ohio State University, Department of Geodetic Science
U.S. Geological Survey

The theme for the Seventh GEOP Research Conference will be set by an introductory review. The conference will be divided into the following subtopics, each introduced by an invited moderator and discussed by a panel:

1. Management Problems Related to Changes in Elevation.
2. Hydrological Effects on Elevations and Shore Line.
3. Geological Effects on Elevations and Shore Line.
4. Special Problems of the Great Lakes.

Individuals interested in attending the conference are requested to send their applications on the standard application form available from the American Geophysical Union, 1707 L Street, N.W., Washington, D.C. 20036.

Further details on the program, accommodations, and registration will be sent to those applicants selected by the committee to attend the conference by April 30, 1974.

GEOP 7 follows the International Symposium on Applications of Marine Geodesy being held June 3–5, 1974, at Battelle in Columbus, Ohio.

Applications for attendance must be received by April 23, 1974.

American Geophysical Union ★ 1707 L Street, N.W. ★ Washington, D.C. 20036

D7

N76-20573

Recent and Late Quaternary Changes in Water Level

R.I. Walcott

PAST GEOP CONFERENCES have focused on such topics as ocean and earth tides and vertical movements and on various other aspects of earth dynamics. In GEOP 7, several of these topics were brought together in considering the classes of problems and processes that arise in coastal areas related to water level. Those who have been following the GEOP conference series in E⊕S or who have attended a number of the conferences will have noted the complex interdependence of solid earth and oceanic dynamics, with the themes of deformation and movement interwoven throughout the various disciplines and specializations of geodesy, geology, climatology, and geophysics–which is the physical ecology of the earth, if you like. On the coasts these interrelationships are most forcefully and dramatically evident.

I have chosen to summarize here our knowledge of changes in water level of both the sea and Great Lakes in very general terms, describing how the information is analyzed and critically reviewing some ideas about the causes of the changes in level.

Changes of Water Level

The amplitude spectrum of periodic water level variations where the amplitude of water level is plotted against frequency is given in a generalized manner for the oceans in Figure 1*a* and for the Great Lakes in Figure 1*b*. These are not measured spectra but are diagrams to summarize the variations in water level and to identify the various bands of water level activity. Water level varies on widely different time scales. In a sense, waves and swell are short-term variations in level, and in geology, in the marine Ordovician, Devonian, and Cretaceous sediments covering large areas of the continents, there is evidence of very long term changes in level. But in this review it is the middle part of the spectrum of water level activity from the tidal to the climatic bands that is of principal importance. These are the bands that contribute significantly to the water level changes that can be measured over a period of a hundred years or so and are thus related to coastal problems.

On the coasts the important variations on a day to day basis are the tidal and wave bands, although in

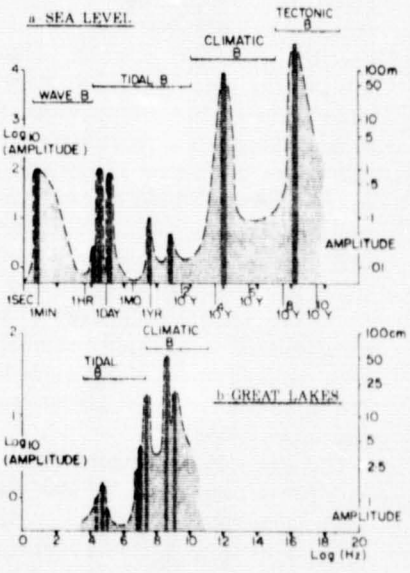

Fig. 1. Diagramatic representation of amplitude of water level against frequency for (*a*) oceans at a typical coastal location and (*b*) Great Lakes.

This article was taken from the keynote address presented at the Seventh GEOP Research Conference, on Coastal Problems Related to Water Level, held at the Ohio State University, Columbus, June 6–7, 1974.

Contribution 519 from the Earth Physics Branch.

terms of a society the climatic band is also important, since the changes are systematic and occur over extensive regions. Water level activity in the range of tidal to yearly period was the subject of the first GEOP conference [*Hendershott,* 1973] and will not be discussed in detail in this review. The amplitude of tides of the ocean coast is generally in the range of 1–5 m and dominates the variance in sea level. In the Great Lakes the tidal band is unimportant, and the largest changes are those that occur in a 1- to 30-yr period, which is the climatic band of the Great Lakes. Tides and seiches can be observed, but the dominant amplitude by far is an annual term [*Dohler and Ku,* 1970].

Variation of the Annual Mean

Direct recorded measurements of water level by gage in both the Great Lakes and Europe go back to the early nineteenth century, and in a few cases in Europe, sea level records are available from the eighteenth century and even earlier. In most of the very old records there is a problem in knowing whether or not the local datum to which the water level was referred had been changed during the time of operation, and this is by far the biggest source of uncertainty in knowing the long-term variations in water level. Some records, plotted as annual mean sea level, are shown in Figure 2; the stations were chosen to obtain a well-distributed set of information not too strongly biased toward any one region. Note how quiet the sea is in the time range of 1 yr to as long as the records are available. The short-term variations in water level are all less than ±10 cm, and a quick inspection by eye shows that most of the variance is in the frequency range of 1 c (cycle) in 5 to 1 c in 15 yr. The amplitude of the variations in insignificant compared with the amplitudes of the waves and the tides (about 1–5 m) at most coastal locations.

The Great Lakes (Figure 3) are in complete contrast. Tides (and seiches) are small, and the mean daily variation (Figure 3*a*) has a root mean square variance of about 5 cm, whereas the yearly variation is typically about 25 cm. The variation shown in annual means (Figure 3*b*) is

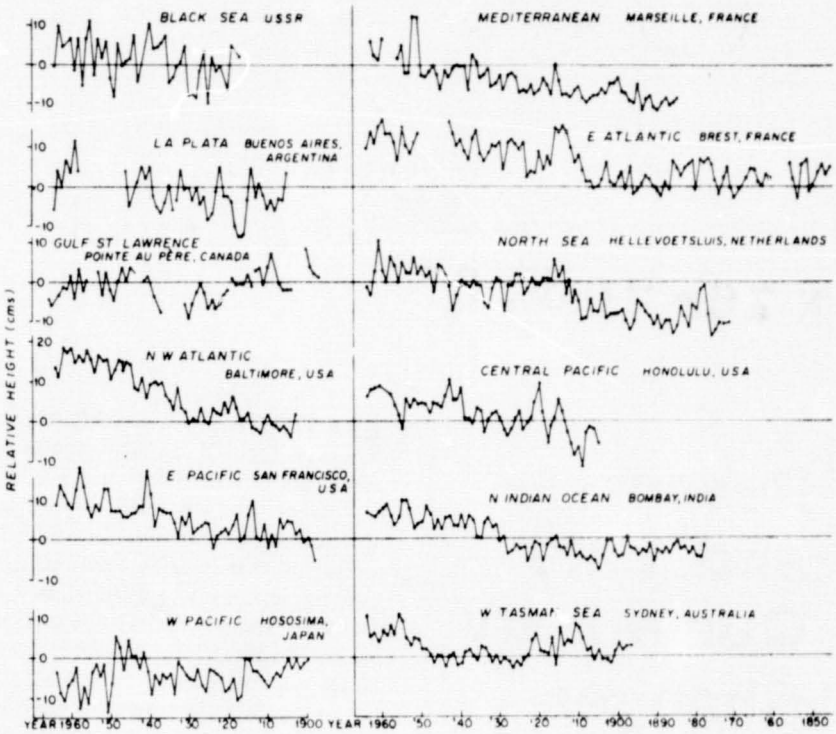

Fig. 2. Mean annual sea level recorded at 12 widely separated tide gages. Data from the International Association of Physical Oceanography, *Publication Scientifique,* nos. 5, 10, 12, 19, and 20, and from International Union of Geodesy and Geophysics *Monographs 21* and *30* (reprints of IAPO *Publication Scientifique,* nos. 24, and 26).

more like ±65 cm, and the dominant power appears in 30-yr and about 12-yr periods. There appears to be a good correlation with variations in precipitation (Figure 3*c*), and thus long-term variations in lake level are presumably climatic in origin.

The secular trend of many stations is of a relative sea level rise the maximum rate of which occurs at Baltimore in the records shown and amounts to 25 cm in the last 70 yr. Of the stations in Figure 2, 7 show this trend clearly; 2, Pointe au Pere

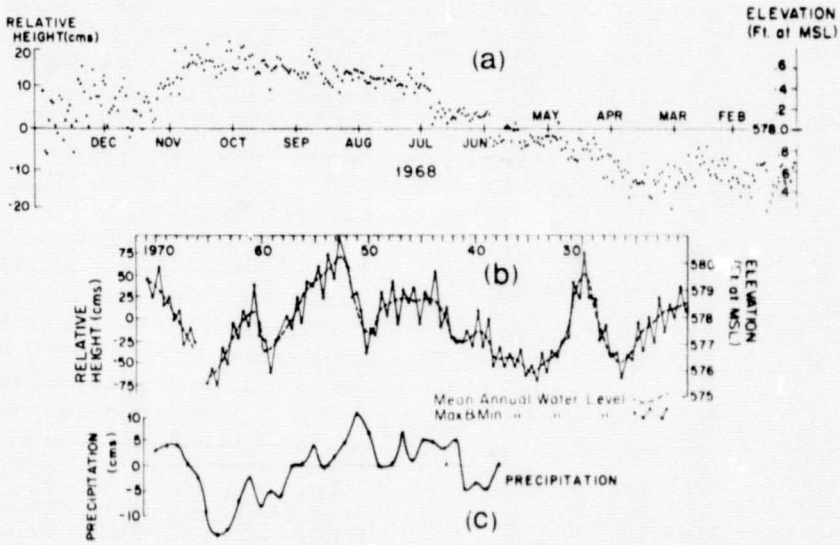

Fig. 3. (*a*) Mean daily water level, Lake Huron, at Thessalon, Ontario, for 1968. Note small daily and large annual variance. (*b*) Mean annual (dashed) and annual extreme mean monthly water levels, Lake Huron, at Goderich, Ontario. (*c*) Variations in the average precipitation at five meteorological stations in Ontario within the watershed of Lake Huron and Lake Ontario. The curve is smoothed by 3-yr running averages.

and Hosojima, Japan, show an opposite trend, and the others are noisy or flat. *Gutenberg* [1941] estimated the mean global secular change in sea level to be 1.2 mm/yr based on an average of about 65 stations the world over. There have been a number of criticisms of individual station records in his analysis, and there is the general criticism that although Gutenberg excluded data from glacioisostatic uplifting areas he included data from glacioisostatic subsiding areas, and therefore a bias is introduced into the data. Moreover, no data were available from more than half the area of the world's oceans, and thus we have to take the rounded value of 1.0 mm/yr secular rise as only very approximate. *Fairbridge and Krebs* [1962] updated Gutenberg's work and gave the world eustatic curve of Figure 4. Again, however, data are unavailable from the southern parts of the Pacific, Indian, and Atlantic Oceans, and, at least for the nineteenth century part of the curve, the data are biased toward galcioisostatically subsiding regions. A compendium of trends in sea level is available in *Publication Scientifique*, no. 13, 1954, from the International Association of Physical Oceanography (IAPO).

Further discussions of worldwide sea level trends are given by *Kuenen* [1954], *Munk and Revelle* [1952], and *Disney* [1955]. Recent discussions of sea level trends in the United States are given by *Hicks* [1972].

In many oceanic gage records there are changes in the long-term trend. In the record from Brest the trend during the nineteenth century seems to be flat, and it rises only gently since 1920, but there was a rapid change of some 10 cm between 1905 and 1920. The record at Hellevoetsluis, Netherlands, is similar, and unusual trends over the same time interval occur at Honolulu and perhaps at Sydney, Australia. This last record is unusually noisy at this period, but if anything the trend is opposite in sign to the trends of northern Europe. None of the other records shows anything unusual in this period, although very similar changes do occur at different times, such as the step in the data at Bombay around 1930.

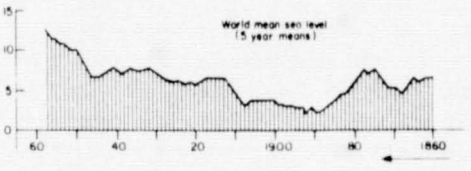

Fig. 4. World mean (eustatic) sea level based on tide gage data from *Fairbridge and Krebs*, [1962].

Thus these short-term anomalies in the secular trend, although they appear to be regionally coherent over large areas, have not been established to be clearly global in character. At Amsterdam 290 yr of water level records are available [*Van Veen*, 1954]. According to *Mörner* [1973], this record and others from southern Scandinavia show a long-term variation in secular trend of sea level in northern Europe as follows: from 1830 to 1930, sea level rose at 1.3 mm/yr; from 1740 to 1830 it rose at 0.15 mm/yr; and from 1682 to 1740 it rose at 0.4 mm/yr. As we can see by Brest and Hellevoetsluis records (Figure 2) the secular trends are very much more uneven than this simple characterization shows.

So far only the trends of mean sea level have been discussed—that is, the averaged or integrated values over specified periods of time—but there are also other characteristics of sea level that show long-term variation. The variation in the annual mean range of sea level is discussed by *Kaye and Stukey* [1973], who show a prominent periodicity in this parameter with a frequency of 1 c in 18.6 yr—the cycle of the lunar nodes.

Late Quaternary Movements of Sea Level

In extending knowledge of sea level back in time beyond direct measurements there is a wide variety of historical, archeological, and geological information. The most abundant and universal data consist of radiocarbon dated materials related to past sea levels, e.g., submerged peat or elevated shells. These materials from a variety of regions show that on a 1000- to 10,000-yr time scale there are pronounced variations in sea level from place to place (Figure 5). The variation in this figure is undoubtedly largely due to movements of the land. In this figure, 5 sea level curves are plotted and compared with a

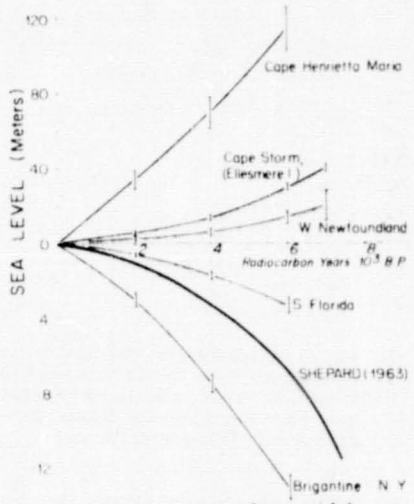

Fig. 5. Sea level curves from widely separated locations in North America. Note the difference in scale below and above zero line. The curves are drawn as smooth lines through the data shown by error bars, which are discussed in the text. Eustatic curve from *Shepard* [1963] is given for reference.

curve published by *Shepard* [1963], which is described as a eustatic—that is, a global-average sea level curve. Each of the curves of Figure 5 is based on discrete data points that have been generalized by drawing smooth best-fit curves by eye and interpolating the point values shown in the figure. The error bars are derived from maximum and minimum positions of sea level consistent with the available data.

Precise determination of late Quaternary eustatic sea levels, the search for which has been going on for some time but which appears to have become of dominating concern in the 1960's after the publication of *Godwin et al.*'s [1958] and *Fairbridge*'s [1961] papers, has proved elusive. As we shall see in the discussion of the analysis of water level data, the idea of a eustatic sea level is not easily formulated in precise terms, but conceptually, it can be understood as a worldwide synchronous change in sea level that might arise by changes in the volume of sea water, in its density, or in the shape of ocean basin(s) [*Fairbridge*, 1962].

A number of the sea level curves that have been referred to as eustatic with varying degrees of assertion are shown in Figure 6. The very considerable scatter shows that the true curve is not well determined, but we can probably be confident that it lies within the limits of the envelope con-

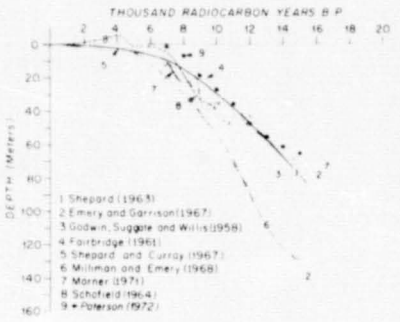

Fig. 6. Eight directly observed or derived (no. 7) sea level curves described as eustatic. The sea level equivalent for Laurentide and Innuitian ice sheets given by *Paterson* [1972] is also shown.

taining all curves. Thus from about 18,000 to 6000 yr B.P., sea level rose eustatically some 100 m to near its present level, and from that time it has remained within 5 m over most of the world. As we have seen in Figure 5, sea level in some locations shows very considerable variations from the eustatic value. Since it is the local value of sea level rise that is important to the coastal problems in any particular locality, it is important for us to determine the reasons for the variations about the mean in relative sea level change.

The principle cause of the eustatic rise in sea level from 18,000 to 6000 years B.P. is the melting of the extensive ice sheets that covered North America and Fennoscandia and the less extensive areas in South America, Alaska, and Siberia. The largest of these by far was the Laurentide Ice Sheet, which, with the contiguous Innuitian ice sheet over the Arctic Archipelago, covered most of Canada. *Paterson* [1972] has calculated the rise in sea level produced by their melting, and his curve is given in Figure 6. Since the two ice sheets covered approximately 2/3 of the total deglaciated area, they account for more than 2/3 of the volume of water released by the melting of the ice, and this would indicate a general agreement with the shallower of the so-called eustatic curves.

Changes in sea level prior to the last glaciation are not well determined. There is some information from the Bahamas [*Broeker et al.*, 1968] and New Guinea [*Chappell*, 1974] that together indicate long-term variations in sea level broadly coinciding, as one might expect, with the cycles of ice buildup and melting insofar as these are known. In this context, Pleistocene sea levels, like the ice sheets themselves, are primarily a climatic phenomenon, and it is easier to determine changes in oceanic climate [*Imbrie and Kipp*, 1971] during the Pleistocene than sea level. The dominant period in temperature is 10^5 to 3×10^5 years, and amplitudes of sea level movement are presumably comparable to that of the last glaciation—100 m. Rates of change of sea level during the Pleistocene have been higher than 10 mm/yr and at present are probably less than 1 mm/yr.

Quasi-Periodic Changes in Sea Level

The most important changes in level in terms of flooding, loss of life, and destruction of property are not the periodic movements of Figure 1 but the transient phenomena of storm surges. These are meteorologically induced rises in water level of comparable amplitude to the tides. The surge is produced by the low pressure of a storm center coupled with high winds that drive the waters to the shore and may last several hours, as with most hurricanes, to a few days for the storm surges of the North Sea. The North Sea is a region particularly prone to surges as anomalously high water levels can be swept in from the north and trapped by the coastal configuration around the Straits of Dover. Since 1897, the year of a particularly severe and destructive storm, there have been 8 major storm-induced surges in the North Sea. The 1953 surge has been described by *Steers* [1971]. The low pressure at the center of the storm over the North Sea was 967 mbar, and it was bounded by a ridge of high pressure over the North Atlantic of 1033 mbar. Sea level rose 70 cm above its predicted value in the center of the North Sea, and levels rose at the coastline up to 3.1 m above normal in Holland and 2.5 m in the Thames estuary [*Rossiter*, 1954; *King*, 1959].

Hurricane-produced surges along the Gulf coast are also frequent. On the Texas coast between 1900 and 1967 there have been 20 surges, with a peak surge height of water level from 60 to 3.9 m [*Bodine*, 1969].

Analysis of Water Level Changes

Water level means the height at some location that is derived for an oscillating surface smoothed in time, mechanically by a still well, as in a tide gage; mathematically by averaging a series of instantaneous values or by the integration of a continuous recording; or naturally by the formation of a beach. The measurement of the height of water level in either sea or lakes, however it is defined and irrespective of whether it is measured instrumentally by a gage or by the recognition and measurement of the elevation of an old, dated shoreline, is simply the difference in height between the water level and some local datum. As such it is defined only locally and can be represented symbolically by $\Delta S_i(t)$, where ΔS is the height of water level above local datum i at time t. To fully specify what is meant by a water level we therefore require definition of the smoothing, the position, the local datum, and the time of the measurement. This is as true for geological data like the elevation of an old shoreline as it is for a tide gage.

Spectrum Analysis of Short Records at a Single Station

With a restricted data set from one locality, *Wunsch* [1972] had considerable success in explaining the variation in water level in terms of the physical processes involved. His data consisted of records over an 8-year period of sea level obtained by a well-maintained tide gage on Bermuda Island. The very short period oscillations of waves were smoothed by the design of the gage, and Wunsch examined the spectrum between 0.5 cph to 1 c in 8 yr. The most important factors affecting the variance of sea level were the linear portion of the tidal spectrum, which accounted for some 70% (M_2 alone at this station was responsible for 60% of the variance) and the weather—in particular, variations in atmospheric pressure at sea level and winds that together accounted for 14%. In the open sea the static relationship between atmospheric pressure and sea level is that of an inverted barometer, and thus to ensure that the pressure a short distance below the surface remains constant,

we require a change in sea level of −0.99 cm/mbar (the sign indicates a sea level fall for an atmospheric pressure rise). This is shown to account for some of the sea level change in the Bermuda records, but the records also show that for very rapid pressure changes the coherence between sea level and pressure falls off, no doubt because sea level does not have time to keep up with pressure changes. The coherence also falls at long periods because the power in sea level rises more rapidly than air pressure, indicating that some other factor is becoming dominant. This is apparently a wind effect and is important for periods exceeding 400 hours. Another interesting relationship is for very extensive pressure disturbances; the ocean tends to compensate the pressure field by geostrophic currents, and sea level tends not to move. Tides and weather therefore account for 84% of the variance. Another 3%, largely in the annual peak, is accounted for by variations in dynamic height where temperature variations of sea level to the 1500-dbar level are computed. Most of the residual 13% is probably due to baratropic motions.

Long-Term Records and Widely Separated Stations

The analysis of widely separated data is a very much more difficult problem. Strictly, in order to compare water levels at different positions, we require a reference datum common to all positions. Such a surface could be an equipotential determined by leveling, in which case the discrimination of changes in water level from one position to another is given by the accuracy of the leveling procedure. There are, however, few places in the world where this information is available to the required accuracy. Alternatively, the analysis can be approached by supposing that the causes of the variation in sea level are sufficiently well understood to recognize all the factors that will contribute to a significant change in water level. Mathematical models can therefore be constructed of the water level variation. As the requirement of accuracy in the model is increased, so will be the number of relevant factors. Conversely, for any particular model of water level variation it is necessary to estimate the probable error of the model.

Simple Partitioning

The most commonly used model is that of a simple partitioning of the sea level variation:

$$\Delta S_i(t) = E(t) + T_i(t) \qquad (1)$$

where ΔE is a simultaneous change of water level that affects all stations equally, and $T_i(t)$ are movements of the local datum i. If the data were globally distributed, ΔE would be the eustatic change in sea level in the sense in which this term is usually used. For data of restricted distribution over the earth partitioned as in (1), the ΔE is not necessarily a eustatic change; it may approximate one, but any uniform change of height of the local datums at each location will appear in the values for ΔE. It is impossible to distinguish by internal criteria alone between a uniform change in water level that is truly eustatic and a uniform change of the local datums. In order to solve equation (1), some hypothesis is required concerning the movement of the local datums T_i, and there will be as many different values for ΔE as there are different hypotheses for the distribution of the T_i.

Since data on water levels are generally available only for discrete times, equation (1) is rewritten

$$\Delta S_{ij} = \Delta E_j + T_{ij} + \epsilon_{ij} \qquad (2)$$

Here j is time, T_{ij} represent a supposed tectonic factor that disturbs the local datums, and the ϵ_{ij} are residuals arising from errors and unexplained effects. As before, to solve (2), hypotheses are required for the form of the T_{ij} and the statistical distribution of the ϵ_{ij}.

Examples. Two examples of simple partitioning are available from southern Scandinavia, explicitly in *Schofield* [1964] and implicitly in *Mörner* [1969, 1971]. These are not the only examples: papers by *Chappell* [1974], *Ward* [1971] and *Mathews* [1973] are based on the same principles and are open to the same errors.

Schofield [1964] used shoreline displacement curves from southern Norway and Sweden and supposed that the ϵ_{ij} are normally distributed and that values of T_{ij} in any particular period j are proportional from one place to another. That is,

$$T_{ij} = q_i \cdot K_j \qquad (3)$$

so that

$$(\Delta S_{ij} - \Delta E_j)/q_i = K_j \qquad (4)$$

With regard to this hypothesis about the T_{ij}, note that q_i is a constant for each location, and therefore the T_{ij} cannot change in sign; i.e., a consequence of this hypothesis is that the zero isobase is fixed.

Mörner [1969, 1971] used accurately elevated and dated transgressive shorelines in the vicinity of the Kattegatt Sea. He did not solve equation (2) directly but tried a number of different formulations for the ΔE_j and thus derived the T_{ij}, which were plotted and discussed in terms of 'reasonableness' and supposed validity. The specific criteria for these judgments are not clearly stated, although he too preferred values for ΔE_j that resulted in a fixed zero isobase. Essentially the assumption made by Mörner is the same as that of Schofield. That they obtain significantly different values for ΔE_j for the same area is presumably a result of the different data used in the analyses.

This criterion of stability is neither necessary nor sufficient to determine the eustatic sea level, as was claimed by both writers. It is not necessary because most physical models of glacioisostatic rebound involve a migration of the zero isobase [*Walcott*, 1973] (i.e., q_i is not constant in time), and it is not sufficient because any uniform change in local datums that affects all positions equally will appear in ΔE, and it is probable that movements of this sort do exist.

The fundamental supposition of simple partitioning as expressed in equations (1) and (2) is that the movements of sea level in different locations can be separated from the movements of the land by using a linear equation. This supposition is incorrect if there is a substantial correlation between movements of the local datums T_{ij} and sea level ΔE_j.

Because a eustatic change constitutes a redistribution of load over the earth's surface, and this load will induce deformation in the solid earth, there is every reason to expect a correlation of movements of the land and movements of sea level. The question becomes to what extent this interdependence of tectonic and eustatic factors introduces an error into the simple partitioning technique. The point is discussed in the following section on deformation of the earth, where it is shown that the error in determining eustatic sea level is probably in excess of 30% of ΔE in many locations.

Deformation and Movements of the Earth's Surface

The error in determining eustatic sea level arises because the earth, like any real body, is deformable. Thus where the earth is subjected to differential surface loading, as at a coastline during a eustatic change, there will be movements of the local datums correlated with the movements of the water. That is, the earth must be stressed to support surface loads, and because the earth has a finite rigidity, these stresses lead to body strains and hence surface displacements. The quantitative relationship between surface load on the one hand and surface displacement on the other can be calculated using various rheological models of the earth. Elastic theory and the elastic parameters for the earth derived by seismology and tidal observations are an obvious first step.

Elastic Deformation

An example from the Great Lakes, although inconclusive in its results, is instructive. The change in water level of the Great Lakes over periods of 50 yr is more than 1 m, and to a first approximation the associated deformation of the earth can be estimated by calculating the displacements caused by loading an infinite elastic half-space. In Figure 7 are shown the vertical displacements in millimeters for a 1-m increase in water level over all the Great Lakes. If a 1-m change in water results in a downward displacement of the ground of f_i, W_i is the elevation of the local datum, and q_i is the rate of vertical movement of the land at the ith gage, then

$$\Delta S_{ij} = W_i + \Delta E_j(1 + f_i) + a_i \cdot j \cdot \Delta t + \epsilon_{ij} \quad (5)$$

where ΔS_{ij} is the mean monthly water level at the jth month and ϵ_{ij} are residuals.

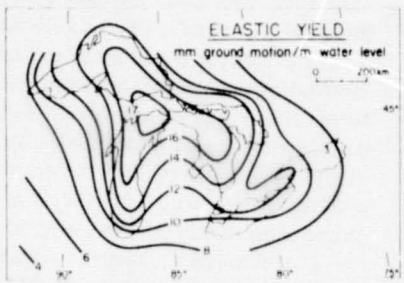

Fig. 7. Vertical displacement in millimeters calculated for a 1-m rise in water level over all the Great Lakes. The elastic constants are taken as Young's modulus 0.8×10^{12} dynes/cm^2 and Poisson's ratio of 0.24.

There are 8 stations, and over a 50-yr period there will be 4800 equations with 624 unknowns. The equations (5) to be solved are nonlinear, but f_i is small—generally between 10^{-2} and 10^{-3}; therefore we solve by first putting $f_i = 0$ to obtain the ΔE_j and by using these values, solve for other parameters.

The values for the parameters are given in Table 1. The partial variance of each parameter is obtained and the root mean variance σ is given. Only the differences in value between stations are of significance, and therfore a base value of zero for all parameters is taken for the most southerly station, Calumet. Note that the relative heights of the local datums W_i and the relative rates of vertical movement are well determined at the 95% confidence level ($\pm 2\sigma$) and that some of the factors f_i are significant at the 1σ level. The estimates for these factors are not the same as those calculated for the elastic half-space; indeed, station Thessalon shows a negative factor. However, any correlation between water level changes of an individual station and lake level changes as a whole will give a significant value to f_i, and such a change could be climatic as well as deformational in origin. Systematic changes in winds, for example, could be correlated with changes in water level, and the negative value at Thessalon may indicate a piling of water up on that shore during periods of relatively high water.

This explanation shows that the statistical precision cited for the relative heights of the local datums is probably not a true estimate of the accuracy of their measurement by a water level transfer. Nevertheless, close monitoring of the parameters of wind, atmospheric pressure at lake level, and lake temperature will provide data to introduce a physically more reasonable model than (5), and very high accuracies of water level transfer of heights would appear technically feasible. Also, in this case

TABLE 1. Values for Parameters of Equation 5 for Mean Monthly Water Levels, 1920–1970

	Lake Michigan-Huron, Base Value at Calumet			
Gage	$W_i \pm 2\sigma$, mm	$a_i \pm 2\sigma$, mm/yr	$f_i \pm \sigma \times 10^3$	$f_i' \times 10^3$
Calumet	0	0	0	0
Milwaukee	3.3 ± 6.9	−0.6 ± 0.3	3.7 ± 4.1	2
Sturgeon Bay	24.4 ± 7.2	1.0 ± 0.3	4.9 ± 4.1	4
MacKinaw City	38.4 ± 6.8	2.0 ± 0.3	3.7 ± 4.1	7
Thessalon	51.5 ± 7.0	3.2 ± 0.3	−5.7 ± 4.1	5
Harbor Beach	28.6 ± 7.2	1.1 ± 0.3	5.5 ± 4.1	5
Goderich	14.0 ± 6.9	0.9 ± 0.3	−4.6 ± 4.1	4
Collingwood	50.6 ± 6.8	3.0 ± 0.3	−2.7 ± 4.1	0

f_i' is the estimated value from Figure 7.

the deformational factors could be accurately determined.

The deformation factor f_i is small in the Great Lakes, but since its magnitude depends on the wavelength of the load, it can be large for oceanic areas. The calculation of the elastic deformation of the earth by surface loading over the oceans was carried out by using the Gutenberg model of the earth given, for example, by *Longman* [1962, 1963]. If the eustatic load were the only load contributing to the factor f_i, it would be an easy task to calculate it once for all places on earth. However, for loading on a global scale there is always a zero sum problem where the actual change in mass integrates to zero and all that occurs is a redistribution of the mass. Figure 8 shows the value for $1 + f_i$ expressed as a percentage for the loading of the oceans by a rise in sea level on the supposition that the rise was caused by the melting of continental ice sheets distributed in the proportion North America : Fennoscandia : Alaska : Argentina :: 10 : 3 : 1 : 1. We see that the value of $1 + f_i$ in the vicinity of the melting ice sheets is less than 1 and as large as 1.27 in the center of the Pacific Ocean.

Viscous Effects

An elastic model for the earth is relevant where viscous relaxation is small, but for the late Quaternary, viscous movements are probably important. However, we have no direct information on the response of the earth to surface loads as large in area as the oceans, apart from the changes in sea level themselves, and it is these changes that will give information on the deep rheology of the earth. Glacioisostatic information that shows a lower mantle of viscosity at least $10^{23}P$ and an asthenosphere with a ratio of the cube of the thickness to viscosity of about 50 km^2/yr [*Walcott*, 1973] is not of definitive value, since the asthenosphere may be much thicker under the oceans than under the shields, and whether the viscosity is $10^{25}P$ or $10^{23}P$ is of critical importance to loads as large as the Pacific Ocean. If it is as large as $10^{25}P$, then relaxation is by thin channel flow, and the relaxation time is about 10^5 years. Therefore there will have been little compensation for the late Quaternary rise in sea level, and the elastic displacements of Figure 8 will be a good approximation. If it were $10^{23}P$, the relaxation time is about 10^4 years, substantial compensation could have occurred, and the appropriate model is that of relaxation of an infinite half-space. In this model, relaxation occurs most rapidly in the center and at equilibrium will amount to about 30% ΔE. In other words, for complete compensation of oceanic loads, movements of comparable amplitude to those of Figure 8 will occur, and these movements will be correlated with changes in water level.

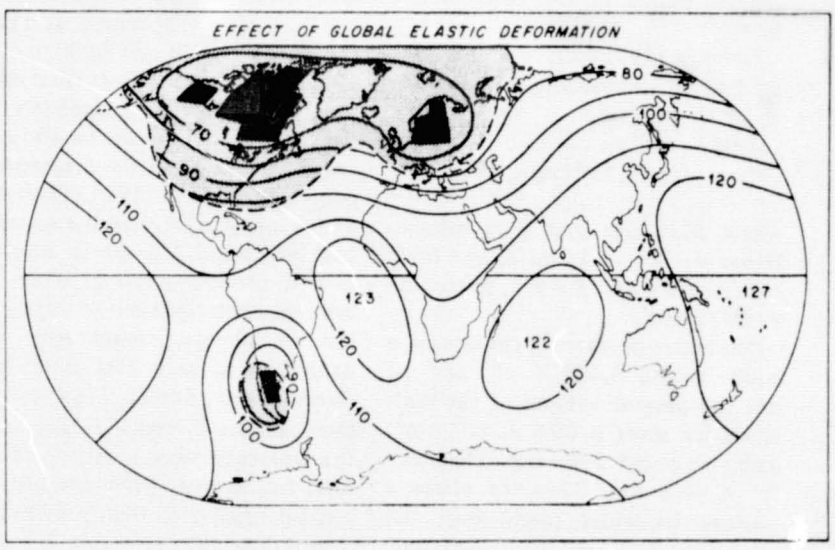

Fig. 8. Vertical displacement caused by elastic deformation of the Gutenberg earth by a rise in sea level derived from melted ice in the black areas. The contours give change in sea level expressed as a percentage of the eustatic (oceanwide average) change in sea level. [From *Walcott*, 1972*a*.]

Most data on Pleistocene sea levels come from the coastlines of the continents, and there considerable complexities in pattern of movement are to be expected because they are at the edge of the surface loading. Some of the possible complexities have been described by *Walcott* [1972*a*] for one particular model of the earth, but the important point is that large variations in movements of the land over extensive areas are possible, and it is these variations that will give the information necessary for determining the deep rheology of the earth and not vice versa. Also, because of these movements the search for the eustatic sea level is, like most interesting geophysical problems, an inverse problem—it is neither directly nor easily solved. Rather than the repetitious production of preferred eustatic curves from a restricted data set, our energies should be more concentrated on the acquisition of better data giving local sea level curves for a variety of regions and environments. With sufficient data it should prove possible to carry out an inversion to obtain not only the eustatic sea level but also the rheological structure of the earth.

In the vicinity of the areas of glacioisostatic rebound like North America and Europe the movements of the land are very much larger than those determined solely by the changes in water level discussed above. The pattern of movements is of a rising dome in the deglaciated area surrounded by a subsiding zone very much larger in area. The maximum uplift in the center is approximately 10 times the maximum subsidence in the peripheral zone. The considerable variations in sea level curves shown in Figure 5 arise from this mechanism of rebound, which for most of the coastlines of North America is the dominant cause of variations in apparent sea level trends [*Fairbridge and Newman*, 1968; *Walcott*, 1972*a*, *b*].

Fluctuations in Holocene Sea Level

Detailed, carefully controlled studies of Late Quaternary sections on

the coast in many regions show evidence of successive transgressions and sometimes regression of sea level, which have been interpreted as oscillations in eustatic sea level. Typically, the oscillations have amplitudes of 1–4 m and half-period of 200–500 yr. These observations are important, because if such oscillations exist, they occur in a time range and amplitude of significance, indeed of concern, to man. *Mörner* [1969] for instance identifies a number of sea level transgressions in the Kattegatt Sea that have been well dated and mapped. The inferred eustatic sea level (but refer to the section on analysis earlier) is shown in Figure 9. The only strong control, however, is at the maximum of the transgressions–the depth of the regressions between is based on a variety of information of unstated precision. Recently *Ters* [1973] has interpreted some 175 radiocarbon dated specimens from the coastline of northwestern France, and she gives a sea level curve shown also in Figure 9. The classic work on oscillations is that of *Fairbridge* [1961] based on worldwide radiocarbon data available at that time (Figure 9). All these curves show oscillations of considerable amplitude with some correlation but also show shifts–significant with regard to the stated precision of their data–in phase and amplitude from one to the other. These curves contrast with Blake's Cape Storm record [*Blake* 1970, Figure 4, 1973], which is very precisely determined, with closely spaced data

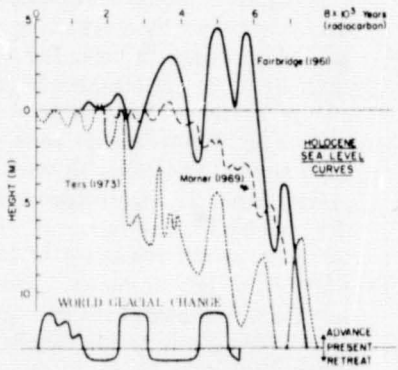

Fig. 9. Three eustatic sea level curves for the Holocene showing fluctuations in level. Note the discordance in amplitude and phase. Fluctuations in world glaciers (*Denton and Karlén*, 1973) shown at bottom of diagram. In this diagram amplitude is poorly determined but phase is well determined.

in the period 3000–8000 yr B.P.; these data points do not depart from a smooth curve by more than 2 m, 1 m being usual. Long-term oscillations with amplitudes exceeding 2 m therefore do not appear to be a global phenomenon, and the oscillations, although real, may not be eustatic, as was claimed by both Ters and Fairbridge. Indeed, the differences in phase and amplitude alone suggest that the curves are dominated by local effects, as was previously suggested by *Curray and Shepard* [1972]. Even the correlations between the curves of Ters and Mörner are insufficient to demonstrate eustasy–it is one thing to demonstrate a regional coherence in northern Europe and quite another to demonstrate a global coherence.

Causes of the Fluctuations in Sea Level

Because of the large volumes of ice still in existence in Antarctica and Greenland and in mountain glaciers, it has been suggested that lesser apparent eustatic changes of the Holocene–the last 6000 years–are, like those of the Pleistocene, produced by changes in the ice volume. A 1-m change in sea level, for instance, is equivalent to a change of 23 m of ice spread uniformly over Antarctica, and at first sight this seems insignificant. However, as *Bloom* [1971] has pointed out, the problem is not this simple, since most of the ice change occurs at the edge of the sheet.

Paterson [1972] has given the well-established empirical relationship for an ice sheet

$$\mathrm{Log}_{10}\, V = 1.23\, [\mathrm{Log}_{10}\, (S - 1)]$$

where S is area and V is volume. Hence $dV/V = 1.23\, dS/S$, and for a circular ice sheet, $S = \pi r^2$, so that $\Delta r = r\Delta V/2.46V$.

One meter of water of the oceans is equivalent to 0.402×10^6 km^3 of ice, the present volume of the Antarctic ice sheet is 30.4×10^6 km^3, and r is about 2000 km. Therefore $\Delta r = 10.6$ km. Thus, to effect a change in water levels over the oceans of 1 m from Antarctic sources, we require a change in the ice margin of on average 10.6 km. As for a change in the volume of Antarctic ice, both an increase [*Hollin*, 1970] and a decrease [*Hughes*, 1973] have been proposed. The former is based on a variety of evidence that supports either an increase or no change in ice volume in the last few thousand years; the latter is largely based on a supposed eustatic rise in sea level in the Holocene and therefore for our purposes is a circular argument. The question is whether an average retreat and advance of some 20–30 km all around the Antarctic ice sheet within the last 6000 years could be detected. No conclusive answer appears to be available at the present time, since most of the margin is difficult to examine. Some parts, however, would be expected to respond to small changes in ice thickness considerably in excess of the average response–the McMurdo Dry Valleys are a case in point–and these do not show large Holocene fluctuations [*Hollin*, 1970]. Greenland being very much smaller than Antarctica requires fluctuations of the ice margin in excess of 100 km on average to produce a 1-m change in sea level, and *Ten Brink* [1974] lists many radiocarbon dates only about 20 km from the present ice edge that are 6000 yr old.

Mountain glaciers of Asia, Europe, and North America show large fluctuations, but their combined volume cannot explain 1 m or more changes in sea level during the Holocene. They cover about 0.23×10^6 km^2 in area [*Thorarinsson*, 1940], and if we use Paterson's relationship as a guide to the upper limit, are equal to 0.5×10^6 km^3 of ice or less. If this volume of ice were to melt completely, the rise in sea level would be about 60 cm. In good supporting agreement, according to *Flint* [1971, Table 4E], all ice today other than the Antarctic and Greenland Ice sheets would, if melted, produce a rise of 50 cm, and even at their maximum during the last glacial age, would have been equivalent to only 3 m in sea level. *Denton and Karlén* [1973] show that changes in these glaciers during the Holocene were broadly synchronous and identify three advances and retreats relative to their present position during the Holocene. However, these changes do not show a systematic relationship with the phase of sea level curves (Figure 9). Thus

there is a problem in the ice volume hypothesis for Holocene sea level changes—there does not appear to be any evidence of the large synchronous fluctuations in ice sheets and glaciers that would be expected if the proposed oscillations are eustatic.

Of course, fluctuations in sea level may be apparent only, and it may be the ground that is moving. *Faure and Hebrard* [1973], for instance, identify apparent sea level movements in the Holocene of Senegal and Mauritania as being noneustatic and suggest ground movements and geoid changes among possible causes. Fluctuating ground movements, independent of the movements of sea level, may exist in the nonseismic regions, but their mechanism is obscure, and to be more than ad hoc suggestions, some critical data and analyses are needed. These do not seem to be available yet. In seismic and volcanic regions, fluctuations of large amplitude are known, but generally the lateral extent of the fluctuations is of the order of tens rather than hundreds of kilometers. *Fleming* [1969], however, has described some extensive patterns of movements of the ground in the Western Mediterranean, and these appear to be closely related to seismicity and current orogeny.

Climatological causes for variations in water level are important and are underrated in the current literature. Storm surges, although short-lived, produce very dramatic and geomorphologically important effects on the coastline. It is during the surge and accompanying storm waves that most of the erosion of cliffs is effected, and the beaches and coastal forms produced under the influence of the normal swell and muted weather conditions are changed and destroyed. On a time scale of a few tens of years, surges are transient phenomena and their effect can be isolated. But in geological time, over periods of a thousand years or more, it is not the effects of individual surges that are important in the record but the superimposed effects of tens or even hundreds of surges. Moreover, changes in the frequency of storm-induced surges may be very important for understanding some sea level records. *Brooks* [1970] has listed the number of storms in Europe for the last 1000 years in 50-yr periods and shows that variations of from 13 to more than 60 storms have occurred. During the whole of the Holocene even greater variations could recur at longer periodicites. It would be expected that variations in the geological record of those centuries that are distinguished by repeated storm surges, the effects of which are piled one on top of the other, can be separated from centuries of comparatively quiet stable conditions. Such variation in weather conditions could be as extensive as the effects of a surge—a thousand kilometers or so. The surprising fact is that these variations have not been identified as such in the record of the Holocene, although they should occur. Whether this is because the effects are overlooked or identified as something else, like a eustatic change, requires the critical appraisal of field geologists.

An ice-melting origin cannot be excluded for the proposed small eustatic changes in sea level given earlier on the basis of tide gage records. Direct monitoring of Antarctic ice margins is inadequate, and one other, rather esoteric, line of evidence is inconclusive. *Munk and Macdonald* [1960, equation 11.11.13] show that a change in sea level from Antarctic and Greenland ice causes inertial changes that result in a shift of the pole and change in the rate of rotation of the earth. The 10-cm change between 1905 and 1955 in the eustatic curve of *Fairbridge and Krebs* [1962], if it is apportioned to Antarctica and Greenland according to their areas, will result in a shift of the pole 2.5 m along 75°W longitude, and the rate of rotation should decrease by about 1 part in 10^8. Observed secular changes in polar position between 1903 and 1957 [*Markowitz*, 1970] are 6 m along $(70 \pm 10)^\circ$ longitude with a nontidal increase in the rate of rotation of about 50 parts in 10^8. Despite the change in sign of variation in the length of day, the calculated movements are not inconsistent with the observed changes considering the many other factors that may cause changes in the earth's rotation. It is clearly important, however, to establish what are the actual changes in eustatic sea level and the source of the water in order to calculate the effect on the earth's rotation in any geophysical analysis of the other causes of variation in rotation.

Conclusions

Trends of sea level over the last few thousand years show large variations from place to place, not only within areas affected by glacioisostatic rebound, but in islands and along coastlines well removed from the near effects of rebound. Such variation is to be expected, since the ground will experience significant vertical displacements by the differential loading of sea level and ice mass changes. Although present rheological models of the earth lead us to expect a complex variation in water level trends, no rheological model is adequate at the present time to generalize the available data, and the pattern of worldwide trends in water level has not yet been physically determined. Instead, it is the information of present and past sea level trends from critical regions that is required for understanding earth structure and processes.

The dominating influences for short-term periodic variation in sea level are tidal and meteorological, and for long-term variation, the deformation of the earth by changes in surface loading and changes in the climate. In the Great Lakes the principal influence is climatic, variation in rainfall over 20-yr periods being the most important.

Oscillations in sea level of some few meters have been identified in several regions, but the belief by many writers that these are eustatic changes related to variable ice volumes is unproven. Indeed, there are considerable difficulties and some negative evidence against both hypotheses. The phases and amplitudes of several of the identified curves differ, and they also differ from identified fluctuations in glacial advance and retreat. The possibility that these oscillations, if correctly identified, are regional and not worldwide phenomena must be seriously considered.

Two alternative suggestions are put forward. Sea level fluctuations may indicate oscillating ground motion in otherwise tectonically stable regions—at best an ad hoc hypothesis—or they may indicate local cli-

matic control of sea level. The cumulative erosional effects of storm surges during periods of unsettled weather may cause identifiable differences in apparent sea level from periods of stable weather.

It is these transient variations in water level such as North Sea storm or Gulf coast hurricane surges that are the most important variations in social terms; they may also be much more important in the geological record than was previously realized.

References

Blake, W., Jr., Studies of glacial history in Arctic Canada, 1, Pumice, radiocarbon dates, and differential postglacial uplift in eastern Queen Elizabeth Islands, *Can. J. Earth Sci., 7,* 634–664, 1970.

Blake, W., Jr., Age of pumice on raised beaches, eastern Arctic Canada, *Geol. Surv. Can., Pap. 73-1,* Part *B*, 141–142, 1973.

Bloom, A.L., Glacio-eustatic and isostatic control of sea level since the last glaciation, in *Late Cenozoic Glacial Ages,* edited by K. Turekian, pp. 355–379, Yale University Press, New Haven, Conn., 1971.

Bodine, B.R., Hurricane surge frequency: Estimated for the Gulf Coast of Texas, *Tech. Mem., 26,* 32 pp., U.S. Army Corps of Eng., Coastal Eng. Res. Center, 1969.

Broecker, W.S., D.L. Thurber, J. Goddard, T.L. Ku, R.K. Mathews, and K.J. Mesolella, Milankovitch hypothesis supported by precise dating of coral reefs and deep sea sediments, *Science, 159,* 297, 1968.

Brooks, C.E.P., *Climate Through the Ages,* 2nd ed., 395 pp., Dover, New York, 1970.

Chappell, J., Geology of coral terraces, Huon Peninsula, New Guinea: A study of Quaternary tectonic movements and sea level changes, *Geol. Soc. Amer. Bull., 85,* 553–570, 1974.

Clark, R.H., and M.P. Persoage, Some implications of crustal movement in engineering planning, *Can. J. Earth Sci., 7,* 628–633, 1970.

Curray, J.R., and F.P. Shepard, Some major problems of Holocene sea levels, paper presented at 2nd National Conference, Amer. Quaternary Assn., University of Miami, Miami, Fla., December 1972.

Denton, G.H., and W. Karlén, Holocene climatic variations–Their pattern and possible cause, *Quaternary Res., 3,* 155–205, 1973.

Disney, L., Tide heights along the coasts of the United States, *Proc. Amer. Soc. Civil Eng., 81,* 666, 1955.

Dohler, G.C., and L.F. Ku, Presentation and assessment of tides and water level records for geophysical investigations, *Can. J. Earth Sci., 7,* 607–625, 1970.

Emery, K.O., and L.E. Garrison, Sea levels 7,000 to 20,000 years ago, *Science, 157,* 684–687, 1967.

Fairbridge, R.W., Eustatic changes in sea level, *Phys. Chem. Earth, 4,* 99–185, 1961.

Fairbridge, R.W., World sea level and climatic changes, *Quaternaria, 6,* 111–134, 1962.

Fairbridge, R.W., and O.A. Krebs, Jr., Sea level and the southern oscillation, *Geophys. J. Roy. Astron. Soc., 6,* 532–545, 1962.

Fairbridge, R.W., and W.J. Newman, Postglacial crustal subsidence of the New York area, *Z. Geomorphol., 12,* 296–317, 1968.

Faure, H., and L. Hebrard, Shoreline fluctuation in Senegal and Mauritania during Holocene time, paper presented at 9th International Quaternary Congress, Christchurch, N.Z., Dec. 2–10, 1973.

Fleming, N.C., Archeological evidence for eustatic change of sea level and earth movements in the western Mediterranean in the last 2,000 years, *Geol. Soc. Amer. Spec. Pap. 109,* 125 pp., 1969.

Flint, R.F., *Glacial and Quaternary Geology,* 892 pp., John Wiley, New York, 1971.

Godwin, H., R.P. Suggate, and E.H. Willis, Radiocarbon dating of the eustatic rise in ocean-level, *Nature, 181,* 1578–1579, 1958.

Gutenberg, B., Changes in sea level, postglacial uplift, and mobility of the earth's interior, *Geol. Soc. Amer. Bull., 52,* 721–722, 1941.

Hendershott, M.C., Ocean Tides, *Eos Trans. AGU, 54,* 76–86, 1973.

Hicks, S.D., Vertical crustal movements from sea level measurements along the east coast of the United States, *J. Geophys. Res., 77,* 5930–5934, 1972.

Hollin, J., Is the Antarctic ice sheet growing thicker?, *Int. Assn. Sci. Hydrol. Publ. 86,* 363–374, 1970.

Hughes, T., Is the west Antarctic ice sheet disintegrating?, *J. Geophys. Res., 78,* 7884–7910, 1973.

Imbrie, J., and N.G. Kipp, A new micropaleontological method of quantitative paleoclimatology: Application to a late Pleistocene Carribean core, in *Late Cenozoic Glacial Ages,* edited by K.K. Turekian, pp. 71–181, Yale University Press, New Haven, Conn., 1971.

Kaye, C.A., and G.W. Stukey, Nodal tidal cycle of 18.6 years, *Geology, 1,* 141–144, 1973.

King, C.A.M., *Beaches and Coasts,* 403 pp., Edward Arnold, London, 1959.

Kuenen, Ph.H., Eustatic changes in sea level, *Geol. Mijnbouw, 16,* 148–155, 1954.

Longman, I.M., A Green's function for determining the deformation of the earth under surface loads, 1, Theory, *J. Geophys. Res., 67,* 845–850, 1962.

Longman, I.M., A Green's function for determining the deformation of the earth under surface mass loads, 2, Computations and numerical results, *J. Geophys. Res., 68,* 485–496, 1963.

Markowitz, W., Sudden changes in rotational acceleration of the earth and secular motion of the pole, in *Earthquake Displacement Fields and the Rotation of the Earth,* edited by L. Mansinha, D.E. Smylie, and A.E. Beck, p. 69, D. Reidel, Dordrecht, Netherlands, 1970.

Mathews, R.K., Relative elevation of Late Pleistocene high sea level stands: Barbados uplift rates and their implications, *Quaternary Res., 3,* 147–153, 1973.

Milliman, J.D., and K.O. Emery, Sea levels during the past 35,000 years, *Science, 162,* 1121–1123, 1968.

Mörner, N.A., The Late Quaternary history of the Kattegatt Sea and the Swedish west coast, *Sverig. Geol. Unders., Ser. C,* no. 640, 488 pp., 1969.

Mörner, N.A., Eustatic changes during the last 20,000 years and a method of separating the isostatic and eustatic factors in an uplifted area, *Palaeogeogr. Palaeoclimatol. Palaeoecol., 9,* 153–181, 1971.

Mörner, N.A., Eustatic changes during the last 300 years, *Palaeogeogr., Palaeoclimatol., Palaeoecol., 13,* 1–14, 1973.

Munk, W.H., and G.F. Macdonald, *The Rotation of the Earth,* 323 pp., Cambridge University Press, London, 1960.

Munk, W.H., and R. Revelle, Sea level and rotation of the earth, *Amer. J. Sci., 250,* 829–833, 1952.

Paterson, W.S.B., Laurentide Ice Sheet: Estimated volumes during Late Wisconsin, *Rev. Geophys. Space Phys., 10,* 885–917, 1972.

Rossiter, J.R., The North Sea storm surge of 31 January and 1 February 1953, *Phil. Trans. Roy. Soc., Ser. A, 246,* 371–399, 1954.

Schofield, J.C., Postglacial sea levels and isostatic uplift, *N.Z. J. Geol. Geophys. 7,* 359–370, 1964.

Shepard, F.P., Thirty-five thousand years of sea level, in *Essays in Marine Geology in Honor of K.O. Emery,* edited by T. Clements, pp. 1–10, University of Southern California Press, Los Angeles, 1963.

Shepard, F.P., and J.R. Curray, Carbon-14 determination of sea level changes in stable areas, in *Progress in Oceanography,* vol. 4, edited by Mary Sears, Pergamon, New York, 1967.

Steers, J.A., The east coast floods, in *Applied Coastal Geomorphology,* edited by J.A. Steers, pp. 198–223, Macmillan, New York, 1971.

Ten Brink, N.W., Glacio-isostasy: New data from west Greenland and geophysical implications, *Geol. Soc. Amer. Bull., 85,* 219–228, 1974.

Ters, M., Les variations du niveau marin depuis 10,000 ans, Le long du littoral Atlantique Francais, in *Recherche sur le Quaternaire Marin,* pp. 114–135, Centre National de la Recherche Scientifique, Paris, 1973.

Thorarinsson, S., Present glacial shrinkage, and eustatic changes of sea level, *Geogr. Ann. 22,* 131–159, 1940.

Van Veen, J., Tide-gauges, subsidence-gauges and floodstones in the Netherlands, *Geol. Mijnbouw, 16,* 214–219, 1954.

Walcott, R.I., Past sea levels, eustasy and deformation of the earth, *Quaternary Res., 2,* 1–14, 1972*a*.

Walcott, R.I., Late Quaternary vertical movements in eastern North America: Quantitative evidence of glacio-isostatic rebound, *Rev. Geophys. Space Phys., 10,* 849–884, 1972*b*.

Walcott, R.I., Structure of the earth from glacio-isostatic rebound, *Annu. Rev. Earth Planet. Sci., 1,* 15–37, 1973.

Ward, W.T., Postglacial changes in level of the land and sea, *Geol. Mijnbouw, 50,* 703–718, 1971.

Wunsch, C., Bermuda sea level in relation to tides, weather, and baroclinic fluctuations, *Rev. Geophys. Space Phys., 10,* 1–49, 1972.

Richard Walcott has been with the Earth Physics Branch of the Department of Energy, Mines and Resources, Ottawa, Canada, as a research scientist since 1967. He studied geology at Wellington, New Zealand and geophysics at Imperial College of London and University of British Columbia. He joined the Geophysics Division, Department of Scientific and Industrial Research, Wellington, New Zealand, in January 1975.

omit

AGU

Seventh GEOP Research Conference Report

THE SEVENTH GEOP (Geodesy/Earth and Ocean Physics) Research Conference, on Coastal Problems Related to Water Level, was held June 6–7, 1974, at the Ohio State University and was attended by 64 persons. On behalf of the GEOP Steering Committee the conference was opened by Hyman Orlin (National Oceanic and Atmospheric Administration/National Ocean Survey), program chairman, who, in his introductory remarks, brought out the fact that a rational coastal zone management must be based on an adequate knowledge of the environment and the natural processes active in altering this environment. Knowledge of the environment involves data gathering and data presentation; knowledge of environmental processes involves an analysis of recent and historic data. This latter information leads to a model for forecasting the future state of the environment, which is the cornerstone of coastal zone management.

Either the future state of the environment pleases us, in which case we do nothing–a do-nothing policy that at least is based on facts–or some attempt is made to moderate those processes that we feel will lead to abhorrent results. Orlin also mentioned that it is superfluous to state that the most pervasive natural force in the coastal zone is that due to water, and the most pervasive unnatural force is that due to man. Thus the aim of the Seventh Geodesy/Earth and Ocean Physics Conference is to examine those characteristics of change that may have a deleterious effect on coastal and lake regions. Hence the conference has been organized to present (1) problems in specific areas, (2) discussions of the hydrological and geological effects of water action in coastal areas, and (3) a presentation of those problems related to large lake regions.

The panel presentations were preceded by the keynote address, delivered by R.I. Walcott (Department of Energy, Mines and Resources, Ottawa). The lecture in its entirety is printed as an article in this issue.

First Session

Management Problems Related to Change in Elevation

Chairman: Pliny Gale, (Turner, Collie and Braden, Inc., Houston)

Members: Billy Jim Garrett (Corps of Engineers, New Orleans), Hugh Dolan (Department of Commerce, Washington, D.C.), Donald C. Steinwert (Department of Water Resources, Sacramento, California), Michele Caputo (University of Bologna)

The chairman, in introducing the panel subject, pointed out that all levels of management in nearly every field of endeavor were concerned with the effects of subsidence in those geographic areas where it occurs in significant amounts. Recognizing that it exists is a prime requirement. Measuring and monitoring the changes caused by it are preliminary to studying the effects from subsidence. These lead into the steps of generating plans and designs to

This report was prepared by G.C. Dohler, Pliny Gale, Ivan I. Mueller, R.B. Perry, and J.F. Poland. Material contained herein should not be cited.

cope with it and then programs of either instituting corrective action to offset continuance of the effects from subsidence or living with the effects.

The panel members reviewed projects that related to the effects of changing elevations in their respective local or professional areas. P. Gale described one program undertaken by the City of Houston in its efforts to combat the subsidence in its region. The specific program used as the example is a comprehensive water supply and distribution system study. A local consulting engineering firm that has been involved with the city in developing many long-range plans was employed and produced the results in a series of reports.

The actual numerical content of the Houston reports was not the accented theme for the panel presentation, but rather the elements of the study and the systematic pursuance of all factors influencing the subject were discussed. Geology, population trends and predictions, aquifer locations and sections, withdrawal of groundwater and its relationship to subsidence, pumping stations, treatment plants, distribution systems, and new sources of surface water supply were dealt with in depth.

As a result of this study and active local interest, constructive steps have been instituted to reduce and hopefully to halt continued subsidence through the reduction of groundwater withdrawal. A definite relationship has been established between the two. It is believed the proposed plan will reduce subsidence and provide an adequate water supply to accommodate projected growth requirements. The population of the study area is expected to be 4.3 million by the year 2000, and the cost to the city is estimated to be of the order of $800 million.

B.J. Garrett explained how southern Louisiana has been seriously affected by changes in land surface elevations. As a result of the great flood of 1927, the U.S. Congress enacted the Flood Control Act of 1928. Under this act and subsequent amendments the U.S. Army Corps of Engineers began development of the flood control plan for the lower Mississippi River and tributaries. The plan authorized by the Flood Control Act provides for the control of the maximum probable flood that may occur in the lower Mississippi valley. The Mississippi River watershed is the largest drainage basin in the United States, and the maximum probable flood at the latitude of Old River has been determined under project conditions to be 100,000 m^3/s. This flood flow is to be routed to the sea by passing ½, or 50,000 m^3/s, through the Atchafalaya basin floodway.

The Atchafalaya River is not a river but a distributary for the Red and Mississippi Rivers. About 500 years ago an enlarged loop in the Mississippi River meandered westward and captured the Red River in the vicinity of Turnbull Island. The meander loop, one arm of which is now known as Old River, cut into an ancient channel of the Mississippi River. The flood waters of the Red and Mississippi entered this new outlet and began excavating the old waterway to form the present Atchafalaya River. The upper end of the channel soon filled with debris, forming an impenetrable raft of logs that continued to grow until Henry Shreve, in 1831, isolated the Atchafalaya from the Mississippi by means of a cutoff at the narrow neck of the Old River loop. The raft, cut off from its major source of debris, ceased to grow. Various groups made unsuccessful attempts to clear the river for navigation between 1839 and 1855. Upon removal of the raft in 1855 by the State of Louisiana, the river enlarged its channel, threatening capture of the Mississippi by 1875. Annual flooding brought ever increasing losses of land and capital to the farmers of the basin until the area was abandoned in the early 1880's.

Changes in land surface elevation in the floodway are caused mainly by sediment reaching the lower basin and depositing therein. As more flow was, and is, routed into the floodway, more deposition occurs. This increased sedimentation in the floodway changes the flood-carrying capacity of the floodway, which in turn necessitates modification of the levee systems and other flood protection works. The rapid acceleration of flow and sedimentation in the lower floodway is attributed to channel enlargement in the upper basin and the transport to the lower basin of sediments that would normally have been deposited in the middle basin. The average annual suspended sediment transported into the basin is about 72 million m^3/yr. However, during the flood of 1973 it was estimated that 290 million m^3 entered the floodway, of which approximately 200 million m^3 were deposited in the floodway. On an average annual basis, about 26 million m^3 are deposited within the floodway. Within the floodway system, settlement through compaction is found in the progressive sinking of the east and west protection levees. However, regional subsidence within the project area, as reported by Gagliano and Van Beek in 1970, through radio carbon dating of buried organic deposits indicates that subsidence within the floodway varies from 10 cm/century to 15 cm/century since sea level reached its present stand about 4300 years ago.

The major management problem associated with changes in surface elevation, is not related directly to subsidence, but to accretions. However, subsidence (regional subsidence) does affect the water-surface-gaging network in the floodway. The problem relates to the application of the adjustment: should the adjustment be prorated over the time interval from last adjustment, or should the application of adjustment begin with the next series of data with no adjustment for previous years?

In discussing the legal and jurisdictional aspects of coastal boundary determinations, H. Dolan carried forward a development of the various conditions met with in attempting to set uniform laws for describing the land-sea demarkation. The Law of Federal Tidal Boundaries in the United States, though derived from English Law, is principally expressed in a line of Supreme Court decisions beginning with Borax versus U.S. in 1935, which adopted the tidally observed 'mean high water' as the boundary. The Submerged Lands Act gave the states rights in the 3-mile territorial sea, the limits of which are ascertained under the criteria of The International Convention of the Territorial Sea and the Contiguous Zone by using the methodology developed by the National Ocean Survey. Most of the coastal states are still litigating the extent of their seaward boundaries. Programs of a number of federal agencies including the U.S. Army Corps of Engineers, Department of Housing and Urban Development, U.S. Geological Survey, Bureau of Land Management, and Environmental Protection Agency utilize tidal determinations.

State laws generally refer to high water or low water as the line dividing ownership; however, many laws pertaining to seashore and wetlands development have been enacted recently that utilize other criteria. These are compiled and discussed in *Technical Report 20* of the University of Michigan Sea Grant Program. Delimitation under these criteria often presents difficult survey problems. The recently enacted Florida Coastal Mapping Act of 1974 is a significant model of baseline legislation on coastal boundary determinations. The authors, Professors Maloney and Ausness, will publish a detailed analysis and explanation in the Fall-Winter issue of the University of North Carolina *Law Review*. The law has long recognized the sea-land intersection as a most significant boundary. Better understanding of the natural and man-made effects on land and water level movements as well as their measurement is essential to the development and articulation of legal norms that will govern property rights in the nearshore coastal areas.

A major construction project described by D.C. Steinwert—the California aqueduct, which supplies a great portion of municipal water used by Los Angeles—had to cope with the significance of vertical movement in design, construction, and operation of the system. This project extends from areas of surplus water in the Sacramento valley to its terminus at Perris reservoir in southern California, a distance of some 885 km. The keystone to the project is the Oroville dam facility, a multipurpose recreational, flood control, conservation, and power generation project. This 235-m-high dam impounds up to 4.3 billion m^3 of water, with a surface area of about 65 km^2, and incorporates an underground powerhouse.

Through a complex system of stretches of natural river, flumes, pipes, lift stations, forebays, and reservoirs, the water is conveyed through many types of terrain, from semiarid desertlike to forested land, from valleys to mountains, and finally through some 55 km of buried pipeline into the Perris reservoir. The size of many of the

conveyance facilities is without precedent; pumps and generators were specially designed, and the logistics of scheduling and constructing a $2-billion project extending over 800 km required completion within a time frame of about 12 yr. In addition to engineering problems related to the unique size of the facilities, very serious problems were associated with vertical movements that could be brought about by ground subsidence and by California's ever-menacing earthquakes.

Land subsidence in the San Joaquin valley was first noted in the midtwenties. Although the magnitude of the problem continued to increase during the next 40 years, very little was understood about it. Surveys conducted during the forties and early fifties, by the U.S. Coast and Geodetic Survey and others, disclosed major areas of subsidence in the valley, and on the basis of data obtained, it was determined that in some areas the ground surface had subsided as much as 2 and 2.5 m just during the period of the surveys. On the basis of 1970 surveys and data from 1926 it was found that subsidence of as much as 7 m had occurred during that period in the area of the canal alignment. Decreasing groundwater levels in the valley and correlated records extending as far back as the early 1900's appeared to have a relationship to the subsidence. Groundwater data obtained in 1905 show that flowing artesian wells were common in the easterly half of the valley; by 1952 the piezometric levels of water in the confined zone had decreased as much as 30–100 m in various areas. The levels of water in the upper, unconfined zone had not changed greatly during the same period.

In 1954, as the state and federal governments moved into more detailed planning for the project, through the results of their studies and others, it was established conclusively that the major deep subsidence occurring in the San Joaquin valley, is directly related to water level decline in the confined zone, and that it slows down or ceases in response to water level recovery. With this information, it was necessary to determine the probable time elements between start of construction and deliveries of surface supplies of water to replace the water being extracted from the deep, confined zone by pumping.

Economic studies of alternate alignments, including full consideration of future modifications and maintenance that might be required because of continuing or residual subsidence, resulted in the selection of the present alignment. This alignment includes reaches of canal with as much as 2 m of extra lined freeboard and structures that could be jacked to higher levels to compensate for the expected subsidence.

It was recognized that additional modifications would be required if subsidence exceeded expected amounts. Such modification work included adding extra lined freeboard. In establishing survey controls for construction in this area in the early 1960's, the controls were 'frozen' as they were established because the ground surface was subsiding so rapidly. As of January 1971, deep subsidence of as much as 1.8 m had occurred since the original frozen surveys. Bridges in the subsidence areas were designed to permit limited vertical adjustment by jacking up to 50 cm or so. However, the subsidence at some of the bridge locations exceeded the jacking limit, and major modifications have been required. These are typical of the deep subsidence problems management continues to cope with in these areas.

In addition to the deep subsidence problem, which is compaction of materials in the confined water zone, management was faced with an equally if not potentially more damaging subsidence phenomenon known as shallow subsidence. The streams that drain from the westerly slopes of the lower San Joaquin valley are normally dry in the summer and are very often dry in winter. Rainfall, though infrequent, usually comes in high-intensity storms lasting only a few hours. Normally, a large part of the annual rainfall occurs in several of these short-duration storms. The alluvial fans formed by the fine-grained soils carried from these watersheds are of low density but have a very high shear strength. When sufficient quantities of water are applied to these soils, the chemical and physical bond diminishes, and a volume decrease results. The downard surface displacement resulting from the compaction of the underlying low-density soils, is defined as shallow land subsidence.

As with the deep subsidence problems, studies of alternate alignments determined that bypassing the shallow land subsidence areas was not feasible. However, the net result of construction without treatment would be excessive maintenance and operational costs and intermittent disruption of water deliveries. In 1957 the state embarked on an intensified two-phase investigation of this particular problem. Phase 1 consisted of a drilling program along the proposed alignment to establish the locations and depths of the low-density soils; the phase 2 objective was to establish various test sites and to determine the most effective method of precompacting the unstable soils.

On the basis of test site studies and the criteria developed during the test program, 7 major reaches of the canal alignment in the lower part of the valley were identified as areas of potential shallow subsidence. Initial canal excavation and consolidation ponding had to be done before permanent structural work could start. Although the maintenance required since construction has generally been limited to repair of cracking in the canal lining, surveillance must be constant to detect problems as they develop.

California is laced with known active earthquake faults. Construction of a water system as long as the California aqueduct would not be economically feasible (and very likely would not even be possible) without crossing some of these faults. Alignments of tunnels such as the Tehachapi crossing, which intercepts the Garlock fault, were designed to daylight between tunnels at the fault crossing. In event of any movement along the fault, access to the damaged aqueduct would be readily available. Attempts were made to avoid the faults, particularly the San Andreas fault, but they still had to be crossed several times, usually in pipeline. The objectives of these crossings were to minimize potential damage to the system and to downstream properties in the event of movement along the fault.

Also faced with the problems of continued subsidence is the city of Venice, Italy. M. Caputo presented historical data, photographs, and charts that confirmed the constant encroachment of the sea upon the city due to sinking of the land mass. For use in estimating the future rate of subsidence, information has been sought to cover the longest period of time possible, and both historical and archeological data have been collected and analyzed. Since the secular sinking of the city and the frequency of the 'acqua alta' depend on the relative height of the ground level with respect to the mean sea level (msl), attention was focused on their relative variation of level. This variation is the sum of two components: the variation of height relative to a point fixed with respect to the center of mass of the earth and the eustatic variation of msl. For a point on the coast the mareograph gives directly the variation of the height with respect to msl; for the same point the variation of height with respect to a fixed point can be measured by spirit leveling. Thus the secular variations of msl were obtained with the mareographs, with the elastic response of the earth taken into account.

To survey the msl variations, the major contributions come from geology and geography, which indicate variations with periods of $10^5 - 10^6$ yr and amplitude of 2×10^4 cm; there are also variations with higher frequency that are of interest. Many archeological monuments located at sea level on the Tyrrhenian Sea have been dated precisely, and their present elevations above the present msl have been accurately measured. Assuming the heights of these monuments with respect to sea level to be a linear function of time, a linear regression has been made to represent the variation of sea level from 600 B.C. to A.D. 100; in that time interval the rise would have been about 1.7 mm/yr.

Since the end of the nineteenth century, data are available from the mareographs of Trieste, Genova, and Marseille, which are located on terrains that seem stable. The correlation of the data in the various places is greater than 0.85. These data suggest a msl rise of 1.5 mm/yr in the interval 1896–1970.

The correlation coefficients of all the mareographs in the Mediterranean Sea are nearly 1; their spectral components, although some are below the 95% confidence level, are common to all of them. In the Lagoon of Venice, four mareographs supplied data for a time interval long enough to allow a dependable analysis. To see the local effects, one can subtract from

the data of each mareograph the corresponding data of a mareograph of an area presumably not affected by subsidence. In all 4 mareographs the analysis of data shows no correlation for the data between 1896 and about 1926; from 1926 to 1967 a linear regression shows that in this interval of time there is an average subsidence of 2.8 mm/yr in the lagoon and the city. Repeated levelings in the region of the Po River mouth and analysis of another mareograph in the south of the Po River show that the phenomenon of the subsidence extends to a 200-km arc of coast including Venice.

From the first results of a study under way there seems to be no correlation between the rate of subsidence and the most obvious geological features such as the bed of the Pliocene.

The high-frequency variation of the msl makes it difficult to determine with accuracy the subsidence in a short interval of time. Geometric leveling can give a description of the subsidence with high accuracy, say, with a propagation error of $1.5 \times D^{1/2}$ mm (D is the distance in kilometers). Obviously, both data are needed.

The many spirit levelings that have been performed in Venice and its hinterland since the beginning of the century indicate that the ground was stable, within observational errors, until 1952; from 1952 to 1970 there was a subsidence of 5–7 mm/yr. The subsidence begins 30 km north of Venice and reaches a maximum in Mestre, 5 km north of Venice.

The results from the great number of loops of leveling that cover the historic center of Venice were presented. It was concluded that in general the msl seems to have risen with respect to the historic center and the lagoon about 4 mm/yr in the last 40 yr, although at some points the rate is much higher. In 50 yr more, assuming that this rate remains constant, the msl would rise so much that in many parts of the historic center almost every high tide would become an 'acqua alta,' which would make life impossible and endanger the safety of most buildings. As to the causes of the subsidence in the historic center and the Lido, there is a correlation between the areas of higher rate of subsidence and the areas where the soil has been subjected to recent loading, e.g., new buildings and soil refills. Another correlation seems to occur within the areas where there has been strong pumping of water from the ground, which is common to most subsiding areas in the Po River valley.

Second Session

Hydrologic Effects on Elevations and Shoreline

Chairman: J.F. Poland (U.S. Geological Survey

Members: R.A. Baltzer (U.S. Geological Survey), C. Bull (Ohio State University), V. Myers (National Weather Service/National Oceanic and Atmospheric Administration), C.I. Thurlow (National Ocean Survey/National Oceanic and Atmospheric Administration), S. Young (National Ocean Survey/National Oceanic and Atmospheric Administration)

In his introductory remarks, J.F. Poland commented that hydrologic effects that represent a significant increase from the 'normal' water depth at the coast can be caused either by sinking of the land surface or by a rise of the sea.

In a discussion of land subsidence due to fluid withdrawal, Poland pointed out that many areas of such subsidence occur in coastal lowlands, whether the cause is groundwater overdraft or removal of fluids from oil and gas fields. In Japan, man-made subsidence has been reported in 31 separate areas, of which all but one lie on the coast. In most of these areas the subsidence is due to fluid withdrawal, decline of artesian head, and compaction of unconsolidated fine-grained beds resulting from the increase in effective stress on the aquifer systems.

The most serious environmental subsidence problem in Japan and probably in the world is the prolonged and continuing subsidence in eastern Tokyo, bordering Tokyo Bay. The artesian head in confined aquifers, initially above sea level, had declined to 60 m below by 1967 because of excessive groundwater draft. As a result of the subsidence (4.2-m maximum), 80 km² of land where 2 million people live had settled below mean high-tide level by 1969. The lowest ground is about 2.5 m below msl. Despite the protective and remedial measures taken, the danger of major and disastrous flooding due to typhoons, or of failure of dikes, water gates, or drain pumps brought about by a violent earthquake, such as the great 1923 earthquake, is ever present. Even after a substitute surface water supply is imported and groundwater levels recover sufficiently to stop the subsidence, any rebound of the ground surface will be small compared with the subsidence.

Land subsidence in the Santa Clara valley bordering San Francisco Bay was first noted in 1933 when bench marks in San Jose established in 1912 were resurveyed by the National Geodetic Survey and found to have subsided 1.2 m. Excessive groundwater pumping produced an overdraft that lowered the artesian head about 58 m from 1916 to 1967. In response to the increased effective stress, the unconsolidated deposits composing the confined aquifer system compacted. The resulting subsidence which began about 1917 had reached 4 m in San Jose and as much as 2.5 m in the bay tidelands by 1969. Remedial measures taken have included extensive construction and raising of levees around the bay and on stream channels, and the repair or replacement of several hundred water well casings ruptured by the compaction of the sediments. The import of surface water to the subsiding area produced a dramatic recovery of artesian head (21 m) from 1967 to 1971 as a result of reduced groundwater pumpage and increased recharge. This recovery of head essentially stopped the subsidence.

Subsidence at the Wilmington oil field in Los Angeles and Long Beach harbor areas was first recognized in 1941. By 1965, it had reached 8.8 m at the center. The subsiding area is intensively industrialized and much of it initially was only 1.5 to 3 m above sea level. The cost of remedial work to maintain structures and equipment in operating condition had exceeded $100 million by 1962. Repressuring of oil zones by water injection began in 1958. By 1969, over a million barrels of water per day was being injected, and the subsidence had been virtually stopped.

In its field studies of land subsidence, the U.S. Geological Survey has developed recording extensometers to measure compaction and expansion of aquifer systems in response to change in stress (change in depth to water). Such stress-strain records obtained from multiple-aquifer systems in subsiding areas indicate that the values of the compressibility and storage parameters are 50 to 100 times greater when total applied stresses are in the virgin range of stressing than when they are in the elastic range, according to Poland.

Hurricane storm tidal inundations are a serious hazard to life and property along the Gulf and Atlantic coasts of the United States; this was recently illustrated by Hurricane Camille on the Mississippi coast in 1969. The tide exceeded 6 m above msl in this storm, according to V. Myers. The problem is accentuated by the recent and prospective increase in population of coastal areas. Furthermore, the hazard varies from point to point depending on the bathymetry of the continental shelf and the climatology of hurricanes.

Myers described a program for evaluating this hazard by calculating tide frequencies on the coast by a synthetic method, from frequencies of 0.1 to 0.005 yr^{-1}. The steps are (1) analyze individual hurricanes (since 1900) to establish index values of intensity and size; (2) collect these statistics into climatological frequency profiles along the coast; (3) translate hurricane atmospheric climatology to hurricane coastal surge climatology by replications with a tested hydrodynamic model; and (4) combine surge climatology with astronomical tide probabilities to form tide frequency probabilities. These frequencies are used for local regulation and guidance under the National Flood Insurance Act of 1968.

General purpose mathematical/numerical modeling systems by which to simulate hydrologic and water-quality-related phenomena in water bodies are being developed for comprehensive investigative and resource management purposes. R.A. Baltzer described one such modeling system that has been developed by the U.S. Geological Survey for simulating hydrologic and water quality conditions in waterways, lakes, estuaries, and coastal embayments. One of the particular models used in this system is a numerical representation of the vertically integrated, two-dimensional, time-dependent set of partial

differential equations for the conservation of mass and of momentum. In addition, the equation for the mass transport and interactions of pollutant/constituents is employed. With the introduction of the appropriate initial and boundary conditions for a particular prototype water body, these equations can be solved by using a clearly coupled, finite-difference technique. Factors such as wind shear at the surface and Coriolis effect are considered in the formulation.

An investigation of proposed harbor and navigational waterway improvements in Tampa Bay, Florida, revealed that by judicious placement of dredged materials, circulation and thus water quality in certain portions of the bay could be substantially improved, according to Baltzer. In addition to evaluating the effects of configural changes in the bathymetry, the modeling system can be used to study the movement of injected waste constituents, the dispersal and dissipation of injected excess thermal energy, the effect of storm surges and other unusual wave phenomena, and the movement, deposition, resuspension, and dispersal of sediment. The modeling system consists of a modular array of computer programs. These programs edit and process prototype initial and boundary condition data, set up a particular simulation, perform the actual mathematical/numerical simulation, analyze the results of the simulation, and prepare the output film plots. The system is designed to be completely general and to have high transferability to appropriate prototype water bodies. Various two- and three-dimensional dynamic simulation models can be used in the system to carry out the mathematical/numerical modeling. These models can be used to estimate the probable areas that would be inundated by tropical storms of various recurrence intervals.

C.I. Thurlow and S. Young discussed tidal observations, with emphasis on instrumentation and the accuracies of measurements. Until the mid-1960's, tide data collected by the National Ocean Survey were in analog form. Although the analog form yields the most satisfactory records, restrictions on personnel for the tabulation and analysis of the data make the continuation of this mode impossible. Demands for tidal datums to determine boundaries throughout the United States are increasing exponentially. In addition, the need to obtain measurements where it is uneconomical and even unreasonable to install a float well has made use of a more simple installation mandatory.

The analog-to-digital tide gage has made possible the use of computers for the reduction of data. Although the instrumentation now on the market needs improvement, the reduction of data by modern methods is possible. The pressure-actuated systems have been on the market for some time. However, the reliability of the measure, relative to that obtained from a float gage, has been controversial. A program is now in progress within the National Ocean Survey to operate all types of tide gages at the same facility for a sufficient period to determine the differences, if any, in the various systems of measure.

Some preliminary results are listed here. Final values will be made available to the public as soon as the comparisons are completed, according to Thurlow and Young.

National Ocean Survey Standard Automatic Tide Gage

Differences between recorded values from the tide gage and simultaneous readings from a tide staff mounted independently of the float well:

Atlantic City, New Jersey, 1967–1972
1 month's mean difference from daily (5 per week) comparisons: 2.1 ± 0.9 cm
1 year of monthly means 2.0 ± 1.1 cm
6 years of monthly means 3.0 ± 2.1 cm

Analog-to-Digital Recorder

Differences between recorded values from the tide gage and simultaneous readings from a tide staff mounted independently of the float well:

Baltimore, Maryland, 1967–1973
Mean differences for 73 months of data involving 1333 staff/gage comparisons:
1 month's mean difference 0.6 ± 0.3 cm
73 months' mean difference 0.6 cm
First standard deviation 0.6 cm
Third standard deviation 2.0 cm
Variance 1.5 cm

National Ocean Survey Standard Automatic Tide Gage Compared with Analog-to-Digital Recorder

Differences are between computed mean sea level and mean tide level values from 1 year of record. The gages were operated simultaneously at the same location for a period of 1 year.

Washington, D.C., 1965
Mean tide level 0.3 ± 0.3 cm
Mean sea level 0.6 ± 0.3 cm

Gas-Purged Pressure-Recording Tide Gage

Mean differences between hourly water level values were recorded simultaneously on an analog-to-digital recorder and a gas-purged pressure-recording tide gage.

Washington, D.C., February 1974
Comparison of 506 hourly heights mean difference 0.6 ± 1.2 cm
Computed mean sea level for the 2 gages yielded a difference of 0.2 cm

Note: The float-operated tide gages all used 30-cm-diameter float wells with bottom-located 2.5-cm-diameter intakes. All floats were 21.6-cm diameter and weighed 2 kg each.

The continental ice sheets of Antarctica and Greenland contain the greatest potential for creating massive worldwide coastal problems related to water level. Obviously, any marked imbalance could have a profound effect on the shorelines of the world. For this reason, the present status of knowledge with respect to the mass balance of these two ice sheets was reviewed by C. Bull. Of the 1.4×10^9 km^3 of water on the surface of the earth, more than 97% is in the oceans and only 2% or so exists as snow and ice. About 90% of the ice (25 or 30×10^6 km^3) is in the Antarctic, and a further 9% (2.6×10^6 km^3) is in the Greenland ice sheet. The melting of this ice, ignoring isostatic changes, would raise sea level by 75–80 m. Obviously, in a conference on coastal problems related to water level a consideration of the mass balance of these two continental ice masses is in order.

For both the Antarctic and Greenland ice sheets the estimates of the annual accumulation of snow and of the annual ablation on land now appear to be reasonably reliable, perhaps within 20%. For the Antarctic ice sheet and the ice shelves the positive annual balance is about 210×10^{16} g, equivalent to 15.5 ± 2.0 g cm^{-2}. For the Greenland ice sheet the annual positive balance is about 17×10^{16} g, equivalent to about 10 g cm^{-2}. Possibly half of the loss of ice from Greenland, and very nearly all of the loss from Antarctica, is in the form of icebergs, and no accurate estimates of the values are available. The most recent estimate (1971) of the total balance of the Antarctic ice sheet is $+42 \times 10^{16}$ g yr^{-1}, equivalent to +3 g cm^{-2}, but the various estimates of the annual loss of ice, in the form of icebergs from the ice sheet, glaciers, and the ice shelves, range from 40×10^{16} to about 180×10^{16} g yr^{-1}, and no one estimate seems much more reliable than the others. The best we can say is that for Antarctica the mean balance is probably +3 ± 5 g cm^{-2} yr^{-1}.

Similar uncertainties exist for the Greenland ice sheet. About equal numbers of estimates give positive and negative balances, and again the main uncertainty is with the quantity of ice lost in the form of icebergs. Experiments now under way and proposed for the near future in tracking individual icebergs and in determining total iceberg flux by high-resolution satellite photography should allow a much more accurate assessment of the balance of these continental ice masses within the next decade.

Even with accurate estimates of the present balance, predictions of future sea level must take into account the possibility of surges of major parts of the Antarctic ice sheet, which could raise sea level by 10 m or so in a period as short as 50 yr, according to Bull.

Third Session

Geologic Effects on Elevations and Shoreline

Chairman: R.B. Perry (National Oceanic and Atmospheric Administration/National Ocean Survey)

Members: M.O. Hayes (University of South Carolina), S.R. Holdahl (National Oceanic and Atmospheric Administration/National Ocean Survey/National Geodetic Survey), J.W. Pierce (Smithsonian Institution)

R. Perry introduced the session by pointing out the need for considering vertical movements in long-range coastal plan-

ning. In tectonically active areas such as the Gulf of Alaska, it is important that there be a good warning system for tsunamis generated in the vicinity.

Where it is feasible, housing and other structures should be located above levels where they may be inundated by abrupt vertical movements or tsunamis. In areas of slow apparent land subsidence relative to sea level, there is greater opportunity for good planning. Barrier beach housing should be elevated and should be built back from the surf zone and away from inlets that may experience strong currents during storm surges. Housing in the wetland areas of coastal bays is very vulnerable to flooding during major storms.

Coastal zone planners as well as housing developers and planners need better access to long-range forecasts of sea level and probable maximum storm surge heights. It was recommended that more permanent tide gages, possibly tied to a real-time warning network, are needed in heavily developed coastal zone areas.

S. Holdahl explained the numerical methods used in estimating the relative and absolute changes of elevation in coastal areas. Long-term records from tide stations are combined with periodic precise leveling to estimate relative changes in elevations. The Houston area, with relatively rapid subsidence, should be resurveyed more often than the Chesapeake Bay area. The Chesapeake Bay area has been covered by a large leveling network that shows maximum vertical velocities of 5 mm/yr in local zones. An average eustatic rise of sea level of 11 mm/yr may be assumed in computing how much of the change is due to sea level rise and how much to land subsidence. That figure can be refined as longer-term data become available.

Coastal zone planning associated with barrier island migration was covered by J. Pierce. We know a great deal about the general worldwide migration of barrier islands as sea level rises. In general, material is eroded from the seaward side and is transported to the landward side of the barrier. As this happens the natural flora and fauna adjust their positions accordingly. Man, however, frequently comes to grief by regarding the barrier beach as a fixed platform. Structures such as lighthouses and dwellings run into problems when they are placed in an area that is retreating owing to erosion. Development should be planned for those parts of the barrier beach that are stable or accreting. Examples were shown of the successful and unsuccessful placement of structures along the North Carolina coast, as well as in several other parts of the world.

The discussion of geological information needed for sound coastal zone planning was continued by M. Hayes. Data are needed on (1) coastal type, including available sources of sediment; (2) whether the coast is erosional, depositional, or neutral; (3) tectonic stability; and (4) active physical processes such as wave conditions, tidal range, sediment erodability, winds, storm frequency, and surge susceptibility. Ideally, these data should be collected and monitored well before planning recommendations are determined. Examples of problems associated with modifications by man were discussed.

A case study of a Massachusetts beach developed a number of practical recommendations to improve stabilization. A study now in progress along the South Carolina coast is expected to determine rates of erosion and deposition that can be portrayed on maps for use by planners.

In the lively discussion that followed it was questioned whether waves and severe weather are not much more important than water level in determining coastal stability. It turns out that the 'signal' of a long-term gradual water change and resulting slow coastal migration may be obscured by a great deal of 'noise' of coastal destruction from large storms. After natural processes heal the damage within a few months or years after the storm, one can see more clearly the significance of the long-term changes. Groins and other coastal protection structures may influence the short-term noise effects, but they do little to alter the long-term coastal migration.

It was pointed out that other measurements such as water temperature and salinity should be taken at permanent tide stations. Another comment was that the present density of permanent shore tide stations probably is adequate, but that more water level measurements are needed on the continental shelves.

In the discussion, S. Holdahl pointed out that (1) the use of gravity measurements, with measured height differences, allows computation of more rigorous heights, but (2) simultaneously repeating gravity and leveling measurements up to 1000-km distances along leveling lines will not provide significantly better estimates of elevation changes, and (3) repeated precise gravity measurements, by themselves, may give better and cheaper estimates of height changes between points separated by great distances.

Fourth Session

Special Problems of the Great Lakes

Chairman: G.C. Dohler (Environment Canada, Ottawa)

Members: F. Blust (NOAA), B. De Cooke (Corps of Engineers), C. Feldscher (NOAA), N. Freeman (Environment Canada, Burlington), M. Lewis (Department of Energy, Mines and Resources, Ottawa), D. Foulds (Environment Canada, Toronto)

The Great Lakes system could be regarded as an extension of the ocean into the North American continent. Problems of managing, preserving, and maintaining a constant surveillance of this large water area requires participation not only by those living along its shores, but also by those living some distance away. To provide the necessary information that is essential for coastal zone management involves the collection of long-time series of water level data. A continuous awareness of the techniques in providing these data as well as their successful application requires searching for the theories underlying short- and long-term water level changes and their impact on mankind.

F. Blust reviewed the importance of charting in the Great Lakes. The present topographic and hydrographic data along the shores might not be adequate for the increasing need of coastal zone management, and requirement for more detailed surveys must be identified. Low-water datums have been used for charting, dredging, and other marine engineering; however, for the determination of lake-land boundaries, some further definitions of and agreements on datums are required.

The long-term variations of lake level create a serious problem for the management of the coastal zone. When the levels are falling, there is a tendency for shoreline development in the floodplain area, and during high-water periods they are subject to erosion, inundation, and even demolition. The International Great Lakes Board has concluded that land use zoning and structural setback requirements are a possible solution to the problem. The development of hydroelectric power is very important in the Great Lakes. Large hydropower plants were constructed at Niagara Falls and Cornwall with a capacity of 4400 and 1700 MW, respectively. The water of the Great Lakes system is also used for cooling several large thermal and nuclear power plants located along the shore.

B. De Cooke explained that the Great Lakes shoreline extends some 18,000 km, of which 8000 km are in the United States. They range from high bluffs of clay shale and rock, through lower rocky shores and sandy beaches, to low, marshy clay flats. Currently, 33% of the shoreline is in residential use, 50% is in agriculture, forest and undeveloped land, 10% is recreational (public), and 7% is used for commercial-industrial and public building.

About 345 km of shoreline has critical erosion mainly due to frost and ice action, storms, and change in lake level. The loss of land, economic losses, and other considerations appear to justify protective measures, including bulkheads, sea walls, revetments, groins, offshore breakwaters and beach fills with an approximate cost of $130 million (1971 prices). The Corps of Engineers has conducted the National Shoreline Study authorized by Congress in 1968. The study indicated the pressing need for a coordinated action in planning and management of the shorelines, and an intensive research for controlling erosion.

Much of the material that the corps dredges from some important harbors and channels is contaminated by pollutants from municipal, industrial, and agricultural sources. To eliminate dumping polluted dredging material in the open lakes, it is necessary to construct contained disposal facilities with 10-yr capacity at har-

bors classified as polluted by the Environmental Protection Agency. There are about 50 harbors in the Great Lakes judged to be polluted, and 25 of them are located near the Detroit area. When public lands are used, the government will bear 75% of the cost of disposal facilities construction, and the balance will be paid by nonfederal interests.

C. Feldscher described the need of water level data for mapping of floodplains and vertical crustal movement. These data are obtained from 63 gages now operated by the Lake Survey Center and 32 gages operated by Environment Canada. All data are referred to the International Great Lakes Datum (1955) established by the Coordinating Committee on Great Lakes Basic Hydraulic and Hydrologic Data. The availability of long and almost continuous water level records, some of them dated prior to 1900, makes it possible to determine the range of lake level fluctuations and the frequency of occurrence of high and low levels. G.C. Dohler and R.J.D. Mackenzie of Environment Canada, did propose a definition of high- and low-water datum based on such a frequency of occurrence, which could be helpful in defining floodplains. The data have also been used extensively to determine the relative movements of the water surface with respect to bench marks at different gages. This study is done by the Vertical Control and Water Level Subcommittee to investigate the crustal movement in the Great Lakes.

N. Freeman presented seiches and other oscillation of water levels in the Great Lakes using the time-dependent spectrum. These fluctuations are excited by storms. He indicated the serious problem of storm surges in Lake Erie, since the water level could change by more than 1.5 m in a short time, causing shoreline erosion and inundation, property damage, and significant material transfers. Statistical techniques have been found to facilitate the real-time prediction of storm surges for issuing warnings to the public. The Shoreline Damage Survey was initiated in July 1973 with the objective of establishing a Coastal Zone Atlas that will include eight data strips for each 10-km reach of shoreline, showing a photomosaic of shoreline, historical and recent shoreline change, histograms of erosion rates, present land use, property values and ownership, damage values, physical characteristics, and existing protective works.

M. Lewis explained the origin and development of the Great Lakes and their relationship to the configuration of rocks of the Precambrian shield, their tectonic movements, and the effects of Tertiary drainage and development and Quaternary continental glaciation. The lakes began life as vast pondings of glacial meltwaters during final retreat of the last (Wisconsin) glaciers from about 15,000 to 10,000 yr ago. As the glacier front retreated and advanced, various outlets were convered or uncovered that allowed the lakes to vary enormously in size and elevation.

About 10,000 yr ago the water levels at Lakes Ontario and Erie were about 80 m and 35 m below the present levels. Because of postglacial rebound of their outlets, the basins were slowly backfilled to the present stage. Lakes Huron and Michigan were originally 131 m below their present level and discharged through a depressed lowland to the northeast at North Bay, Ontario, into the Ottawa–St. Lawrence valley. Differential uplift of this outlet raised the lake levels and transferred the drainage to present outlets. The level in Lake Superior was about 30 m above present level. It was held back by a morainic drain of unconsolidated till. The threshold eventually eroded down to bedrock at St. Mary's River and lowered the level. The differential uplift (tilting) is still proceeding today approximately 6 mm/yr across the region. The products from erosion will continue to infill the offshore lake basins at a rate of about 7.1 mm/yr.

D. Foulds showed a movie entitled 'Not Man's to Command' produced by Environment Canada. It was made for the general public and explains the causes of lake level fluctuations, pointing out that these changes are mostly caused by weather and not because of man's interference. The film stresses that regulation is a compromise between conflicting interests of many users. The problem is not readily solvable by simply opening or closing dams because of (1) the rights of those downstream who would be flooded, (2) the time required for a flow increase to have an appreciable effect on the lake level, (3) the possibility that natural events can increase the supply more rapidly than one could reduce it, and (4) inadequacy during drought conditions of the natural supply for the needs of some interests. The overall solution that seems best is to learn to live with the fluctuations that exist and to design our works accordingly, rather than to try to enlarge the outlets to the sea. Foulds also mentioned that the lake forecast was done by statistical approach; a significant improvement could be made only if the weather could be predicted several months in advance.

Eighth Geodesy/Solid-Earth and Ocean Physics (GEOP) Research Conference

Lunar Dynamics and Selenodesy

Keynote Speaker: William M. Kaula, Department of Planetary and Space Science, University of California, Los Angeles

FAWCETT CENTER FOR TOMORROW
THE OHIO STATE UNIVERSITY
COLUMBUS, OHIO

OCTOBER 10–11, 1974

Sponsored by: **American Geophysical Union**
Defense Mapping Agency
National Aeronautics and Space Administration
National Oceanic and Atmospheric Administration
Ohio State University, Department of Geodetic Science
U.S. Geological Survey

The theme for the Eighth GEOP Research Conference will be set by an introductory review. The conference will be divided into the following subtopics, each introduced by an invited moderator and discussed by a panel:

1. Gravity Field: W.L. Sjogren (Jet Propulsion Laboratory, Pasadena, California)
2. Geometric Implications: Lunar Mapping, Figure: F.J. Doyle (USGS, Washington, D.C.)
3. Dynamic Implications: Ephemeris, Librations: D.H. Eckhardt (Air Force Cambridge Research Laboratory)
4. Tectonic Implications: Structure, Evolution: J.W. Head III (Brown University, Providence, R.I.)

Individuals interested in attending the conference are requested to send their applications on the standard application form available from the American Geophysical Union, 1707 L Street, N.W., Washington, D.C. 20036.

Further details on the program, accommodations, and registration will be sent to those applicants selected by the committee to attend the conference by September 3, 1974.

Applications for attendance must be received by August 23, 1974.

American Geophysical Union ★ 1707 L Street, N.W. ★ Washington, D.C. 20036

D8

N76-20574

The Gravity and Shape of the Moon

William M. Kaula

THIS REVIEW discusses the current knowledge of the gravity and geometry of the moon, and their implications as to lunar structure. Measurements pertaining to the gravity field are, first and foremost, Doppler tracking of spacecraft that have orbited the moon, but also the laser ranging from the earth to the moon and the gravity meters and accelerometers landed with the Apollo spacecraft. Measurements pertaining to the geometry include (1) those related to the shape: the metric photography and laser altimeters on Apollo 15, 16, and 17; the electromagnetic sounder on Apollo 17; the landmark tracking from earlier Apollo orbiters; and occultations, plus (2) measurements related to the orientation: the laser ranging and interferometry from the earth. The review does not cover determinations of topography from photography taken for geologic or landing reconnaissance purposes. The discussion of tectonic implications is limited to inferences of a quantitative nature. The emphasis is on work since 1970; see *Kaula* [1969, 1971] for reviews of earlier work.

This article was taken from the keynote address presented at the Eighth GEOP Research Conference, on Lunar Dynamics and Selenodesy, which was held at the Ohio State University, Columbus, October 10 and 11, 1974.

Gravity

Of the global gravity field of the moon, only the second- and third-degree harmonics can be said to be known reliably. The best determination thereof is that of *Sjogren* [1971], who used tracking of the 2700- to 6100-km-altitude Lunar Orbiter 4 to filter out higher harmonic effects. Sjogren's results for the third harmonics have been largely confirmed through their effects on the physical librations (J.G. Williams, personal communication, 1974). These results are given in Table 1.

For most of the front face of the moon, the broad regional variations of about 150-km resolution are rather well known, since orbiters could be tracked continuously. This coverage is due mainly to Lunar Orbiter 5, which had an 85° inclination, a minimum altitude of 100 km over latitude 2°N, and a maximum altitude of 1600 km. The essentials of its information were obtained by *Muller and Sjogren* [1968]. The lack of far-side tracking makes it difficult to fit orbital elements to more than one revolution of data. Hence major features in the representation of the earth-side field tend to have spurious features of opposite sign north and south of them. This defect occurs regardless of whether this representation is in terms of accelerations or of surface masses. The defect is relieved within

TABLE 1. Spherical Harmonic Coefficients of the Lunar Gravitational Field [From *Sjogren*, 1971]

Coefficient	Unnormalized* 10^{-6}	Normalized† 10^{0}
C_{20}	−204.8	−91.6
C_{22}	22.1	34.2
C_{30}	− 10.7	− 4.0
C_{31}	31.6	29.3
S_{31}	4.3	4.0
C_{32}	5.5	16.1
S_{32}	2.7	7.9
C_{33}	1.8	12.9
S_{33}	− 0.99	− 7.1

*Neuman or Ferrers harmonics:

$$1/4\pi \int_{\text{unit sphere}} Y_{lm}^2 \, d\sigma = (l+m)!/[(l-m)!(2l+1)(2-\delta_{om})]$$

†Neuman or Ferrers harmonics: $1/4\pi \int_{\text{unit sphere}} Y_{lm}^2 d\sigma = 1$

latitudes ±21° by coverage from lower-inclination orbiters, as used in the surface mass solutions of *Gottlieb* [1970] and *Wong et al.* [1971].

The low altitude of some Apollo CSM's and subsatellites has enabled pushing the resolution as low as 30 km for a limited part of the moon's face. The most extensive such coverage is by the Apollo 16 subsatellite: essentially a strip from 50°W to 40°E between the equator and 10°N, in which the Apollo 16 subsatellite was below 30-km altitude. The Apollo 15 satellite was between 40 and 60 km over a strip between 20° and 30°S [*Muller et al.*, 1974; *Sjogren et al.*, 1974*a*; *Sjogren and Wollenhaupt*, 1973*b*]. More limited low-altitude coverages correspond to the CSM ground tracks: strips about 80 km in width and 4000 km in length [*Sjogren et al.*, 1972*a*; *Sjogren et al.*, 1974*b*, *c*]. Higher-altitude coverages, 60 to 180 km, were obtained by Apollo 15 over the zone 20°S to 30°N for most of the front face [*Sjogren et al.*, 1974*a*].

The failure to fit orbits accurately for more than one revolution at a time indicates that there is information about the far side in the data. However, solutions for spherical harmonic coefficients to eighth degree by *Liu and Laing* [1971] and to thirteenth degree by *Michael and Blackshear* [1972] did not succeed in obtaining plausible representations for the far side. A significant improvement has recently been obtained by *Ferrari* [1975]. He fitted a fifteenth-degree solution to Kepler elements for the Apollo 15 and 16 subsatellites plus Lunar Orbiter 5 and obtained a reasonable far-side field by using a priori sigmas. Further application of modern inversion theory seems appropriate.

The leading features observed in the gravity field are shown in Figure 1 [*Sjogren*, 1973] and Table 2 (of variable reliability). Most noticeable, of course, are the mascons. Seven of these positive features are larger (in the sense of anomaly X area) than the largest negative features (other than the ring around the Orientale mascon). Discrimination of the depth of the mass excesses came with the low-altitude Apollo passes. While the traditional ambiguity persists that an external gravity field can be exactly satisfied by a mass distribution at any level, as shown in Figure 2, the 'shoulders' on the gravity profile require that there be density variations at a shallow depth. The same analyses obtain central surface densities as much as 800 kg/cm², equivalent to about 2.5 km of basalt [*Muller et al.*, 1974; *Sjogren and Wollenhaupt*, 1973*b*].

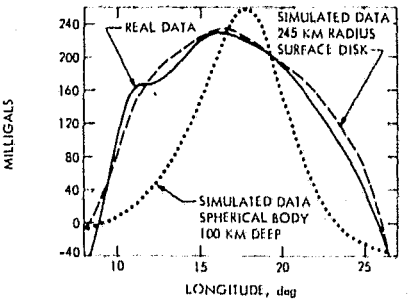

Fig. 2. Gravity profile for a low-altitude pass over Mare Serenitatis [*Sjogren et al.*, 1972*c*].

A unique feature is the Orientale 'bull's eye' complex of a central positive, a negative ring, and a positive apron, successively smaller in absolute magnitude and larger in area. Also distinct is the large mildly positive area over the southern highlands.

Other marked features of the gravity field are less than 300 km in extent and 150 mgal in magnitude. The most important characteristic of the lunar gravity field is, in fact, its mildness for longer wavelengths. From the most detailed data, the 1.5 × 10^6 km² covered by the 30-km-altitude Apollo 16 subsatellite passes, the rms mean anomaly for 300-km squares is only ±26 mgal; for 150-km squares it is ±33 mgal. (In calculating these values,

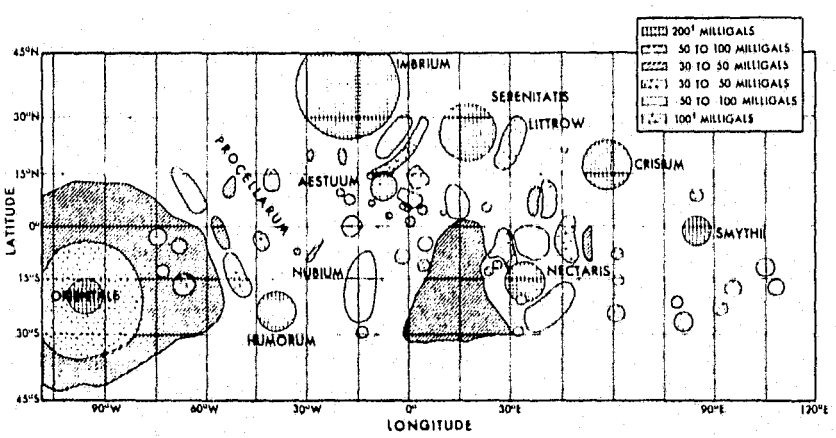

Fig. 1. Principal features of the gravity field [*Sjogren*, 1973].

TABLE 2. Leading Features of the Lunar Gravity Field Based on Figure 1

Name	Latitude	Longitude	Mean Anomaly, Mgal	Area, 10^3 km^2	Mass Excess 10^{16} kg*
Imbrium	40°N	15°W	+200	400	+200
Serenitatis	25°N	20°E	+200	200	+100
Crisium	15°N	60°E	+200	150	+ 70
Smythii	5°S	85°E	+230	90	+ 50
Humorum	25°S	40°W	+120	110	+ 30
Nectaris	20°S	35°E	+120	130	+ 40
Aestuum	10°N	10°W	+200	60	+ 30
Orientale Mascon	20°S	100°W	+200	50	+ 25
Orientale Ring	15°S	90°W	−150	600	−200
Orientale Apron	10°S	80°W	+ 40	1100	+120
Littrow Trough	20°N	30°E	−150	60	− 20
Southern Highlands	20°S	15°E	+ 40	500	+ 50
Nubium	20°S	15°W	− 80	150	− 30
Southeast of Nectaris	25°S	40°E	− 80	110	− 20
North of Nectaris	5°S	35°E	− 80	70	− 15

*Approximately 0.14×10^{-6} lunar mass.

allowance has been made for (1) the altitude of the spacecraft, (2) the difference between line-of-sight and vertical accelerations, (3) the absorption of low-degree harmonics in the reference orbit, and (4) error of estimation of 150-km-square means). These figures are less than 1.5 times the rms terrestrial values for the same areas—despite mean gravity, and hence stress implications, being only one-sixth as much. It is possible that the Apollo 16 strip is unrepresentatively mild. A higher figure compared with the earth is obtained from the long-wavelength features of the gravity field. From the data in Table 1, the rms normalized coefficient of degree l is about $\pm 1.5 \times 10^{-4}/l^2$. Extending this rule to degree 5 gives a rms anomaly for 1100-km squares of ±27 mgal compared with ±14 mgal for terrestrial 1100-km squares. (A power spectrum estimate by *Wong et al.* [1971] gives ±38 mgal for 1100-km squares and ±93 mgal for 300-km squares but is severely distorted by use of *Liu and Liang*'s [1971] harmonics).

Dynamics

The variations of the lunar gravity field interact with another observable, the wobbles in the moon's rotation known as the physical librations. Interest in the librations has been stimulated in recent years through the great improvement in the accuracy with which they are measured by laser ranging [*Bender et al.*, 1973] and interferometry (VLBI) [*Counselman et al.*, 1973*a*, *b*] from the earth.

For a year or two the librations were the major source of error in the laser ranging from the earth to the moon. This was partly because of inaccuracy in the harmonic coefficients and partly because of inadequate computation of their effects and planetary effects on the librations. Linear estimates of the third and fourth harmonic effects obtained terms up to 10" in amplitude [*Eckhardt*, 1973; *Kaula and Baxa*, 1973]. Since then, Eckhardt has extended his iterative technique [*Eckhardt*, 1970] to include the third and fourth harmonics and planetary effects to a precision of 0.01", and Williams and Slade numerically integrated the librations including the same effects [*Williams et al.*, 1973]. This work has been a long and tedious task to make sure that all planetary perturbations, orientation effects, etc., are included.

The aforementioned integrations assume a rigid moon. *Peale* [1973] has investigated the implications of elasticity and finds the effects to be no more than about 0.01": the moon is rather small and tight, and the libration periods are far from the free-oscillation period. However, possibly other frequencies should be examined (J.G. Williams, personal communication, 1974). With any plausible dissipation factor $1/Q$, the meteorite flux is probably too small to excite any perceptible free librations, but this area is also not completely closed to speculation (S.J. Peale, personal communication, 1974).

The principal parameters determined by observation of the librations are the moment-of-inertia ratios β and γ:

$$\beta = (C - A)/I: 631.1 \pm 0.4 \times 10^{-6}$$
$$\gamma = (B - A)/I: 226.8 \pm 1.0 \times 10^{-6}$$

[*Williams et al.*, 1974], where I is the mean moment of inertia and C, A, and B are, respectively, the moments about the principal axes near the rotation axis, the mean direction of the earth, and the direction orthogonal to these two. Combined with the second-degree harmonics from Table 1,

$$J_{20} = [C - (A + B)/2]/MR^2 : 204.8 \pm 3.0 \times 10^{-6}$$
$$J_{22} = (B - A)/4MR^2 : 22.1 \pm 0.5 \times 10^{-6}$$

a redundant set of data is obtained that yields 0.3951 ± 0.0045 for I/MR^2 [*Kaula et al.*, 1974]. Nearly all the uncertainty in I/MR^2 comes from the gravity field determination.

An odd finding from the recent work on physical libration theory is that, because of the third harmonics in the gravity field, the principal axis with moment of inertia A is shifted about 200" east and 60" south of the mean earth direction [*Williams et al.*, 1973]. The essence of the situation in longitude is sketched in Figure 3: the S_{33} harmonic exercises a torque on the earth slightly offsetting the torque by the C_{22} harmonic. The consequence of this offset for orientation of the moon is that the mean direction of the earth will be, under foreseeable circumstances, a much more accurately known direction than the principal axis of inertia. This condition exists because the offset is not directly observed but is calculated from observations of the moon's gravity harmonics through orbiter perturbations. For a long time to come these harmonics will not be known to the requisite 3- or 4-figure accuracy.

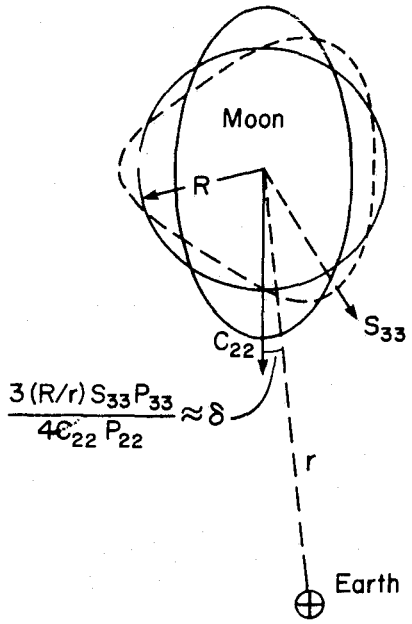

Fig. 3. Offsetting torques on the moon's gravity field by the earth.

Geometry

It is evident that the accurate laser ranging to retroflectors at the Apollo 11, 12, and 15 sites and VLBI to Alsep transmitters at the Apollo 12, 14, 15, 16, and 17 sites are the appropriate means to obtain the orientation of the moon with respect to external references: the earth, sun, and stars [*Bender et al.*, 1973; *Counselman et al.*, 1973*a*, *b*; *Fajemirokun*, 1971]. The same observing system affords a geometric control system of high accuracy referred to the moon's center of mass. Unfortunately, it is rather sparse. A purely photogrammetric control system was proposed at one time, but a rather complete global network is needed for accurate results [*Brown*, 1968]. The actual Apollo coverage is limited to about 20% of the surface, between longitudes 60°W, 155°E, and latitudes 32°N, 28°S [*Light*, 1972*a*, *b*; *Helmering*, 1972].

Hence the essential control of the selenodetic survey comes from the orbits of the Apollo spacecraft, determined by tracking from the earth. This orbital reference gives an overall tie to the center of mass of the moon—thus serving as a substitute for a selenoid—and gives the relative location of successive camera stations to a greater accuracy than the photogrammetry: a few meters standard deviation. However, the relative locations of adjacent orbits are determined more poorly, with errors of the order of some tens of meters.

The main cause for the imperfection in the control system defined by the Apollo orbits is the imperfect knowledge of the gravity field. The resulting errors have a long-wave systematic character that shows up as warps with respect to the photogrammetry. In the short run, the ephemerides provided by NASA have rather severe warps, consequences of the relatively simple operational orbit determination procedures, erroneous models of the gravity field, and spacecraft oscillations due to astronaut actions. In the long run, a more ideal system should be attained by a process of iteration and mutual adjustment between the orbital dynamics and the photogrammetry, taking advantage of the strengths of each.

The heart of the Apollo photogrammetric system is the mapping camera of 76-mm focal length and 74° × 74° angular coverage. Supplementary components are the stellar camera of 76-mm focal length and 24° × 18° angular coverage; the laser altimeter of ±2-m accuracy; and timing of ±0.001-s accuracy. The control network being established from this sytem by the DMA Aerospace and Topographic Centers has one point for each 900 km² of ±30-m horizontal location accuracy [*Light*, 1972*a*, *b*; *Doyle*, 1972; *Helmering*, 1973].

The principal product of the mapping camera system is a series of 1 : 250,000 orthophotomaps. The system also supports a panoramic camera of 610-mm focal length and 11° × 108° angular coverage, designed to cover most of the same area at poorer geometric accuracy but better resolution (±2 m). The panoramic photography is used for 1 : 50,000 and 1 : 10,000 maps of areas of special interest.

The topographic maps are principally of value for yielding quantitative information about such characteristics as the slopes of a variety of geologic features. For the more global variations in elevation the laser altimeter furnishes the most direct estimate. The altimeter was programmed to operate without, as well as with, the mapping camera, making measurements at intervals of 33 km. About 6000 points were obtained along the Apollo 15, 16, and 17 ground tracks. The principal constraint on the accuracy of these elevations is the orbit determination. The absolute errors may be as much as 400 m. However, for relative elevations between successive points the uncertainty is less than 10 m. Relative elevations between adjacent tracks have errors of less than 100 m, since

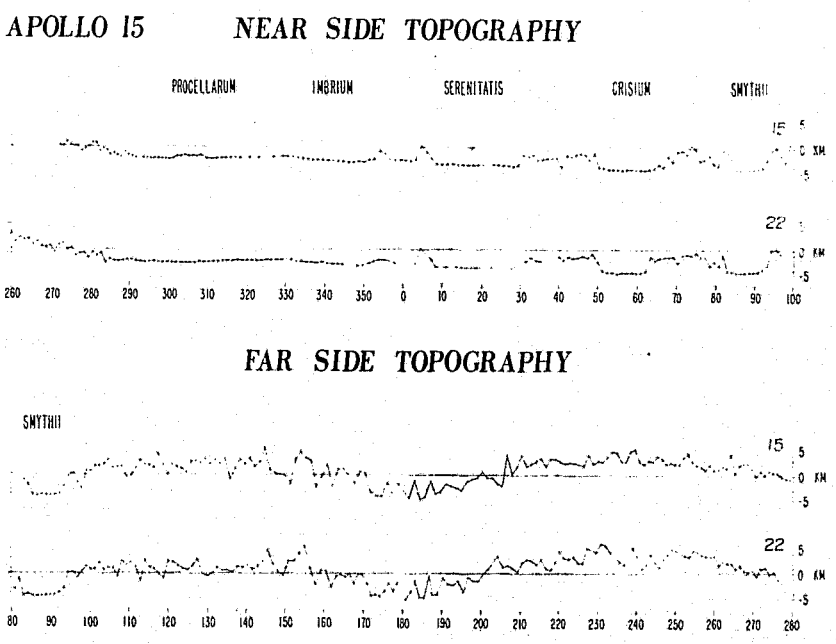

Fig. 4 Topographic elevations measured by the Apollo 15 laser altimeter [*Kaula et al.*, 1973].

the orbits are similarly affected by the main error source, the gravity field model.

The broad variations of topography measured by the altimeter (Figure 4) are most obviously analyzed in terms of harmonic components. The mean radius is estimated as 1737.7 km, and the offset of center of figure from center of mass (CFCM) as −2.5 km in the direction 24°E. The amplitude of the second harmonic is about 700 m for Apollo 15's ground track, with the major axis at longitude 90°; it is 1200 m for Apollo 16, with axis longitude 50° [*Kaula et al.*, 1973]. Perhaps more meaningful are variations of elevation with terrain type, as shown in Table 3 [*Kaula et al.*, 1974]. The ringed maria also show a distinct inverse correlation of depth with width, as is evidenced by Serenitatis, Crisium, and Smythii in Figure 4.

Additional topographic information is anticipated from the Apollo 17 radar sounder [*Phillips et al.*, 1973*a*, *b*; *Brown et al.*, 1974].

Tectonic Implications

The major variations in structure that give rise to the lunar gravity and shape are, as for any planetary body, caused mainly by circumstances of origin and the subsequent thermal evolution. Infalls subsequent to origin, such as the Imbrium and Orientale events, have strong regional effects and influence the locus of volcanism but do not greatly affect the moment of inertia, the broad variations of the gravity field, etc.

Origin is a much more important influence relative to evolution for the moon than for a larger body such as the earth. The outer parts of the moon were heated sufficiently at formation to differentiate a thick crust. The 2.5-km CFCM offset is

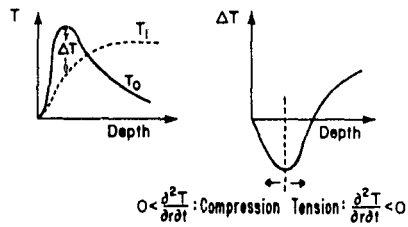

Fig. 5. Principal tectonic effect of lunar thermal evolution.

largely a consequence of the convection associated with this separation. Since origin, the global evolution has been essentially that sketched in Figure 5: a cooling off of the outer parts together with a heating up of the inner parts. These changes would have contradictory effects, since the shallow cooling off would put the outer shell in compression, whereas the deeper heating up would put it in tension. Hence the lunar tectonic regime should show compressive characteristics on a regional scale but possibly tensile characteristics on a global scale.

The contrast between the relatively mild gravity field (Figure 1) and the marked variations in elevations (Table 3) indicates that isostatic compensation prevails. If it is assumed that this compensation is mainly by variations in thickness of a light crust (as it is on earth), and if the uniform seismic velocity 20—60 km deep under eastern Procellarum is taken to denote anorthositic gabbro [*Toksoz et al.*, 1974], then an extrapolation can be made to obtain the variations of crustal thickness with terrain type, and thence a mean thickness of about 60 km, as shown in Figure 6 [*Kaula et al.*, 1974]. This thickness is somewhat more than the absolute minimum necessary to account for the CFCM offset (40 km) [*Kaula et al.*, 1972], as it should be.

The effect of this mean crust necessary to account for isostatic compensation of the topography is to reduce the moment-of-inertia ratio I/MR^2 by 0.0032 from uniform, 0.4. The probable value I/MR^2 of 0.3950 thus allows either a small iron core of 260-km radius, as has been recently inferred from seismology [*Nakamura et al.*, 1974], or a moderate gradient from magnesian to iron silicates in the mantle [*Kaula et al.*, 1974; *Toksoz et al.*, 1974].

Radioactive dating constraints indicate that lunar origin took place about 4.6×10^9 years ago, and that crustal formation was complete about 4.45×10^9 years ago, but that widespread brecciation, shocking, metamorphism, etc., occurred at a 'cataclysm' about 4.0×10^9 years ago [*Tera et al.*, 1974]. This cataclysm was presumably the formation of the great basins, which constituted the penultimate stage of major events shaping the lunar surface [*Howard et al.*, 1974]. The lateness of this cataclysm, 700 m.y. after origin, makes it probable that

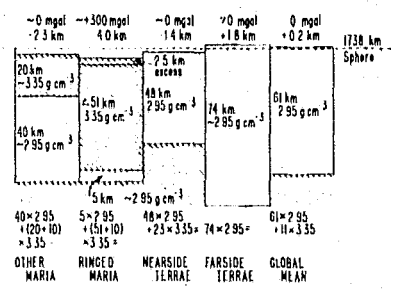

Fig. 6. Mean crustal thicknesses inferred from altimetry and gravimetry [*Kaula et al.*, 1974].

the impacting bodies were from outside the earth-moon system and hence were of high velocity (more than 10 km/sec) [*Wetherill*, 1975]. Such high-energy impacts would have removed considerably more mass than they added. Since the lithosphere would have already attained a considerable thickness—at least 200 km—more than 500 m.y. after crustal formation, the isostatic recovery would be incomplete, and the basins would be still marked by negative gravity anomalies.

But, except for the Orientale ring, we do not have a clear-cut example of a large negative gravity anomaly associated with a basin. Instead, there are the notorious mascons. The moon is like the earth and Mars

TABLE 3. Mean Elevations by Terrain Type

Terrain Type	Portion of Global Surface	Apollo 15 Track, km	Apollo 16 Track, km	Apollo 17 Track, km	Weighted Mean, km
Ancient Cratered	0.57	+1.9	+2.1	+0.9	+1.8
Imbrian and Nectarian Basins	0.23	−1.7	−1.2	−1.3	−1.4
Ringed Maria	0.06	−4.1	−4.1	−3.7	−4.0
Other Maria	0.14	−2.0	−2.5	−2.1	−2.3

in that the most prominent association of the gravity field with geology is a correlation of positive anomalies with the most recent volcanism. The moon differs from the earth and Mars in that 'most recent' is more than 3×10^9 years ago, the magnitudes of the anomalies are much smaller in stress implication, and the associated topographic features are depressions rather than elevations. The fundamental cause of both the volcanism and the mascons is the thermal evolution sketched in Figure 5. Continued internal heating led to melting. Because rock decreases about 10% in density upon melting, the magma would have exerted great stress, enough for some of it to force its way to the surface before cooling.

The greatest amount would have come up where the lithosphere was structurally weakest, the deepest basins: the ringed maria. Probably the bulk of the magma solidified before it reached the surface. The extraordinary length of some sinuous rills indicates that the magma had a much lower viscosity, and hence more basic composition, than is characteristic of terrestrial lava flows. The absence of large maria on the far side suggests that the greater crustal thickness was too much for the magma to overcome. This explanation further implies that the great far-side basin around 30°S, and 180° is a negative anomaly, supported by lithospheric strength.

Aside from internal heating being a fundamental cause, there is much left to be explained about the length scale, time history, etc., of mascon formation and the associated volcanism. Most remarkable is the lack of distinct negative rings around the mascons (other than Orientale). The simplest local hypotheses for mascon formation [e.g., *Wise and Yates*, 1970] shift the mass a minimum distance, out from under the surrounding higher topography; such shifts would result in negative rings. The magma constituting the mascon excess apparently traveled a long way, either vertically or horizontally. The evidence from perturbations of Apollo 15 and subsequent orbiters (as in Figure 2) that the excess is a shallow plate [*Phillips et al.*, 1972] associates it with the most recent flow, which occurred when the lithosphere had become most capable of sustaining loads. This still leaves as a question the history of flows from basin formation to the final mare surface flows. The evidence of 'shadow' craters, for example, indicates that there was a long period of dwindling activity. Subsidiary is the thermal effect of transfer of surface matter from the basin to the surroundings [*Arkani-Hamed*, 1973].

The $1/l^2$ rule of variation with wavelength of normalized spherical harmonic gravity potential coefficients of the earth is most likely the consequence of (1) a white spectrum in the generating density variations plus (2) the density variations occurring predominantly near the surface. The white spectrum in turn suggests that the characteristic wavelengths of the phenomena causing the spectrum are shorter than the wavelength of the highest wave number to which the rule applies. In the case of the above-described apparent drop-off in the lunar coefficients between wave numbers 3 and 18, at least two explanations are possible: either the characteristic wavelength is intermediate between these two wave numbers, or the predominant depth for the density variations is considerable. Consistent with the latter hypothesis is the low correlation of the long wavelength gravity field with surface features.

Conclusions

The simpler history of the moon makes it an easier planet to interpret than the earth. However, there are ambiguities arising from insufficiency of data as well as from lack of ingenuity in explanation. It is particularly irksome that there is a strong correlation of terrain type with the direction of the earth, so that the most common terrain type, the ancient heavily cratered terrae, is virtually unsampled. The unmanned lunar satellite proposed for late in the decade should remedy this deficiency. Meanwhile, more about the moon's structure and history can be winnowed from data already at hand.

Acknowledgements

This work is partially supported by NASA grants NGL 05-007-002, NGL 05-007-283, and NAS 9-12757. Institute of Geophysics and Planetary Physics Publication 1392.

Bibliography

Determination

Bender, P.L., and 12 others, The Lunar laser ranging experiment, *Science, 182*, 229–238, 1973.

Brown, D.C., A unified lunar control network, *Photogramm. Eng., 34*, 1272–1292, 1968.

Brown, W.E., Jr., and 13 others, Elevation profiles of the moon, *Geochim. Cosmochim. Acta, 38, Suppl. 5*, 3037–3048, 1974.

Counselman, C.C., H.F. Hinteregger, and I.I. Shapiro, Astronomical application of differential interferometry, *Science, 178*, 607–608, 1972.

Counselman, C.C., H.F. Hinteregger, R.W. King, and I.I. Shapiro, Precision selenodesy via differential interferometry, *Science, 181*, 772–774, 1973*a*.

Counselman, C.C., H.F. Hinteregger, R.W. King, and I.I. Shapiro, Lunar baselines and libration from differential VLBI observations of Alseps, *Moon, 8*, 484–489, 1973*b*.

DeBra, D.B., J.C. Harrison, and P.M. Muller, A proposed lunar orbiting gravity gradiometer experiment, *Moon, 4*, 103–112, 1972.

Doyle, F.J., Photographic systems for Apollo, *Photogramm. Eng., 36*, 1039–1044, 1970.

Doyle, F.J., Photogrammetric analysis of Apollo 15 records, *NASA Spec. Publ. SP-289*, 25:27–36, 1972.

Eckhardt, D.H., Lunar libration tables, *Moon, 1*, 264–275, 1970.

Eckhardt, D.H., Physical librations due to the third and fourth degree harmonics of the lunar gravity potential, *Moon, 6*, 127–134, 1973.

Eckhardt, D.H., and K. Dieter, A nonlinear analysis of the moon's physical libration in longitude, *Moon, 2*, 309–319, 1971.

Fajemirokun, F.A., Application of laser ranging and VLBI observations for selenodetic control, *Dept. of Geod. Sci. Rep. 157*, 230 pp., Ohio State Univ., Columbus, 1971.

Fajemirokun, F.A., F.D. Hotter, and H.B. Papo, Selenodetic computer program library, *Dept. of Geod. Sci. Rep. 197*, 196 pp., Ohio State Univ., Columbus, 1973.

Ferrari, A.J., An empirically derived lunar gravity field, *Moon, 5*, 390–410, 1972.

Ferrari, A.J., Lunar gravity derived from long-period satellite motion—a pro-

posed method, *Celestial Mech., 7*, 46–76, 1973.

Ferrari, A.J., and W.G. Heffron, Effects of physical librations of the moon on the orbital elements of a lunar satellite, *Celestial Mech., 8*, 111–120, 1973.

Ferrari, A.J., Lunar gravity, The first far-side [illegible] submitted to *Science*, 1975.

Gavrilov, I.V., On the standardization of the selenodetic frame of reference, *Moon, 8*, 155–514, 1973.

Gottlieb, P., Estimation of local lunar gravity features, *Radio Sci., 5*, 301–312, 1970.

Helmering, R.J., Selenodetic control derived from Apollo metric photography, *Moon, 8*, 450–460, 1973.

Kaula, W.M., The gravitational field of the moon, *Science, 166*, 1581–1588, 1969.

Kaula, W.M., Selenodesy and planetary geodesy, *Eos Trans. AGU, 52*, IUGG 1–4, 1971.

Kaula, W.M., and P.A. Baxa, The physical librations of the moon, including higher harmonic effects, *Moon, 8*, 287–307, 1973.

Kaula, W.M., G. Schubert, R.E. Lingenfelter, W.L. Sjogren, and W.R. Wollenhaupt, Analysis and interpretation of lunar laser altimetry, *Geochim. Cosmochim. Acta, 36, Suppl. 3*, 2189–2204, 1972.

Kaula, W.M., G. Schubert, R.E. Lingenfelter, W.L. Sjogren, and W.R. Wollenhaupt, Lunar topography from Apollo 15 and 16 laser altimetry, *Geochim. Cosmochim. Acta, 37, Suppl. 4*, 2811–2819, 1973.

Kaula, W.M., G. Schubert, R.E. Lingenfelter, W.L. Sjogren, and W.R. Wollenhaupt, Apollo laser altimetry and inferences as to lunar structure, *Geochim. Cosmochim. Acta 38, Suppl. 5*, 3049–3058, 1974.

King, R.W., C.C. Counselman, H.F. Hinteregger, and I.I. Shapiro, Study of lunar librations using differential very-long-baseline observations of Alseps, *Proc. Soc. Eng. Sci. Meet.*, Durham, N.C., in press, 1974.

Light, D.L., Altimeter observations as orbital constraints, *Photogramm. Eng., 38*, 339–346, 1972*a*.

Light, D.L., Photo geodesy from Apollo, *Photogramm. Eng., 38*, 574–587, 1972*b*.

Liu, A.S., and P.A. Laing, Lunar gravity analysis from long-term effects, *Science, 173*, 1017–1020, 1971.

McLean, R., Establishment of selenodetic control through measurements on the lunar surface, *Dept. of Geod. Sci. Rep. 143*, 83 pp., Ohio State Univ., Columbus, 1970.

Michael, W.H., Jr., and W.T. Blackshear, Recent results on the mass, gravitational field, and moments-of-inertial of the moon, *Moon, 3*, 388–402, 1972.

Moutsoulas, M.D., Rotation of the moon and lunar coordinate systems, *Moon, 5*, 302–331, 1972.

Moutsoulas, M.D., Selenographic control, *Moon, 8*, 461–468, 1973.

Mueller, I.I. (Ed.), A general review and discussion on geodetic control on the moon, *Dept. of Geod. Sci. Rep. 127*, 131 pp., Ohio State Univ., Columbus, 1969.

Mueller, I.I. (Ed.), Investigations related to geodetic control of the moon, *Dept. of Geod. Sci. Rep. 198*, 97 pp., Ohio State Univ., Columbus, 1973.

Mulholland, J.D., Lunar dynamics and observational coordinate systems, An interpretive review, *Moon, 8*, 548–556, 1973.

Mulholland, J.D., and E.C. Silverberg, Measurement of physical librations using laser retroreflectors, *Moon, 4*, 155–159, 1972.

Muller, P.M., and W.L. Sjogren, Mascons: Lunar mass concentrations, *Science, 161*, 680–684, 1968.

Muller, P.M., W.L. Sjogren, and W.R. Wollenhaupt, Lunar gravity: Apollo 15 Doppler radio tracking, *Moon, 10*, 195–205, 1974.

Papo, H.B., Optimum selenodetic control, *Dept. of Geod. Sci. Rep. 156*, 260 pp., Ohio State Univ., Columbus, 1971.

Papo, H.B., Orientation of the moon by numerical integration, *Moon, 8*, 539–545, 1973.

Peale, S.J., Some effects of elasticity on lunar rotation, *Moon, 8*, 515–531, 1973.

Peterson, C.G., Compilation of lunar pan photos, *Photogramm. Eng., 39*, 73–79, 1973.

Phillips, R.J., Techniques in Doppler gravity inversion, *J. Geophys. Res., 79*, 2027–2036, 1974.

Phillips, R.J., J.E. Conel, E.A. Abbott, W.L. Sjogren, and J.B. Morton, Mascons: Progress toward a unique solution for mass distribution, *J. Geophys. Res., 77*, 7106–7114, 1972.

Phillips, R.J., and 14 others, Apollo lunar sounder experiment, *NASA Spec. Publ. SP-330*, 22:1–26, 1973*a*.

Phillips, R.J., and 13 others, The Apollo 17 lunar sounder, *Geochim. Cosmochim. Acta, 37, Suppl. 4*, 2821–2831, 1973*b*.

Riotte, W., An investigation to improve selenodetic control on the lunar limb utilizing Apollo 15 trans-earth photography, *Dept. of Geod. Sci. Rep. 176*, 108 pp., Ohio State Univ., Columbus, 1972.

Roberson, F.I., and W.M. Kaula, Apollo 15 laser altimeter, *Apollo 15 Preliminary Science Report NASA Spec. Publ. SP-289*, 25:48–50, 1972.

Rodinov, B.N., and 16 others, New data on the moon's figure and relief based on results from the reduction of Zond-6 photographs, *Cosmic Res., 4*, 410–417, 1971.

Sjogren, W.L., Lunar gravity estimate: Independent confirmation, *J. Geophys. Res., 76*, 7021–7026, 1971.

Sjogren, W.L., Lunar gravity anomalies (map), *Geochim. Cosmochim. Acta, 37, Suppl. 4, 1*, iii–iv, 1973.

Sjogren, W.L., and W.R. Wollenhaupt, Lunar shape via the Apollo laser altimeter, *Science, 179*, 275–278, 1973*a*.

Sjogren, W.L., and W.R. Wollenhaupt, Gravity: Mare Humorum, *Moon, 8*, 25–32, 1973*b*.

Sjogren, W.L., P. Gottlieb, P.M. Muller, and W.R. Wollenhaupt, Lunar gravity via Apollo 14 Doppler radio tracking, *Science, 175*, 165–168, 1972*a*.

Sjogren, W.L., P. Gottlieb, P.M. Muller, and W.R. Wollenhaupt, S-band transponder experiment, *Apollo 15 Preliminary Science Report, NASA Spec. Publ. SP-289*, 22:1–6, 1972*b*.

Sjogren, W.L., P.M. Muller, and W.R. Wollenhaupt, Apollo 15 gravity analysis from the S-band transponder experiment, *Moon, 4*, 411–418, 1972*c*.

Sjogren, W.L., P.M. Muller, and W.R. Wollenhaupt, S-band transponder experiment, *NASA Spec. Publ. SP-315*, 24:1–7, 1972*d*.

Sjogren, W.L., W.R. Wollenhaupt, and R.N. Wimberly, S-band transponder experiment, *NASA Spec. Publ. SP-330*, 14:1–4, 1973.

Sjogren, W.L., W.R. Wollenhaupt, and R.N. Wimberly, Lunar gravity via the Apollo 15 and 16 subsatellite, *Moon, 9*, 115–129, 1974*a*.

Sjogren, W.L., R.N. Wimberly, and W.R. Wollenhaupt, Lunar gravity: Apollo 16, *Moon, 11*, 35–40, 1974*b*.

Sjogren, W.L., R.N. Wimberly, and W.R. Wollenhaupt, Lunar gravity: Apollo 17, *Moon, 11*, 41–52, 1974*c*.

Sprague, M.D., An investigation to improve selenodetic control on the lunar far side utilizing Apollo mission trans-earth trajectory photography, *Dept. of Geod. Sci. Rep. 155*, 192 pp., Ohio State Univ., Columbus, 1971.

Sweet, H.J., An investigation to improve selenodetic control through surface and orbiter lunar photography, *Dept. of Geod. Sci. Rep. 144*, 54 pp., Ohio State Univ., Columbus, 1970.

Talwani, M., G. Thompson, B. Dent, H.-G. Kahle, and S. Buch, Traverse gravimeter experiment, *NASA Spec. Publ. SP-330*, 13:1–13, 1973.

Van Flandern, T.C., Some notes on the use of the Watts limb-correction charts, *Astron. J., 75*, 744–746, 1970.

Williams, J.G., M.A. Slade, D.H. Eckhardt, and W.M. Kaula, Lunar physical librations and laser ranging, *Moon, 8*, 469–483, 1973.

Williams, J.G., W.S. Sinclair, M.A. Slade, P.L. Bender, J.P. Hauser, J.D. Mulholland, and P.J. Shelus, Lunar moment-of-inertia constraints from lunar laser ranging (abstract), in *Lunar Science V*, p. 845, Lunar Science Institute, Houston, Tex., 1974.

Wollenhaupt, W.R., and W.L. Sjogren, Comments on the figure of the moon based on preliminary results from laser altimetry, *Moon, 4*, 337–347, 1972*a*.

Wollenhaupt, W.R., and W.L. Sjogren, Apollo 16 laser altimeter, *Apollo 16 Prelim. Sci. Rep., NASA Spec. Publ. SP-315, 30*, 1–5, 1972*b*.

Wollenhaupt, W.R., R.K. Osburn, and

G.A. Ransford, Comments on the figure of the moon from Apollo landmark tracking, *Moon, 5*, 149–157, 1972.

Wollenhaupt, W.R., W.L. Sjogren, R.E. Lingenfelter, G.Schubert, and W.M. Kaula, Apollo 17 Laser Altimeter, *Apollo 17 Prelim. Sci. Rep., NASA Spec. Publ. SP-315, 33*, 41–43, 1974.

Wong, L., G. Buechler, W. Downs, W. Sjogren, P. Muller, and P. Gottlieb, A surface-layer representation of lunar gravitational field, *J. Geophys. Res., 76*, 6220–6236, 1971.

Interpretation

Arkani-Hamed, J., On the formation of lunar mascons, *Geochim. Cosmochim. Acta, 37, Suppl. 4*, 2673–2684, 1973.

Booker, J.R., and R.L. Kovach, Mascons and the moon's gravity field, *Phys. Earth Planet. Interiors, 4*, 180–184, 1971.

Hartmann, W.K., and C.A. Wood, Moon: Origin and evolution of multi-ring basins, *Moon, 3*, 3–78, 1971.

Head, J.W., Some geologic observations concerning lunar geophysical models, in *Proc. Sov. Amer. Conf. Cosmochim. of Moon and Planets*, National Aeronautics and Space Administration, Washington, D.C., in press, 1975.

Howard, K.A., D.E. Wilhelms, and D.H. Scott, Lunar basin formation and highland stratigraphy, *Rev. Geophys. Space Phys., 12*, 309–327, 1974.

Hulme, G., Mascons and isostasy, *Nature, 238*, 448–450, 1972.

Kaula, W.M., Interpretation of the lunar gravitational field, *Phys. Earth Planet. Interiors, 4*, 185–192, 1971.

Lammlein, D.R., G.V. Latham, J. Dorman, Y. Nakamura, and M. Ewing, Lunar seismicity, structure, and tectonics, *Rev. Geophys. Space Phys. 12*, 1–21, 1974.

Lingenfelter, R.E., and G. Schubert, Evidence convection in planetary interiors from first-order topography, *Moon, 7*, 172–180, 1973.

McGetchin, T.R., M. Settle, and J.W. Head, Radial thickness variation in impact crater ejecta: Implications for lunar basin deposits, *Earth Planet. Sci. Lett., 20*, 226–236, 1973.

Nakamura, Y., G. Latham, D. Lammlein, M. Ewing, F. Duennebier, and J. Dorman, Deep lunar interior inferred from recent seismic data, *Geophys. Res. Lett., 1*, 137–140, 1974.

Phillips, R.J., and R.S. Saunders, Interpretation of gravity anomalies in the irregular maria (abstract), in *Lunar Science V*, pp. 596–597, Lunar Science Institute, Houston, Tex., 1974.

Ransford, G.A., and W.L. Sjogren, Moon model—An offset core, *Nature 238*, 260–262, 1972.

Schaber, G.C., Lava flows in Mare Imbrium: Geologic evaluation from Apollo orbital photography (abstract), in *Lunar Science IV*, pp. 653–655, Lunar Science Institute, Houston, Tex., 1973.

Scott, D.H., The geologic significance of some lunar gravity anomalies, *Geochim. Cosmochim. Acta, 38, Suppl. 5*, 3025–3036, 1974.

Short, N.M., and M.L. Forman, Thickness of impact crater ejecta on the lunar surface, *Mod. Geol., 3*, 69, 1972.

Solomon, S.C., Density within the moon and implications for lunar composition, *Moon, 9*, 147–166, 1974.

Tera, F., D.A. Papanastassiou, and G.J. Wasserburg, Isotopic evidence for a terminal lunar cataclysm, *Earth Planet. Sci. Lett., 22*, 1–21, 1974.

Toksoz, M.N., Geophysical data and the interior of the moon, *Annu. Rev. Earth Planet. Sci., 2*, 151–177, 1974.

Toksoz, M.N., A.M. Dainty, S.C. Solomon, and K.R. Anderson, Velocity structure and evolution of the moon, *Geochim. Cosmochim. Acta, 37, Suppl. 4*, 2529–2547, 1973.

Toksoz, M.N., A.M. Dainty, S.C. Solomon, and K.R. Anderson, Structure of the moon, *Rev. Geophys. Space Phys., 12*, 539–567, 1974.

Wetherill, G.W., Pre-mare cratering and early solar system history, in *Proc. Sov. Amer. Conf. Cosmochim. of Moon and Planets*, in press, 1975.

Wilhelms, D.E., and J.F. McCauley, Geologic map of the near side of the moon, *U.S. Geol. Surv. Misc. Geol. Inv. Map 1-703*, 1971.

Wise, D.U., and M.T. Yates, Mascons as structural relief on a lunar 'Moho,' *J. Geophys. Res., 75*, 261–268, 1970.

Wood, J.A., Bombardment as a cause of the lunar asymmetry, *Moon, 8*, 73–103, 1973.

OMIT

AGU

Lunar Dynamics and Selenodesy

REPORT OF THE EIGHTH GEOP RESEARCH CONFERENCE

THE EIGHTH GEOP (Geodesy/Earth and Ocean Physics) Research Conference, on Lunar Dynamics and Selenodesy, was held October 10 and 11, 1974, at the Ohio State University. The conference, the last in the second year of the series, was attended by 66 persons.

The meeting was opened by William M. Kaula, who also delivered the traditional introducto-

This report was prepared by Frederick J. Doyle, Donald H. Eckhardt, James W. Head, William M. Kaula, Ivan I. Mueller, and W. L. Sjogren. Material contained herein should not be cited.

ry address, printed in its entirety elsewhere in this issue. The presentations and the discussions are summarized below by panel sessions.

First Session

Panel on Gravity Determination and Interpretation

Chairman: W. L. Sjogren (Jet Propulsion Laboratory, California Institute of Technology)

Members: R.H. Tolson (Langley Research Center), A.J. Ferrari (California Institute of Technology), M.P. Ananda (Jet Propulsion Laboratory), W.R. Wollenhaupt (Johnson Space Center), R.J. Phillips (Jet Propulsion Laboratory), C. Bowin (Woods Hole Oceanographic Institution), A.W.G. Kunze (University of Akron)

During the introduction, W.L. Sjogren displayed the diagram shown as Figure 1, which indicated the various attacks that are being made on the lunar gravity data. There are many avenues, and each approach has its advantages over another, depending on what parameters are being sought. The basic data, however, are only of one class, namely, spacecraft Doppler, which provides line-of-sight velocity measurements.

There now exist data from 13 orbiting spacecraft (Lunar Orbiter 1, 2, 3, 4, and 5; Explorer 35; RAE-B; Apollo 15 and 16 subsatellites; and Apollo CSM 14, 15, 16, and 17). The large omission in this data block is the lack of any direct far-side observations. The earth-based radio tracking is nonexistent during the periods of occultation—almost half the orbital period for the Apollo missions. Therefore any determination of far-side gravity variations must come from an extensive analysis of a long history of the spacecraft orbital elements.

The parameters being sought vary from spherical harmonic coefficient values, to global geoid heights, to acceleration profiles over very local anomalies, to front-side surface mass distributions. Each of these areas was discussed by one or more participants emphasizing his particular motivation. For example the homogeneity constant, determined from the polar moment of inertia C, is derived from the J_{20} and C_{22} harmonic coefficients; loading and stress estimates for local anomalies including the mascons are determined from acceleration profiles and global isostatic conditions from total geoid maps.

The status of spherical harmonic representation of the lunar gravity field was reviewed by R.H. Tolson. Current models are limited by the poor distribution of satellite orbit geometries, the occultation of satellites on the lunar far side, and a limited number of arcs that are free of nongravitational forces. Most gravity fields have been based on Doppler tracking data from the Lunar Orbiter series; however, data from Explorer 35 and 49 and the Apollo particle and fields satellites are currently being analyzed. The Explorer satellite orbits are relatively high and are free of perturbations from high-frequency gravity field components. Thus these satellites should be useful in estimation of the low-order potential coefficients needed to place constraints on the internal structure.

Tolson compared about a dozen gravity fields in terms of the values of the individual coefficients, the power spectra, and the surface gravity anomaly contours. The gravity fields varied from third to thirteenth degree. Half of the fields were generated by using the Doppler data directly as the observable; the other half utilized two-stage filtering in which short arcs of Doppler data are processed to obtain mean orbital elements, which are in turn processed to obtain the gravity field.

The second-degree zonal coefficient is particularly important for placing a constraint on the internal structure. A value of $2.054 \pm 0.012 \times 10^{-4}$ for this coefficient is obtained from selected Doppler-derived fields. Values of this coefficient determined from mean elements are generally smaller, having an average value of $1.997 \pm 0.016 \times 10^{-4}$, and are thought to be less accurate because of inadequate separation of the zonal harmonics in the mean element approach. Using values of β and γ determined from lunar libration studies yields C/MR^2 values of 0.397 ± 0.003 and 0.386 ± 0.005, respectively.

A comparison of the third-degree normalized coefficients shows consistency between the gravity fields of about 1×10^{-5}, with C_{31} being the most consistent coefficient. Fourth-order fields show limited consistency at the 10^{-5} level except for J_4, which can be estimated as $-7 \pm 3 \times 10^{-6}$. This estimate is obtained by combining the mean element solutions and the Doppler derived value of J_2 given above. Higher-order coefficients show no consistency at the 10^{-5} level. Thus the current satellite tracking data set does not generally provide sufficient constraints to permit individual coefficient estimates beyond third or fourth degree.

The power spectra of typical high-order fields are shown in Figure 2. The lower curve is the spectrum generated from a point mass representation of the near-side gravity field. Such representations should yield realistic high-degree spectra. As we discussed above, the spherical harmonic fields are realistic through at least the third degree and to a lesser extent through the fourth degree. Thus, in the regions where the two representations are valid, the spectrum appears to follow the empirical formula $16 \times 10^{-6}/n^2$. The high-degree spherical harmonic fields demonstrate what appears to be excessive power in the higher-frequency terms, whereas the point mass representations appear to underestimate the power in the low and intermediate frequencies. Caution must therefore be exercised in using either representation for studies of internal stress or density variations.

Gravity anomaly contour maps generated from gravity fields of degree less than about 10 do not resolve the ringed maria anomalies. Higher-order fields, which do resolve the mascons, generally produce far-side and polar gravity anomalies 5 to 10 times larger than those expected. This is the manifestation of the excessive power in the high-degree terms shown in Figure 1.

W.T. Blackshear, in an unpublished result, has mapped the covariance on the gravity coefficients into an uncertainty

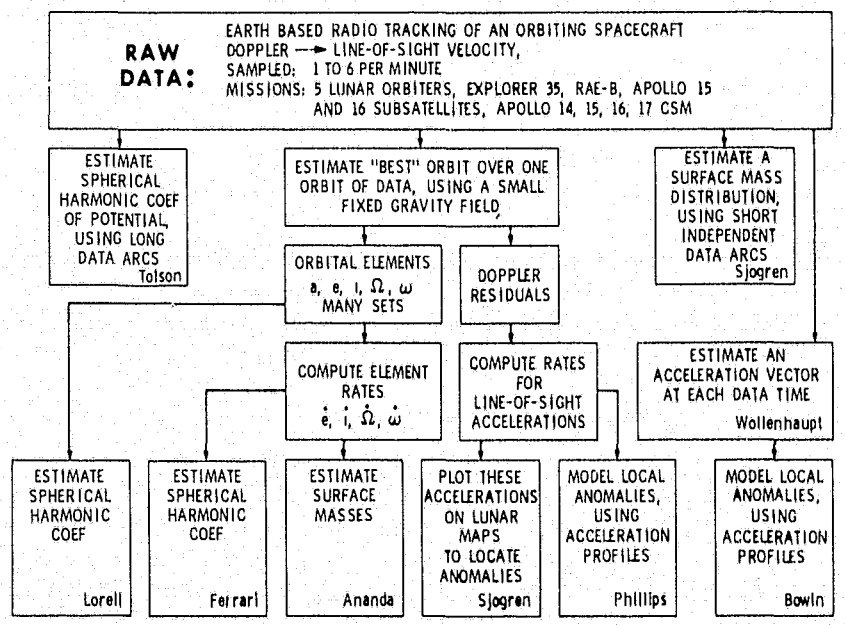

Fig. 1. Analysis of lunar gravity data.

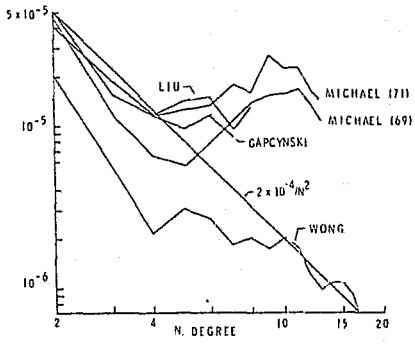

Fig. 2. Power spectra of high-order fields.

in the gravity anomaly on the near and far side. He found that the near-side equatorial uncertainty was 5 mgal, whereas the far-side uncertainty was about 7 mgal. Thus the data are nearly as sensitive to the far-side field as to the near-side field. However, the data do not constrain the entire set of gravity coefficients. The implication is that the far-side field can only be determined if additional constraints are introduced to the existing data. The optimal constraint would be to have new data in the polar and far-side regions. In lieu of this, reduced rank solutions or geophysical constraints, to reduce the power in the high-frequency terms, should be explored.

Our meeting was highlighted when A.J. Ferrari presented his very recent work using data from the Apollo subsatellites. A gravity model of degree and order 14 had been obtained from these data, yielding a maximum resolving ability of 384 km in the equatorial region.

Radial accelerations from the model, when evaluated at 100 km above the lunar surface, are in good agreement with results obtained by using the residual analysis method. The model clearly resolved the mascon features at Mare Serenitatis, Mare Imbrium, Mare Humorum, and Sinus Aestuum-Medii. Other large prominent mascons at Crisium, Nectaris, Orientale, and Grimaldi are all resolved as positive anomalies but are shifted approximately 5° from the topographic centers of these features. The mascon at Mare Smythii was not resolved. Possible new small front-side mascons were found at Aristarchus, and one was found in the southeastern highlands at 30°S latitude and 60°E longitude.

The far-side lunar gravity map, which is the first believable one, shows all the highland regions to be areas of broad positive gravity. The only large (over 400 km) far-side ringed basin that resolved as a potential mascon was Mare Ingenii. Ringed basins such as Apollo, Korolev, Moscoviense, and Mendeleev were all strong negative gravity regions. Hertzsprung appeared to be a relative low in a broad highland region. A large negative gravity region exists at 40°S latitude and 190°E longitude, which corresponds closely to the known topographic depression. The lunar far side, in contradistinction to the front, is characterized by the broad strong gravity regions of the highlands, with interspersed local negative regions corresponding to the larger ringed basins. From this evidence it appears that the far-side basins are craterlike and are not equivalent to front-side mare (filled circular basins).

Ferrari's work was not the complete answer, for when the accuracy of the low-order harmonic was presented, it did not change Tolson's previous picture of a definite need for a magnitude improvement in J_2 and C_{22}.

M.P. Ananda discussed a mass point representation of the gravity field derived from 120 days of Apollo 15 subsatellite data. The data consisted of the mean rates of the orbital elements rather than the elements themselves.

The estimated masses consisted of only 68 points placed about 20° apart over the region of ±30° about the equator and 100 km below the lunar surface. This was a factor of 4 reduction in the number of parameters that Ferrari used and eliminated the use of any a priori condition. About 90% of the information was extracted from the data. However, the residuals showed systematic signature indicating that further information can be recovered. A radial acceleration contour map, evaluated at 100-km altitude from the lunar surface, showed the front side in close agreement with the result derived from the residual analysis method. The only discrepancy was the Mare Crisium anomaly; all other known mass anomalies were recovered. The far-side map showed the highland regions as positive gravity areas and the basins such as Korolev, Moscoviense, Mendeleev, and Tsiolkovsky as negative gravity regions. The results were very similar to Ferrari's solutions and added confidence to the reality of the far-side field. Ananda's further efforts will include selecting optimum mass anomaly grid points, combining Apollo 15 and 16 subsatellite data, studying various data blocks, studying the effects of depths and shapes of mass anomalies, adjusting for known low-order gravity harmonics, and applying geophysical constraints.

Sjogren described the results from the short independent arc (≈70 min) approach using a grid of surface masses as the estimated gravity field.

The short integration periods reduced the effects of solar pressure modeling, gas leak perturbations, and integration errors. The reductions fitted the observations to almost the noise level, so that only very small systematic signatures were visible in the residuals. The cost of this method, however, was the complete loss of any far-side information.

Three different reductions have been accomplished over the past several years. The first was a quasi least squares reduction in that the entire 580 point masses estimated were obtained from overlapping blocks of 50 parameters each rather than from a complete simultaneous inverse. In 1971, 600 surface disks (50-km radius and infinitely thin) were estimated simultaneously with some 1100 state parameters. There were 11,000 observations, primarily from the lunar orbiter series (500 from Apollo 8 and 12). These results provided the first good estimate for a radial acceleration mapping over the front face from ±50° latitude. It revealed the mascons, the Orientale ring structure, and the Oceanus Procellarum's mild variations. In 1973 another reduction using almost 20,000 observations from the Apollo missions (Apollo CSM 14, 15, 16, and 17 and the Apollo 15 and 16 subsatellites) was finished. However, in this reduction many suface features were modeled with disks placed at their optical centers (i.e., mascons and craters). The disk radii were different, depending on the size of the structure. There were 960 parameters (350 disks) in this solution. With this result, estimated features had a single quantitative value—a realistic value where adjacent variations had been accounted for. These results are the best present front-side quantitative values. They can be improved upon by more detailed modeling, which is the next step in the analysis.

A sidelight to this approach was the analysis of the Mariner 9 (Mars orbiting spacecraft) data. Here the entire planet was modeled by using 92 equally spaced masses, and the short arcs (2 hours) were evenly spread over the entire surface (rather than over just 200° of longitude, as in the lunar case). The results were remarkable in that again surface features were detected and the expansion of the mass points into spherical harmonics produced coefficient values that were almost identical to the straightforward harmonic estimates. However, the harmonics solutions had their problems when it was attempted to attain higher order, and they did not have the resolution of the mass points. Also, they had large systematic residuals after their long integrations and many iterations.

W.R. Wollenhaupt outlined his plans for incorporating the Apollo photographic data into the Doppler data solutions for gravity parameter estimates. He displayed results from simulations indicating that indeed one could significantly improve the results from Doppler-only reductions. He stressed the importance of a close interface with the photographic reduction personnel and the need to iterate between themselves on independent reductions. He was confident that the direct photographic ray data on the far side would be powerful in resolving the major far-side anomalies.

Sjogren reviewed the residual analysis approach, a method developed by P.M. Muller and Sjogren in 1968, when they accidentally found the large gravity anomalies in the circular basins (mascons). It was a quick and easy way

to pinpoint anomalies, although quantitative values were somewhat distorted. The reduction was accomplished by essentially removing all known motion from the raw Doppler observations and analyzing the remaining line-of-sight velocities as variations in the lunar potential. These Doppler residuals were fitted with third degree splines having continuous second derivatives. Differentiation of these splines produced line-of-sight accelerations (which were mapped on a lunar chart according to the spacecraft selenocentric location at the observation time). Data from the Apollo missions have provided many detailed mappings over such features as mascons, craters, and mountain chains. Some 20 craters have been detected, all revealing negative gravity or mass deficiencies. Also, features not correlated with surface structure have been found.

The resolution of the data is almost proportional to the spacecraft altitude, and therefore the orbits of the command and service modules just prior to lunar landing have some of the most detailed structure. The Apollo 16 subsatellite was at a relatively low 15- to 20-km altitude over the region from the equator to 10°N and from 50°W to 40°E longitude. The Apollo 15 satellite at a 30° inclination never attained any low altitudes in the northern hemisphere (i.e., <100 km) and reached a minimum of 40 km in the southern hemisphere at 30°S latitude. This provided excellent coverage over Mare Humorum and Mare Orientale.

A measure of ground truth was obtained from Apollo 17 with a surface gravimeter. A comparison with Sjogren's results by using appropriate adjustment terms showed a very good agreement (i.e., 10 mgal for a −200-mgal anomaly).

R.J. Phillips reviewed two aspects of the modeling of local lunar gravity anomalies. He discussed the use of semi-global models, such as the 1971 Aerospace-JPL disk solution, to derive local mass distributions. On a local basis, such global models are useful within the limitations of the model error variance and resolution. Such aspects can be controlled by using the techniques of generalized inversion theory.

Phillips reviewed orbit simulation techniques for constructing local gravity models. Residual line-of-sight gravity data are typically biased by the least squares removal of the Keplerian orbit. In the orbit simulation approach, the gravity vectors for a particular model and spacecraft orbit are integrated along track. The least squares Keplerian orbit is removed, permitting a comparison with the actual line-of-sight residual gravity data.

Phillips stressed the nonuniqueness of the modeling and the importance of additional geological and geophysical information to constrain the interpretation.

C. Bowin presented a model for the mascons that was a two-body model rather than a single-body model, which he contended was being proposed by almost all analysts.

In the case of mare fill with a reasonable density contrast (+0.5 g/cm³) with crustal material, this would require a fill thickness of about 16 km for Mare Serenitatis to account for the observed gravity values at 100-km height. Such a great thickness would require a 16-km-deep hole prior to filling, and such a topographic depression is inconsistent with gravity anomalies away from the mare basins, where near-isostatic conditions appear to prevail. It would also be inconsistent with the depths of the topography of Mare Nectaris and Mare Orientale basins, which have but little fill, and with estimates of mare thicknesses based on buried crater dimensions. A two-body mascon solution, however, required only a 2-km thickness of fill and a 12-km rise of a lunar M discontinuity beneath Mare Serenitatis to account for the observed gravity anomalies. The top of the mantle dome or plug is placed at 60-km depth to match observed seismic-velocity structure. Bowin claimed that this mascon structure had an anomalous gravity field that was in good agreement with anomalies observed at several heights above Mare Serenitatis. Almost all agreed that the model was correct; however, the problem of estimating the two masses independently probably was not possible with the existing data set.

A.W.G. Kunze also considered a mascon model and proposed the integral

$$2\pi GM = \int_{-\infty}^{\infty}\int_{-\infty}^{\infty} g(X, Y)\, dx\, dy$$

to be zero over the mascon regions. In mascon maria the integral included the negative ring anomaly surrounding the positive mascon peak, and the uncompensated masses thus determined were small. Consequently, regional isostasy was approached in all mascon maria except Mare Orientale (isostatically overcompensated by the adopted definition). It therefore appeared that most lunar mascons were supported isostatically by mass deficits at depth, and that the observed gravity profiles were essentially the superposition of gravity highs caused by the excess density of the basaltic mare fill and broader gravity lows produced by compensating density deficits at depth. It was pointed out to Kunze that the negative ring structure was not sufficiently consistent with the mascons and that his density inversion had problems also.

Second Session

Panel on Dynamics

Chairman: Donald H. Eckhardt (Air Force Cambridge Research Laboratories)

Members: J.G. Williams (Jet Propulsion Laboratory), P.L. Bender (National Bureau of Standards and University of Colorado), C.C. Counselman (Massachusetts Institute of Technology), S.J. Peale (University of California, Santa Barbara)

In the seventeenth century, Galileo discovered the libration in latitude; Hevelius discovered the libration in longitude; and in 1693 Cassini elegantly described the moon's rotations that cause the optical librations as the sum of two uniform motions that are synchronized with the period and precession of its orbit. By 1750, Cassini's figure of 2.5° for the inclination of the moon's equator to the ecliptic I was brought down to 1°29' by Mayer, and the moon's librations were then predictable to about 1", as seen from the earth.

The principal improvements concerning our knowledge of the librations over the subsequent two centuries came from the theoreticians such as Lagrange; they provided the dynamical explanations for Cassini's 'laws' and showed that physical librations with amplitudes less than 0.5", as seen from the earth, must also exist. The physical librations were just marginally discernible, and the dynamical theory was developed to a level far superior to the quality of the observations. Then came the revolutionary improvements in the resolution of our observations of the librations: lunar laser ranging and differential VLBI are now providing resolution improvements by a factor of 10^4 over what existed a decade ago. The theoreticians are still scurrying to try to keep up with the observers, and our knowledge of the moon's dynamics and of the theoretical implications of its rotations is rapidly growing.

The three dynamical equations that represent the rotations of the moon are complicated, mutually coupled, and nonlinear. To solve them one must first adopt an ephemeris of the moon. The semianalytic solution starts with a semianalytic (numeric coefficients and symbolic arguments) tabulation of terms composing Fourier series expansions of the lunar coordinates. The numeric solution starts with a numerically integrated ephemeris. A purely analytic solution would start from a purely analytic ephemeris; the construction of such a solution has not yet been achieved with a precision comparable with that of the semianalytic or numeric solutions.

D. Eckhardt discussed his latest semianalytic solution for the physical librations. His model is a rigid moon with its gravity potential developed through the fourth-degree harmonics. The lunar ephemeris used is the improved lunar

theory of Deprit. The moon is considered to be moving about the earth according to the main (three body) problem of lunar theory, and it is torqued by the earth and the sun. The perturbations caused by additive and planetary terms in the lunar theory must be added separately.

The dynamical equations are solved iteratively with a digital computer performing all the semianalytic mathematical manipulations required. Each of the many Fourier series involved is allowed up to 510 terms. The computer sets and monitors the truncation level of each operation and decides upon convergence once all solution correction terms in an iteration have amplitudes less than a specified criterion. Because successive corrections decrease rapidly, the solutions are internally consistent to about 1 order of magnitude better than the 0.04" convergence criterion used. Tables are generated for all terms in τ, ρ, $I\sigma$, p_1, and p_2 that have amplitudes greater than 0.001"—about 450 terms for each parameter set. The parameters varied to produce partial differences are β, γ, and C/MR^2, each third-degree harmonic individually, and all fourth-degree harmonics as a block.

J.G. Williams reported on the Jet Propulsion Laboratory numeric solution for the physical librations, their comparison with semianalytic solutions, and their fit to the lunar laser ranging data. His lunar model is similar to Eckhardt's, and his ephemeris is one of the JPL series of numeric lunar ephemerides. A simple fourth-order Runge-Kutta scheme is used to integrate τ, ρ and $I\sigma$ as functions of time. The partial derivatives of the libration angles with respect to the initial conditions are obtained by finite differences.

Williams compared his solution with Eckhardt's by adjusting the initial conditions of the numeric solution for a least squares fit with the semianalytic solution. The comparison is now better than 0.1" (84 cm) selenocentrically over a three-year interval. The true discrepancy is several times larger because the second-order effects in the long-period, additive, and planetary terms have not yet been derived for the semianalytic solution. Like the semianalytic solution, the numeric solution fitted to it would have no free librations. Even if the numeric solution is used for the adjustment of observations, it must be compared with the analytic or semianalytic solutions to test for the existence of free librations.

Five years of lunar laser ranging data from McDonald Observatory, Texas, have now been fitted with an rms residual of 45 cm. A number of libration-related parameters and the coordinates of four lunar retroreflectors are adjusted in the fit. The values of β, γ, C_{32}, S_{32}, and S_{33} are very well determined from the data. The remaining third-degree harmonics are sensitive enough to be determined in future work. The retroreflector coordinates are accurate enough to serve as control points for selenodetic networks.

P.L. Bender discussed work in which lunar range residuals from solutions generated at JPL and at the University of Texas at Austin are used to solve for low-degree lunar gravitational harmonics in different ways. One approach is to introduce a covariance matrix for the calculated residuals to allow for uncertainties in the earth's orientation. A second approach consists of solving for single-day corrections to UT0 directly from the McDonald Observatory data. The results are being combined with the normal equations for Sjogren's Lunar Orbiter 4-a solution to obtain improved values for the low-degree harmonics. It appears that about 6 degrees of freedom in present spacecraft tracking solutions for lunar gravity can be tied down by proper combination with the normal equations for lunar range solutions.

C. Counselman reported progress by the MIT-Haystack-Goddard-AFCRL group in studying the libration through differential VLBI. Two relative-position coordinates of a pair of Apollo lunar surface experiments package (Alsep) transmitters are determinable within less than 1 m from a several-hour-long series of observations. Over the last 19 months, nearly 500 such series have been obtained.

Data from these observations have been analyzed so far with libration ephemerides based on Eckhardt's semianalytic development and on JPL's numeric integration, and with a numerically integrated lunar orbit generated at MIT by fitting laser ranging data. When VLBI observations are analyzed one day at a time, the fit obtained by adjusting only the selenodetic coordinates of an Alsep is good, and results from simultaneous observations on different base lines are consistent within 1 m. However, a serious discrepancy between observed and computed values of the VLBI observable, equivalent to tens of meters in Alsep position, accumulates over a month. This discrepancy is surprising in view of the relatively good fit to three years of laser ranging observations, within 10 ns rms, which has been obtained with the same orbit and libration ephemerides. Inconsistencies in the relative orientations among these ephemerides, the equator, and the ecliptic are suspected inasmuch as VLBI is much more sensitive than ranging observations to the position angle of the moon.

R.W. King is continuing to study these problems at MIT and AFCRL with assistance from the Lunar Laser Ranging Experiment (Lure) team and the JPL ephemeris group. VLBI observations of the Alseps are also continuing through the cooperation of Goddard Space Flight Center and the Spacecraft Tracking and Data Network. The quality of these observations is expected soon to improve with the installation of new instrumentation recently developed at MIT and Haystack Observatory.

Until only three years ago, the dynamical figure of the moon used in physical libration solutions was represented only by the second-degree harmonics of its gravity potential. The higher-degree harmonics had been neglected because they seemed to be of little significance, whereas their inclusion would have greatly complicated the equations. When this assumption was closely examined, it was found to be quite invalid; the third-degree harmonics were found to lead to significant physical librations.

Other assumptions based on cursory analyses are now also being reconsidered. Williams, for example, questioned whether the moon should really be considered a rigid body. He suggested that it may be possible to measure the potential disturbance Love number of the moon through its effect on the librations. A frequent assumption has been that there are no free librations. If this assumption could be justified, six parameters could be eliminated from the data reductions by taking a priori zero amplitudes for the free libration amplitudes. S.J. Peale made a very careful analysis of the validity of the assumption.

The only likely excitation of the free librations is by impact of large meteorites, whereas the damping will be due to internal energy dissipation during the periodic distortions from rotation and tides. Peale bracketed the meteorite energy rate by dividing the crater size distribution for those craters that have formed during the last 3 b.y. by this time span and using two scaling laws to relate crater diameter and impact energy. He then assumed extreme values of impact velocity of 10 and 30 km/sec to calculate momentum impulse rates. Assuming a uniform flux density over the lunar surface but keeping the velocity vectors parallel to the ecliptic plane and integrating over the impact parameters and differential momentum impulse rate, Peale finally arrived at angular momentum impulse rates. Tidal friction is the most important dissipation mechanism in nearly all cases of decay of the free librations. The tidal dissipation is modeled by allowing each periodic term in the expanded potential of the tidal distribution of mass a phase lag whose magnitude is $1/Q$, the specific dissipation factor.

Peale compared decay time estimates with the average times between excitations by meteorite impact. An impact that excites a free libration in longitude with amplitude greater than 0.01" to 0.1" may occur several times during each decay time to once in many decay times depending on which set of assumptions is used. Until critical assumptions in Peale's analysis are refined, the possibility of small-amplitude free librations of the moon cannot be ignored in data reductions.

Third Session

Panel on Geometric Control and Mapping

Chairman: Frederick J. Doyle, U.S. Geological Survey

Members: W. Wollenhaupt (NASA Johnson Space Center), L. Schimerman (Defense Mapping Agency Aerospace Center), M. Tiernan (Jet Propulsion Laboratory), R.W. King (Air Force Cambridge Research Laboratory), A. Elassal (U.S. Geological Survey), C. Shull (Defense Mapping Agency Topographic Center)

Lunar mapping started when Galileo first turned his new telescope toward the moon in 1610. For nearly 300 years, visual observations provided sketch maps whose detail increased with every improvement in telescope quality.

Lunar latitude and longitude are defined by the equator, which is the great circle perpendicular to the polar axis of rotation, and the prime meridian, which contains the mean direction of the line from the center of the earth to the center of the moon. To relate this system to the physical surface of the moon, the coordinates of a small circular crater, Mosting A, are accepted as the fundamental point. Control point networks have been computed for the visible face of the moon by measuring on telescope photographic plates the distance and direction in the sky from Mosting A to other identified features. Coordinates of the same feature differed by several kilometers in the separate solutions—which is not surprising, since the resolution of the best telescope plates is about 800 m.

In 1960 the control network computed by Schrutka-Rechtenstamm was used by the Army Map Service (AMS) to compile the first topographic map of the moon using photogrammetric techniques. Pairs of photographs made at maximum and minimum optical librations were employed in a specially constructed stereoscopic plotter to compile maps at 1 : 5,000,000 and 1 : 2,500,000. This effort made obvious the inadequacies of the existing control, and both AMS and Aeronautical Chart and Information Center (ACIC) undertook new control solutions.

ACIC then undertook a new topographic mapping program at 1 : 1,000,000 for the visible face and 1 : 500,000 for the equatorial zone using new photographs from Pic du Midi and Flagstaff. These have been the basic documents for lunar exploration.

In October 1959, lunar mapping entered a new phase when the Soviet spacecraft Lunik 3 flew around the moon and televised a series of pictures of the hitherto unseen far side. These were used to produce a chart at scale 1 : 10,000,000. In July 1965, another Soviet spacecraft Zond 3 televised much better pictures from the far side and a new map in nine sheets at scale 1 : 5,000,000 was compiled.

The U.S. Ranger missions, the Soviet Luna landers, the U.S. Surveyor landers, and the first three U.S. Lunar Orbiters contributed detail maps of restricted local areas.

Lunar Orbiters 4 and 5 were placed in polar orbits and photographed nearly the complete lunar surface. From these pictures a four-sheet planimetric map at scale 1 : 2,750,000 was compiled. Accuracy is a few hundred meters on the front side of the moon but degenerates to about 15 km on the far side.

The early Apollo missions carried Hasselblad cameras, which made negligible contributions to lunar mapping. But on Apollo 15, 16, and 17, a photogrammetrically designed system consisting of terrain cartographic camera, stellar camera, laser altimeter, panoramic camera, and precise timing, was carried. The coverage provided by this system, extending 32° north and south and from 165° east to 65° west longitude, is a new source of precise data for current studies on lunar geometry and mapping.

Fundamental to mapping from the Apollo data is the spacecraft position in the selenodetic coordinate system at the time each photograph was exposed. W. Wollenhaupt described the NASA spacecraft ephemeris computations that produce this information. Original position data were computed from Doppler tracking by using existing models for lunar gravity field and librations. When these data were incorporated in photogrammetric solutions, discrepenacies of several kilometers were disclosed. The accuracy of this weighted least squares solution is estimated to be $\sigma_\phi = 2000$ m, $\sigma_\lambda = 500$ m, and $\sigma_r = 1200$ m within an arc of tracking data. When the ephemeris is projected one spacecraft revolution outside the tracking arc, the accuracy deteriorates to $\sigma_\phi = 2800$ m, $\sigma_\lambda = 1100$ m, and $\sigma_r = 1600$ m.

To improve this accuracy, a new sequential estimator program has been developed that will permit the incorporation of unmodeled spacecraft accelerations due to venting, uncoupled thrusting, etc. With these improvements the predicted accuracy will be $\sigma_\phi = 1000$ m, $\sigma_\lambda = 500$ m, and $\sigma_r = 500$ m within the tracking arc, but with little improvement when the ephemeris is extended one revolution outside the tracking data.

The eventual solution will incorporate the photogrammetric condition equations and the laser altimetry, together with improved gravity and libration models. It is hoped to obtain a final accuracy of spacecraft position of the order of 30 m in all three coordinates.

Responsibility for photogrammetric triangulation was assigned by NASA to the Defense Mapping Agency. The DMA Aerospace Center has completed Apollo 15 and 17 triangulations and is now computing an Apollo 16 triangulation based on measurements by the DMA Topographic Center; Aerospace Center has responsibility for incorporating the three missions into a unified solution. These efforts were described by L. Schimerman.

To provide data for strip and block photogrammetric solutions, over 50,000 images on 1500 photographs from 31 lunar orbital revolutions have been measured. The solutions are constrained by exposure station positions based on spacecraft ephemerides, camera orientations resulting from stellar photograph reductions, and spacecraft-to-lunar-surface distances defined by the laser altimetry. Because of excessive discrepancies between ephemeris positions and photogrammetric positions, an initial Apollo 15 control system has been adopted based on the tracking data for revolution 44, which produced the best fit between ephemeris and photogrammetric positions. A capability for photogrammetrically projecting orbital positions to the lunar surface with an accuracy of 25 to 65 meters has been demonstrated, and large photogrammetric blocks based on current spacecraft ephemerides indicate maximum positional inconsistencies of 300 m between most widely separated points.

Extension of the Apollo control system to higher latitudes is being accomplished through triangulation of Apollo mission high oblique photographs and relation to positions defined by earlier earth-based telescopic systems. Improvement to the absolute basis for the system is also being sought by photogrammetric tie to lunar surface retroreflectors and radio transmitters being observed by earth-based laser ranging and very long baseline interferometry (VLBI). Triangulation of photographs taken by the astronauts on the surface at the Apollo 14 and 15 landing sites is also being performed to precisely relate the positions of the retroreflectors and radio transmitters at these sites.

The Apollo 17 orbiting spacecraft carried a VHF coherent imaging radar. M. Tiernan described the geometry of feature position determination by measurement of the radar records. Thirteen craters in the southern region of Mare Serenitatis were selected. The along-track and across-track distances between the craters were determined together with their selenocentric radius. These values were compared with those produced by the DMA photogrammetric procedures. Excluding three craters that were apparently misidentified or poorly measured and a systematic bias in radius, the mean differences were $\Delta_\phi = 192$ m, $\Delta_\lambda = 160$ m, and $\Delta_r = 50$ m. Major sources of error were probably crater identification, specular reflection resulting in measurements to other than crater centers, radar calibration, and spacecraft ephemeris. The technique shows promise for mapping in areas where lack of illumination prohibits photography.

R.W. King reported the use of differential VLBI observations of the

Alsep transmitters to determine the relative coordinates of the Apollo 12, 14, 15, 16, and 17 landing sites. These observations can contribute to the reduction of Apollo 16 and 17 orbital metric photography by locating the Alseps at the landing sites for these missions with respect to the Apollo 15 Alsep. The determination of the position of the Apollo 15 Alsep transmitter with respect to that of the retroreflector at that site, reported by Schimerman, can then be used to locate all the Apollo sites in a unified selenodetic system.

The coordinates determined by VLBI depend directly on the coordinates adopted for the Apollo 15 reflector and on the correct modeling of the moon's physical libration and orbit. Considerable effort is being spent to compare the reference system defined by the MIT software with that used at JPL. These comparisons involve not only the lunar libration and orbit but also the planetary ephemerides, precession, nutation, observing site coordinates, UT1, and polar motion.

Data obtained on approximately 150 tracking days between March 1973 and July 1974 are currently being reduced to obtain Alsep 16 and 17 coordinates. An accuracy of 5 to 15 m seems possible within the next six months.

The integrated combination of terrain camera and stellar camera on the Apollo 15, 16, and 17 missions provides a unique opportunity to determine the position of the moon with respect to the stellar coordinate system. A. Elassal described the photogrammetric triangulation solution being conducted jointly by the U.S. Geological Survey and the National Geodetic Survey. Features of the program are ability to accept all inputs with appropriate weights, inclusion of the moon's rotation rate and the right ascension and declination of its axis as unknowns to be adjusted, and a rigorous error propagation. Observed image coordinates are taken from the Aerospace and DMA Topographic Center projects rather than being reobserved. Solutions have been performed for blocks taken from the Apollo 15 and 16 missions. The lunar orientation and rotation computed from these solutions differ significantly from the latest Eckhardt model, as is shown in Table 1.

Possible explanations for these differences are changes in the locking angles between the terrain and stellar cameras from their preflight calibrated values or a computational error in the application of the angles in the DMA data.

A rigorous error propagation was performed on the triangulation of revolution 17 from Apollo 16. Using the a posteriori estimate of image coordinate residuals gives the following mean values for the estimates of computed surface point coordinates: $\sigma_\phi = 37$ m, $\sigma_\lambda = 80$ m, $\sigma_r = 75$ m. These are the values that can be expected in a unified triangulation accepting any specified libration model.

The task of producing maps from the Apollo 15, 16, and 17 missions has been assigned by NASA to the DMA Topographic Center. These operations were described by C. Shull. From the mapping camera photographs, map series at 1 : 250,000 are being compiled for most of the area covered by the three missions. The orthophoto image base is obtained from rectified and scaled mosaics in flat areas, and from optical orthophotos in rugged terrain. Versions are produced both with and without contours, which are derived in conventional stereoplotter instruments. On some maps, the orthophoto imagery is affected by the presence of Newton rings and other film faults on the original photography. Where this occurs, a diagram appears at the bottom of the map describing the film faults.

For sites of special scientific interest, maps at scales of 1 : 50,000 and 1 : 10,000 are being produced from the panoramic camera photographs. Control points at intervals of 40 to 50 mm on the panoramic photographs are identified on the mapping camera photographs, and their positions are computed by analytical triangulation of the mapping camera photographs. Additional control, if needed, is established by using the AS-11A analytical stereoplotter on which all stereographic compilation is performed. These additional control points also serve as a base for mosaics of rectified panoramic photographs. The rectification is performed on a special Apollo transforming printer. In areas of large elevation differences, orthophotographs are produced on the Universal automatic map compilation equipment (Unamace). Control for these orthophotographs is established by analytical triangulation of the panoramic photographs using a panoramic preprocessor program developed to reduce the panoramic photograph to an equivalent metric frame.

TABLE 1. Lunar Orientation and Rotation: Comparison of Values

	δ'	α	δ
	Apollo 15		
Computed value	13°09'30"	−87°11'15"	22°34'30"
99% confidence	±01'	±08'	±05'
Eckhardt	13°12'	−87°01' to −87°11'	22°20'30"
	Apollo 16		
Computed value	13°10'48" to 13°10'17"	−86°28'30"	22°41'45"
99% confidence	±30'	±05'40"	±02'
Eckhardt	13°08'39" to 13°09'59"	−86°30' to 86°24'	22°45' to 22°43'

Fourth Session

Panel on Tectonic Implications: Structure and Evolution

Chairman: James W. Head (Brown University)

Members: Gerald Schubert (University of California at Los Angeles), John Wood (Smithsonian Astrophysical Observatory), Nafi Toksoz (Massachusetts Institute of Technology), D.W. Strangway (University of Toronto)

The surface of the moon offers a number of clues about the tectonic setting and history of that planetary body. There is no evidence in the moon's present surface morphology for any of the classic terrestrial ocean basin or continental features associated with plate tectonics. Structural features typical of the last 3.8 b.y. of lunar history are primarily limited to small tensional and compressional features generally associated with the filling of the maria and minor readjustments of mare basins. Mountain ranges, classic terrestrial tectonic features, are limited in terms of their time of formation on the moon to the period prior to about 3.8 b.y. ago. They also formed in a radically different way. Lunar mountain ranges define the circular rings of major, multiple-ringed basins, which formed as gigantic impact craters.

The mountains associated with these events are up to 5 to 6 km high and formed both at the crater rim itself and along circular fractures as major portions of the crust collapsed inward toward newly excavated craters. Between 50 and 60 of these major basins have been recognized on the moon. The characteristics, distribution, sequence, and filling of these basins provide considerable evidence for understanding the structure and evolution of the moon. Surface structure suggests that the major tectonic activity on the moon occurred during and just after the formation of the lunar crust. By about 3.8 b.y. ago, the lunar crust had attained a state and thickness that precluded subsequent major tectonic activity. Important evidence for the characteristics of the interior that led to this tectonic history are found in geophysical and petrologic experiments and studies.

Gerald Schubert discussed the implications of the lunar offset of center of figure/center of mass in terms of what

thickened at the rate of about 220 km/b.y. during this period. In particular, the shallowest melting progressed from 140- to 280-km depth during the period of mare filling, in agreement with the depth of origin of mare basalts and with the need for a reasonably thick lithosphere to sustain the stresses associated with mascon gravity anomalies. The disappearance of melting in the mantle coincided roughly with the termination of magmatic events. At the present the whole moon is cooling. The deep interior, below a depth of 1000 km may be hot enough for partial melting.

Present-day temperatures generally exceed the melting temperatures of Fe or Fe/FeS combinations in the deep lunar interior. Thus if there were a concentration of Fe or Fe/FeS in the center, these would be molten, and the moon would have a molten core.

Dave Strangway discussed the variety of lunar magnetic data and outlined implications for lunar evolution from the information. Returned lunar basalt and breccias are magnetized, and lunar suface magnetic anomalies have been detected at the Apollo 16 site by using the lunar portable magnetometer. Measurements from lunar orbit reveal surface anomalies at the 50- to 100-km scale of surface magnetization. Lunar breccias appear more magnetic than basalts because they have more metallic iron, and the metallic iron in mare basalts occurs in larger fragments that are generally soft. Breccias are shocked and heated and appear to derive their magnetic characteristics from excess fine-grained iron rather than from a stronger field.

Modeling work is under way on regional anomalies detected by satellite to determine direction of magnetization. Directional information will be significant in determining the nature and origin of the field originating these anomalies (internal, external, transient, or impact-induced).

Knowledge of the origin of the magnetic field will help to put constraints on lunar thermal history. Strangway discussed a model in which there is a present-day partially molten core, a heat flow between 24 and 30 ergs $cm^{-2}\ s^{-1}$, and a crust that developed early in the moon's history by melting of the outer 150 km. The deep interior is below the Curie point of iron for the first 1 to 1.5 b.y., so that it is able to carry the memory of an early field that magnetized the cold interior. The magnetized mare basalts and breccias cooled in this field from above the Curie point of iron (~800°C.) and acquired a thermoremanent magnetization. In this model the moon's deep interior will recently have warmed up enough to erase the memory of the ancient field from the deep interior and to develop the core, which has been detected seismically.

Summary Session

In the final discussion, the following measures were emphasized as desirable to exploit existing data and to prepare for a future lunar orbiter: addition of high satellites (Lunar Orbiter 4, Explorer 49) to the data set being analyzed for the far-side gravity field, with the hope of getting an improved J_2 as well; use of far-side metric camera data; singular-value analysis and other statistical techniques to obtain more meaningful measures of the accuracy of the results; and simulation studies of possible lunar orbiters with the existing data set. The solution of dynamical problems associated with the physical librations is progressing satisfactorily toward ultimate accuracies of the order of ± 0.5 m for the location of fundamental control points and $\pm 0.1''$ for the moon's orientation. Full exploitation of the mapping photography appears to require both more iteration with orbital dynamics solutions and interaction with the geologic applications of the end product.

Although appreciably more should be inferred about the far-side and polar regions from existing data, the resulting picture will inevitably be considerably smoothed and highly vulnerable to bias. These considerations, together with the significantly different character of the far-side and polar geology, make a high-inclination orbiter with altimetric and gravimetric capabilities an extremely attractive means of attaining a better-rounded understanding of lunar gravity and geometry, and of their implications for origin and evolution.

List of Participants

Name	Address	Conferences Attended
Agnew, Duncan	IGPP/P.O.Box 109, La Jolla, California 92037	6
Aki, K.	Massachusetts Institute of Technology, 54-526 Cambridge, Massachusetts 02139	2
Alewine, R. W.	California Institute of Technology, P.O.Bin 2 Arroyo Annex, Pasadena, California 91109	6
Allen, C.	California Institute of Technology, P.O.Bin 2 Arroyo Annex, Pasadena, California 91109	6
Allen, Rex	U.S.Geological Survey/NCER, 345 Middlefield Rd. Menlo Park, California 94025	6
Allen, Wm. A.	USAETL-Research Institute, 701 Prince St. Alexandria, Virginia 22314	7
Ananda, Mohan	Jet Propulsion Laboratory, California Institute of Technology, 4800 Oak Grove Dr., Pasadena, California, 91103	8
Anderle, R. J.	Computation and Analysis Laboratory, USNWL, Dahlgren, Virginia 22448	2
Anderson, D.L.	California Institute of Technology Pasadena, California 91109	6
Anderson, J.D.	Jet Propulsion Laboratory, California Institute of Tech., 4800 Oak Grove Dr., Pasadena, California, 91103	5
Andrews, D. J.	U.S.Geological Survey, 345 Middlefield Rd. Menlo Park, California 94025	6
Anton, J.	Systems Control, Inc., 260 Sheridan Ave., Palo Alto, California 94306	6

Apel, J.R.	Atlantic Oceanographic & Meteorological Labs., NOAA, 15 Rickenbacker Causeway, Miami, Fla.	1, 4
Archuleta, R.	IGPP/P.O. Box 109, La Jolla, California 92037	6
Argentiero, P.	Goddard Space Flight Center, 4452 Faraday Place, Washington, D.C. 20016	4
Argote, M.L.	Centro de Investigacion Cientifica de Baja California Gastelum 898, Ensenada, Baja California, Mexico	1
Balazs, E.I.	NOAA, NGS, 6001 Executive Boulevard, Rockville, Maryland 20852	1, 4, 7
Bally, A. W.	Shell Oil Co., P. O. Box 2099, Houston, Texas 77001	3
Baltzer, R. A.	U.S.G.S., National Center - 430 Reston, Virginia 22092	7
Barker, T.	IGPP/P.O. Box 109, La Jolla, California 92037	6
Beaumont, C.	Department of Oceanography, Dalhousie Univ., Colurs Rd., Halifax, Nova Scotia, Canada	1, 6
Bender, P.L.	Joint Institute for Lab. Astrophysics, Univ. of Colorado, Boulder, Colorado 80302	2, 6, 8
Bennett, J.E.	Office of Naval Research, 800 N. Quincy St., Arlington, Virginia 22217	4, 7
Berbert, J.	NASA Goddard, Code 590, Greenbelt, Maryland 20771	4
Berger, J.	University of California, San Diego, IGPP/ P.O.Box 109, LaJolla, California 92037	1, 6
Blackshear, W.T.	NASA, Langley Research Center M/S401B, Hampton, Virginia	5
Blankenburgh, J.Chr.	Granon, 13, 1430 As, Norway	7
Bliamptis, E. E.	AF Cambridge Research Laboratory, L.G. Hanscom Field, Bedford, Massachusetts	6

Bloom, A.L.	Department of Geological Sciences, Cornell University, Ithaca, New York 14585	3
Blust, F. A.	NOAA, NOS, Lake Survey Center, 630 Federal Building, Detroit, Michigan 48091	7
Bonilla, M.G.	U.S.G.S., 345 Middlefield Road, Menlo Park, California 94025	6
Booker, J.	University of Washington, Geophysics Program, AK-50, Seattle, Washington 98102	6
Boore, D. M.	Stanford University Geophysics Department Stanford, California 94305	6
Bowin, C.	Woods Hole Oceanographic Laboratory, Woods Hole, Massachusetts 02543	3,8
Briedis, D.	Stone & Webster Consult. Eng. Boston, Massachusetts	6
Brown, R. D.	Computer Sciences Corporation, Colesville Rd., Silver Spring, Maryland	4
Brown, W. E.	Jet Propulsion Laboratory, 4800 Oak Grove Dr. M.S.183-701, Pasadena, California 91103	4
Brune, J. N.	IGPP-University of California La Jolla, California 92037	6
Buchanan-Banks, J.	U.S.G.S., 345 Middlefield Road, Menlo Park, California 94025	3,6
Budiansky, B.	Harvard University, Pierce Hall, Cambridge, Massachusetts 02138	6
Buckley, N.A.	Federal Power Commission, No. 1 Snow's Court, N.W., Washington, D.C. 20037	7
Buglia, J. J.	NASA-Langley Research Center, MS401B Hampton, Virginia 23665	4
Buland, R.	IGPP/P.O.Box 109, La Jolla, California 92037	6

Burke, K.	Erindale College, University of Toronto, 3359 Mississauga Rd., Mississauga, Ontario, Can.	3
Burns, J. A.	Cornell University, Center for Radiophysics & Space Research, Ithaca, New York 14850	5
Bush, G. B.	Johns Hopkins University, Applreel Physics Lab., 8621 Ga.Ave., Silver Spring, Md.20910	4
Cabaniss, G. H.	AFCRL (LWH), L. G. Hanscom Field. Bedford, Massachusetts 01730	1, 3
Calame, O.	University of Texas, Department of Astronomy Austin, Texas	8
Campbell, D. B.	M.I.T., Haystack Observatory Westford, Massachusetts 01886	5
Caputo, M.	Istituto Di Geodesia, Facolta Di Scienze, Universita Degli Studi, Viale Risorgimento, 2, 40136, Bologna, Italy	7
Carroll, D. G.	Gravity & Astronomy Division, National Geodetic Survey, Rockville, Maryland 20852	4
Carter, N.L.	Department of Earth & Space Science, State University of New York, Stony Brook, N.Y. 11790	3,7
Castle, R.O.	U.S.Geological Survey, 345 Middlefield Rd., Menlo Park, California 94025	1, 3, 6
Cathles, L.	Ledgemont Laboratory, Kennecot Copper Co. 128 Spring Street, Lexington, Massachusetts 02173	3
Cazenave, A.	Centre National d'Etudes Spatiales, BP no.4 91 Bretigny/orge, France	2
Chapman, Wm. H.	U.S.Geological Survey, 1340 Old Chain Bridge Rd., McLean, Virginia 22101	4, 5, 7
Cherry, T.	Systems, Science, Software, P.O. Box 1620 La Jolla, California 92037	6
Chinnery, M. A.	Department of Geological Sciences Brown University, Providence, Rhode Island	2

Chovitz, B.	Geodetic Research & Development Lab. NOS/NOAA, Rockville, Maryland 20852	4, 8
Christensen, E.	Jet Propulsion Laboratory, California Institute of Technology, 4800 Oak Grove Drive, Pasadena, California 91103	5
Church, J. P.	U.S.Geological Survey, 345 Middlefield Rd. Menlo Park, California 92037	6
Coakley, J. P.	Canada Centre for Inland Waters, 867 Lakeshore Rd., Box 5050, Burlington, Ontario, Canada	7
Collias, E. E.	Department of Oceanography, University of Washington, Mail Stop WB-10, Seattle, Washington	1
Colombo, G.	Facolto di Ingogerio, Universite de Padova 35100 Padova, Italy	5
Compton, H. R.	Langley Research Center, NASA Hampton, Virginia 23665	8
Conlon, R.	Stone & Webster Consulting Engineers Boston, Massachusetts	6
Converse, G.	U. S. Geological Survey, 390 Main Street, San Francisco, California 94105	6
Cook, K. L.	Department of Geology, University of Utah. Salt Lake City, Utah 84112	6
Counselmann, C.C.III	Massachusetts Institute of Technology, 54-626, Cambridge, Massachusetts 02139	2, 3, 5, 6, 8.
Cornaby, B.	Battelle Columbus Laboratory, 505 King Avenue, Columbus, Ohio 43201	7
Crowell, J.C.	Department of Geological Sciences, University of California, Santa Barbara, California 93106	6
Dahlen, F. A.	Department of Geology & Geophysical Sciences Princeton University, Princeton, New Jersey 08540	2
Davies, M. E.	The Rand Corporation, 1700 Main Street Santa Monica, California 90406	8

Davis, T. M.	Naval Oceanographic Office, Mathematical Modeling Project, Suitland, Maryland	4
Day, S.	IGPP/P.O.Box 109, La Jolla, California 92037	6
Decker, B. L.	Defense Mapping Agency, Aerospace Center Second & Arsenal Streets, St.Louis AFS, Missouri 63118	2, 4, 5, 8
DeCooke, B.G.	U.S.Army Corps of Engineers, 150 Michigan Avenue, Detroit, Michigan	7
Dehlinger, P.	Marine Sciences Institute, University of Connecticut, SE Branch, Groton, Connecticut	1
Deprit, A.	Cincinnati Observatory Cincinnati, Ohio 45208	5
Dicke, R. H.	Palmer Physical Laboratory, Princeton University, Princeton, New Jersey 08540	2
Dixon, J. F.	Jet Propulsion Laboratory, California Institute of Technology, 4800 Oak Grove Drive, Pasadena, California 91103	5
Dixon, J.	Code TN-3, Johnson Space Center Houston, Texas 77058	8
Dohler, G.	Marine Sciences Directorate, 615 Booth Street, Ottawa, Canada KIA OE6	7
Dolan, H.	Department of Commerce - Room 3518, 14th & Constitution Ave., Washington,D.C. 20230	7
Douglas, B.C.	Wolf R & D Corporation, 6801 Kenilworth Avenue, Riverdale, Maryland 20840	4
Doyle, F.J.	U.S.Geological Survey, 1340 Old Chain Bridge Road, McLean, Virginia 22101	8
Dunbar, W. S.	Department of Physics, University of Toronto Toronto, Ontario, Canada	3
Dziewonski, A.	Department of Geology, Harvard University Cambridge, Massachusetts 02138	6

Ealum, R. L.	Defense Mapping Agency Aerospace Center Geophysical & Space Sciences Division, St. Louis AFS, Missouri 63118	4
Eckerman, J.	NASA/GSFC, Greenbelt, Maryland 20771	4
Elachi, C.	Jet Propulsion Laboratory, 4800 Oak Grove Drive, Pasadena, Californai 91103	1
Eldholm, O.	Lamont-Doherty Geological Observatory, Columbia University, Palisades, New York 10964	3
Emrick, H.W.	USAF, DFEGM, Colorado Springs, Colorado	4
Esposito, P.	Jet Propulsion Laboratory, California Institute of Technology, 4800 Oak Grove Drive, Pasadena, California 91103	5
Eckhardt, D.H.	Air Force Cambridge Research Laboratories Hanscom Air Force Base, Massachusetts 09730	8
Elassal, A. A.	U. S. Geological Survey, 12201 Sunrise Valley Drive, Reston, Virginia 22092	8
Fahnestock, R.K.	State University of New York, Geology SUNY Fredonia, New York 14063	7
Faller, J.E.	Joint Institute for Laboratory Astrophysics NB8, Boulder, Colorado 80302	3
Falzone, A.J.	U.S.Naval Observatory, 37th & Massachusetts Aves., Washington, D.C. 20008	1
Feldscher,C.B.	Lake Survey Center, NOS,NOAA, 630 Federal Building, Detroit, Michigan 48226	3,7
Farrell, W.E.	Cooperative Institute for Research in Environmental Sciences, University of Colorado, Boulder, Colorado 80302	1
Ferrari, A. J.	California Institute of Technology, Division of Geological and Planetary Sciences, Pasadena, California 91109	8
Filloux, J. H.	Scripps Institute of Oceanography, P.O.Box 109, La Jolla, California 92037	1

Fischer, I.	Defense Mapping Agency Topographic Center 6500 Brooks Lane, Washington, D.C. 20315	4, 7
Fix, J. E.	Teledyne Geotech, P.O.Box 28277 Dallas, Texas 75228	1
Fliegel, H.F.	Jet Propulsion Laboratory, CPB-300, 4800 Oak Grove Drive, Pasadena, California 91103	6
Fosque, H.S.	NASA Headquarters , 600 Independence Ave. Washington, D. C. 20546	2
Foucher, J-P	Gravity Division, Earth Physics Branch, 3 Observatory Crescent, Ottawa, Ontario K1A OE4, Canada	3
Foulds, D.	Environment Canada, Water Planning & Management, 135 St.Claire Ave., W. Toronto, Ontario	7
French, R. B.	Department of Geology, University of Michigan Ann Arbor, Michigan 48104	2
Freeman, N.	Canada Center for Inland Waters, 867 Lakeshore Rd., E., Burlington, Ontario, Canada	7
Fubara, D.M.	Battelle Memorial Institute, 505 King Ave. Columbus, Ohio 43201	1, 3, 7
Fuller, M.	University of Pittsburgh, 506, Langley Hall Pittsburgh, Pennsylvania 15213	2
Gabrysch, R.K.	U.S.Geological Survey (WRD) Room 1112, 2320 La Branch St., Houston, Texas 77004	7
Gale, P.	Turner, Collie & Braden, Inc., P.O.Box 13089 Houston, Texas 77019	7
Gallet, R.M.	ERL/NOAA, R, Boulder, Colorado 80302	1
Garrett, B.J.	U.S.Army Corps of Engineers, New Orleans District, P.O.Box 60267, New Orleans, Louisiana	7
Garrett, C.	Department of Oceanography, Dalhousie University, Halifax, Nova Scotia Canada	1
Gealey, W.K.	Chevron Overseas Petroleum, Inc., 555 Market Street, San Francisco, California 94105	3

Gergen, J.	USNOAA, NGS, 6001 Executive Blvd. Rockville, Maryland 20852	1
Godbey, T. W.	Aerospace Electronics, General Electric, French Road Plant, Utica, New York 13503	4
Goodkind, J. M.	Department of Physics, University of California, San Diego, La Jolla, California 92037	1
Goodman, L. R.	NOAA, Wallops Station; Bldg. E106 Wallops Island, Virginia 23337	4
Goldstein, R.	Jet Propulsion Laboratory, Califonia Institute of Technology, 4800 Oak Grove Drive, Pasadena, California 91103	5
Goldstein, S.	University of Virginia, Department of Astronomy Charlottesville, Virginia	5
Graber, M. A.	NOS, NOAA, Satellite Applications Div., C16 Rockville, Maryland 20852	1, 2, 3
Gracie, G.	University of Toronto, 3359 Mississauga Road, Mississauga, Ontario, Canada	3
Greenberg, R.	Lunar & Planetary Laboratory, University of Arizona, Tucson, Arizona 85721	5
Griffith, J. S.	Lakehead University, Department of Mathematical Sciences, Thunder Bay, Ontario, Canada 87B 5E1	8
Gripshover, S.	U.S.Naval Weapons Laboratory, Code KGR Dahlgren, Virginia 22485	4
Gubbins, D.	CIRES/NOAA, University of Colorado, Boulder, Colorado 80302	2
Guinot, B.	Bureau International de l'Heure, 61 Avenue de l'Observatoire, 75014, Paris, France	2
Haardeng-Pedersen, G. P.	Memorial University of Newfoundland, St. John's, Newfoundland, Canada	2
Hammond, J. A.	AFCRL/LWG, L. G. Hanscom Field, Bedford, Massachusetts 01730	1, 4
Hammond, D. L.	Naval Research Laboratory Washington, D. C. 20375	4

Hanks, T.	California Institute of Technology Seismological Labs., Pasadena, California 91109	6
Hannon, W. J.	Lawrence Livermore Laboratory P.O.Box 808, L-44, Livermore, California 94550	6
Hanson, M.E.	Lawrence Livermore Laboratory, P.O.Box 808 Livermore, California 94550	6
Harris, H. C.	DMAAC/Geodetic Survey Squadron F. E.Warren AFB, Wyoming 82001	2
Harrison, C.G.A.	University of Miami, 10 Rickenbacker Causeway, Miami, Florida 33149	2
Harrison, J. C.	CIRES, University of Colorado Boulder, Colorado 80302	1
Haubrich, R.A.	University of California, San Diego, IGPP - P.O.Box 109, La Jolla, California 92037	1,2
Hayes, M.O.	Coastal Research Division, Geology Department University of South Carolina, Columbia, South Carolina 29208	7
Heacock, J.G.	Office of Naval Research, 800 N. Quincy Street, Arlington, Virginia 22217	1
Head, J.W.	Brown University, Providence, Rhode Island 02912	8
Hegemier, G.	AMES - IGPP, University of California, San Diego, La Jolla, California 92037	6
Heinrichs, D. F.	Office of Naval Research, Arlington Virginia 22217	4
Heinecke, U.	Technical University, Nienburger Str. 6 3 Hannover, West Germany	7
Hendershott, M.	Institute of Geophysics & Planetary Physics University of California, La Jolla, California	1,2
Henricksen, L.	AGU, 6th Floor, 1909 K St., N.W. Washington, D. C. 20036	4
Herron, T.J.	City College of New York, Convent Avenue & 133rd Street, New York, New York	3,4

Hicks, S. D.	NOX, NOAA, 6001 Executive Blvd. Rockville, Maryland 20852	7
Holdahl, S.	NGS, NOS/NOAA, 6001 Executive Blvd. Rockville, Maryland, 20852	3,4,7
Hord, C. W.	Laboratory for Atmospheric and Space Physics LASP - University of Colorado, Boulder, Colorado 80302	5
Hotter, F.	DMA, Aerospace Center, Box 6 St. Louis, Missouri 63118	1,2,3
Howell, D. E.	S.C. State Dev. Board, Division of Geology 800 Dutch Square Plaza, Suite 117, Columbia, South Carolina 29210	6
Hubbard, W. B.	Planetary Sciences Dept., LPL, University of Arizona, Tucson, Arizona 85721	5
Ingalls, R. P.	M.I.T. Haystack Observatory Westford, Massacusetts 01886	5
Ingram, H. W.	Transcontinental Gas Pipeline Corporation P.O. Box 1396, Houston, Texas 77001	7
Isacks, B. L.	Department of Geological Sciences Cornell University, Ithaca, New York 14850	3
Jachens, R. C.	Lamont-Doherty Geological Observatory Seismology Department, Palisades, New York	1
Jackson, B. V.	Institute of Geophysics, UCLA, Los Angeles, California 90066	1
Jackson, D.	Department of Planetary & Space Sciences University of California, Los Angeles, California	6
Jensen, O. G.	Department of Physics, York University Downsview M3J IP3, Ontario, Canada	2
Johnston, M.	U.S.Geological Survey/NCER, 345 Middlefield Road, Menlo Park, California 94025	6

Johnson, L. E.	CIRES, University of Colorado PSRB#1, Boulder, Colorado 80302	1
Jordan, S. K.	TASC, 6 Jacob Way, Reading, Maine 01867	4
Julian, G. M.	Physics Department, Miami University, Oxford, Ohio 45056	3
Jurdy, D. M.	Department of Geology, University of Michigan, Ann Arbor, Michigan 48104	2
Kahn, W. D.	Goddard Space Flight Center, NASA, Code 590 Greenbelt, Maryland 20770	4
Kanomori, H.	California Institute of Technology Pasadena, California 91109	6
Karcz, I.	Geology Department, State University of New York, Binghamton, New York 13901	3
Karig, D. E.	Department of Geological Sciences, University of California, Santa Barbara, Santa Barbara, California 93106	3
Karpov, A. V.	Consulting Engineer, 641 Lexington Avenue, 13th Floor, New York, New York 10022	2
Kaula, W. M.	Department of Planetary & Space Sciences University of California, Los Angeles, California 90024	2,5,6,8
Khan, M. A.	University of Hawaii, Goddard Space Flight Center Code 592, Greenbelt, Maryland 20771	4
King, C-Y	U.S.Geological Survey, 345 Middlefield Road Menlo Park, California 94025	6
King, G.C.P.	Department of Geophysics, Cambridge University, Cambridge, England	6
King, R. W.	Air Force Cambridge Research Laboratories Hanscom Air Force Base, Bedford, Massachusetts	8
Klepczynski, W. J.	U.S.Naval Observatory, 34th and Massachusetts Ave., N. W., Washington, D.C. 20390	2
Ku, L-F	Tides and Water Levels, #8 Temp. Building, Carling Avenue, Ottawa, Ontario, Canada	1,4,7

Kunze, A.W.G.	University of Akron, Department of Geology 312 Kolbe Hall, Akron, Ohio 44325	8
Kuo, J. T.	Columbia University, New York, New York 10027	1
Lambeck, K.	Groupe de Recharches de Geodesie Spatiale Observatoire de Paris, 92 Meudon, France	1,2,5,8
Lambert, A.	Department of Energy, Mines and Resources, Gravity Division, Earth Physics Branch Ottawa, Ontario KIA OE4, Canada	1
Lander, J. F.	NGSDC, Environ, Data Service NOAA, Boulder, Colorado 80302	6
Larsen, J. C.	NOAA-Joint Tsunami Research Effort 2525 Correa Road, Honolulu, Hawaii 96822	1
Leitao, C. D.	NASA Wallops Station, Building N161 Wallops Island, Virginia 23337	4
Lennon, G. W.	Institute of Coastal Oceanography and Tides Bidston Observatory, Birkenhead, Chesire L43 7RA, U.K.	1
Levine, J.	National Bureau of Standards, Division 271, Boulder, Colorado 80302	1,6
Lewis, C.F.M.	Geological Survey of Canada, 601 Booth St., Ottawa, Canada, KIA OE8	7
Lill, G.G.	NOAA/NOS, 6001 Executive Blvd. Rockville, Maryland 20852	1,7
Lindh, A. G.	Department of Geophysics, Stanford University, Stanford, California	6
Loewy, A.	2400 S. Ocean Drive, Hollywood Beach, Florida	7
Lomnitz, C.	Instituto de Geofisica, Universidad Nacional Auto., Mexico 20, D.F., Mexico	6
Loomis, A.	Jet Propulsion Laboratory, 4800 Oak Grove Drive, Pasadena, California 91103	1,4
Lorell, J.	Jet Propulsion Laboratory, California Institute of Technology, 4800 Oak Grove Drive, Pasadena, California 91103	5

Lovberg, R.	IGPP, University of California, San Diego LaJolla, California 92037	6
Lucas, J. R.	NOAA/NGS, Code 121, Rockwall Building, Rockville, Maryland 20852	5,8
MacDoran, P.	Jet Propulsion Laboratory, CPB-300, 4800 Oak Grove Drive, Pasadena, California 91103	6
Malbourne, W. G.	Jet Propulsion Laboratory/ CPB-208 Pasadena, California 91103	6
Mansinha, L.	University of Western Ontario, Department of Geophysics, London 72, Ontario Canada	1,2,5,6
Markowitz, W.	Nova University, 8000 N. Ocean Drive Dania, Florida 33004	2
Marsh, J. G.	Goddard Space Flight Center, Greenbelt, Maryland 20870	4
Masursky, H.	U.S.Geological Survey, 601 E. Cedar, Flagstaff, Arizona 86001	5
Mason, R.	U.S.Geological Survey, 390 Main Street, Rm.7021, San Francisco, California 94105	6
Mather, R. S.	Goddard Space Flight Center, Code 553, Geodynamics Branch, Greenbelt, Maryland 20771	2,3
Matthews, J.B.	Institute of Marine Science, University of Alaska, Fairbanks, Alaska 99701	1,4
Mauk, F. J.	University of Michigan, C. C. Little Building Department of Geology, Ann Arbor, Michigan	1,2
McCarthy, D. D.	U.S. Naval Observatory, Washington, D. C. 20390	2
McConnell, R. K.	Earth Sciences Research, Inc., 133 Mt.Auburn Street, Cambridge Massachusetts 02138	3
McDonald, W.	Lamont-Doherty Geological Observatory Palisades, New York 10964	1

McLure, P.	Goddard Space Flight Center Greenbelt, Maryland 20771	1,2
Melchior, P.	Observatoire Royal de Belgique, Av. Circulaire 3, 1180 Bruxelles, Belgium	1,2
Menard, H. W.	Scripps Institute of Oceanography, Box 109, La Jolla, California 92037	3,6
Merriam, J.	Physics Department, Memorial University of Newfoundland, St. John's, Newfoundland, Canada	2,5
Meyer, D. L.	Defense Mapping Agency Aerospace Center St. Louis, AFS, Missouri 63118	8
Meyers, H.	NOAA/Environmental Data Service, NGSTD Ctr. Solid Earth Data Services Division, Boulder, Colorado 80302	4,7
Miller, S. P.	Massachusetts Institute of Technology, 54-611 Cambridge, Massachusetts 02139	2
Mofjeld, H. O.	NOAA/AOML, Physical Oceanography Laboratory 15 Rickenbacker Causeway, Virginia Key, Miami, Florida 33149	1
Molnar, P.	Institute of Geophysics & Planetary Physics University of California, San Diego, P.O.Box 109 La Jolla, California 92037	3
Montgomery, R. B.	John Hopkins University, Department of Earth and Planetary Sciences, Baltimore, Maryland	1,4
Mooers, C.N.K.	University of Miami, Division of Physical Oceanography, School of Marine & Atmospheric Science, 10 Rickenbacker Causeway, Miami, Florida 33149	1
Morrison, F.	NGS, National Ocean Survey NOAA, 6001 Executive Boulevard, Code C121, Rockville, Maryland 20852	4,6,8
Morrison, N. L.	P.O.Box 2012, Rockville, Maryland 20852	6

Mourad, A. G.	Battelle Memorial Institute, 505 King Avenue Columbus, Ohio 43201	1,3,4
Mulholland, J. D.	Department of Astronomy, University of Texas Austin, Texas 78712	2,8
Muller, P.M.	Jet Propulsion Laboratory CPB-104, 4800 Oak Grove Drive, Pasadena, California 91103	2
Munk, W. H.	University of California, San Diego, IGPP/P.O. Box 109, La Jolla, California 92037	2
Murphy, J. P.	NASA Headquarters, Code ES, 600 Independence Avenue, Washington, D.C. 20546	1,2,4,6
Mulcahy, M.	Department of Geology and Geophysical Science Princeton University, Princeton, New Jersey 08540	2
Myers, V.A.	NOAA 8060 13th Street Silver Spring, Maryland 20910	7
Nathanson, F.	Technology Service Corporation, 8555 16th Street Silver Spring, Maryland 20910	4
Nava, A.	IGPP-University of California La Jolla, California 92037	6
Needham, P.	DMA/PRA, U.S. Naval Observatory, Building 56 Washington, D. C. 20305	1,2
Newberry, A. W.	Jet Propulsion Laboratory, 4800 Oak Grove Drive, Pasadena, California 91103	6
Nowroozi, A. A.	Lamont-Doherty Geological Observatory Palisades, New York 10964	1
Nummedal, D.	University of South Carolina Columbia, South Carolina 29208	7
Nur, A.M.	Department of Geophysics, Stanford University Stanford, California 94305	2,6
Nyland, E.	Institute of Earth and Planetary Physics, University of Alberta, Edmonton, Alberta, Canada	3
O'Connell, R.J.	Hoffman Laboratory, Harvard University 20 Oxford Street, Cambridge, Massachusetts	2,3,6

Oldenburg, D.	IGPP-University of California La Jolla, California 92037	6
Orlin, H.	Special Assistant to the Director, NOS, for Earth Science Activities, NOAA, Rockville, Maryland 20852	1,4,7
Orphal, D.L.	Physics International Company, Applied Mechanics Department, 2700 Merced Street, San Leandro, California 94577	6
Ortiz, N.G.	Centro de Investigacion Cientifica de Baja California, Gastelum 898, Ensenada, Baja California, Mexico	1
Pannella, G.	Department of Geology, University of Puerto Rico, Caam, Puerto Rico	2
Parker, R.	IGPP-University of California, San Diego, La Jolla, California 92037	6
Parsons, B.	Department of Earth & Planetary Sciences Massachusetts Institute of Technology Cambridge, Massachusetts 02139	3
Parks, P. E.	Virginia Polytechnic Institute, Department of Geological Sciences, Blacksburg, Virginia 24001	1
Paul, A. K.	NOAA/ERL, Space Environmental Laboratory Boulder, Colorado 80302	1
Peale, S. J.	Joint Institute for Laboratory Astrophysics University of Colorado, Boulder, Colorado 80302	2,5,8
Pearlman, M.	Smithsonian Astrophysical Observatory, 60 Garden Street, Cambridge, Massachusetts 02138	2
Perry, R. B.	NOS/NOAA, Cx6, 6001 Executive Boulevard Rockville, Maryland 20852	7
Peschel, H.	Technical University, Thomas Mann Str. 43 Dresden A20, DDR	7
Pfluke, J.	U.S.Geological Survey/OERCS, 345 Middlefied Road, Menlo Park, California 94025	6
Phillips, R. J.	Jet Propulsion Laboratories, 4800 Oak Grove Drive, 241-208, Pasadena, California 91103	8

Pierce, J. W.	Smithsonian Institution, Division of Sedimentology, Washington, D.C. 20560	7
Pitman, III W. C.	Lamont-Doherty Geological Observatory Columbia University, Palisades, New York 10964	3
Plafker, G.	U.S.Geological Survey, 345 Middlefield Road Menlo Park, California 94025	6
Platzman, G. W.	University of Chicago, Department of Geophysical Sciences, Chicago, Illinois 60637	1
Plugge, R. J.	Martin Marietta, 6851 S. Kendall Boulevard Littleton, Colorado	4
Podolak, M.	Yeshira University, Belfer Graduate School of Science, Department of Physics, New York, New York 10033	5
Poland, J. F.	U. S. Geological Survey, 2800 Cottage Way Sacramento, California 95825	7
Poling, A. A.	NOAA-NOS, 6001 Executive Boulevard Rockville, Maryland 20852	1
Pollack, H. N.	University of Michigan, Department of Geology Ann Arbor, Michigan 48104	1,2
Pope, A. J.	NOAA-NOS-NGS, 6001 Executive Boulevard Rockville, Maryland 20852	1
Prescott, W. H.	U.S.Geological Survey, 345 Middlefield Road Menlo Park, California 94025	6
Priestley, K.	Seismological Laboratory, Mackay School of Mines, University of Nevada, Reno, Nevada 89507	6
Quinn, F. H.	Great Lakes Environmental Research Laboratory/ NOAA, 630 Federal Building & U. S. Courthouse Detroit, Michigan 48226	7
Rabinowitz, P.	Lamont-Doherty Geological Observatory, Columbia University, Palisades, New York 10964	3
Raleigh, B.	U.S.Geological Survey, 345 Middlefield Road Menlo Park, California 94025	6

Ramasastry, J.	Goddard Space Flight Center, Code 553 Greenbelt, Maryland 20771	2
Ransford, G. A.	5111 Briggs Avenue, La Crescenta, California 91214	8
Rapatz, W. J.	Department of Environment, Marine Sciences 512-1230 Government Street, Victoria, B.C. Canada	4,7
Reasenberg, R.D.	M.I.T., Department of Earth & Planetary Sciences Massachusetts Institute of Technology, Cambridge, Massachusetts 02138	5,8
Reid, I.	IGPP-University of California, La Jolla, California 92037	6
Reid, J.L.	Scripps Institution of Oceanography, P.O. Box 1529, La Jolla, California 92037	4
Reyes, A.	IGPP-University of California, La Jolla California 92037	6
Rinehart, J. S.	NOAA, Environmental Research Laboratories Boulder, Colorado 80302	1
Rives, S.R.	Johns Hopkins University, 34th and Charles Streets, Baltimore, Maryland 21218	1
Rizzo, P.	E, D'Appollonia Consulting Engineers, 10 Duss Road, Pittsburgh, Pennsylvania 15235	6
Robinson, E. S.	Virginia Polytechnic Institute, Department of Geological Sciences, Blacksburg, Virginia 24061	1,4
Robinson, J.V.	FBM Geoballistice Division, U.S.Naval Weapons Laboratory, Dahlgren, Virginia 22448	4
Rochester, M. G.	Memorial University of Newfoundland, St. John's, Newfoundland, Canada	2,8
Rodgers, D. A.	California Division of Mines & Geology 1416 Ninth Street, Room 118, Sacramento, California 95814	6
Rondy, D. R.	Lake Survey Center, NOAA, 630 Federal Building & U.S.Courthouse, Detroit, Michigan	7
Rundle, R. T.	Headquarters Defense Mapping Agency, Building 56, Naval Observatory, 34th and Massachusetts Avenue, N.W., Washington, D.C. 20305	8
Ruthven, D.W.	U.S.Geological Survey, 345 Middlefield Road Menlo Park, California 94025	6

Ryall, A.	Seismological Laboratory, Mackay School of Mines, University of Nevada, Reno, Nevada 89507	6
Sakata, S.	IGPP-University of California, San Diego, La Jolla, California 92037	6
Sanford, A.R.	New Mexico Technology, Geoscience Department Socorro, New Mexico 87801	6
Saunders, R. S.	Jet Propulsion Laboratory, 183/501, 4800 Oak Grove Drive, Pasadena, California 91103	5
Savage, J. C.	U. S. Geological Survey, 345 Middlefield Road Menlo Park, California 94025	6
Schimerman, L.A.	Defense Mapping Agency Aerospace Center 2nd & Arsenal Streets, St. Louis AFS, Missouri 63118	8
Schloissin, H. H.	University of Western Ontario, Department of Geophysics, London 72, Ontario, Canada	5
Schmidt, V.A.	University of Pittsburgh, 506 Langley Hall Pittsburgh, Pennsylvania 15213	2
Schnelzer, G.	Terrestrial Science Laboratory, AFCRL(LWH) L.G.Hanscom Field, Bedford, Massachusetts 01730	2
Scholz, C.	Lamont-Doherty Geological Observatory Columbia University, Palisades, New York 10964	3
Schubert, G.	Department of Planetary & Space Sciences University of California, Los Angeles, California	8
Schutz, B. E.	University of Texas, Aerospace Engineering Department, Tay.227, Austin, Texas 78712	2,4,5,8
Schwarz, K-P	Technische Hochschule Graz, Institute of Geodesy IV, A-8010 Graz, Steyrergasse 17, Graz, Austria	8
Schwimmer, P.M.	Defense Mapping Agency, Building 56, Naval Observatory, Washington, D.C. 20305	4
Sclater, J.	Department of Earth & Planetary Physics Massachusetts Institute of Technology, Cambridge, Massachusetts 02139	3

Seeber, G.	Technical University, Nienburger Str. 6 3 Hannover, West Germany	7
Seeger, C. R.	Geography and Geology Department, Western Kentucky University, Bowling Green, Kentucky 43101	3
Severy, N.I.	CIRES, University of Colorado, Boulder, Colorado 80302	1
Shaffer, R.	N. Mexico Institute of Mining, New Mexico Technology, Socorro, New Mexico 87801	6
Shapiro, A.	Naval Research Laboratory, Washington, D.C.	4
Shelton, J.	P.O.Box 48, La Jolla, California 92037	6
Shirey, W. H.	NASA, Code SM - NASA HG Washington, D.C. 20546	8
Shull, C. W.	Defense Mapping Agency Topographic Center 6500 Brooks Lane D/Cartography, Washington, D.C.	8
Simon, R. M.	Lawrence Livermore Laboratory, P.O.Box 808-L-51, Livermore, California 94550	6
Singh, R. N.	Physics Department, Memorial University of Newfoundland, St. John's, Newfoundland, Canada	2
Siry, J. W.	Goddard Space Flight Center, Greenbelt, Maryland 20771	1,3,6
Sjogren, W.L.	Jet Propulsion Laboratory, California Institute of Technology, 4800 Oak Grove Drive, Pasadena, California 91103	8
Slade, M.A.	Jet Propulsion Laboratory, CPB 300, 4800 Oak Grove Drive, Pasadena, California 91103	8
Sleep, N.H.	Department of Geology and Geophysics, Room 54-514, Massachusetts Institute of Technology, Cambridge, Massachusetts 02139	3
Slichter, L.B.	UCLA, Institute of Geophysics, Los Angeles, California 90024	1
Smith, D.E.	Goddard Space Flight Center, Code 553, Geodynamics Branch, Greenbelt, Maryland 20771	2
Smith, D.	GSFC-NASA, Code 921, Greenbelt, Maryland	6

Smith, S.	University of Washington, 15th Ave., N.E. & N.E.40th, Seattle, Washington 98105	6
Smith, S.L.	Naval Weapons Laboratory, Dahlgren, Virginia	4
Smoluchowski, R.	Princeton University Princeton, New Jersey 08540	5
Smylie, D. E.	York University, Toronto, Departmentof Physics, Downsview 463, Ontario Canada	1,2,5
Snodgrass, F. E.	University of California, San Diego, P.O.Box 109, La Jolla, California 92037	1
Snyder, R. L.	Nova University, Oceanographic Laboratory 8000 N. Ocean Boulevard, Dania, Florida 3304	1
Sousk, S. F.	American Geophysical Union, 1909 K Street, N.W. Washington, D. C. 20036	5
Spilhaus, A. F. Jr.	American Geophysical Union, 1909 K Street, N.W. Washington, D. C. 20036	1,
Spring, W.	New York University, Department of Oceanography & Meteorology, University Heights, N.Y.U. Bronx, New York	4
Stein, R.S.	P.O.Box 4847, Brown University Providence, Rhode Island 02912	8
Steinwert, D. C.	State of California, Department of Water Resources P.O.Box 388, Sacramento, California 95802	7
Stephen, M.F.	Coastal Research Division, Geology Department Department of Geology, University of South Carolina, Columbia, South Carolina 29208	7
Stepp, J. C.	U.S.Atomic Energy Commission, Directorate of Licensing, Washington, D.C. 20014	3,6
Stipe, J. G. Jr.	Physics Department, Boston University, 111 Cummington Street, Boston, Massachusetts	2
Stock, G.	University of California, San Diego La Jolla, California 91034	1
Stoughton, H. W.	P.O.Box 599, Ann Arbor, Michigan 48104	3

Strange, W.	Computer Science Corporation 8728 Colesville Road, Silver Spring, Maryland	4
Strangway, D.	University of Toronto, Department of Geology Toronto, Canada	8
Strickland, A.T.	Code SM, NASA Headquarters, Washington, D. C. 20546	8
Stuart, W.D.	U.S. Geological Survey, 345 Middlefield Road Menlo Park, California 94025	6
Sturges, W.	Florida State University, Department of Oceanography, Tallahassee, Florida 32306	1,4
Suh, J.H.	Colorado School of Mines, Geophysics Department Golden, Colorado 80401	1
Swanson, R.L.	NOAA/MESA, Marine Sciences Research Center Building J, State University of New York, Stony Brook, New York 11790	7
Swetnick, M.J.	NASA Headquarters, Earth Observations Programs, Washington, D. C. 20546	4
Talwani, M.	Lamont-Doherty Geological Observatory Columbia University, Palisades, New York 10964	3
Tapley, B. D.	Aerospace Engineering and Engineering Mechanics University of Texas at Austin, Taylor Hall 227 Austin, Texas 78712	2,4,8
Teng, T-L	University of Southern California/Geodetic Science Los Angeles, California	6
Thacker, C.	NOAA/AOML, 15 Rickenbaker Causeway Miami, Florida 33144	7
Thatcher, W.	U.S. Geological Survey, 345 Middlefield Road Menlo Park, California 94025	6
Thurlow, C.I.	Tidal Datum Planes Section, NOS Rockville, Maryland 20852	7
Tiernan, M.	Jet Propulsion Laboratory, California Institute of Technology, 4800 Oak Grove Drive, Pasadena, California 91103	8
Toksoz, N.	Massachusetts Institute of Technology, 54-518 Department of Earth & Planetary Science, Cambridge, Massachusetts 02139	6,8

Tolson, R. H.	Langley Research Center, NASA Hampton, Virginia 23665	4,5,8
Toomre, A.	Massachusetts Institute of Technology, 2-371 Cambridge, Massachusetts 02139	2
Trask, D. W.	Jet Propulsion Laboratory, 4800 Oak Grove Drive, Pasadena, California 91103	2
Tullis, T. E.	Brown University, Department of Geological Science, Providence, Rhode Island 02912	6
Turcotte, D. L.	Cornell University, Department of Geological Science, Ithaca, New York 14850	6
Turcotte, T.	Weston Geophysics, Weston, Massachusetts	6
Uliana, E. A.	Naval Research Laboratory, Code 7112 U Washington, D. C. 20375	4
Van der Voo, R.	Department of Geology & Mineralogy, University of Michigan, Ann Arbor, Michigan 48104	2
Van der Wal, J.H.M.	Meetkundige Dienst Van De Rijkswaterstaat Kanaalweg 3B, Delft, Holland	7
Van Flandern, T. C.	U.S.Naval Observatory, Washington, D.C. 20390	2
Vanicek, P.	Department of Surveying Engineering, University of New Brunswick, Fredericton, New Brunswick Canada	3
Vaughan, G. W.	National Weather Service, Akron-Canton Regional Apt., North Canton, Ohio 44720	7
Velez, N.	Centro de Investigacion Cientifica, de Baja California, Gastelum #898, Ensenada, Baja California, Mexico	1
Vincent, S.	Computer Sciences Corporation, System Sciences Division, 8728 Colesville Road, Silver Springs, Maryland 20910	4
von Schwind, J. J.	Department of Oceanography, Naval Postgraduate School, Monterey, California 93940	1,4
Walcott, R.I.	Earth Physics Branch, Department of Energy, Mines & Resources, Ottawa, Ontario KIA OE4, Canada	3,7

Walsh, J. B.	Department of Earth & Planetary Sciences Massachusetts Institute of Technology Cambridge, Massachusetts, 02139	6
Walter, H.G.	Observatoire de Paris, Section d'Astrophysique Dep. Dano, Sol-Ter, 92 Meudon, France	2
Walter, L. S.	GSFC-Code 650.3, Laboratory for Meteorological Sciences, Greenbelt, Maryland 20771	6
Warburton, R. J.	University of California, San Diego, P-C Building Department of Physics, La Jolla, California 92037	1
Ward, W. R.	Harvard Observatory, 60 Garden Street Cambridge, Massachusetts 02138	3
Watts, A. B.	Lamont-Doherty Geological Observatory Columbia University, Palisades, New York 10964	3
Weertman, J.	Material Science Department, Northwestern University, Evanston, Illinois 60201	6
Weiffenbach, G.	Smithsonian Astrophysical Observatory 60 Garden Street, Cambridge, Massachusetts	2,4
Weissel, J.K.	Lamont-Doherty Geological Observatory Columbia University, Palisades, New York 10964	3
Westhusing, J. K.	Lockheed Electronics Co., ASD Dept.626-30 16811 El Camino Real, Houston, Texas 77058	6
Wexler, J. A.	NOAA/NOS, Rockville, Maryland 20852	7
Whitten, C. A.	American Geophysical Union, 9606 Sutherland Road, Silver Springs, Maryland 20901	2,3,4
Wigen, S.O.	Marine Sciences Directorate, 512 Federal Building, Victoria, B.C., Canada	1,3
Williams, J. G.	Jet Propulsion Laboratory, 4800 Oak Grove Drive Pasadena, California 91103	8
Williamson, R. G.	Wolf Research & Development Corporation, 6801 Kenilworth Avenue, Riverdale, Maryland 20840	8
Willis, D. E.	Department of Geological Sciences, University of Wisconsin, Milwaukee, Wisconsin 53201	3,6
Wilson, C. R.	Institute of Geophysics & Planetary Physics University of California, San Diego, La Jolla, California 92037	2

Wimbush, M.	Nova University Oceanographic Laboratory 8000 North Ocean Drive, Dania, Florida 33004	1
Winkler, G.M.R.	U.S. Naval Observatory, Washington, D.C.20390	2
Wolgemuth, K.	Dickinson College, Carlisle, Pennsylvania 17013	7
Wollenhaupt, W.	Johnson Space Center, Houston, Texas 77058	8
Wood, J. A.	Smithsonian Astrophysical Observatory 60 Garden Street, Cambridge, Massachusetts 02138	8
Wood, M.C.	National Center for Earthquake Research, USGS 800 Menlo Ave., Menlo Park, California 94025	1
Won, I.J.	School of Mines, Columbia University New York, New York 10027	1
Wood, M.D.	U.S.Geological Survey/NCER, 345 Middlefield Road, Menlo Park, California 94025	6
Wu, F. T.	Suny University, Department of Geodetic Science Binghamton, New York	6
Wunsch, C.	Room 54-1324, Massachusetts Institute of Technolcgy, Cambridge, Massachusetts 02139	1
Yionoulis, S. M.	JHU/APL, 8621 Georgia Avenue Silver Spring, Maryland	4
Young, S.	Tidal Datum Planes Section, NOS Rockville, Maryland 20852	7
Yuen, D.	University of California/Geophysics Los Angeles, California	6
Zetler, B. D.	IGPP, University of California, San Diego P.O.Box 109, La Jolla, California 92037	1

OSU Personnel	GEOP
Agajelu, S.	8
Arur, M.G.	8
Bossler, J.D.	1
Bull, C.	2,3,7
Christodulidis, D.	3,8
Dermanis, A.	5,8
Ewing, D.R.	1,2
Gopalapillai, S.	1,2,3,4,5,7
Ghosh, S.	5
Hajela, D.P.	1,2,3,4,5,8
Heitkamp, H.	1
Hower, J.C.	8
Joshi, C.S.	1
Jiwalai, W.	8
Kumar, M.	1,2,3,4,5,6,7,8
Lakhoo, R.A.L.	1
Leick, A.	2,3,5,8
Marino, R. J.	8
McLuskey, D.	5,8
Moose, R. E.	1
Moritz, H.	5
Mueller, I.I.	1,2,3,4,5,6,7,8
Noltimier, H.C.	2,3
Papo, H.	2
Rapp, R. H.	2,3,4,8
Reed, G.B.	1
Reilly, J.P.	1,2,3,4,5
Rummel, R.	8
Saxena, N.	1,2,3,4,5,6,7,8
Smith, G.	1,5,6
Sprinsky, W.	1,5
Soler, T.	1,2,3,4,5,7,8
Steward, H.	1,2,3,5
Tscherning, C.C.	5,7
Tseng, C.L.	8
Uotila, U.O.	1,2,3,5,8
van Gelder, B.H.	1,2,3,5,7,8